BASIN DEVELOPMENT, ENVIRONMENT OF DEPOSITION AND DEFORMATION OF A PRECAMBRIAN (?) CONGLOMERATIC FLYSCH SEQUENCE AT BATHURST HARBOUR, S.W. TASMANIA.

by

PETER RODERICK WILLIAMS, B.Sc. (Hons.)

VOLUME TWO

DIAGRAMS AND PLATES

UNIVERSITY OF TASMANIA

HOBART

(NOVEMBER 1979)

CONTENTS

DIAGRAMS

CHAPTER 6. Stratigraphic and Sedimentological characteristics of the Clytie Cove Group.

6:1 Typical stratigraphic sequences of formations of the Clytie Cove Group.

6:2 Graph of bed thickness against bed number, Mt. Rugby Conglomerate.

6:3 Stratigraphic column, White Point section.

6:4: a. Graph of thickness of coarse divisions against bed number, White Point section.

b. Smoothed average of bed thickness of layers against bed number, White Point section.

6:5 Graph of bed thickness of conglomeratic beds against bed number, White Point section.

6:6 As above.

6:7: a. Stratigraphic column, Long Bay Shale.

b. Stratigraphic column, Narrow Sandstone and Conglomerate and Joan Point Sandstone.

6:8: a. Narrow Formation; graph of layer thickness against bed number.

b. Narrows Formation; graph of coarse division thickness against bed number.

6:9 Narrows Formation; graph of conglomeratic division thickness against bed number.

6:10 Thickness of coarse divisions. Generalised diagram for the Clytie Cove Group as a whole.

6:11 Facies changes in the Clytie Cove Group.

6:12 Grainsize analyses of the White Point section. Graph of bed number against maximum grainsize.

6:13 Relationship between bed thickness and grainsize, White Point section.

3:1 Early generation folds, Clytie Cove Group.

3:2 Modified primary deformation structures from the Mt. Mackenzie Formation.

3:3 Slump zone, pseudonodules and early faults from the Mt. Mackenzie Formation.

3:4 Early deformation structures - Clytie Cove Group.

3:5: a. Mudstone intrusions of sandstone beds.

b. Major D_{2c} anticline, from Mt. Stokes.

3:6 Early isoclinal folds, D_{2c}.

3:7 D_{2c} folds with strongly discordant S_{3c} surface.

3:8 Style of D_{3c} folds.

3:9 Saddle folds related to D_{3c} event.

3:10 Lithological banding parallel to cleavage (S_{3c})

3:11 As above.

3:12 Anastomosing cleavage in the core of the Clytie Cove Syncline.

3:13 Form of S_{3c}.

3:14 Mesoscopic banding parallel to cleavage.

3:15 Banding in the core of a fold in a sandstone layer.

3:16 Relationship between S_{3c} and sedimentary flames.

3:17 Microscopic form of cleavage seams.

3:18 Sedimentary mobilisation of mudstone.

3:19 Cleavage development in other rock types.

3:20 Form of water escape folds, Joan Point Sandstone.

5:1 Fabric and structure of the Mt. Rugby Conglomerate.

5:2 Photomicrographs, Mt. Rugby Conglomerate.

5:3 Long Bay Shale, Antimony Point.

5:4 Sedimentary structures, Long Bay Shale.

5:5 Turbidity current deposited beds, Long Bay Shale.

5:6 As above.

5:7 Thin-bedded sandstone deposited from turbidity currents, Long Bay Shale.

5:8 Photomicrographs, Clytie Cove Group and correlates.

5:9 Structure of the Narrows Sandstone and Conglomerate.

5:10 Outsized clasts and pebbly sandstone, Mt. Rugby Conglomerate correlate.

5:11 Fabric of conglomerate, Mt. Rugby correlate, Mt. Fulton.

5:12 Photomicrographs of rocks from the Mt. Fulton area.

5.13 Sedimentary structures at Mt. Fulton.

5:14 As above.

5:15 Cross-bedding structure, Joan Point Sandstone correlate.

5:16 Forms of graded bedding, Clytie Cove Group.

5:17 Graded bedding and fabric around clasts.

5:18 Projecting clasts and outsized clasts.

5:19 Fabric of beds with large clasts and outsized clasts.

5:20 As above.

5:21 Form of graded conglomerate, Clytie Cove Group.

5:22 Granule conglomerate deposited over a scoured sandstone.

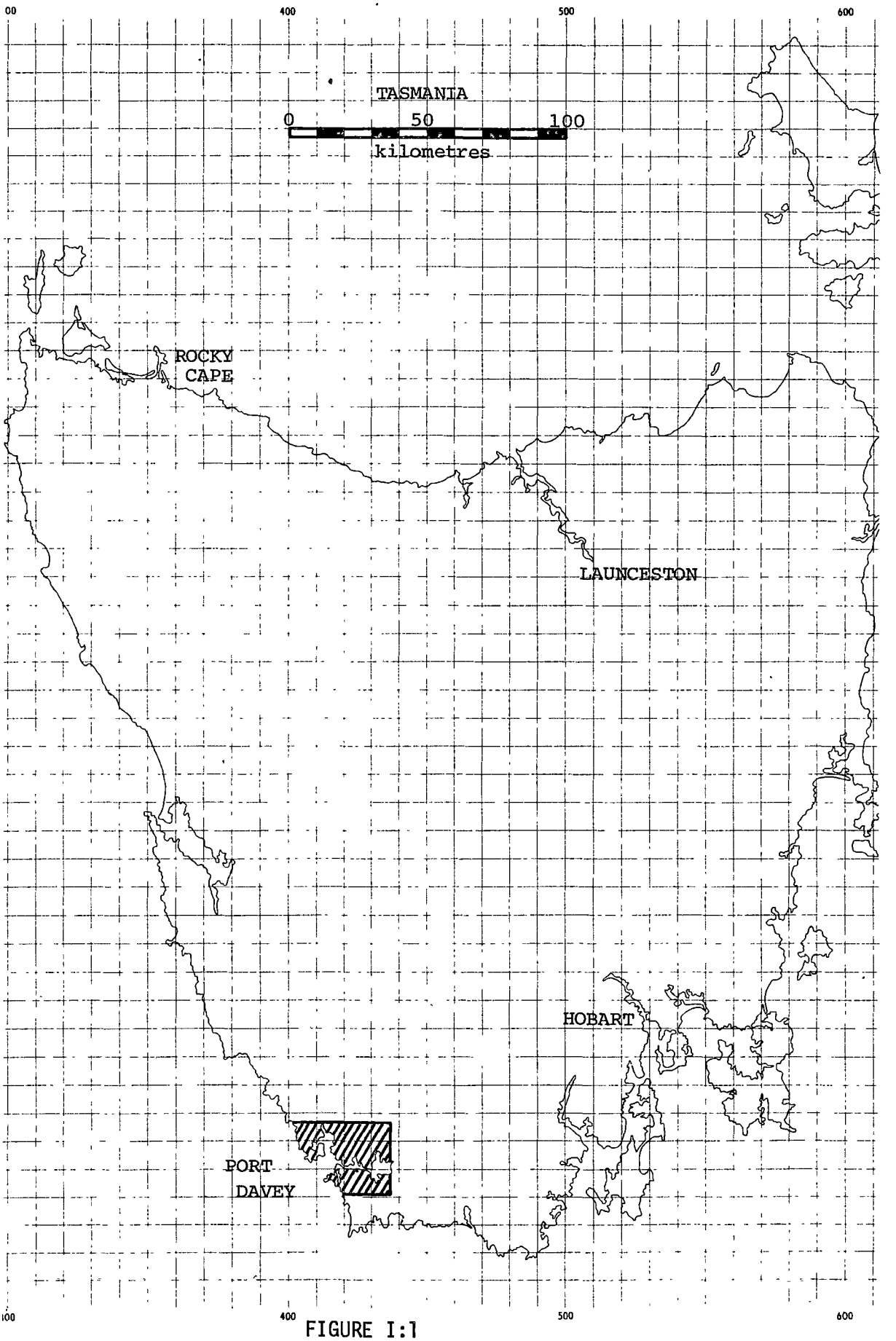
00
400
500
600
TASMANIA
0
50
100
kilometres
ROCKY
CAPE
LAUNCESTON
HOBART
PORT
DAVEY
100
400
500
600

FIGURE I:1

CHAPTER 1

DIAGRAMS

ASPECTS OF THE TECTONICS OF TASMANIA RELATED TO THE GEOLOGICAL HISTORY OF THE PORT DAVEY-BATHURST HARBOUR REGION.

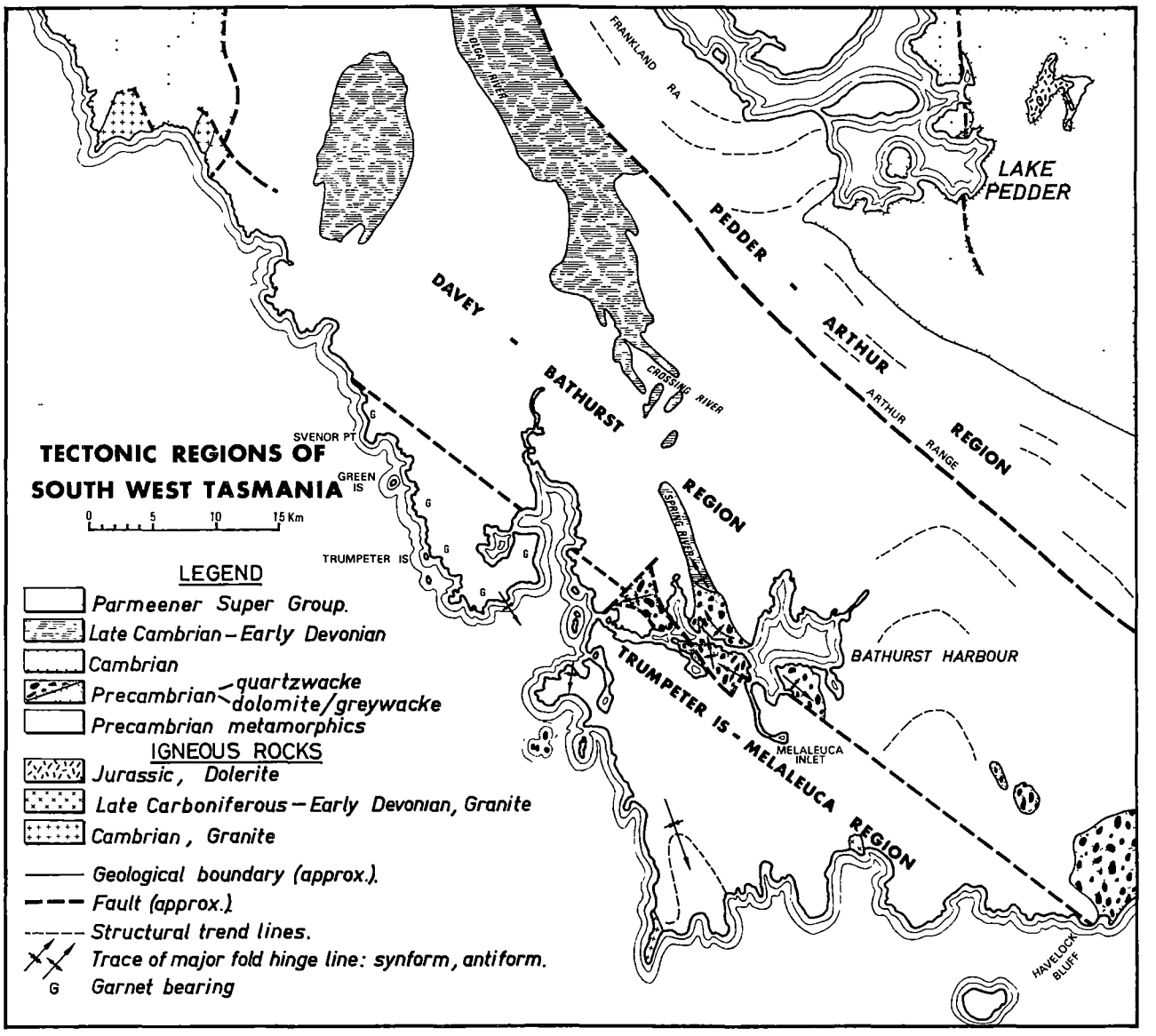
TECTONIC REGIONS OF
SOUTH WEST TASMANIA
0 5 10 15 Km
LEGEND
Parmeener Super Group.
Late Cambrian – Early Devonian
Cambrian
Precambrian – quartzwacke
dolomite/greywacke
Precambrian metamorphics
IGNEOUS ROCKS
Jurassic, Dolerite
Late Carboniferous – Early Devonian, Granite
Cambrian, Granite
Geological boundary (approx.).
Fault (approx.)
Structural trend lines.
Trace of major fold hinge line: synform, antiform.
G Garnet bearing
FRANKLAND RA
LAKE PEDDER
PEDDER - ARTHUR REGION
DAVEY - BATHURST REGION
ARTHUR RANGE
DUCK RIVER
CROSSING RIVER
SVENOR PT
GREEN IS
TRUMPETER IS
SPRING RIVER
BATHURST HARBOUR
MELALEUCA INLET
TRUMPETER IS - MELALEUCA REGION
HAVELOCK BLUFF

FIG 1 2

FIGURE 1:3

Generalised stratigraphy of the Clytie Cove Group. Nowhere in the region is there a continuous sequence from the Mt. Rugby Formation to the Joan Point Sandstone. Conformable relations between successive formations are exposed in different sections around Bathurst Harbour. Thicknesses are taken from the thickest exposed succession of each formation, and so the thickness is a maximum stratigraphic thickness, not allowing for structural effects. Major conglomerate bodies are indicated by circled units. Circled and stippled layers represent units of conglomerate and sandstone. The wedges coloured in triangles represent a megabreccia unit.

GENERALISED STRATIGRAPHY :

CLYTIE COVE GROUP

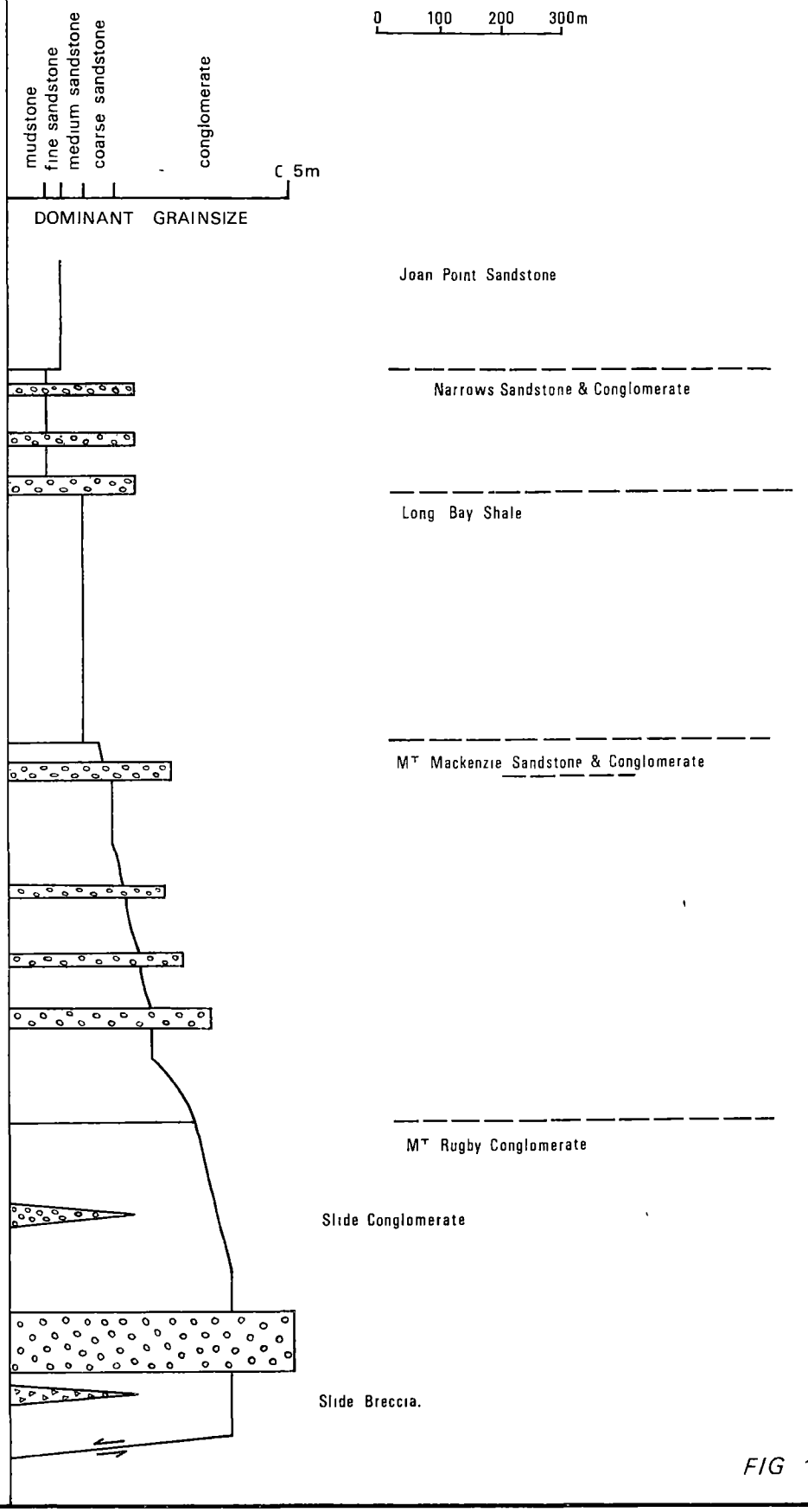

FIG 13

CHAPTER 2

DIAGRAMS AND PLATES

REGIONAL GEOLOGICAL STRUCTURE OF THE PORT DAVEY - BATHURST HARBOUR REGION

FIGURE 2:1

Geological map from east of Trixies Cove (GR350984) to Moulters Inlet (GR364963).

FIGURE 2:2

Mesoscopic folds mirror the regional trend of dominant layering. Parasitic folds do not verge towards the major closures. The style is conjugate in nature. See text.

FIGURE 2:3

Cleavages and kink-bands associated with the folds shown in figure 2:2.

a. N.E. trending cleavage in quartzite (39 values) apparently associated with dextral folds contoured at 1.3, 6.4, 14 and 27% per 1% area. Dots represent cleavage poles associated with sinistral folds.

b. Kink-bands, (o) dextral, (.) sinistral, in laminated quartzite. Heavy lined girdles are kink-band planes of best fit.

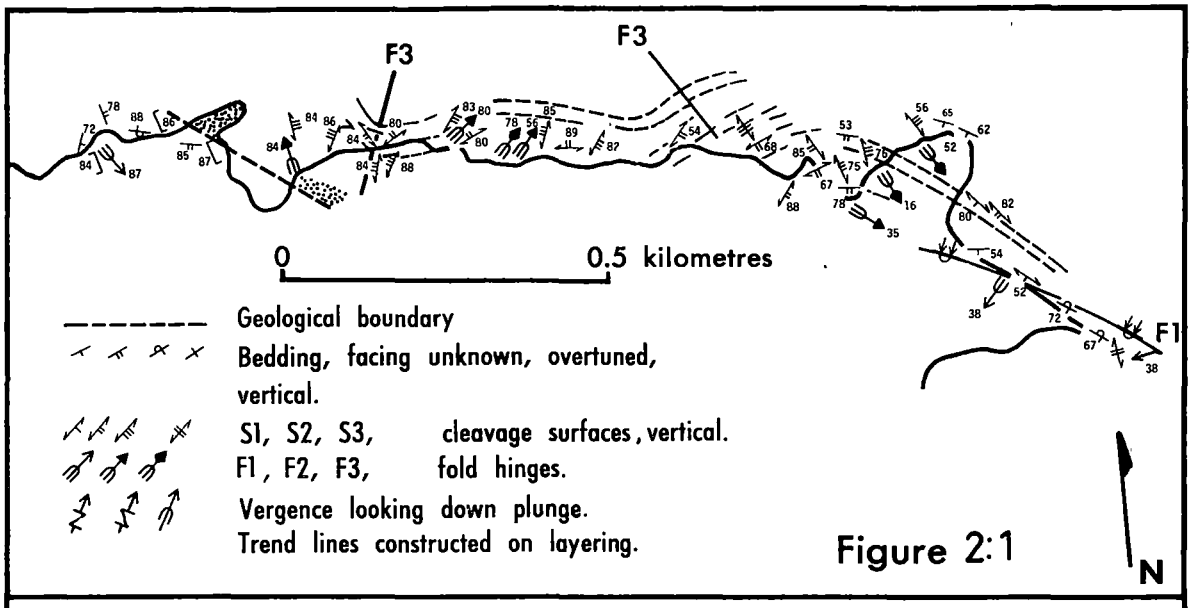

Figure 2:1

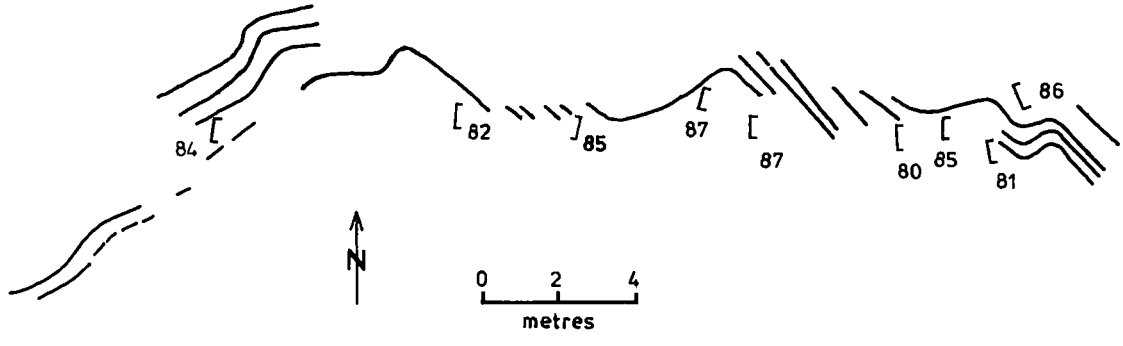

FIG. 2:2

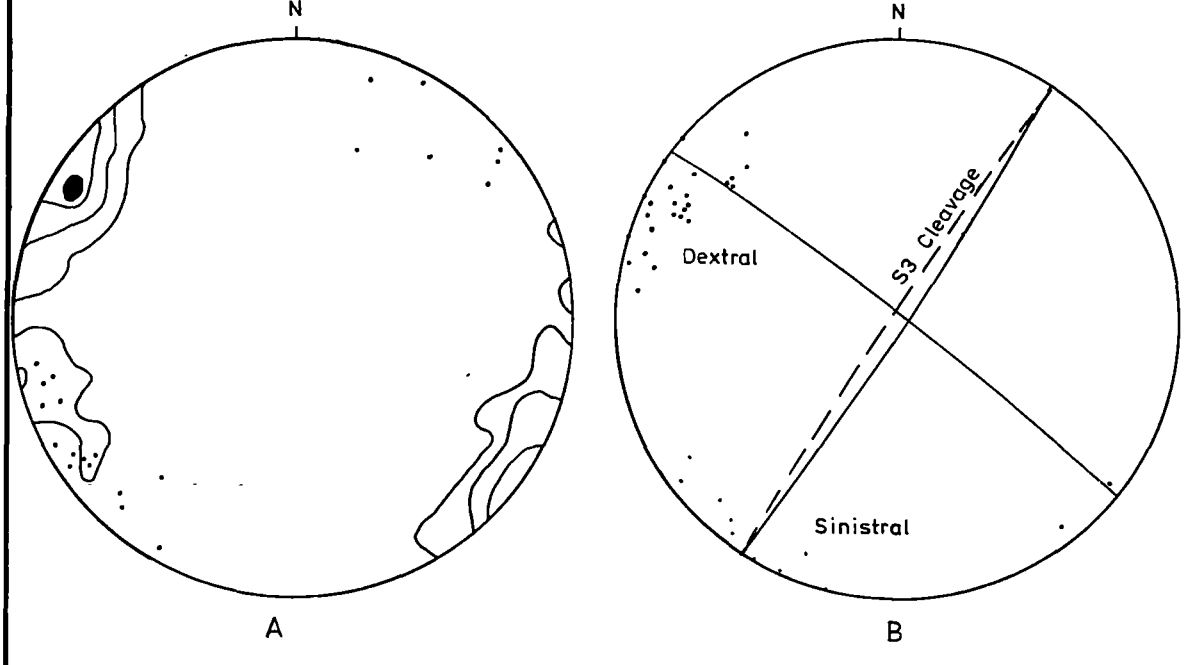

FIG. 2:3

PLATE 2:1

a. Kink-band in laminated quartzite from east of Trixies Cove. Substantial grainsize reduction of quartz in the hinge areas. NX, magnification x 10. Specimen 48151.

b. Form of the cleavage, parallel to kink-bands, in micaceous quartzite unit. S_2 horizontal, S_3 diagonal from lower left. PPL, magnification x 20. Specimen 48152.

c. Large scale mechanical layering in the quartzite layer is parallel to S_1. Folds in layers above and below the quartzite are F_2, and produce a cleavage at a low angle to layering. Hammer handle 0.4 m long. (GR 308967).

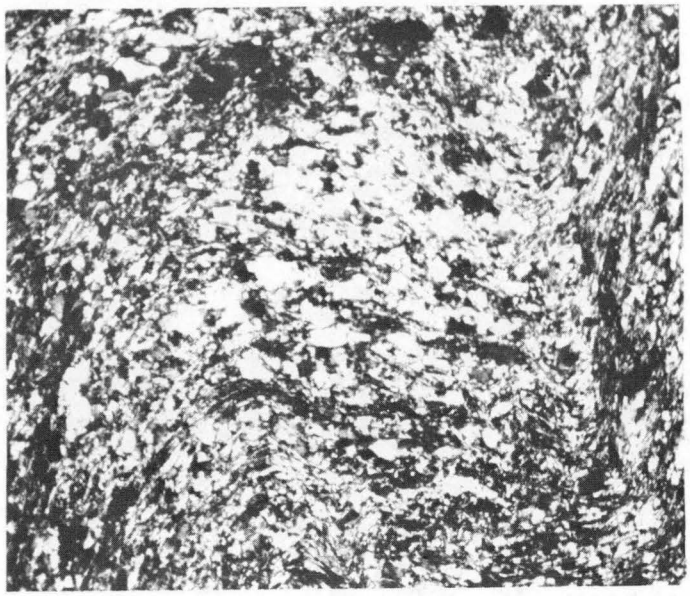

a

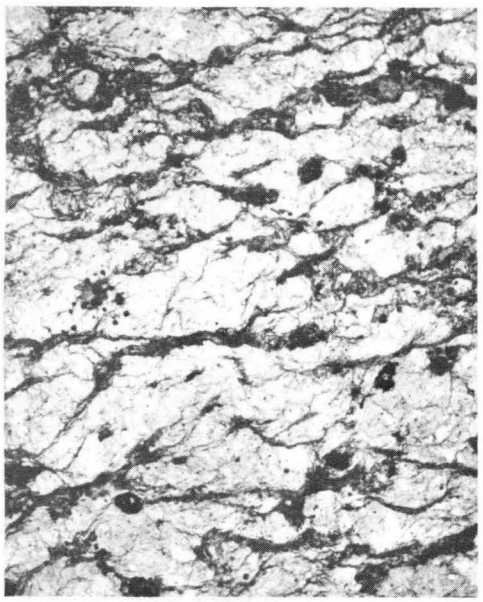

b

c

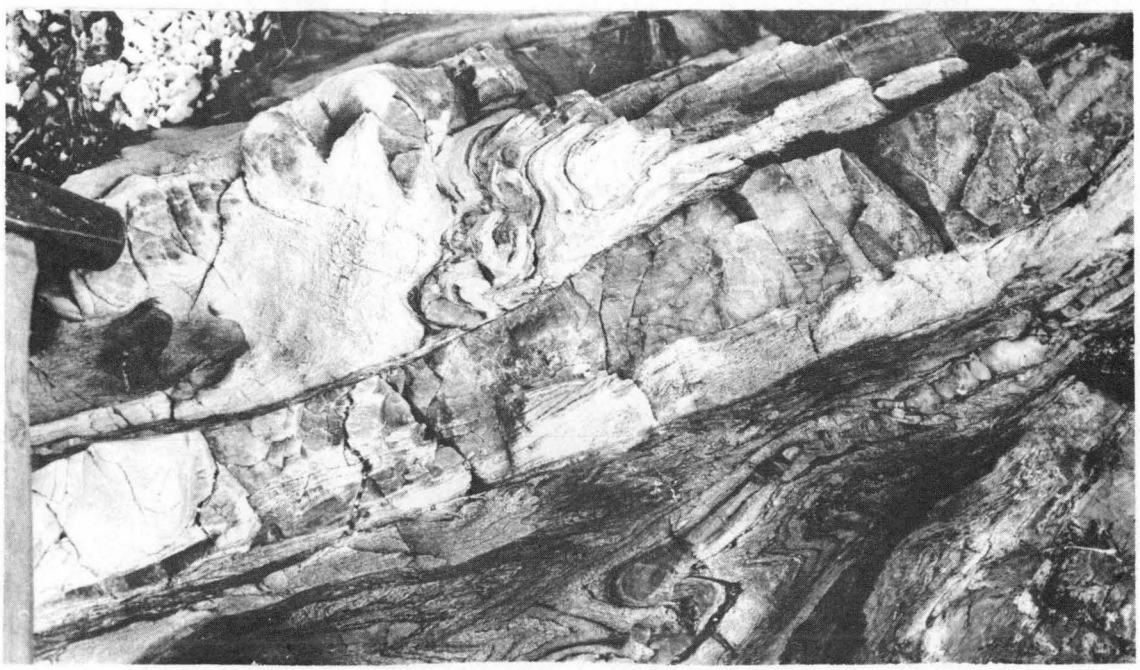

PLATE 2:1

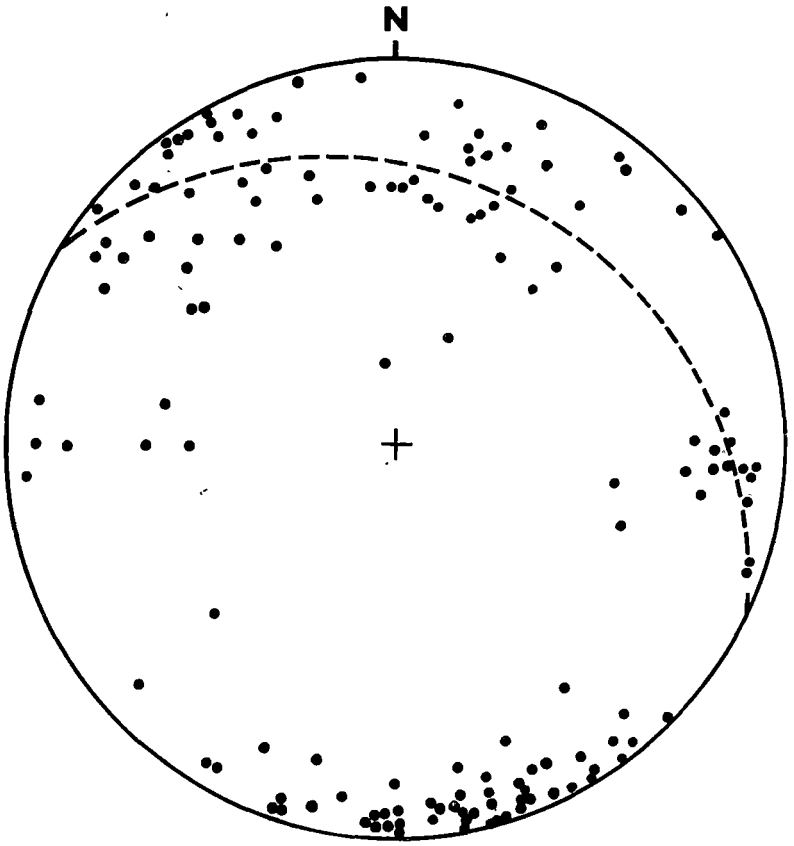

Figure 2:4

PLATE 2:2

Mesoscopic folds

a. Isolated isoclinal fold cores preserved in micaceous quartz-schist. Loaparte Cove. Scale in centimetres.

b. Isoclinal and party isolated F_1 folds in laminated quartzite. Mt. Rugby, eastern flank. Lens cap 50 mm diameter.

c. Intrafolial style of F_2 folds. Cleavage weakly developed, but at a low angle to layering. Biro for scale, 150 mm long. (GR 285038).

a

b

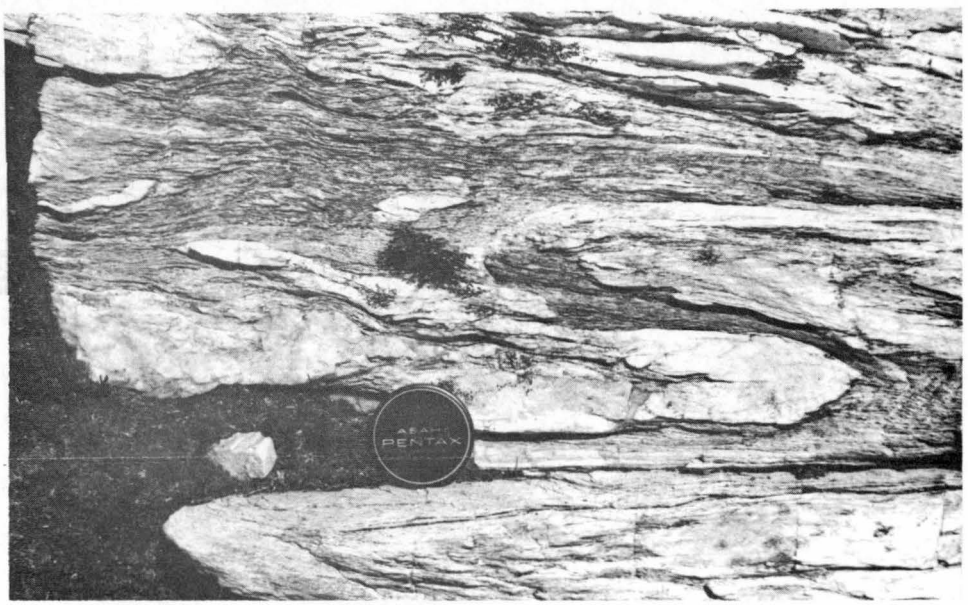

c

PLATE 2:2

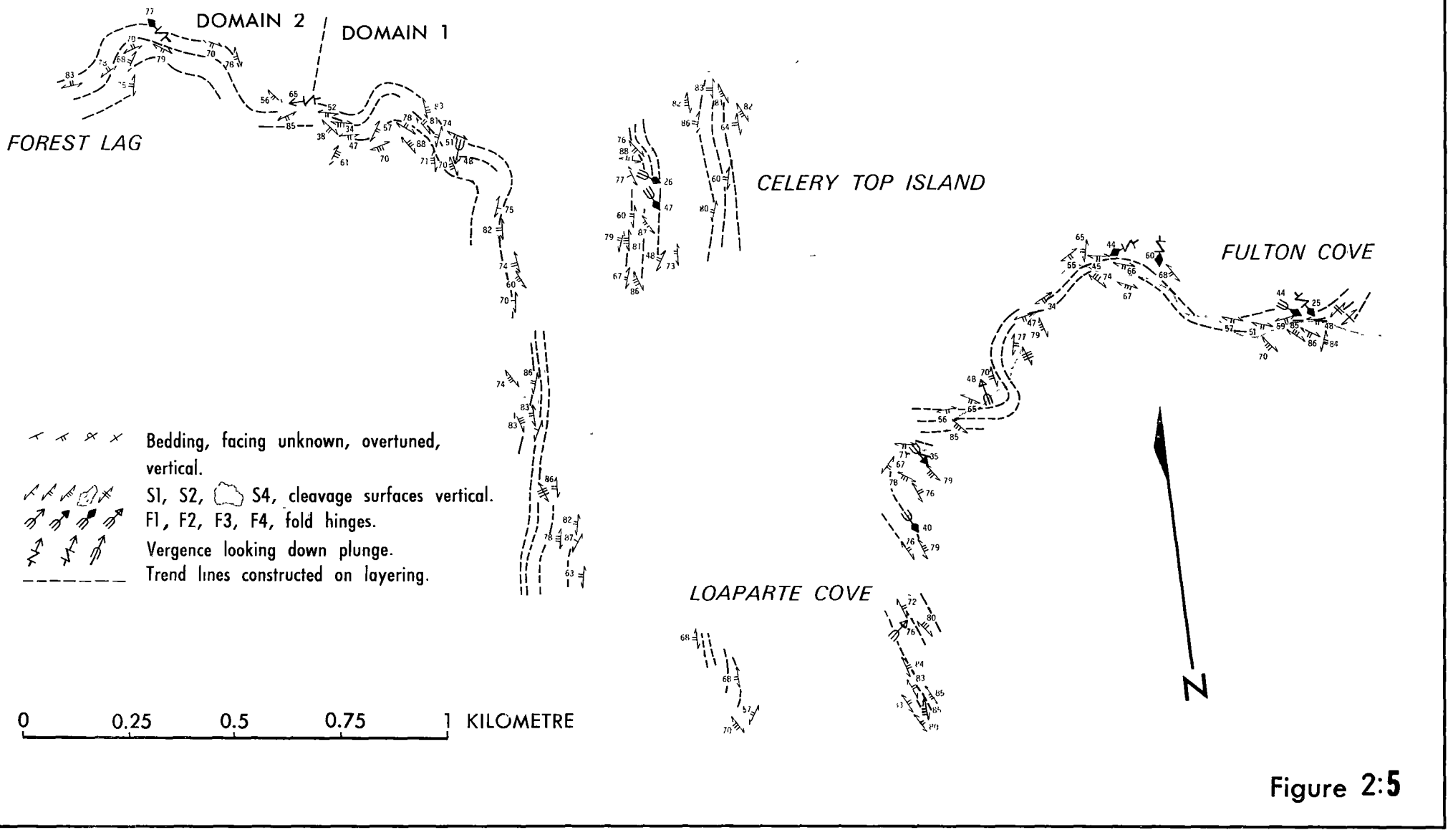
DOMAIN 2
DOMAIN 1
FOREST LAG
CELERY TOP ISLAND
FULTON COVE
LOAPARTE COVE
Bedding, facing unknown, overtuned, vertical.
S1, S2, S4, cleavage surfaces vertical.
F1, F2, F3, F4, fold hinges.
Vergence looking down plunge.
Trend lines constructed on layering.
0
0.25
0.5
0.75
1 KILOMETRE
N

Figure 2:5

FIGURE 2:6

Equal area projections of orientation data from Melaleuca Inlet to Fulton Cove.

a. Poles to layering from domain 1, west of Loaparte Cove (see fig. 2:5). Cone axis plunges 70° to 151°. Semi-angle is 70°. 22 values.

b. Poles to layering from domain 2, east of Forest Lag. Cone axis plunges 80° to 285°, semi-angle is 80°. 31 values.

c. Poles to layering from Loaparte Cove to Fulton Cove. 66 values.

d. Poles to the S_4 cleavages from Fulton Cove to Melaleuca Inlet, 67 values.

e. Poles to layering, Celery Top Island, 21 values.

f. Poles to S_4 cleavage from the Celery Top Island, 10 values.

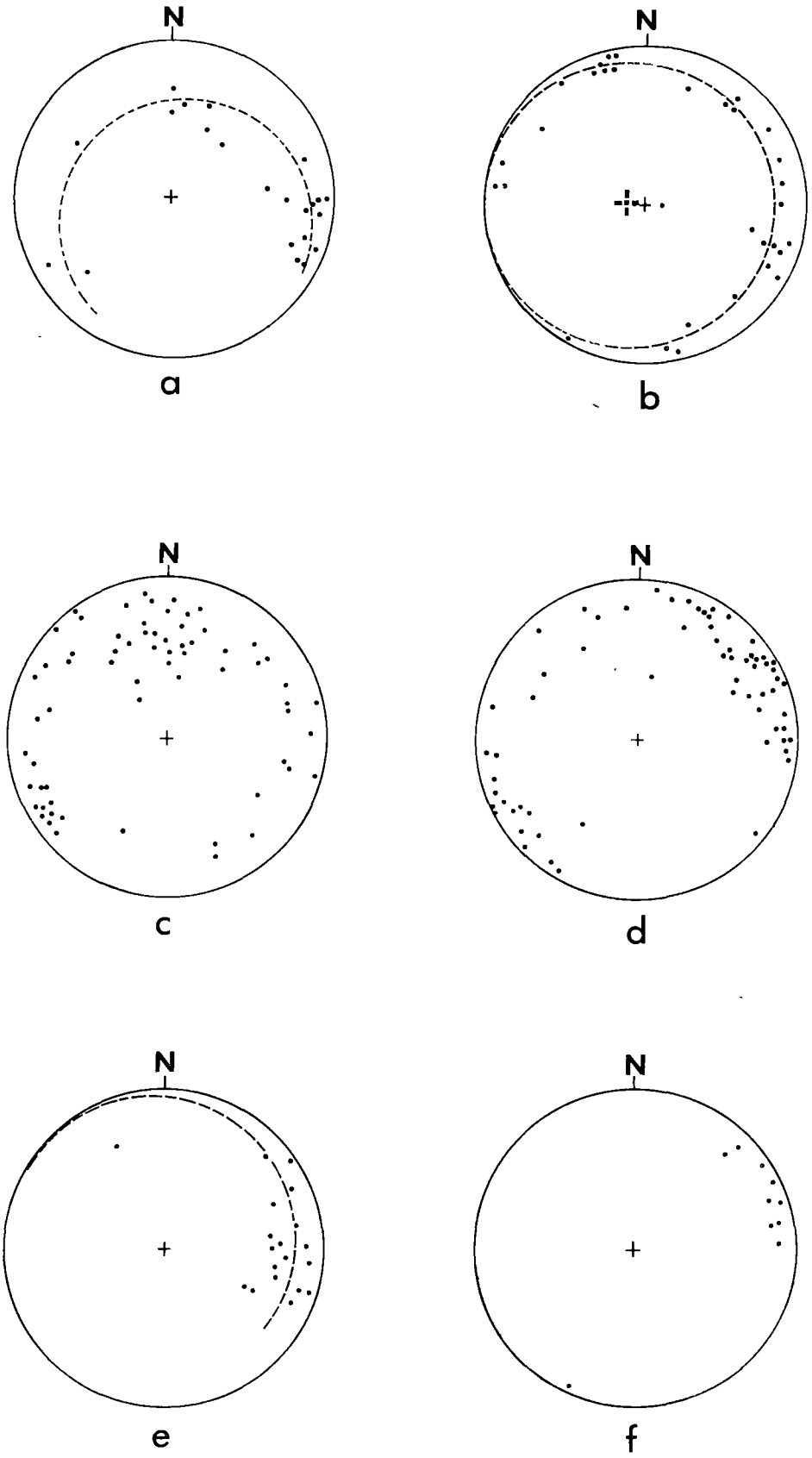

Figure 2:6

FIGURE 2:7

Equal area projections of orientation data from Mt. Rugby.

a. 23 poles to layering from north of the Mt. Rugby Conglomerate boundary. Great circle of best fit plunges 47° to 265°.

b. 12 poles to S_3 cleavage from quartzite units. x indicates the direction of pseudo-ripples, approximately parallel to the fold hinge spreading both S_2 and S_3.

c. Fold hinge directions from the quartzite units.

d. Poles to layering in the phyllite east of Mt. Rugby. 53 values.

e. Orientation of kink-bands in phyllite east of Mt. Rugby
(.) clockwise rotation looking vertically downwards.
(+) anticlockwise rotation looking vertically downwards.

f. 28 poles to layering from units adjacent to the Clytie Cove Group contact. -¦- marks the poles of the great circles of best fit.

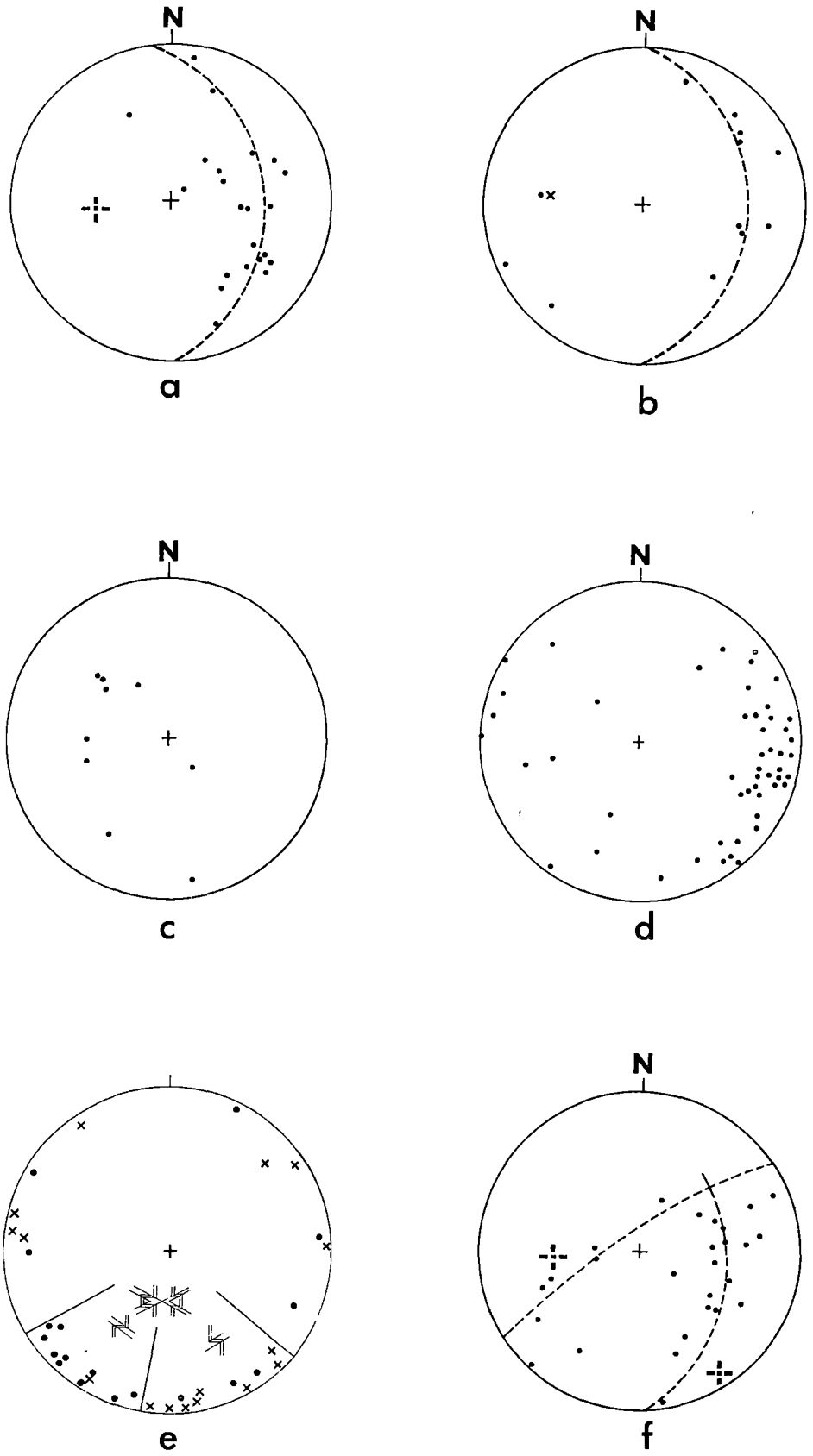

Figure 2:7

FIGURE 2:8

Equal area projections of orientation data from Horseshoe Inlet, Mt. Parry and Bathurst Channel.

a. Poles to layering ($=S_2$) from around Horseshoe Inlet, 38 values.

b. Poles to S_3 cleavage from around Horseshoe Inlet, 39 values.

c. Poles to layering ($=S_2$) from Mt. Parry, 76 values.

d. Poles to S_3 cleavage from Mt. Parry, 28 values.

e. Poles to S_2 cleavage from east of Bramble Cove, 81 values.

f. Poles to S_3 cleavage from east of Bramble Cove, 55 values.

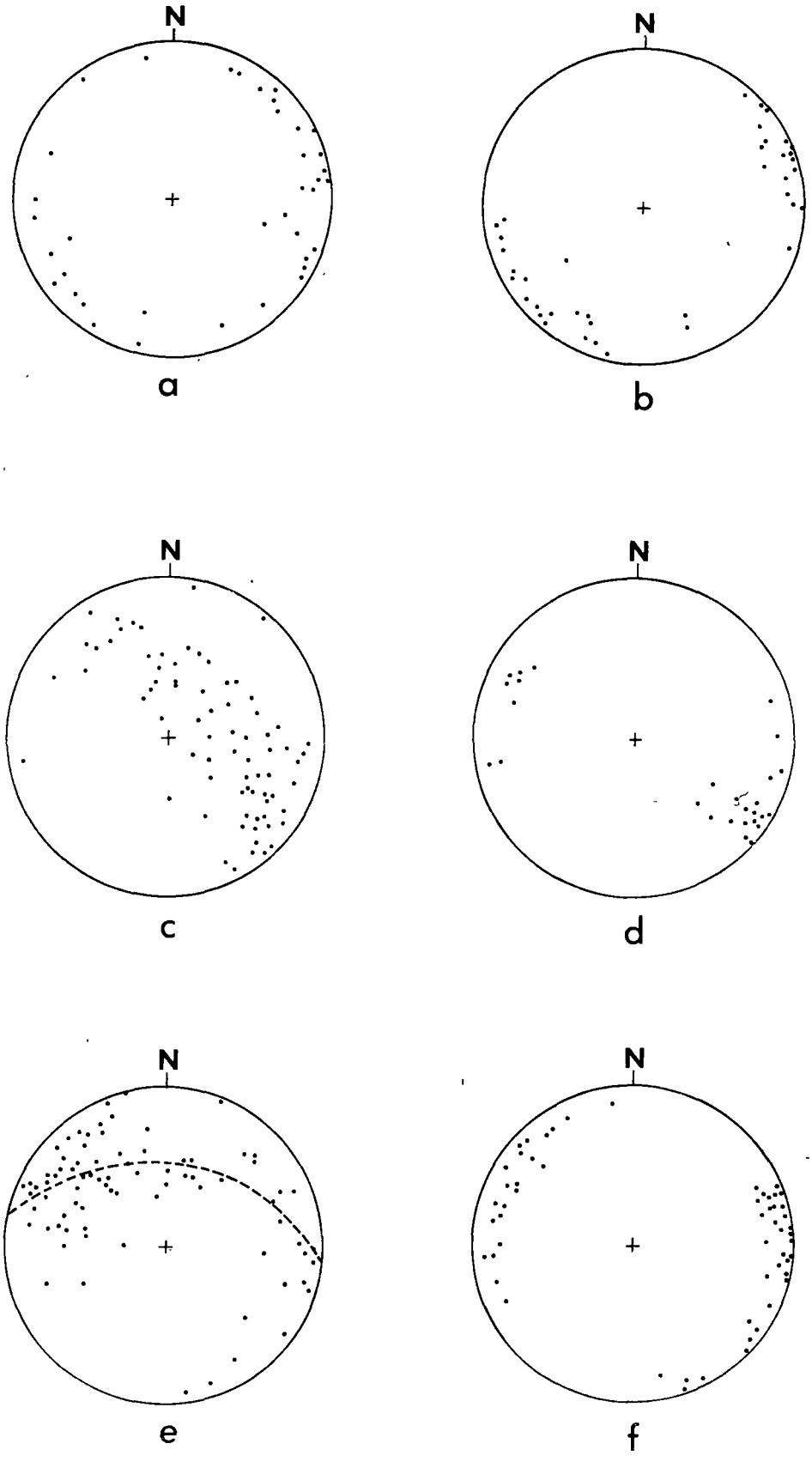

Figure 2:8

PLATE 2:3

a. Clastic, dykes, orientated parallel to the S_3 cleavage, intruding downwards from thin siltstone layers. Bramble Cove. Scale in centimetres.

b. Sedimentary brecciation of siliceous mudstone beds, overlain by graded sandstone bed. Bramble Cove. Scale in centimetres.

c. Load casts of sandstone into siliceous mudstone beds. A truncation of the deformed laminae by overlying beds shows the sedimentary origin of the structure. Clastic dykes are present in the underlying siltstone - mudstone succession. Scale in centimetres. Bramble Cove.

a

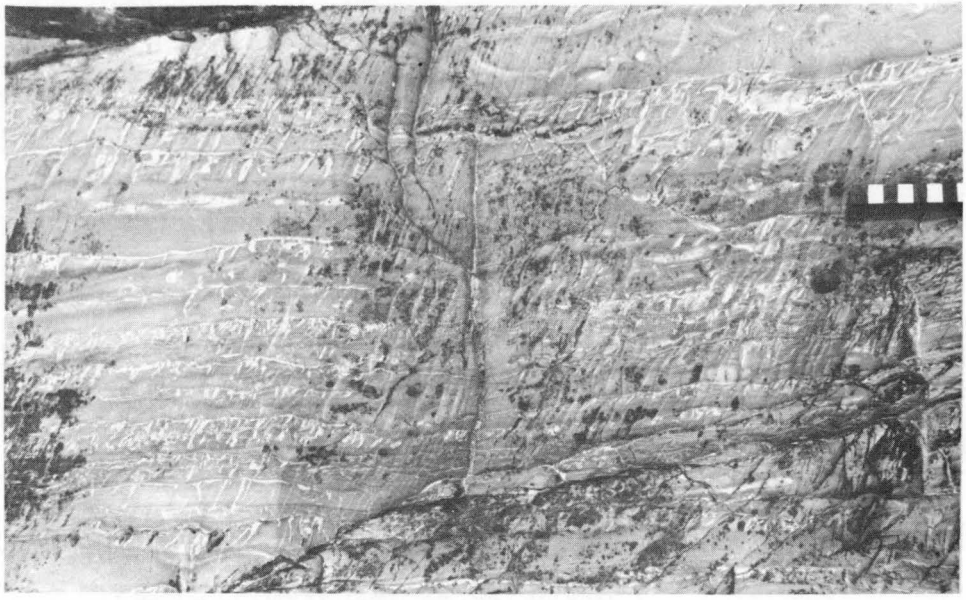

b

c

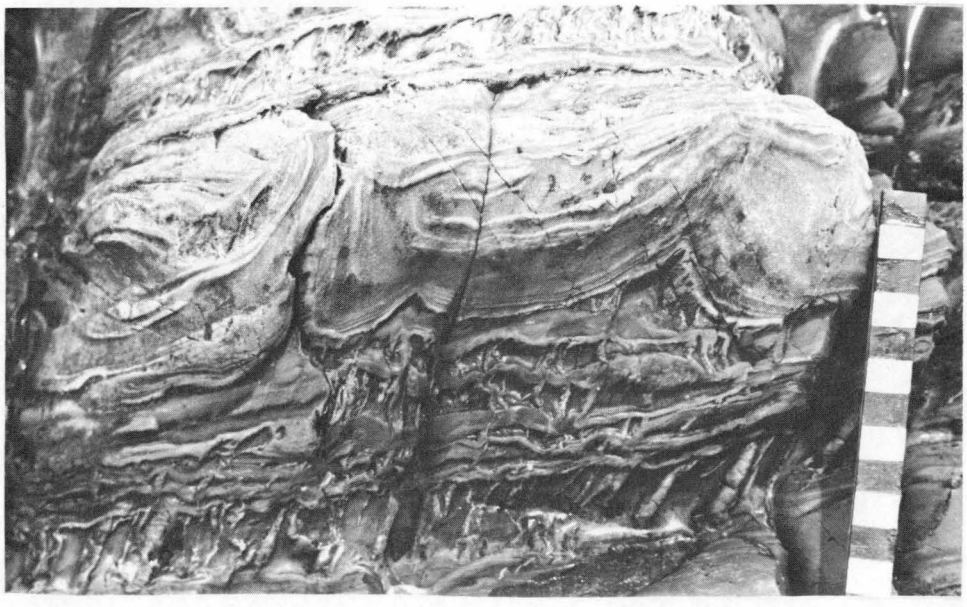

PLATE 2:3

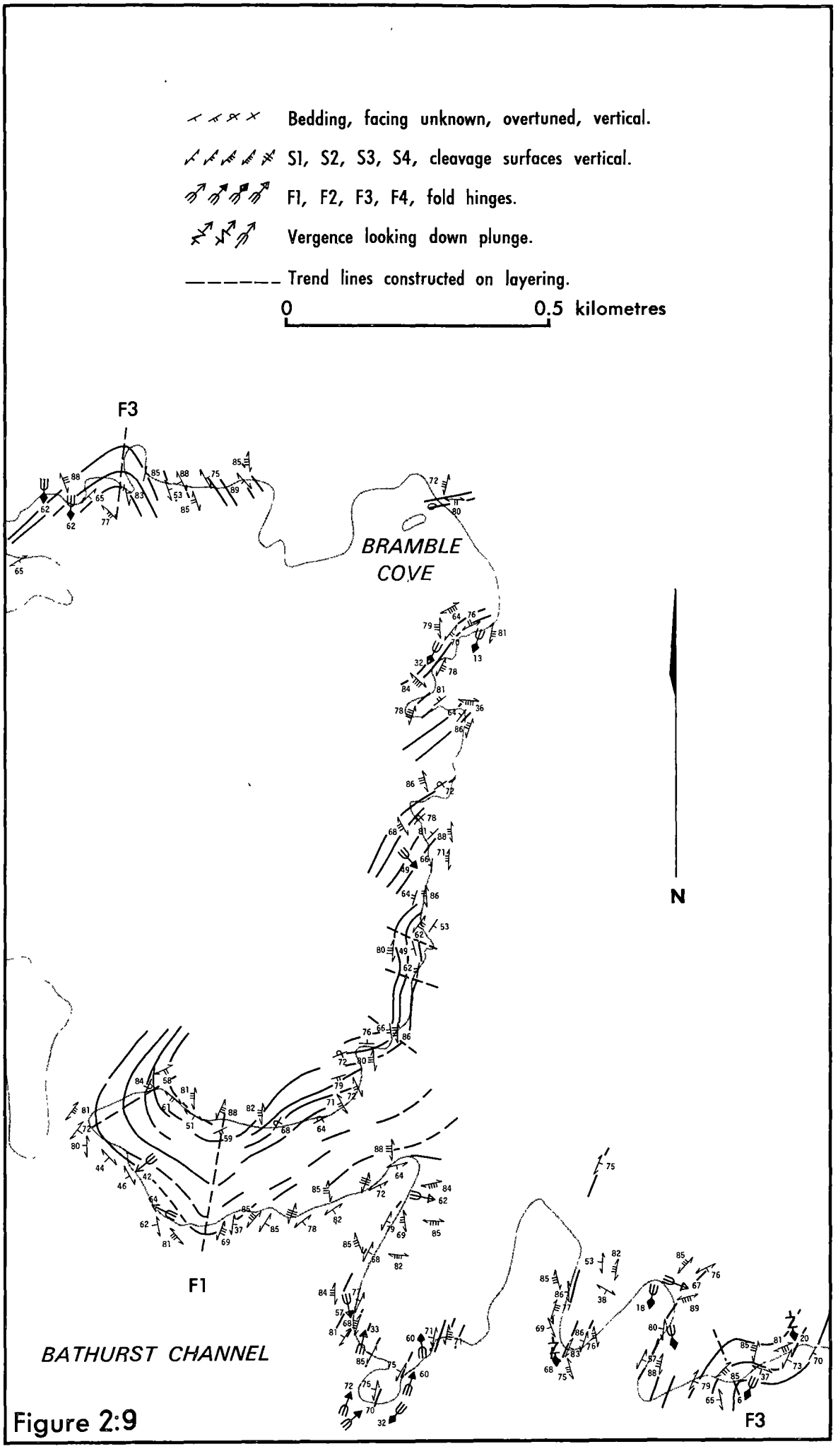
Bedding, facing unknown, overtuned, vertical.
S1, S2, S3, S4, cleavage surfaces vertical.
F1, F2, F3, F4, fold hinges.
Vergence looking down plunge.
Trend lines constructed on layering.
0
0.5 kilometres
F3
BRAMBLE COVE
N
F1
BATHURST CHANNEL
F3

Figure 2:9

FIGURE 2:10

Equal area projections of orientation data from Bramble Cove.

a. Poles to bedding, showing the geometry of F_1 folding.
x indicates overturned beds.
-¦- shows the fold hinge directions.
37 values.

b. Poles to elements altered during post-F_1 deformation.
(.) bedding, 21 values.
(x) overturned bedding, 5 values.
(o) S_3 cleavage, 20 values.
-¦- pole to great circle of best fit.

c. Geometry of F_3 folding west of Bramble Cove.
(.) bedding poles, 20 values.
(o) S_3 cleavage poles, 10 values.

d. Poles to S_2 cleavage east of Bramble Cove, 36 values.

e. Poles to S_2 cleavage at Mt. Parry, east of Bramble Cove, 81 values.

f. Poles to S_3 cleavage at Mt. Parry, east of Bramble Cove, 84 values.

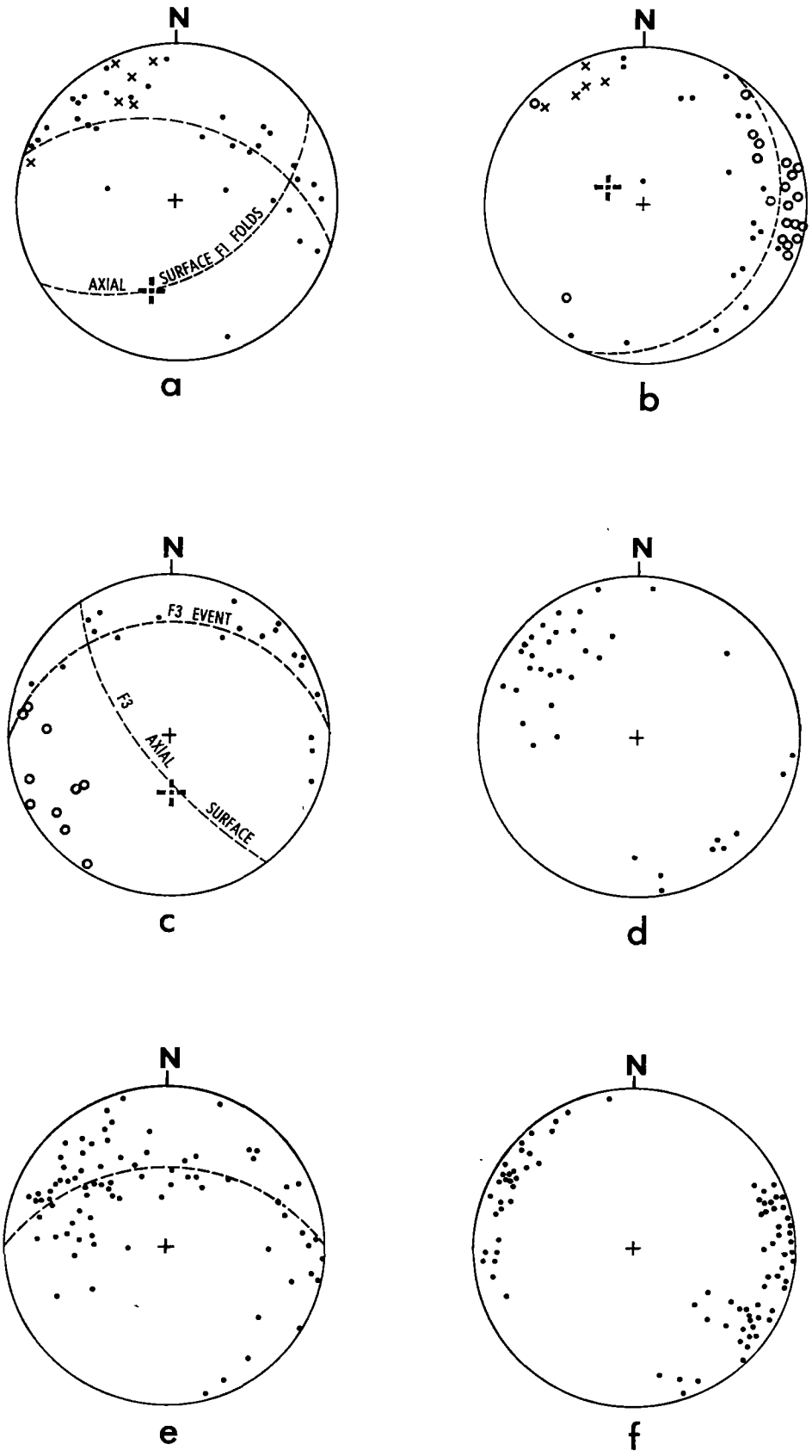
N
AXIAL
SURFACE F1 FOLDS
a
N
b
N
F3 EVENT
F3
AXIAL
SURFACE
c
N
d
N
e
N
f

Figure 2:10

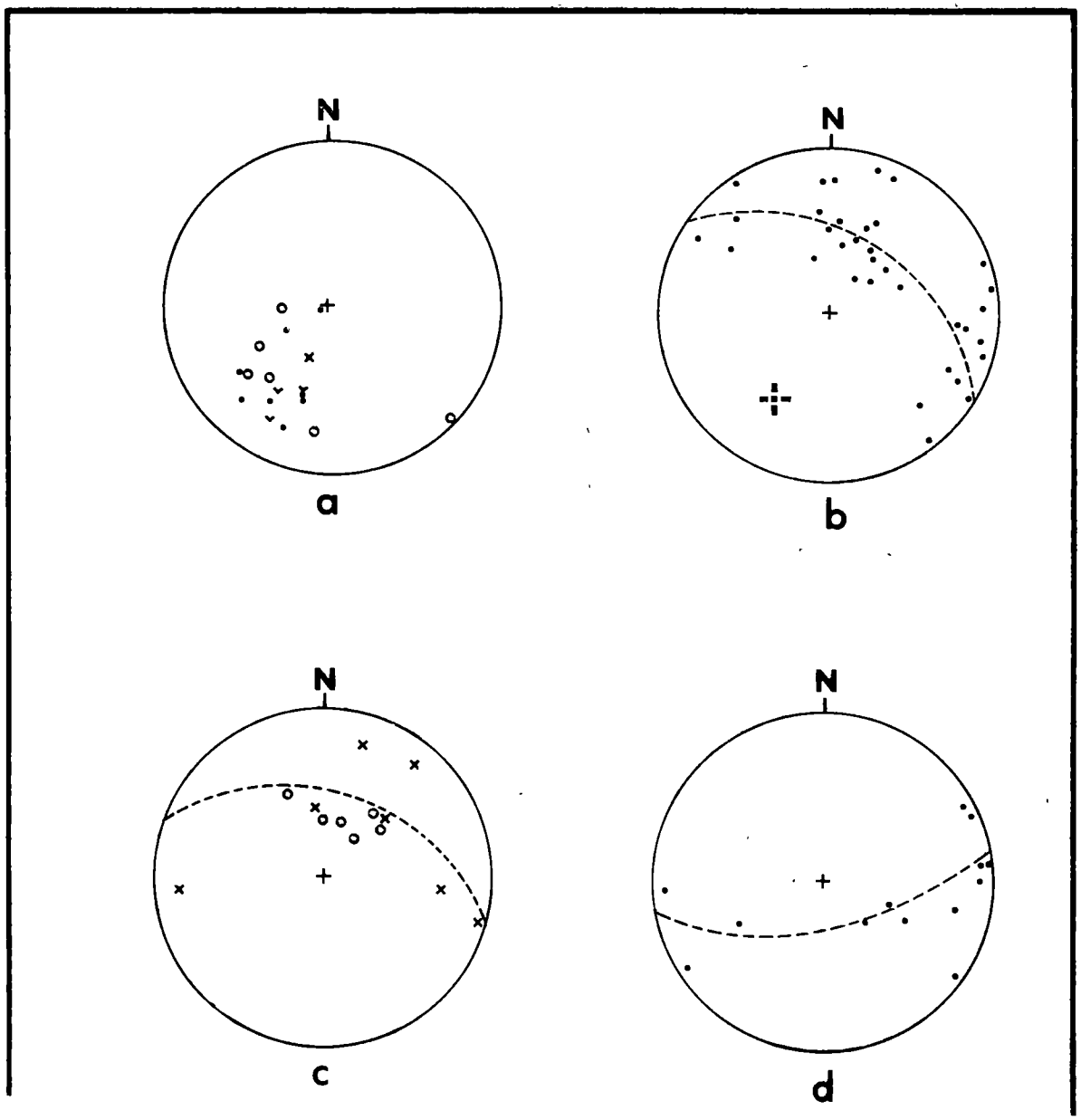

Equal area projections of orientation data from the Mt. Lindsay region.

a) (o) F_1 hinge lines
   (x) F_2 hinge lines
   (·) F_3 hinge lines
   (v) F_4 hinge lines

b) Poles to the S_2 cleavage from Mt. Lindsay, 35 values. Pole to the great circle of best fit (⊹) plunges 40° to 214°.

c) Poles to the S_4 cleavage (o) and F_3 axial surfaces (x) from Mt. Lindsay.

d) Poles to the S_2 cleavage from north of Mt. Lindsay. Pole to the great circle plunges 20° to 355°.

FIGURE 2:11

PLATE 2:4

a. Intensely flattened isoclinal F_1 folds from South-East Bight (GR068050). Note the contrast in thick and thin layers, and the apparent "cross-bedding" in the thicker layer.

b. Large scale mechanical layering in the quartzite sequence at Woody Point (GR1507). Oblique layering is S_1.

c. "Mushroom" interference effects of F_1 and F_2 structures at South-East Bight. Scale in centimetres.

a

b

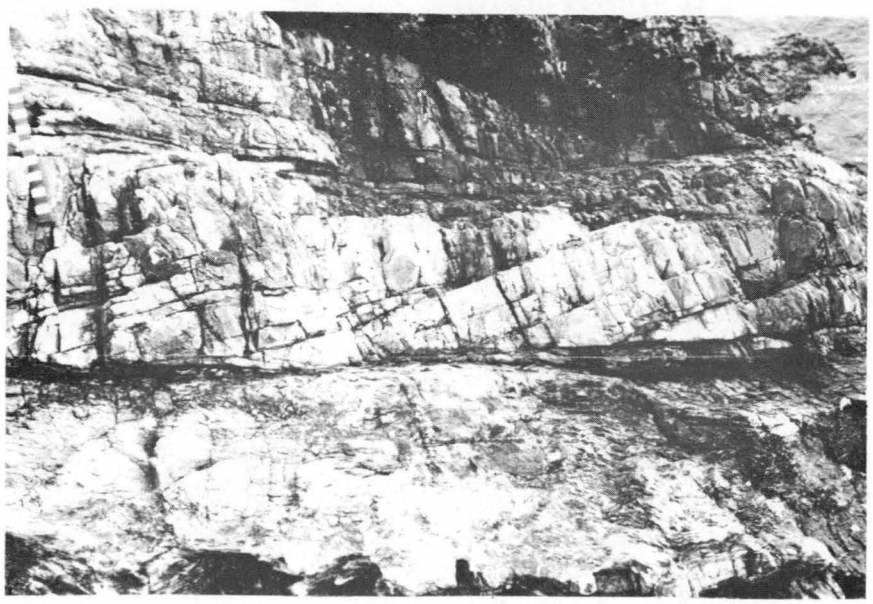

c

PLATE 2:4

FIGURE 2:12

Orientation data for the Spain Bay, Davey Head and Coffin Creek areas.

a. 48 poles to layering (.) and 47 fold hinge directions (⊙) from the Coffin Creek area. Average fold hine plunges 45° to 195°.

b. Poles to layering from the Davey Head (.) and South-East Bight (GR068050) (o). Average fold hine plunges 50° to 186°.

c. 40 poles to layering from the Spain Bay area. Average fold hine plunges 50° to 183°.

d. 122 S_3 cleavage readings from Spain Bay area, contoured 0.4, 2, 4.5, 8.5 and 12% per 1% area.

e. Poles to late cleavages in the Davey Head area, (.) = S_4, (o) = S_5.
These may represent conjugate cleavages.

f. F_3 and F_4 fold hinges in the Spain Bay area.
46 values.

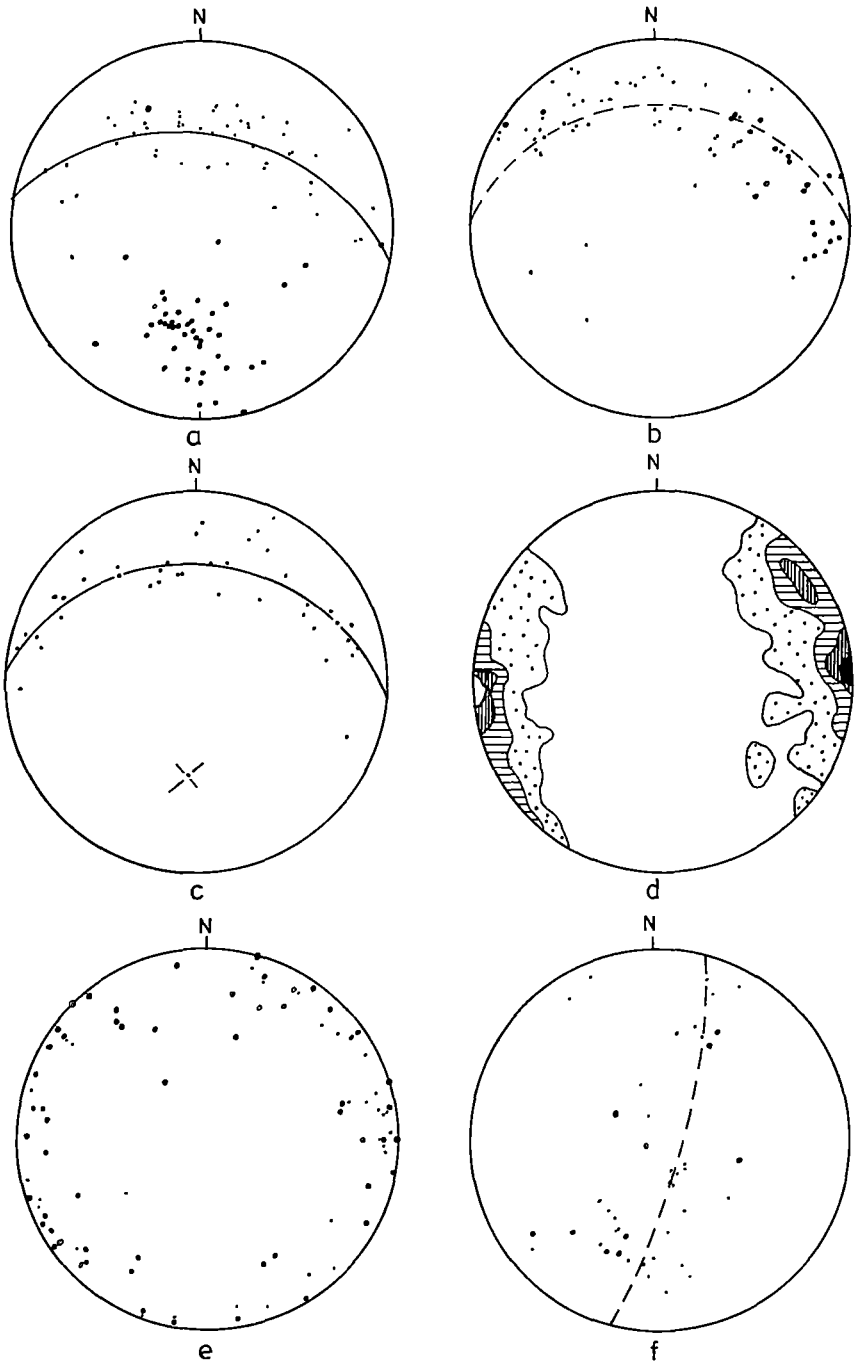

FIG 2:12

PLATE 2:5

TEXTURES IN METAMORPHOSED QUARTZITE

a. Weakly recrystallised fabric in quartzite from Mt. Parry. Large detrital grains show undulose extinction and quartz grains in the matrix are aligned and neocrystalline.
Detrital grain boundaries are sutured.
(Specimen 48153, NX, magnification x 10).

b. A slightly elongate mortar texture, with quartz triple junction self boundaries dominating the texture.
Quartzite from Mt. Rugby.
(Specimen 48154, NX, magnification x 10).

c. A lepidoplastic texture in quartzite from Mt. Rugby. The textural development is controlled by the percentage of mica flakes.
(Specimen 48155, NX, magnification x 10).

d. Ribbon texture in quartzite from Mt. Rugby. This is an inherited texture from an earlier deformation event, forming a vein within a lepidoblastic texture. It possesses the same quartz optic axis fabric as the surrounding rock.
(Specimen 48156, NX, magnification x 10).

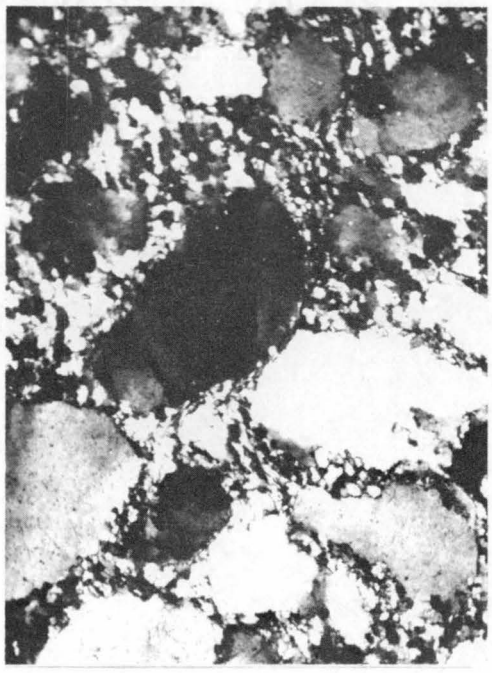

a

b

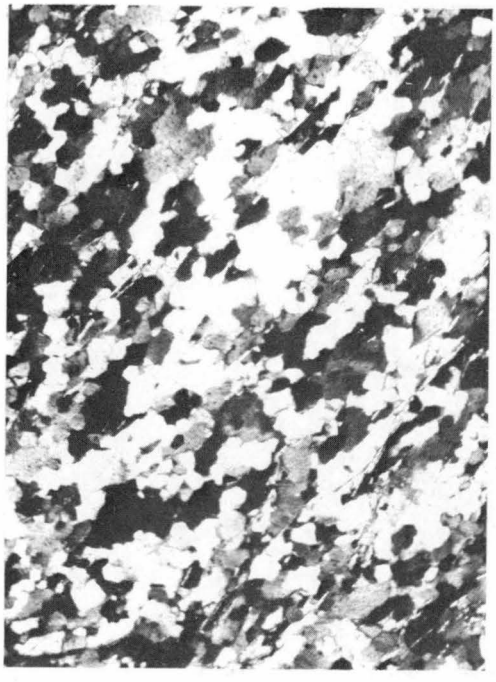

c

d

PLATE 2:5

PLATE 2:6

TEXTURES IN RELATIVELY UNMETAMORPHOSED SANDSTONE AND FINE-GRAINED ROCKS

a. Open framework sandstone with detrital quartz grains in a recrystallised siliceous matrix. Note lack of quartz grain alignment in the matrix, and the solution effects (sculpturing) of grain boundaries.
(Specimen 48157, NX, x 10)

b. In micaceous quartz wacke, grain boundary alteration is less, and micaceous seams have formed parallel to cleavage. These anastomose around detrital grains.
(Specimen 48158, PPL, x 10)

c. Metamorphic phyllite with albite porphyroblasts (note discordant inclusion trails). The mica grains are metamorphic.
(Specimen 48159, PPL, x 20)

d. Deformed mudstone of the Clytie Cove Group. Abundant silica grains, opaque minerals and mica is detrital. No major recrystallisation.
(Specimen 48160, PPL, x 20)

a

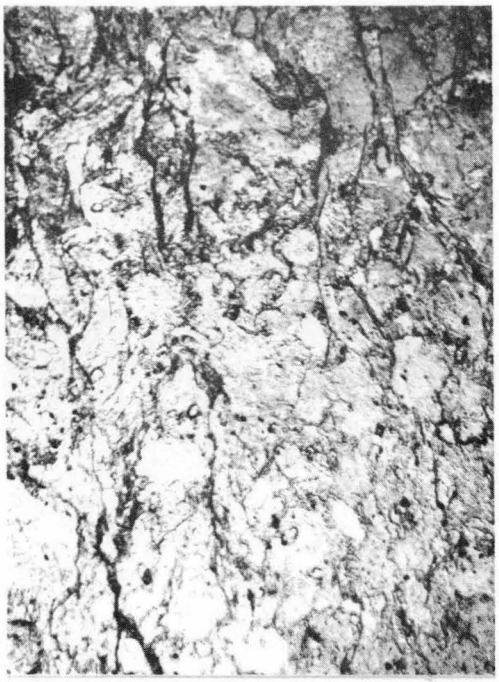

b

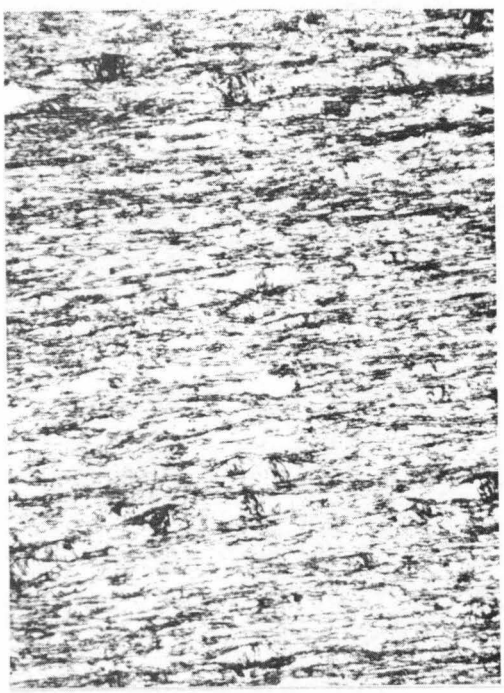

c

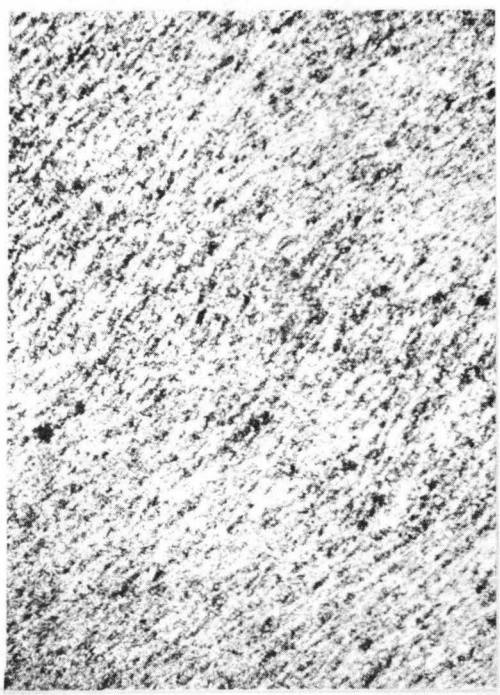

d

PLATE 2:6

PLATE 2:7

CLEAVAGE DIFFERENTIATION, AND BOUNDARY CONGLOMERATES AT ANTIMONY POINT

a. Strongly differentiated cleavage with major grain boundary changes and recrystallisation, S_2 of the metamorphic sequence.
(Specimen 48161, PPL, x 20)

b. Differentiated crenulation cleavage (S_{3c}) of the Clytie Cove Group. Recrystallisation restricted to the limbs of microfolds. (Specimen 48162, PPL, x 10)

c. Tectonic conglomerate adjacent to the boundary of the metamorphic sequences and the Clytie Cove Group. Inferred tectonic transport direction to the right (geographically upwards). Photograph is 0.2 m across.

d. Slightly brecciated conglomerate belonging to the Clytie Cove Group, adjacent to the metamorphic sequences at Antimony Point. The good cleavage visible is parallel to the boundary. Scale is in centimetres.

a

b

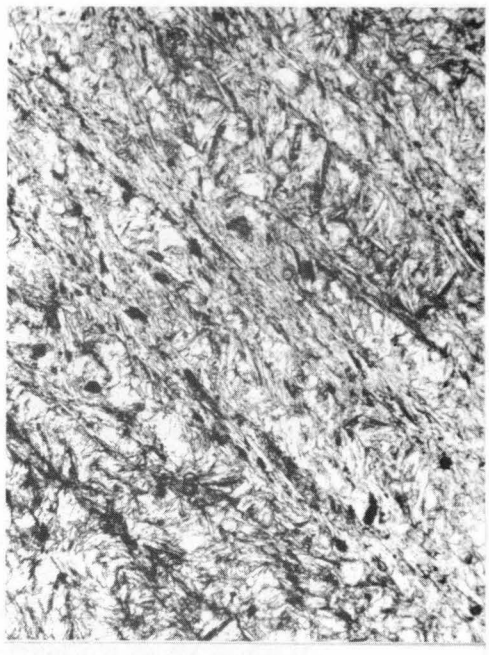

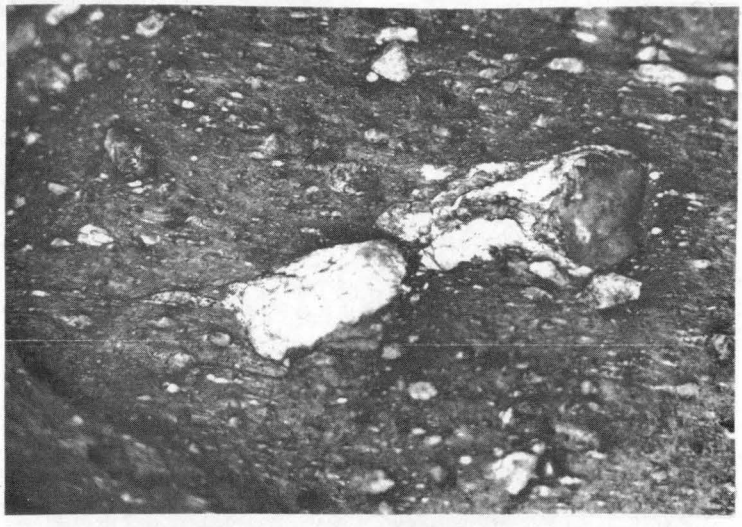

c

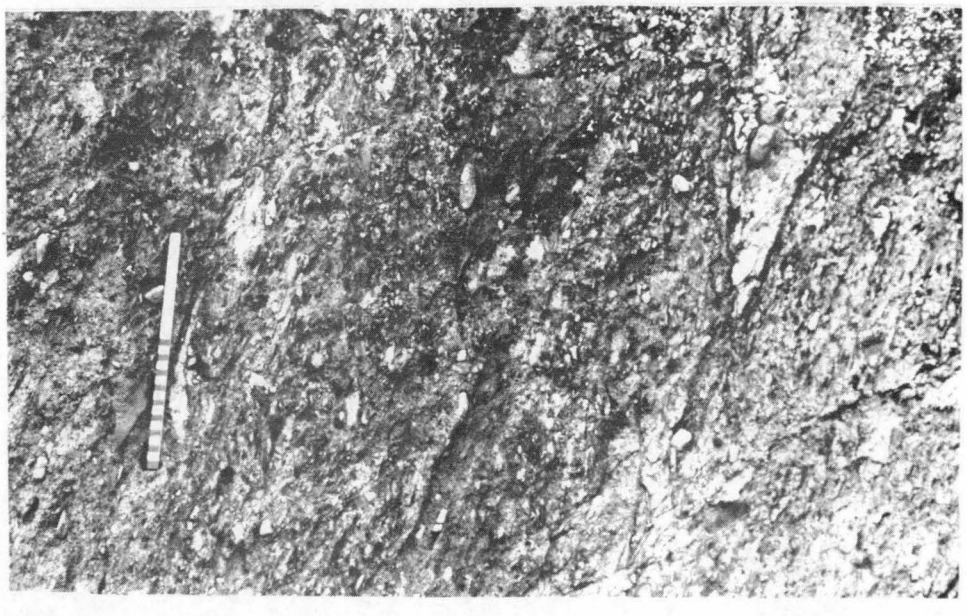

d

PLATE 2:7

FIGURE 2:13

QUARTZ OPTIC AXIS FABRIC DIAGRAMS

a. Bimodal poorly sorted sandstone of the Clytie Cove Group Specimen 48157. 200 quartz optic axes from the matrix contoured at 0.25, 1.25, 2.25, 3.25% per 1% area. Cleavage is indicated by the great circle.

b. 200 quartz optic axes from clasts from the same specimen, contoured at 0.25, 1.7, 2.7, 3.2% per 1% area. Cleavage is indicated by the great circle.

c. Bimodal quartzite from metamorphosed Precambrian breccia west of the Parker Bay Fault. Specimen 48163. 200 matrix grains contoured at 0.25, 1.25, 1.75, 2.75% per 1% area. Great circles indicate fabric symmetry.

d. 140 quartz clast optic axes from specimen 48163 contoured at 0.35, 2.5, 3.2, 4.0% per 1% area.

e. 157 quartz clast optic axes from specimen 48153 from Mt Parry, contoured at 0.3, 1.6, 2.9, 3.5% per 1% area.

f. 204 quartz matrix optic axes from specimen 48153, contoured at 0.25, 1.25, 2.25, 3.75% per 1% area.

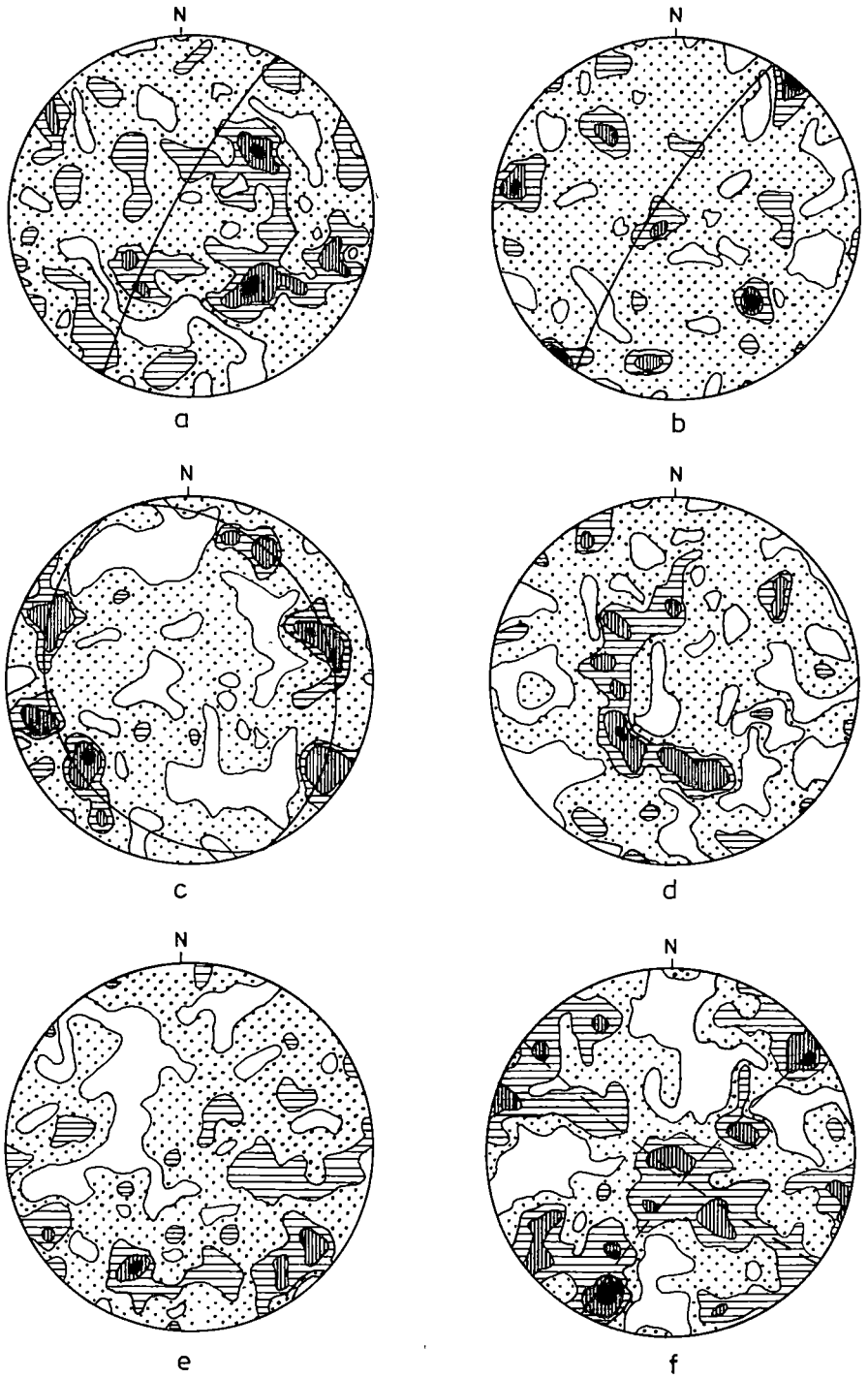

FIG. 2:13

FIGURE 2:14

QUARTZ OPTIC AXIS DIAGRAMS FROM ROCKS PREVIOUSLY ASSIGNED TO THE CLYTIE COVE GROUP

a. 154 quartz grains from metasiltstone at Bramble Cove, contoured at 0.3, 1.6, 3, 4% per 1% area. Shows a well-defined fabric. Specimen 48164.

b. 111 quartz optic axes from quartzite at Mt Rugby. Great circle represents cleavage defined by the alignment of muscovite. Specimen 48154. Contoured at 0.5, 2, 4, 7, 9% per 1% area.

c. 150 quartz optic axes from quartzite at Mt Rugby, contoured at 0.75, 1.7, 2.3, 4.3, 5.7% per 1% area. Great circle represents cleavage. Specimen 48155.

d. 150 quartz optic axes from quartzite at Mt Rugby, contoured at 0.33, 1.67, 3, 5% per 1% area. Great circle represents cleavage. Specimen 48156.

e. 60 poles to mica flakes contoured at 1, 20, 30, 40% per 1% area. Specimen 48154.

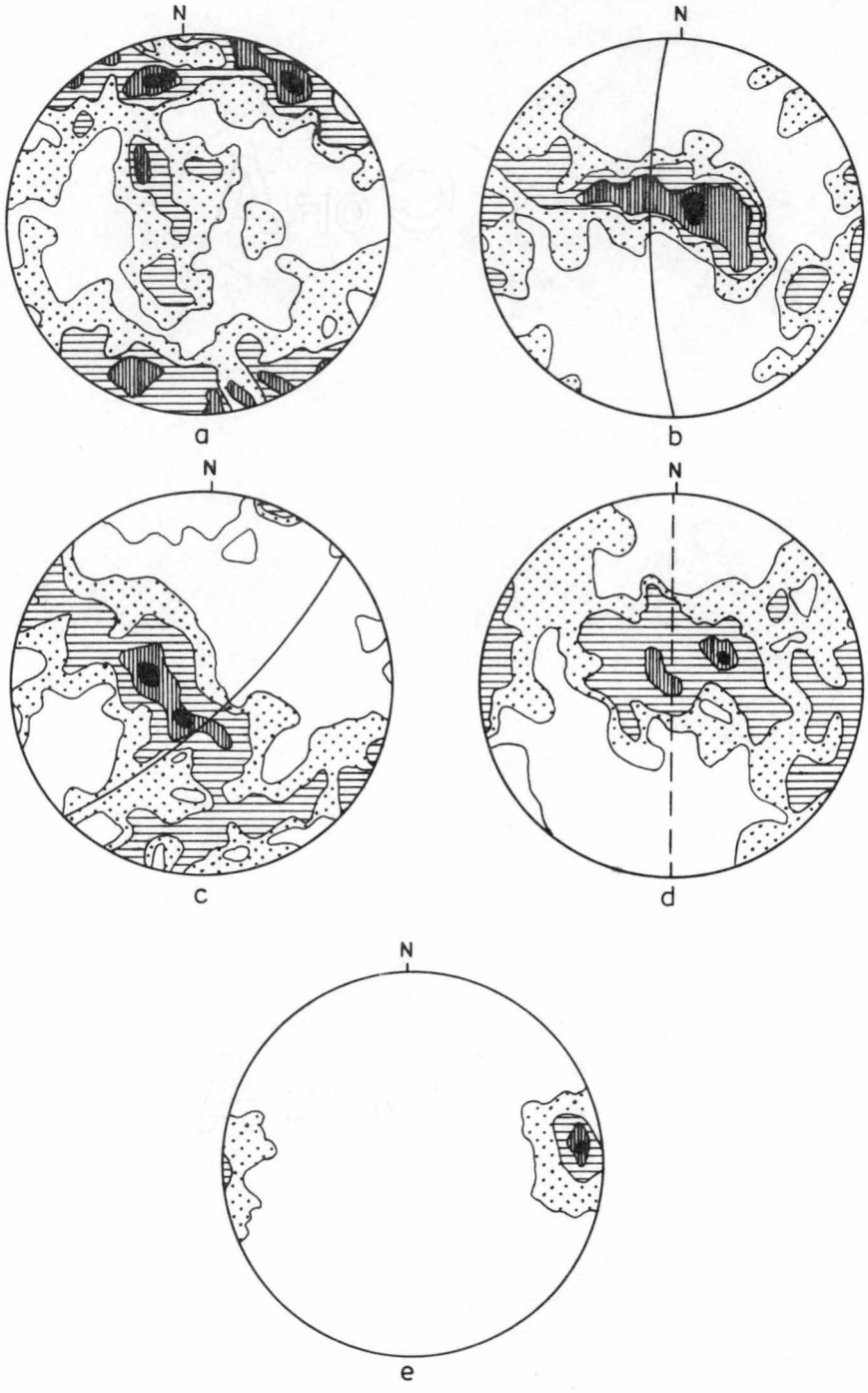

FIG 2:14

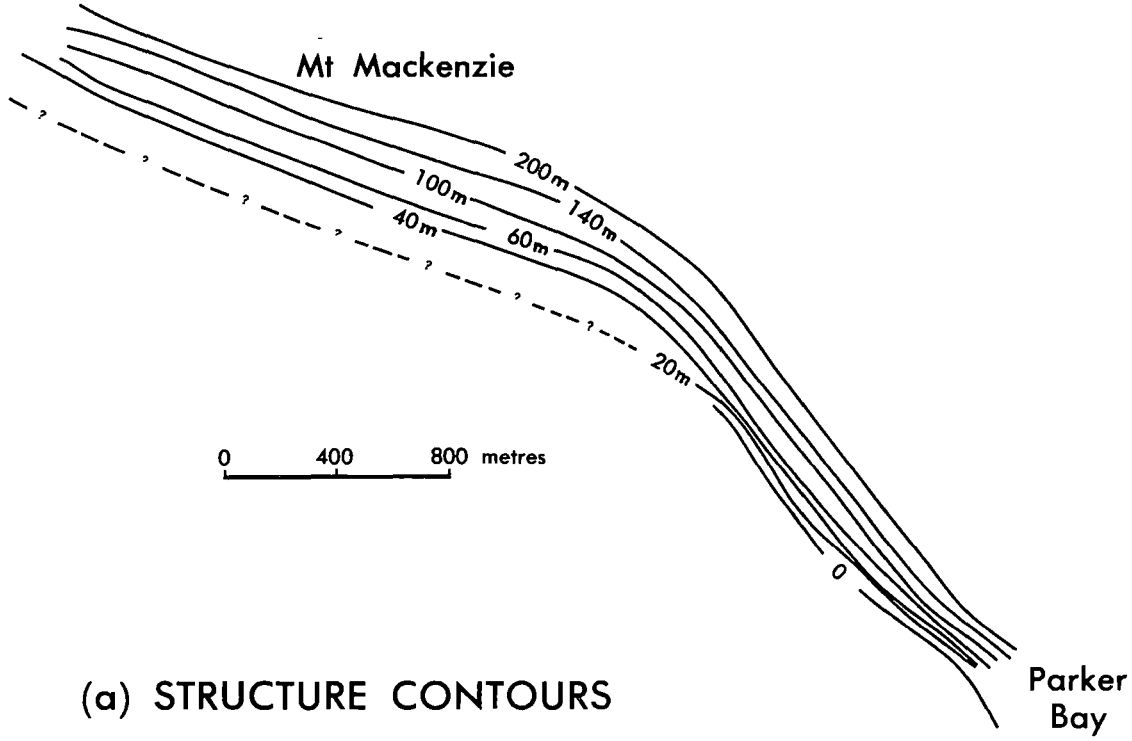

(a) STRUCTURE CONTOURS

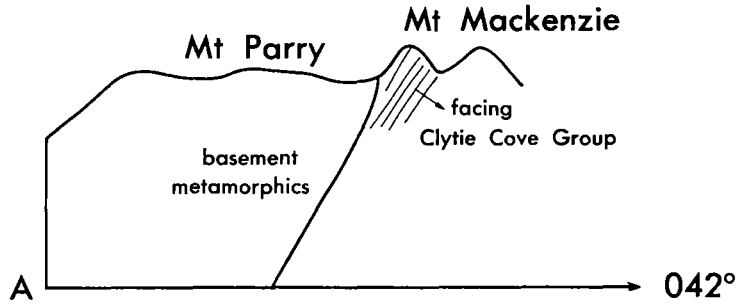

A : 41206728

0 400 800 metres

(b) CROSS SECTION

PARKER BAY FAULT

Figure 2:15

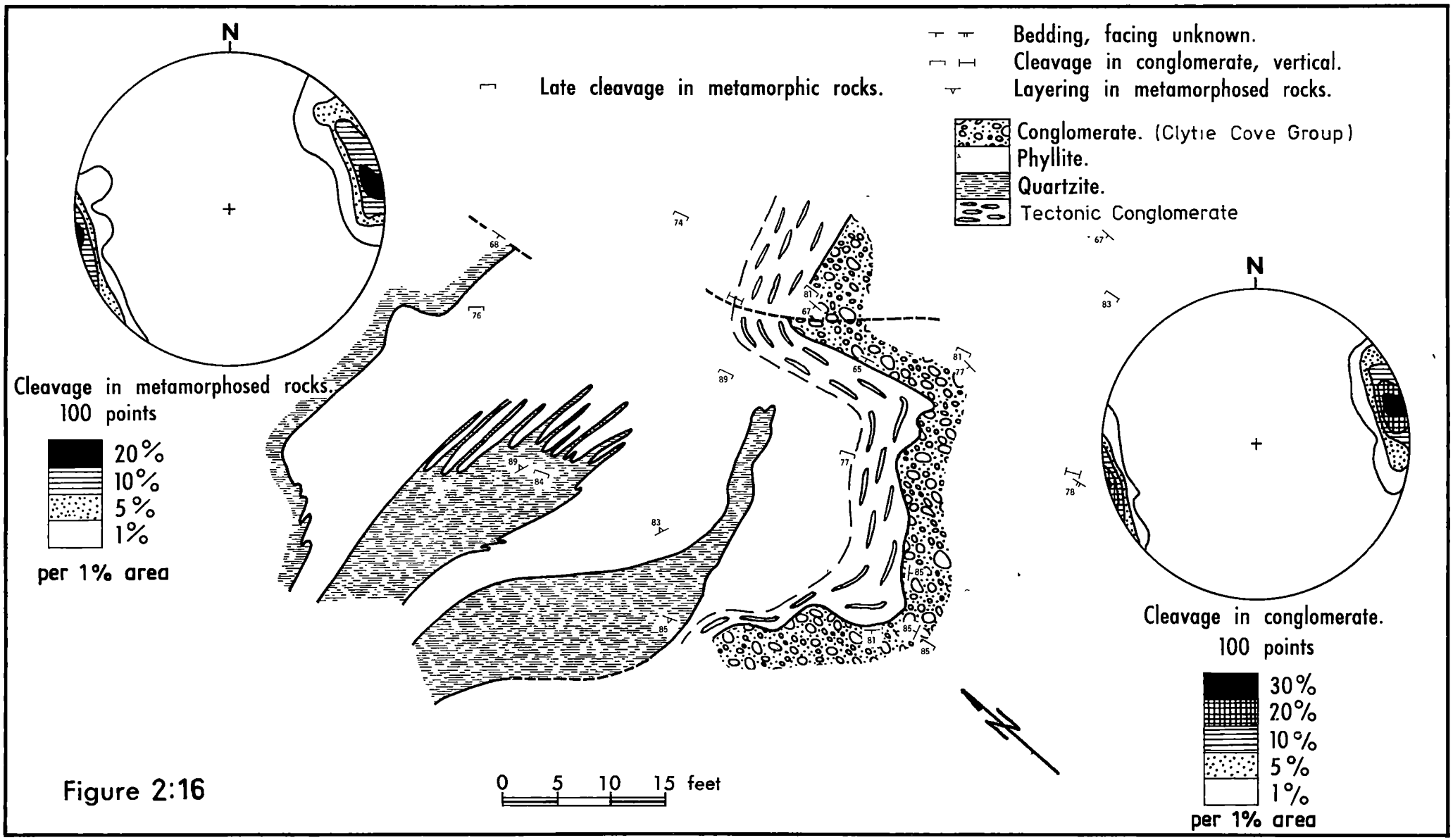
N
Cleavage in metamorphosed rocks.
100 points
20%
10%
5%
1%
per 1% area
Late cleavage in metamorphic rocks.
Bedding, facing unknown.
Cleavage in conglomerate, vertical.
Layering in metamorphosed rocks.
Conglomerate. (Clytie Cove Group)
Phyllite.
Quartzite.
Tectonic Conglomerate
N
Cleavage in conglomerate.
100 points
30%
20%
10%
5%
1%
per 1% area
0 5 10 15 feet

Figure 2:16

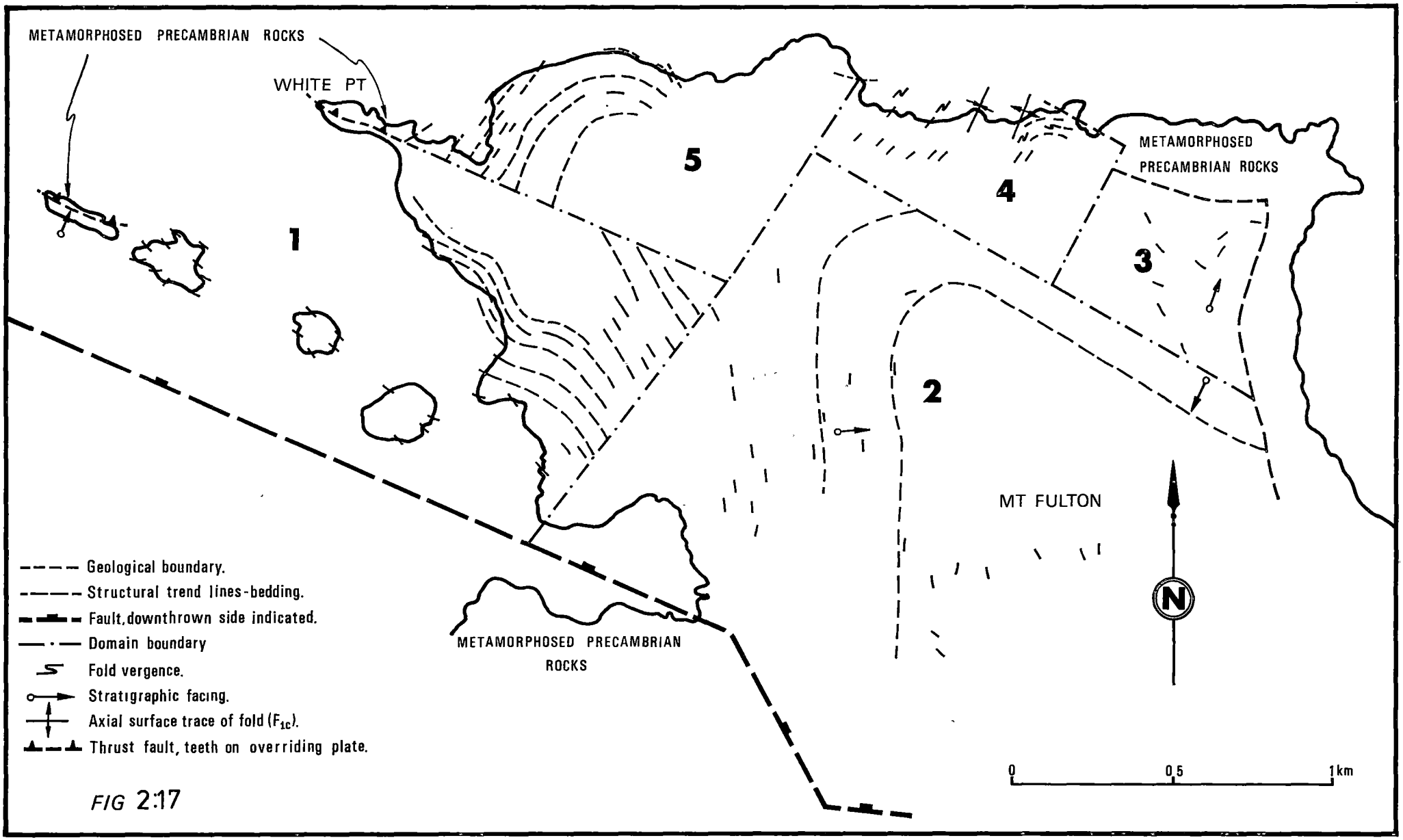
METAMORPHOSED PRECAMBRIAN ROCKS
WHITE PT
1
2
3
4
5
METAMORPHOSED PRECAMBRIAN ROCKS
MT FULTON
METAMORPHOSED PRECAMBRIAN ROCKS
N
0
0.5
1km
Geological boundary.
Structural trend lines-bedding.
Fault, downthrown side indicated.
Domain boundary
Fold vergence.
Stratigraphic facing.
Axial surface trace of fold (F_{1c}).
Thrust fault, teeth on overriding plate.

FIG 2:17

FIGURE 2:18

EQUAL AREA PROJECTIONS OF ORIENTATION DATA FROM THE MT FULTON AREA

a. Poles of bedding from domain, 1, 87 values. Contour intervals 0.5, 3, 6, 11% per 1% area. Pole of great circle fit, 70° to 335°.

b. Pole of bedding from domain 2, 84 values. Contour intervals 1, 3, 5, 10% per 1% area. Pole of best great circle fit 70° to 168°, best conical fit plunges 70° to 150° with semi-angle 80°.

c. Poles of cleavage from domain 1, 83 values. Contour intervals 0.5, 2, 12, 30% per 1% area.

d. Poles of cleavage from domain 2, 59 values. Contour intervals 0,7, 2.5, 13, 27% per 1% area.

e. Bedding-cleavage intersection lineations from domain 1, 79 values. Contour intervals 0.6, 3, 11, 22% per 1% area.

f. Bedding-cleavage intersection lineations from domain 2, 71 values. Contours at 0.7, 2, 5, 9% per 1% area.

g. Poles to bedding from domain 5, 49 values. Contours at 1, 3, 7, 11% per 1% area.

h. Poles to cleavage from domain 5, 26 values. Contours at 2, 10, 13, 17% per 1% area.

i. Poles to bedding from domain 4, 74 values. Contours at 1, 2, 4, 6, 9% per 1% area. Pole to the best great circle 70° to 005°.

j. Cleavage poles from domain 4.

k. Bedding-cleavage intersection lineations and fold hinges from domain 4, 37 values. Contours at 2, 4, 10, 15% per 1% area.

l. Bedding and cleavage poles from domain 3.

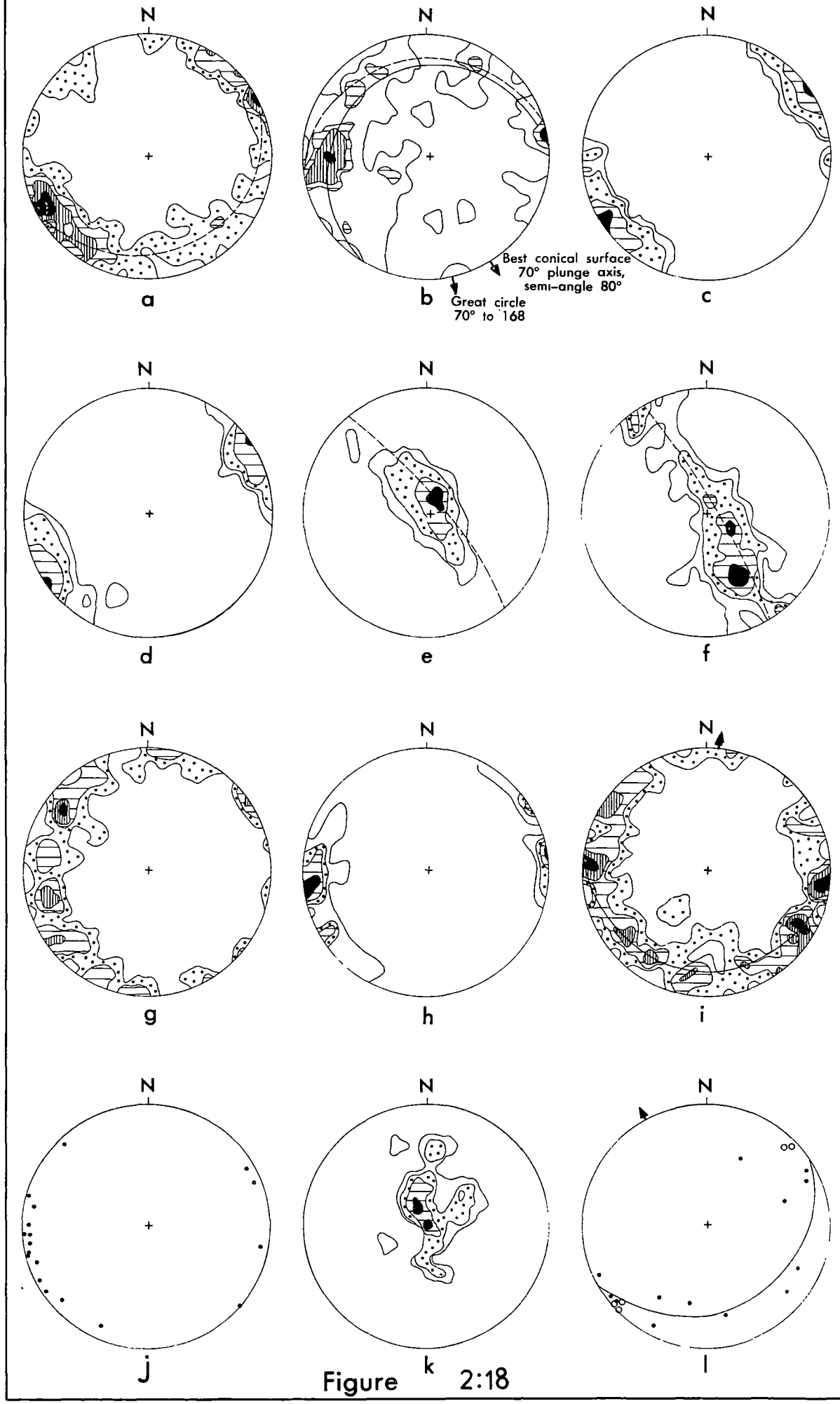
N
a
b
Best conical surface
70° plunge axis,
semi-angle 80°
Great circle
70° to 168
c
d
e
f
g
h
i
j
k
l

Figure 2:18

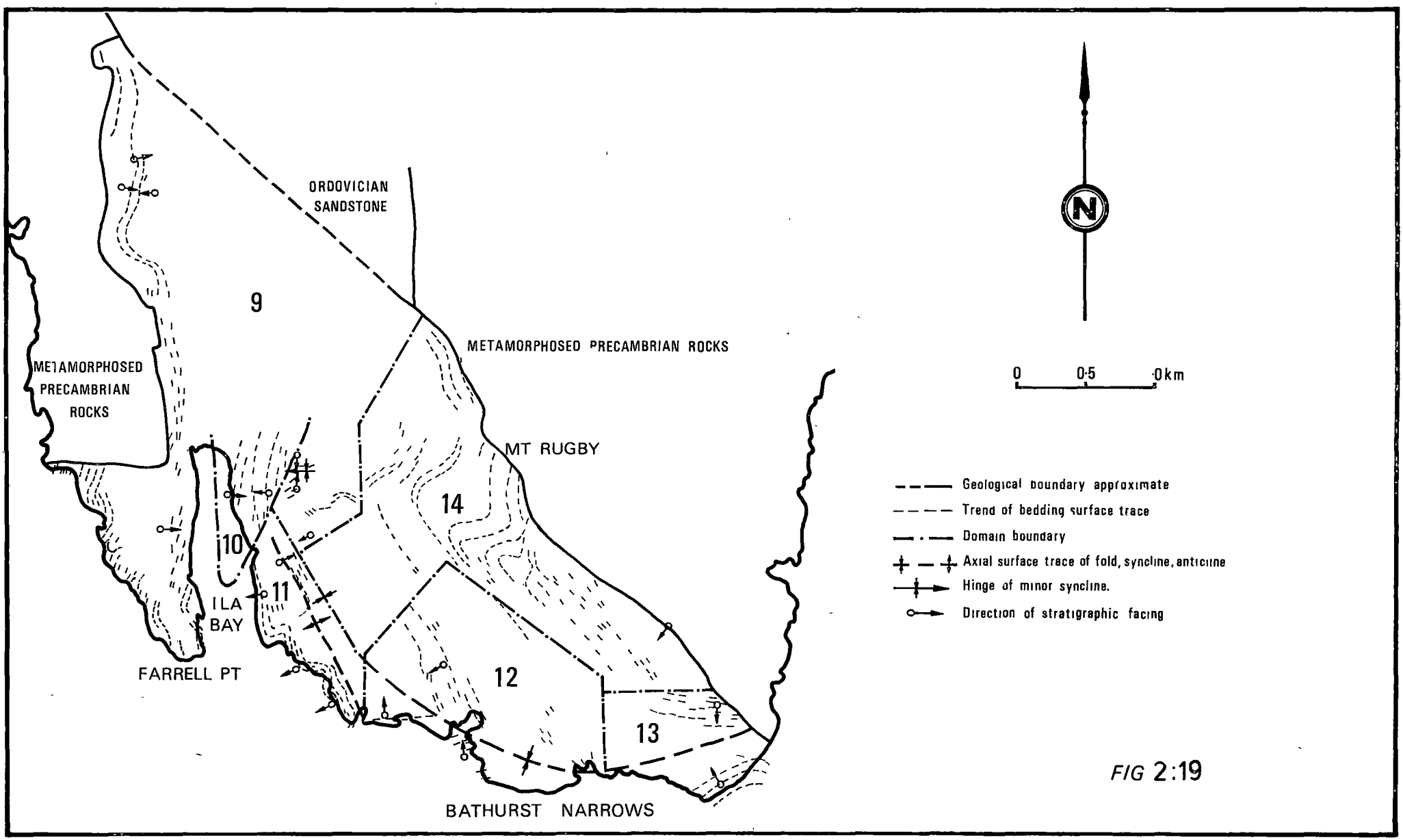
ORDOVICIAN SANDSTONE
METAMORPHOSED PRECAMBRIAN ROCKS
METAMORPHOSED PRECAMBRIAN ROCKS
MT RUGBY
9
10
11
12
13
14
ILA BAY
FARRELL PT
BATHURST NARROWS
N
0 0·5 0km
Geological boundary approximate
Trend of bedding surface trace
Domain boundary
Axial surface trace of fold, syncline, anticline
Hinge of minor syncline.
Direction of stratigraphic facing

FIG 2:19

FIGURE 2:20

All diagrams from Mt Rugby unless stated otherwise.

a. Poles to bedding from domain 9. Contours at 0.5, 2.7, 6, 11% per 1% area. 93 values.

b. Poles to bedding from domain 10, 42 values. ◑ represents overturned beds.

c. Poles to cleavage from domains 9 and 10, 69 values. Contours at 0.5, 3, 10, 20% per 1% area.

d. Poles to bedding from domain 11, 53 values. Contours at 1, 3, 5, 12% per 1% area. Pole to great circle of best fit plunges 60^{o} to 184^{o}.

e. Poles to bedding from domain 12, 60 values. Contours at 1, 2.5, 6, 13% per 1% area. Axis of conic surface of best fit plunges 70^{o} to 247^{o}. Semi-angle is 60^{o}.

f. Poles to bedding from domain 13, 34 values. Hinge 25^{o} to 236^{o} represents D_2 spread, and D_3 hinge plunges 60^{o} to 292^{o}.

g. Poles to cleavage from domains 11, 12 and 13, 64 values. Contours at 1, 4, 8, 16% per 1% area.

h. Poles to bedding (.) and cleavage (⊙) from domain 14. Pole to best great circle fit plunges 25^{o} to 311^{o}.

i. Poles to bedding (.) and cleavage (⊙) from domain 15.

j. Poles to bedding (.) and cleavage (⊙) from siliceous clastic sediments.

k. Poles to bedding from domain 1, Mt Berry-Mt MacKenzie. 23 values. Pole to great circle of best fit plunges 60^{o} to 266^{o}.

l. Poles to cleavage from domain 1. Mt Berry-Mt MacKenzie.

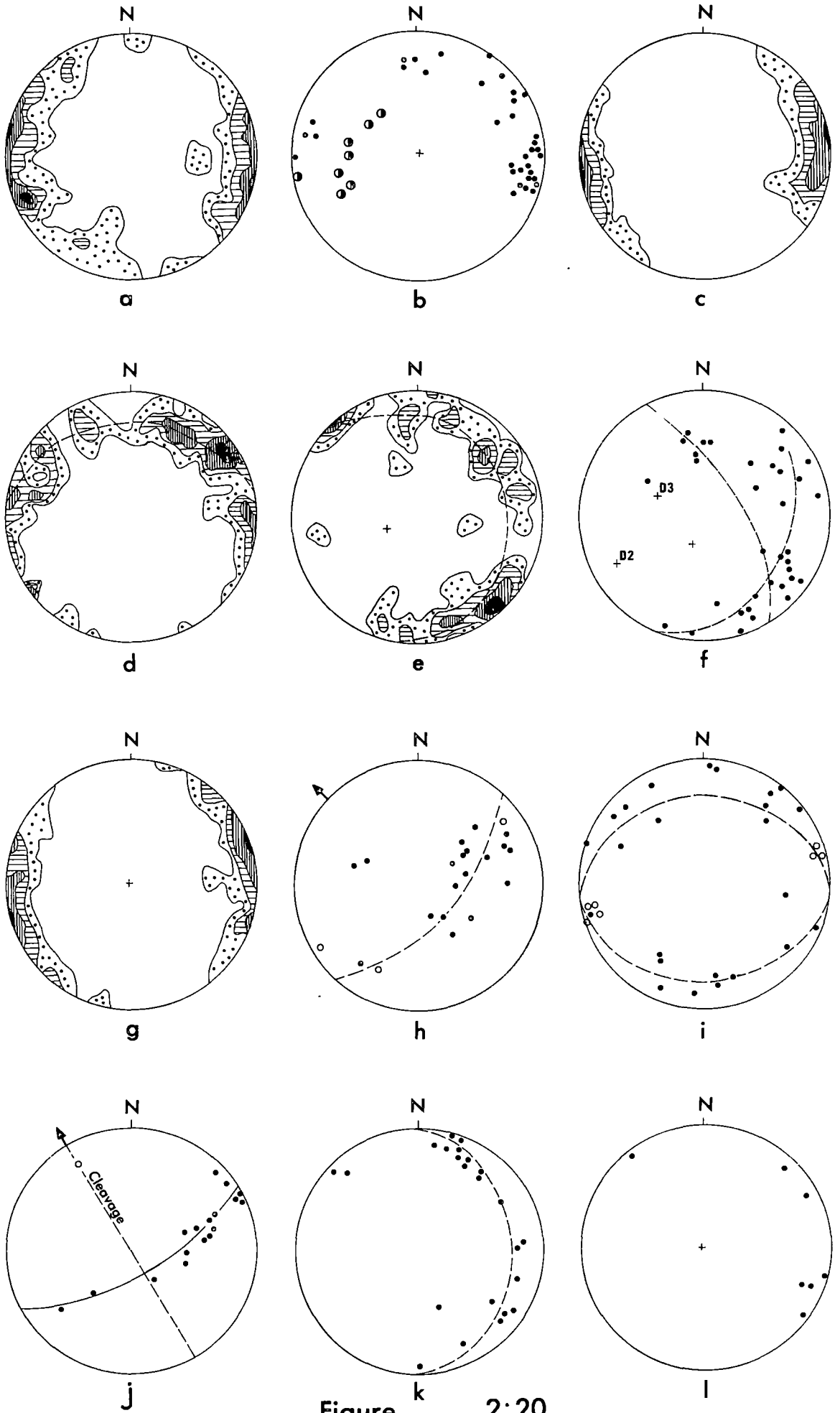

Figure 2:20

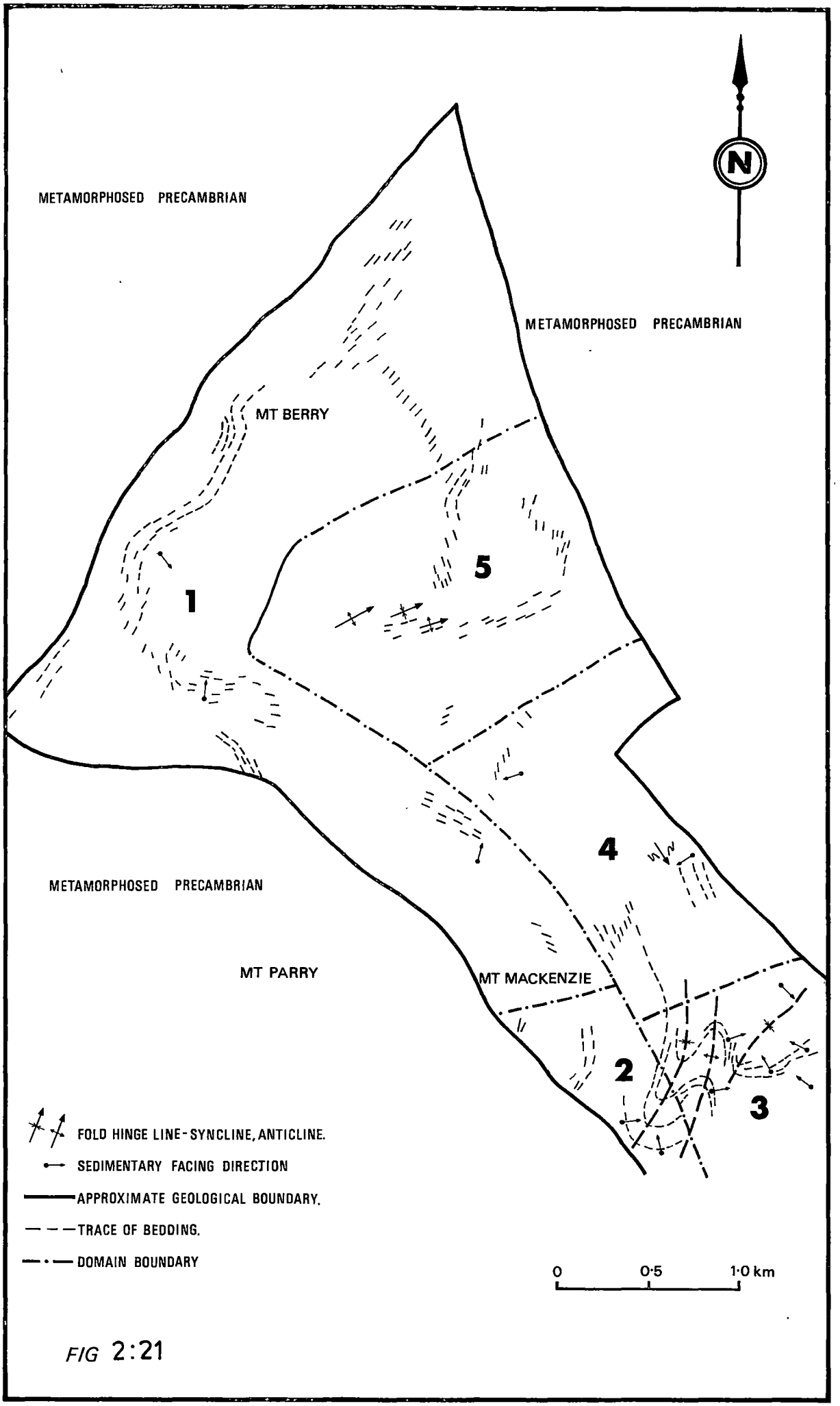
METAMORPHOSED PRECAMBRIAN
METAMORPHOSED PRECAMBRIAN
MT BERRY
1
5
4
METAMORPHOSED PRECAMBRIAN
MT PARRY
MT MACKENZIE
2
3
N
FOLD HINGE LINE - SYNCLINE, ANTICLINE.
SEDIMENTARY FACING DIRECTION
APPROXIMATE GEOLOGICAL BOUNDARY.
TRACE OF BEDDING.
DOMAIN BOUNDARY
0
0·5
1·0 km

FIG 2:21

FIGURE 2:22

EQUAL AREA PROJECTIONS OF ORIENTATION DATA FROM MT MACKENZIE, MT BERRY AND MT BEATTIE

a. Poles of bedding (.) and cleavage (⊙) from domain 2, Mt MacKenzie. Pole to the great circle plunges 10° to 326°.

b. Poles of bedding, domain 3, Mt MacKenzie. 42 values contoured at 1, 4, 8, 13% per 1% area.

c. Poles of cleavage, domain 3, Mt MacKenzie. 25 values contoured at 2, 6, 14, 22% per 1% area.

d. Poles of bedding, domain 4, Mt MacKenzie. 33 values showing two fold directions plunging 59° to 184° and 48° to 096°.

e. Poles of cleavage, domain 4, Mt MacKenzie.

f. Poles of bedding (.) and cleavage (⊙), domain 5, Mt Berry. Axis of conic surface of best fit plunges 70° to 075° and has a semi-angle of 80°.

g. 129 minor fold hinge lines from Mt Beattie to Balmoral Hill contoured at 0.5, 1, 2, 5, 10, 15, 23% per 1% area.

h. 247 poles of bedding from the Clytie Cove syncline contoured at 1, 2, 4, 6% per 1% area.

i. Poles to cleavage within the Clytie Cove syncline. 51 values contoured at 1, 5, 10, 15% per 1% area.

j. Poles to cleavage from the Mt Beattie anticline.

k. 113 poles of cleavage measured outside the major fold cores from Mt Beattie to Balmoral Hill, contoured at 1, 6, 11, 18% per 1% area.

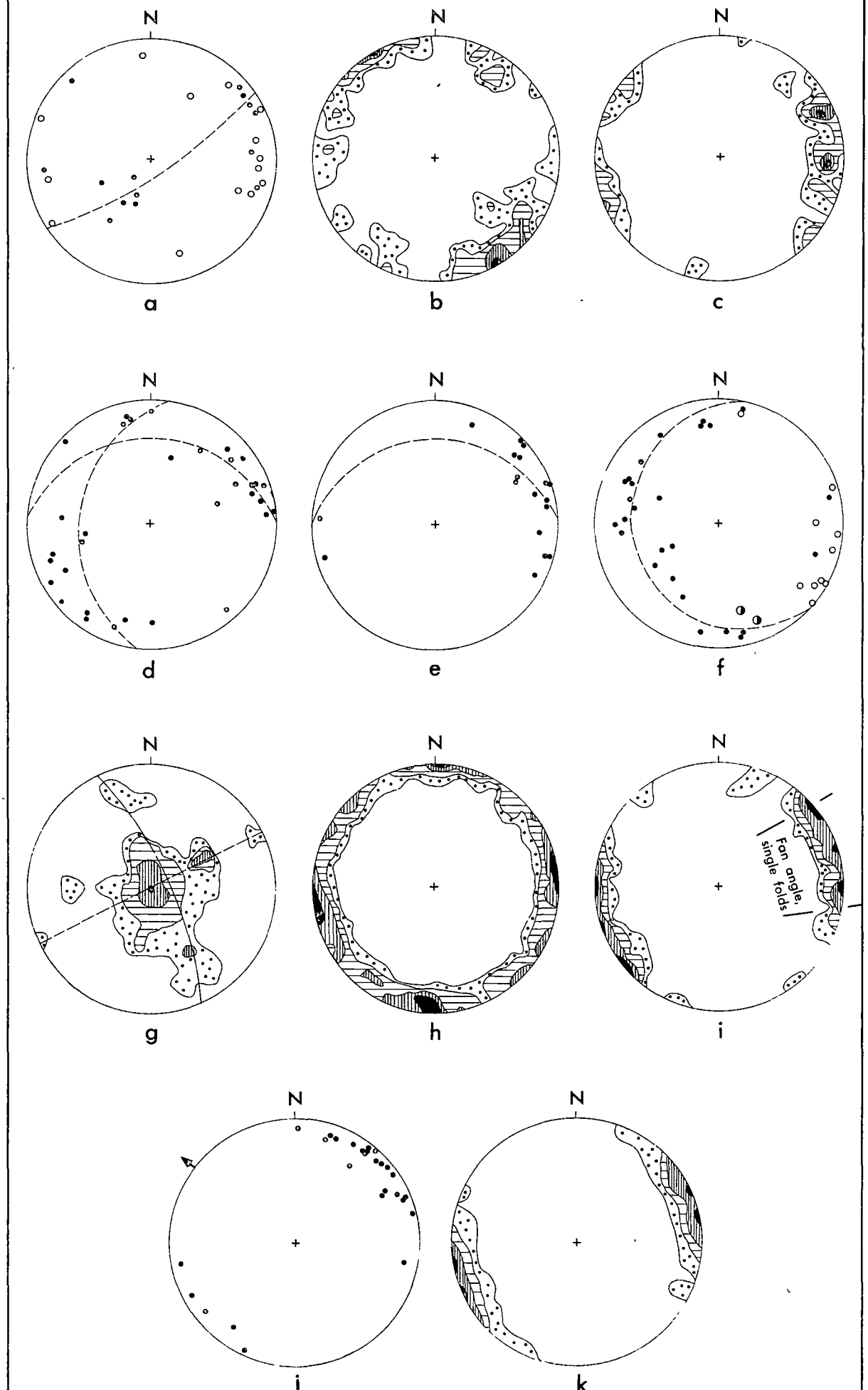

Figure 2:22

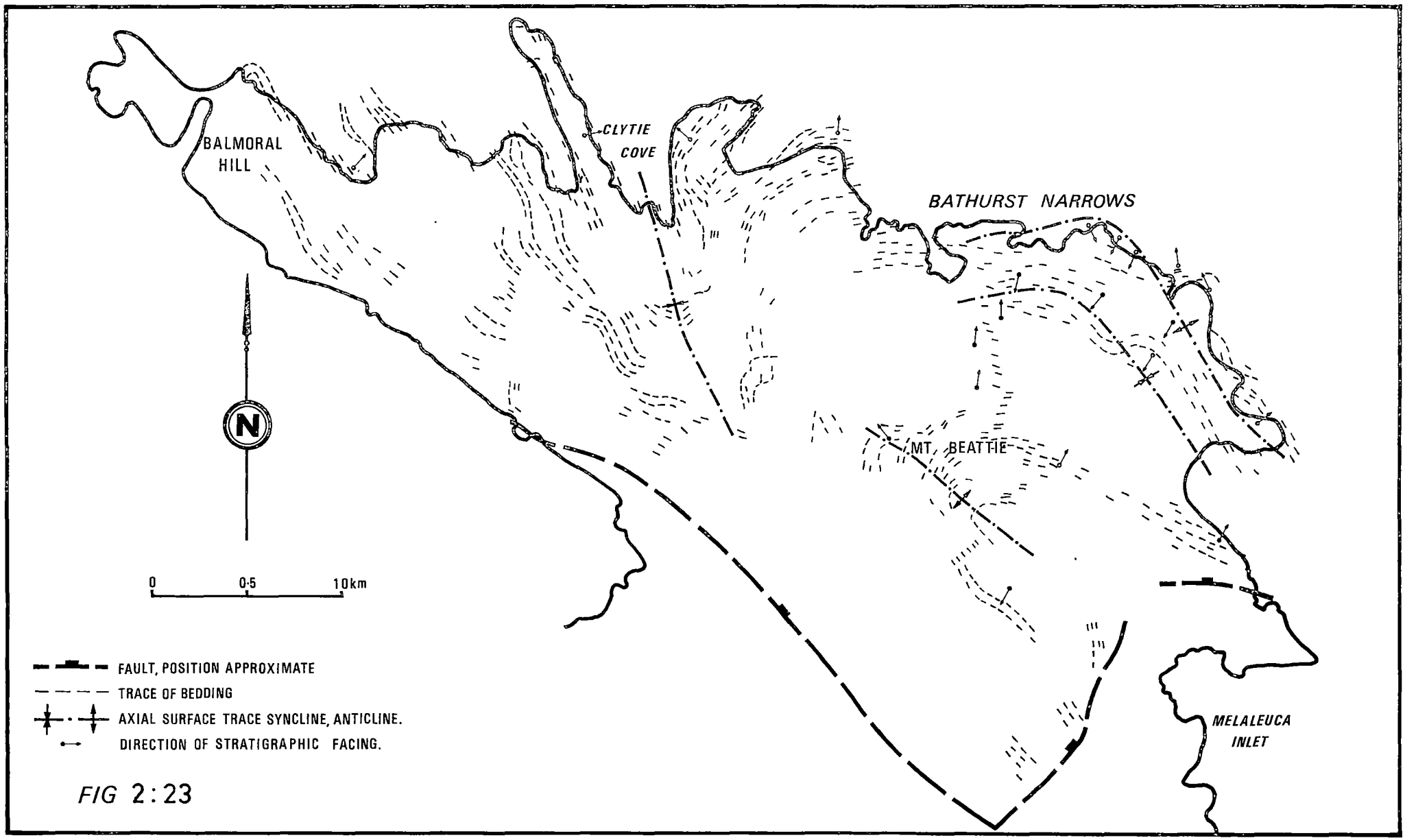
BALMORAL HILL
CLYTIE COVE
BATHURST NARROWS
MT. BEATTIE
MELALEUCA INLET
N
0
0·5
10km
FAULT, POSITION APPROXIMATE
TRACE OF BEDDING
AXIAL SURFACE TRACE SYNCLINE, ANTICLINE.
DIRECTION OF STRATIGRAPHIC FACING.

FIG 2:23

CHAPTER 3

MINOR STRUCTURES AND MICROFABRIC OF THE CLYTIE COVE GROUP ROCKS

DIAGRAMS AND PLATES

PLATE 3:1:a

Isoclinal fold formed by movement of beds soon after deposition. No cleavage has developed, but flame-like structures have formed parallel to the axial surface.
Apparent refolding indicates formation of the fold by "rolling" of the top limb over the bottom limb.

PLATE 3:1:b

Disrupted bedding developed as a response to downslope movement. The general style is over-folding, but the presence of box-folds shows that horizontal constraint was substantial.

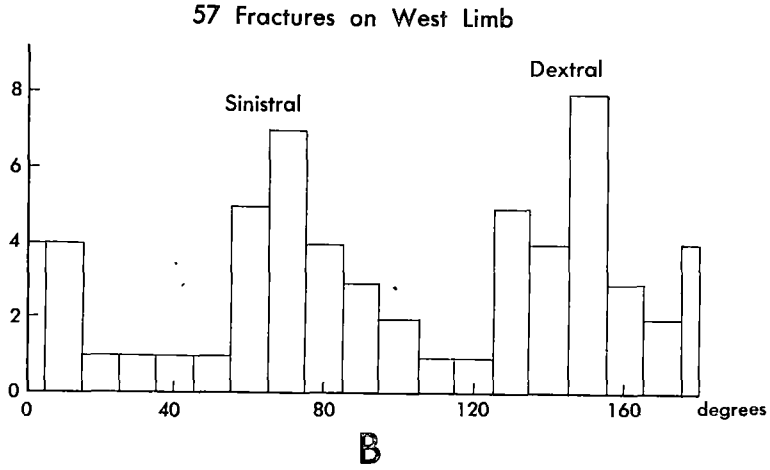

B

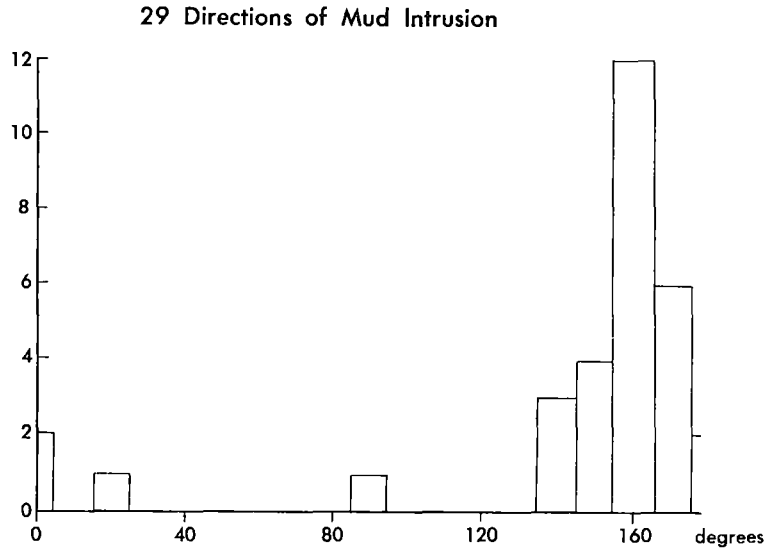

A

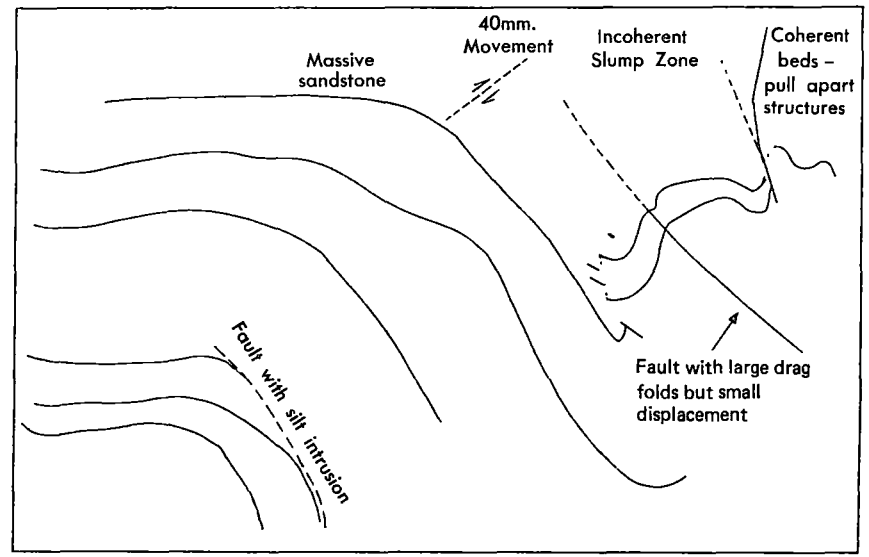

SOFT SEDIMENT FOLD AT 04556660

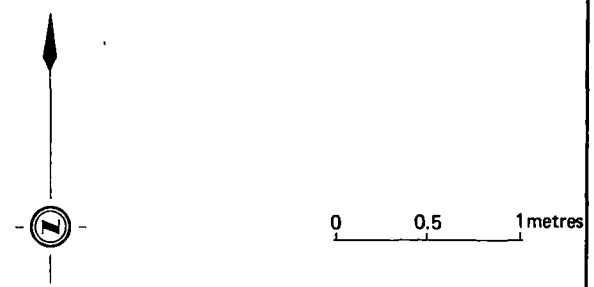

FIG. 3:1

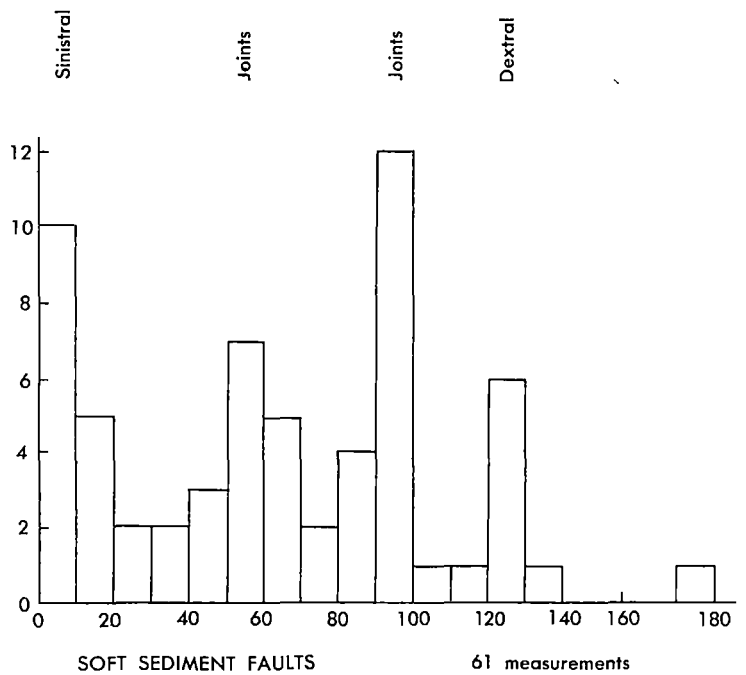
Sinistral
Joints
Joints
Dextral
12
10
8
6
4
2
0
0
20
40
60
80
100
120
140
160
180
SOFT SEDIMENT FAULTS
61 measurements

Figure 3:2

PLATE 3:2

Primary deformation structures from the Mt MacKenzie Sandstone and Conglomerate. Elongated pseudo-nodules showing "refraction" and parallelism with mud concentrations. Mud-streamers run parallel to sandstone layer in upper left of the lower plate. The mud-streamers are now parallel to grain-elongation in sandstone layers. "Refraction" is probably due to differential compaction of the mudstone-sandstone system during later deformation.


PENTAX

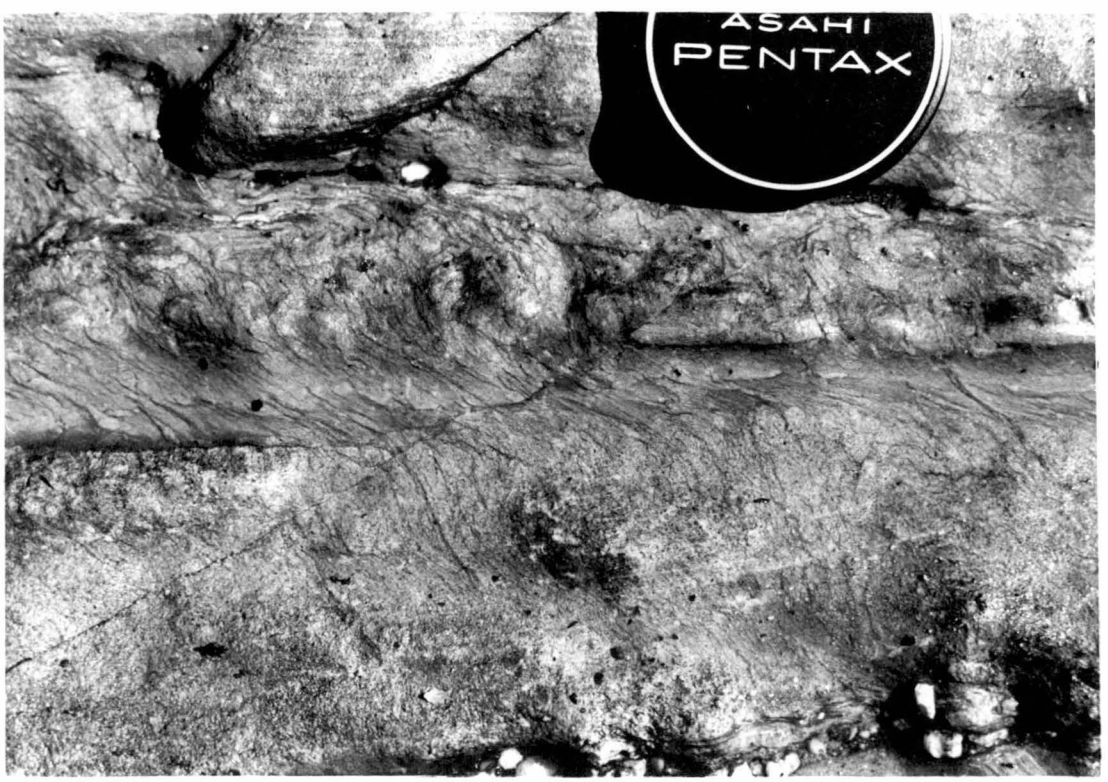
ASAHI
PENTAX

PLATE 3:3:a

Slump zone beneath a sandstone bed showing no major basal instability. The slump material arose from the part of the bed which is removed. Two directions of mud intrusion are apparent.

PLATE 3:3:b

Nature of pseudo-nodules formed from the terminated bed. Mud intrusion direction dominated by pseudo-nodule direction or by "post-nodule" faults. "Post-nodule" faults are controlling bed break-up.

ASAHI
PENTAX

PLATE 3:4:a

Massive remobilisation of mudstone between fault-bounded sandstone blocks. This photograph is from the axial region of the soft-sediment fold shown in figure 3:1.

PLATE 3:4:b

Early faults and folds which do not penetrate a large number of beds at Farrell Point. The thrust-fault nature indicates overriding and hence compression from a shallow angle to bedding. No mud intrusion is associated with this fold set.

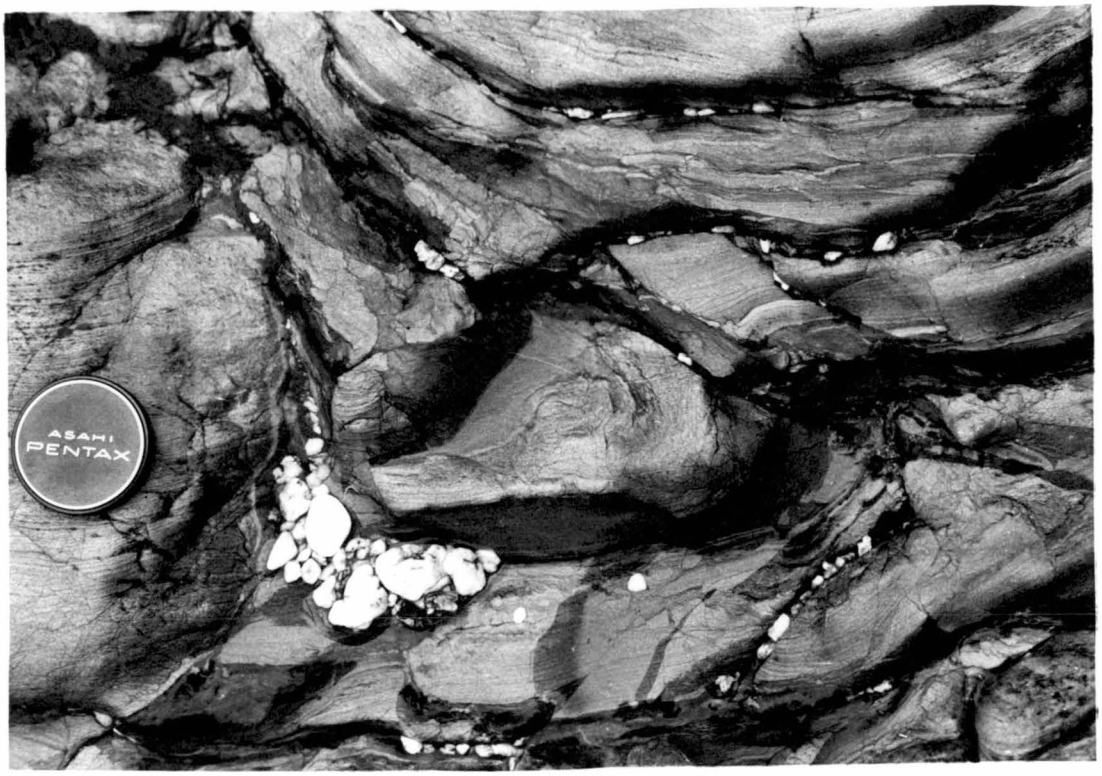
ASAHI
PENTAX

PLATE 3:4:c

Normal faults in the Long Bay Shale at Southern Cross Bay

PLATE 3:4:d

Normal faults and a thrust fault at Southern Cross Bay. "Striping", or mud-differentiation, is parallel to the normal faults, but cross-cuts the thrust fault. "Striping" is much more closely spaced than the faulting, and so not directly related.

ASAHI
PENTAX

PLATE 3:5:a

Mud intrusion formed in a medium-sandstone bed. The location of the mud zones is apparently controlled by bedding irregularities. Note the downward intrusion at the top of the photograph, and the association with a small fault.

PLATE 3:5:b

Major second generation anticline looking east from Mt Stokes (GR201037).

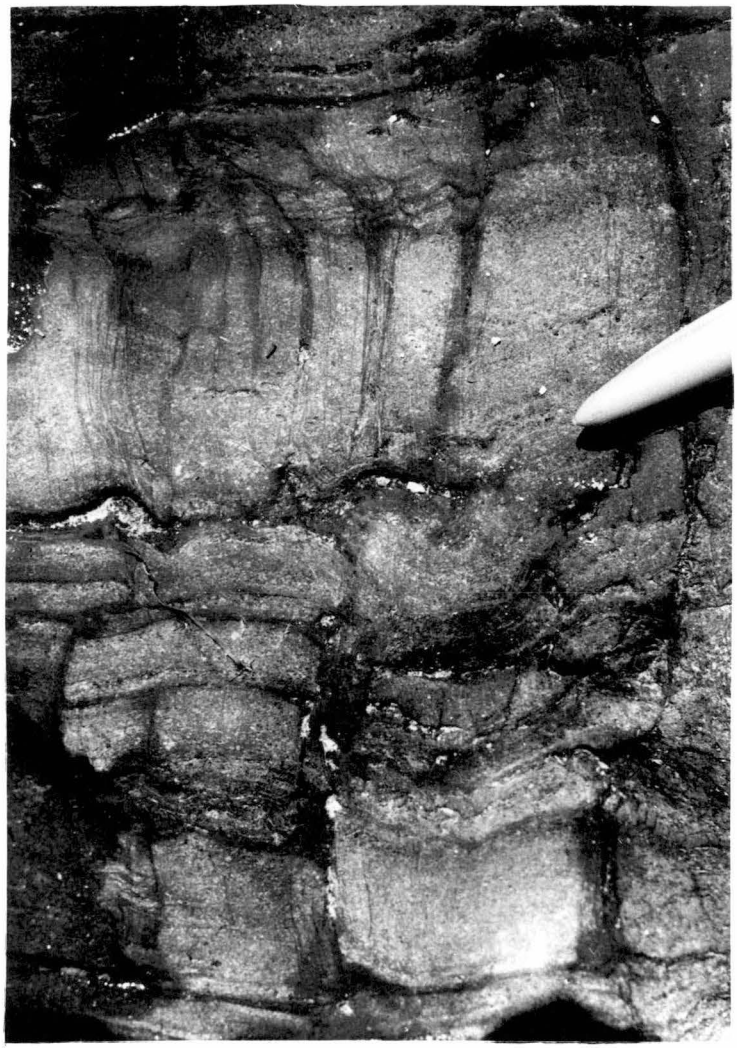

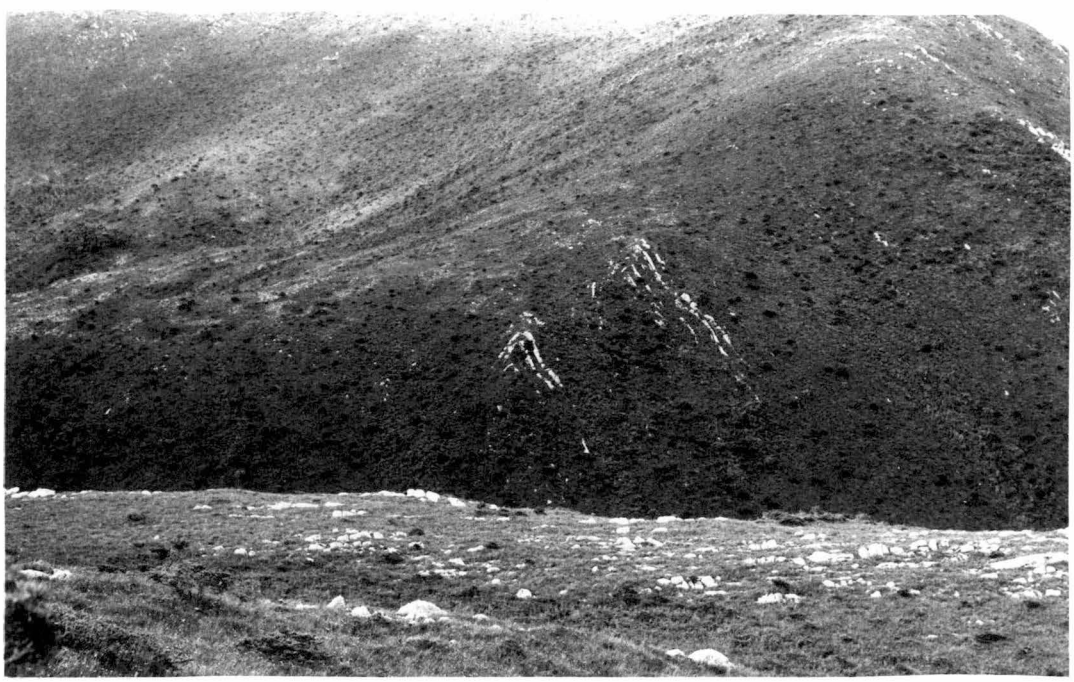

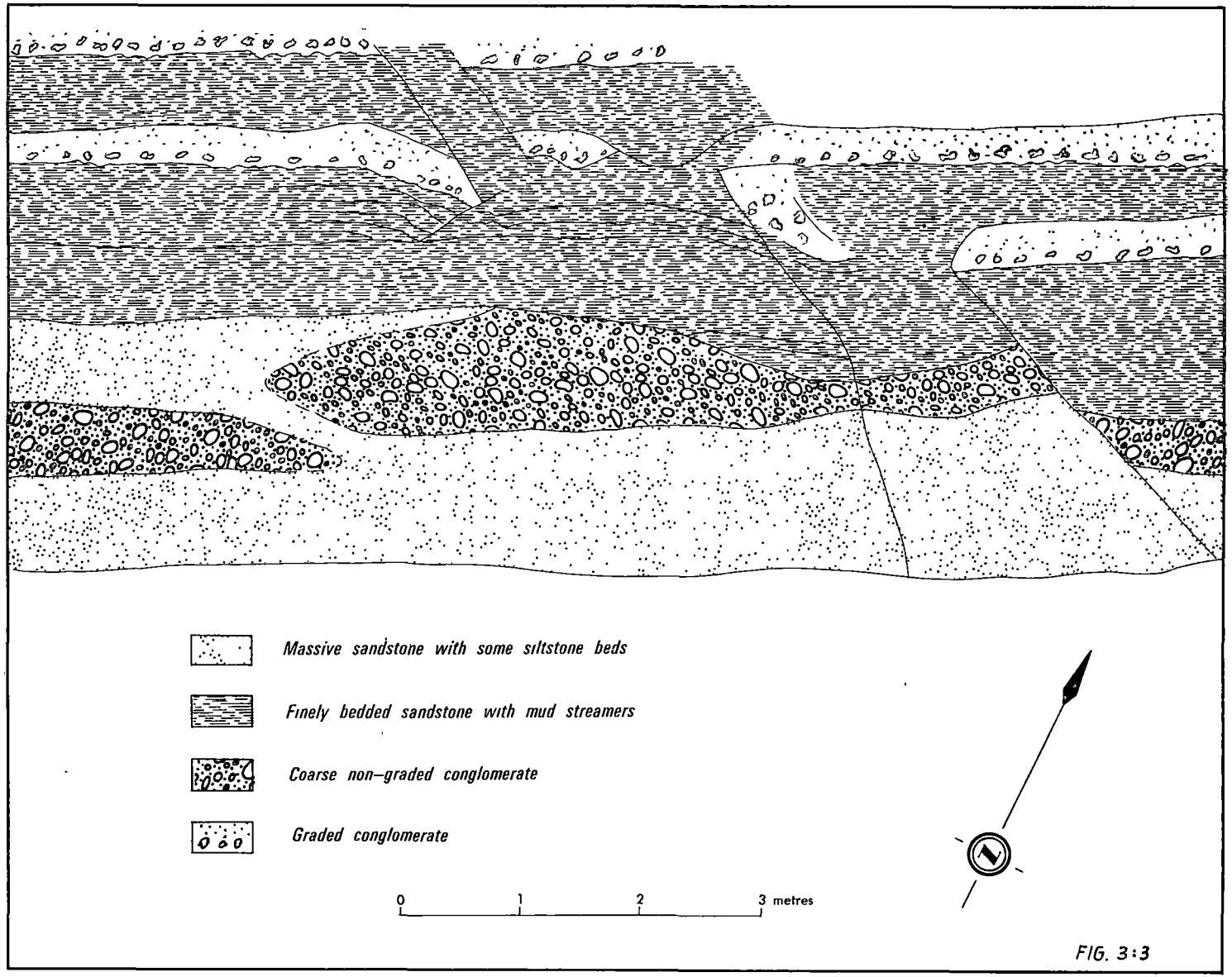
Massive sandstone with some siltstone beds
Finely bedded sandstone with mud streamers
Coarse non-graded conglomerate
Graded conglomerate
0
1
2
3 metres
N

FIG. 3:3

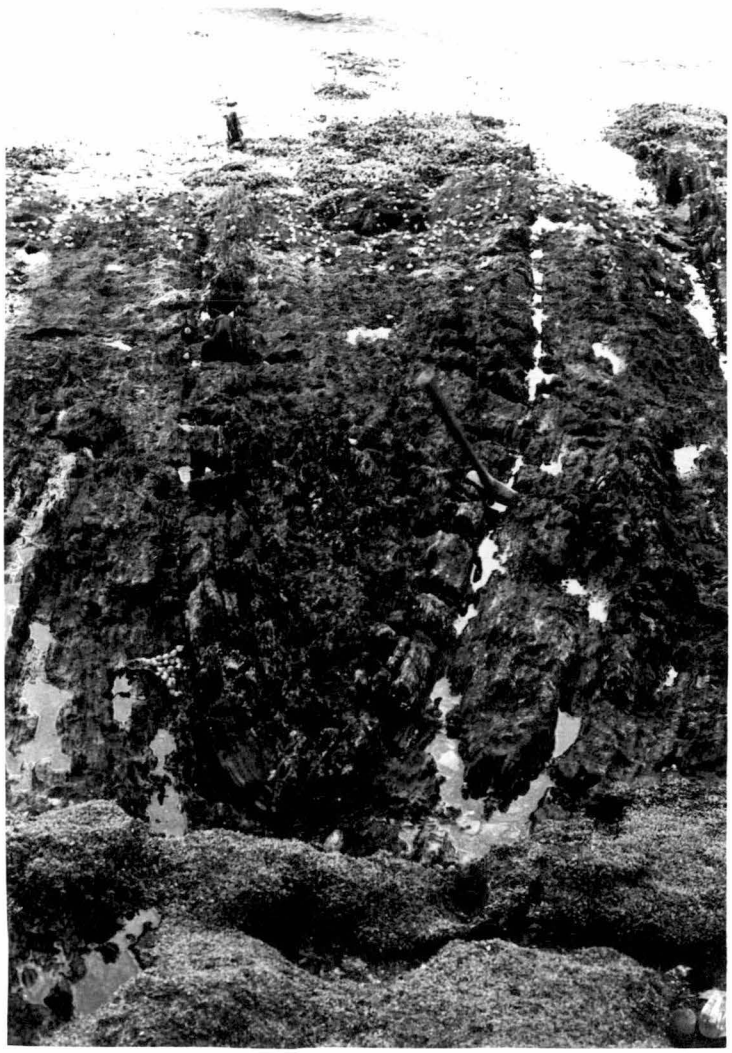

PLATE 3:6

PLATE 3:7:a

A second phase fold with clear cross-cutting third-phase cleavage. "Stripey" nature of the cleavage is apparent.

PLATE 3:7:b

Style of second generation fold in the Mt Fulton region. Cleavage is poorly developed.

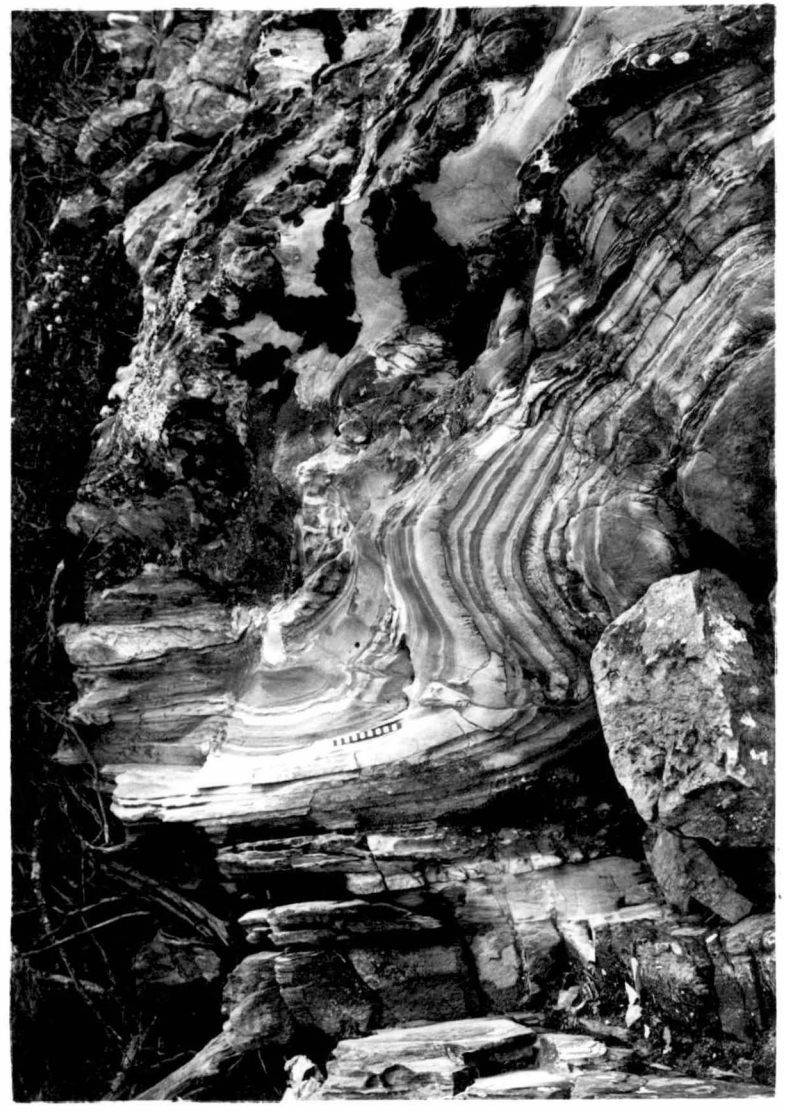

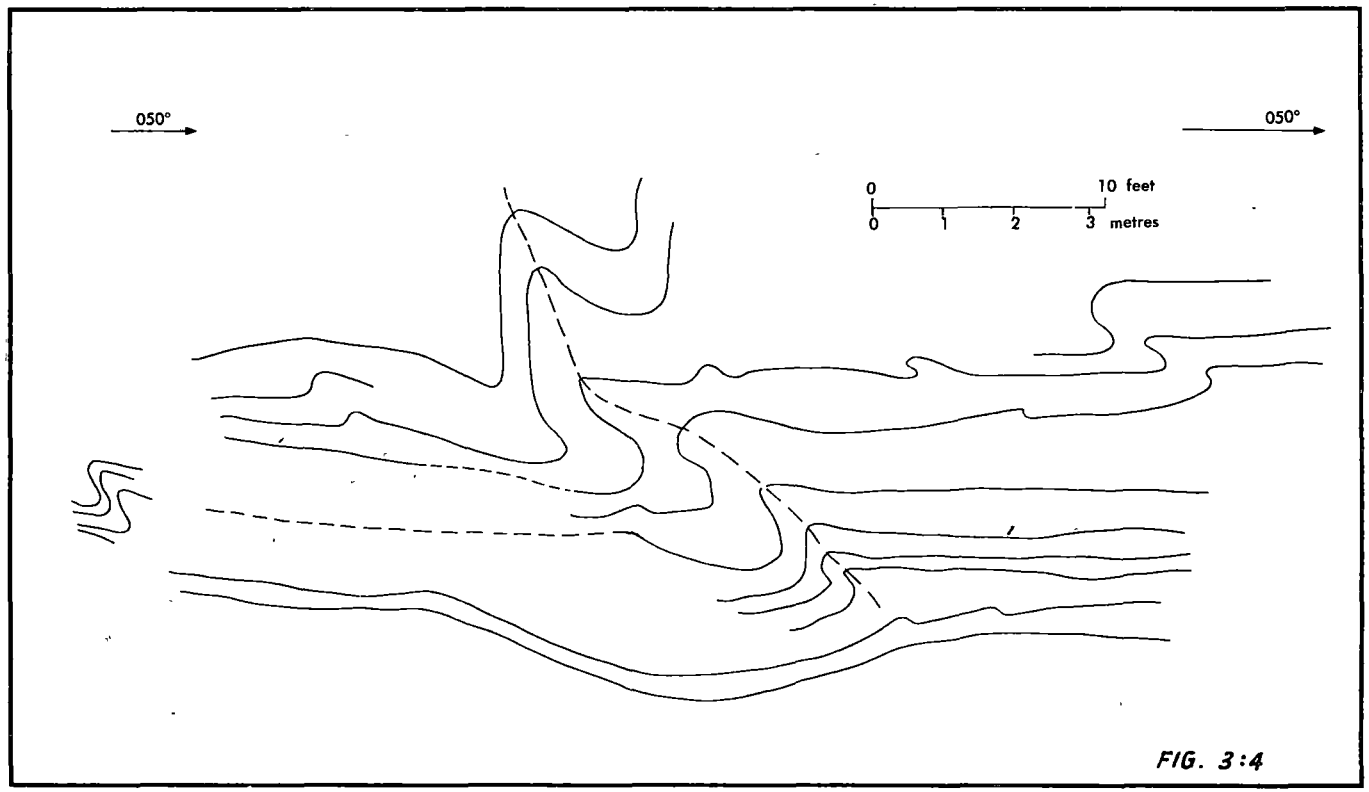

FIG. 3:4

FIGURE 3:5

Geological map along Farrell Point and the eastern side of Joe Page Bay.

FIGURE 3:6

The effect on D_{2c} folds of removing 29% homogeneous plane strain, probably imposed during D_{3c}, perpendicular to the D_{3c} axial surface.

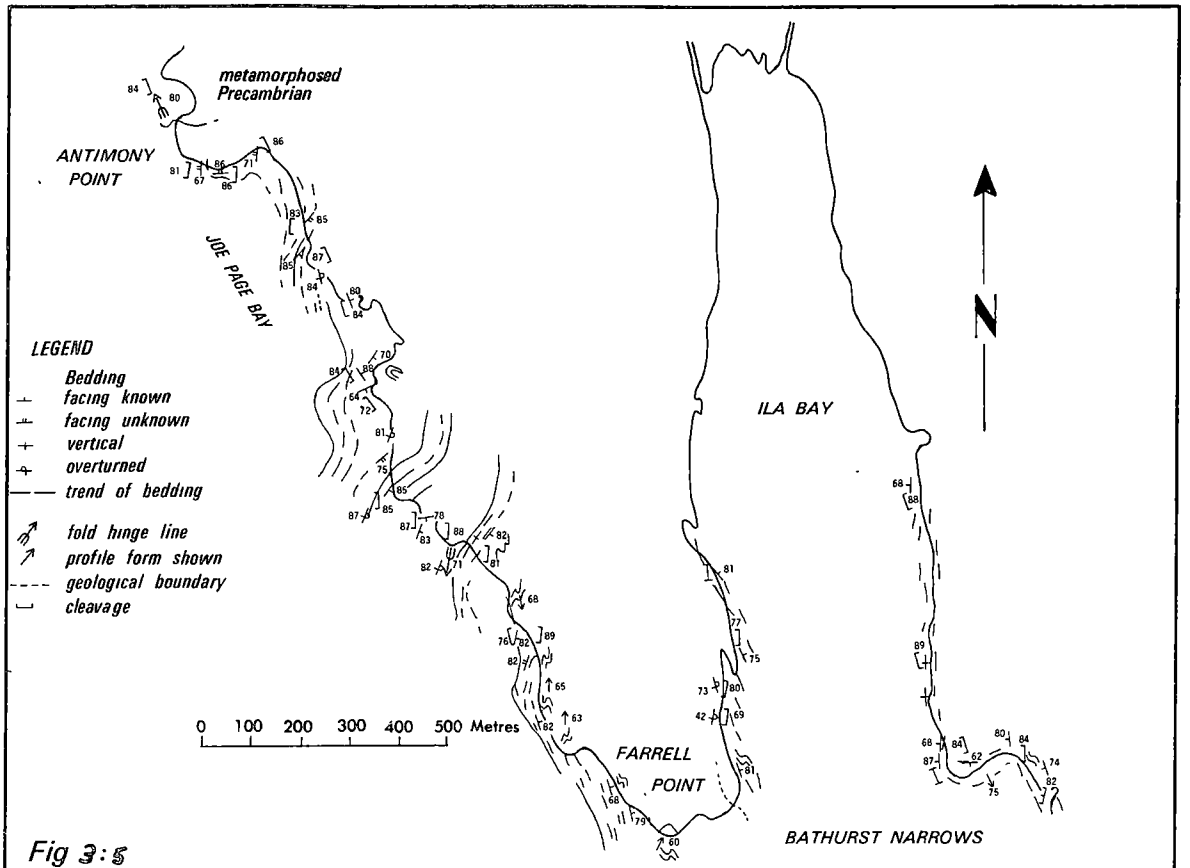
metamorphosed
Precambrian
ANTIMONY
POINT
JOE PAGE BAY
ILA BAY
FARRELL
POINT
BATHURST NARROWS
N
LEGEND
Bedding
facing known
facing unknown
vertical
overturned
trend of bedding
fold hinge line
profile form shown
geological boundary
cleavage
0 100 200 300 400 500 Metres

Fig 3:5

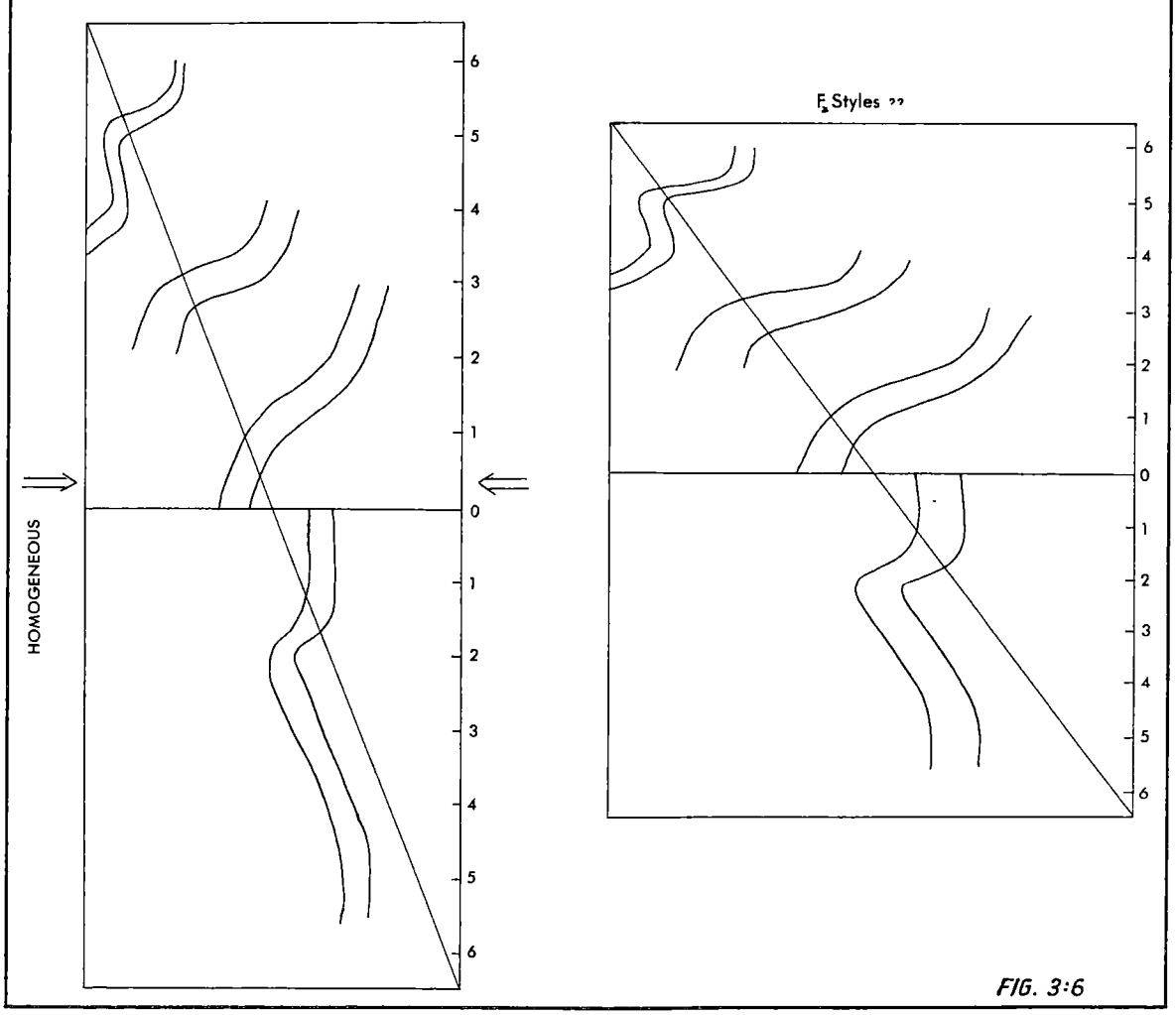
HOMOGENEOUS
F2 Styles ??

FIG. 3:6

PLATE 3:8:a

D_{3c} folds verging towards right, showing a well developed axial surface cleavage and disharmony between layers of different thickness. Scale bar in centimetres.

PLATE 3:8:b

Multiple hinge line developed in a large symmetrical fold. Distance between hinge lines is 1.2 m.

PLATE 3:9

Saddle fold formed by the reversal of plunge of D_{3c} mesoscopic fold. Top photograph looking south, the bottom photograph looking north.

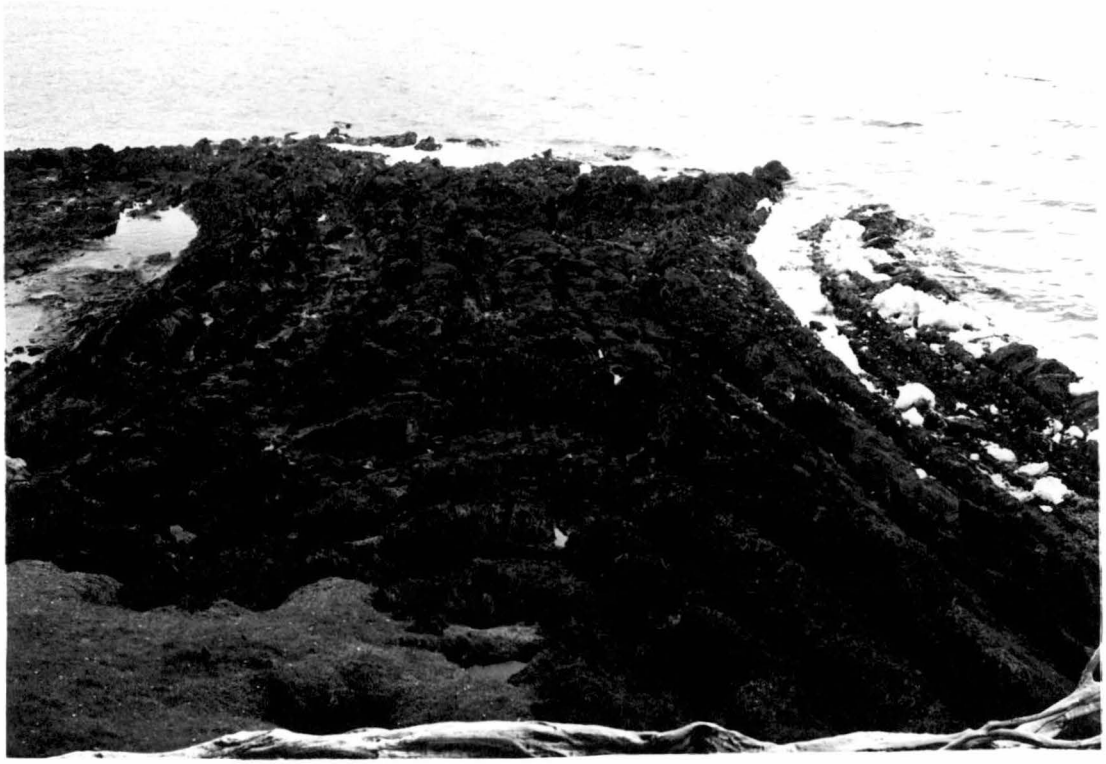

FIGURE 3:7

a. Map of interfering folds (GR23500346)

Fold hinge line


Bedding


Cleavage

b. Poles to bedding:

. Fold 2

⊡ Fold 3

⊙ Fold 4

c. Equal area projection of readings from around fold 1.

. bedding

⊙ fold hinge


cleavage

This indicates folds similar to fold 2 interfere with fold 1.

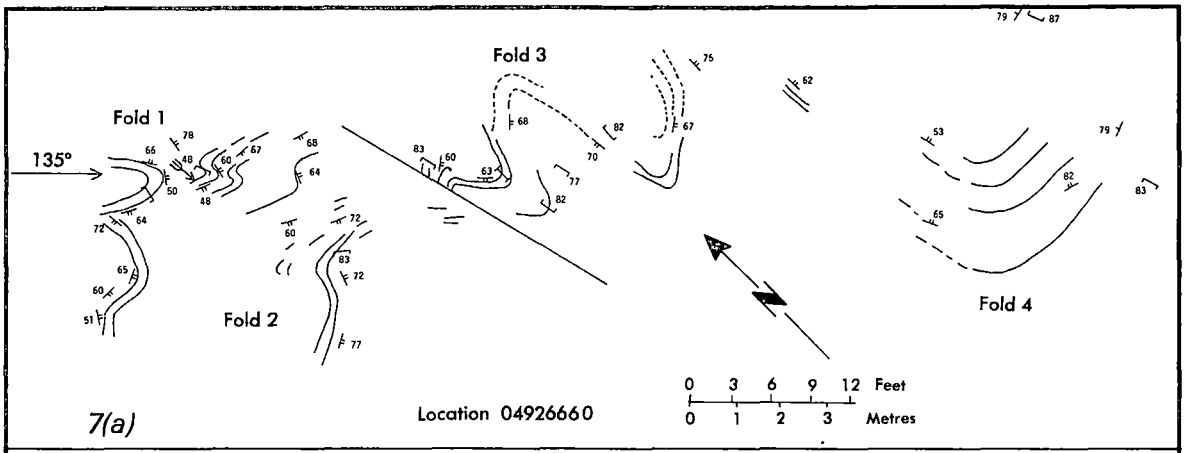

7(a)

Location 04926660

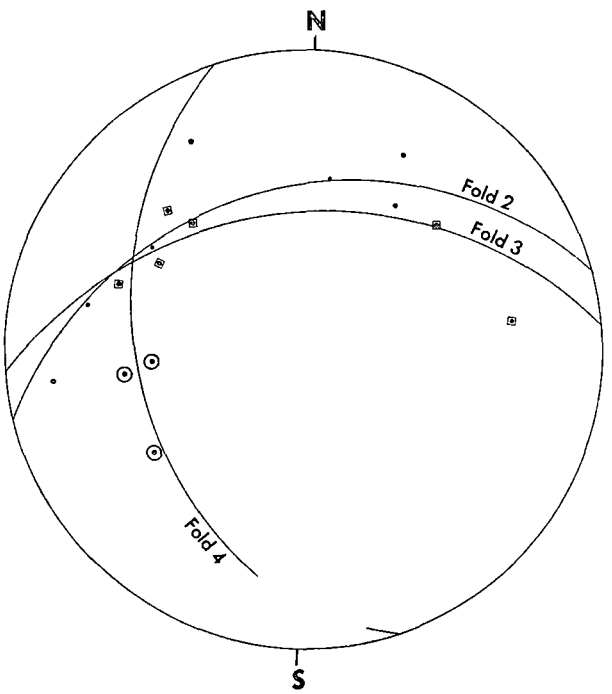

7(b)

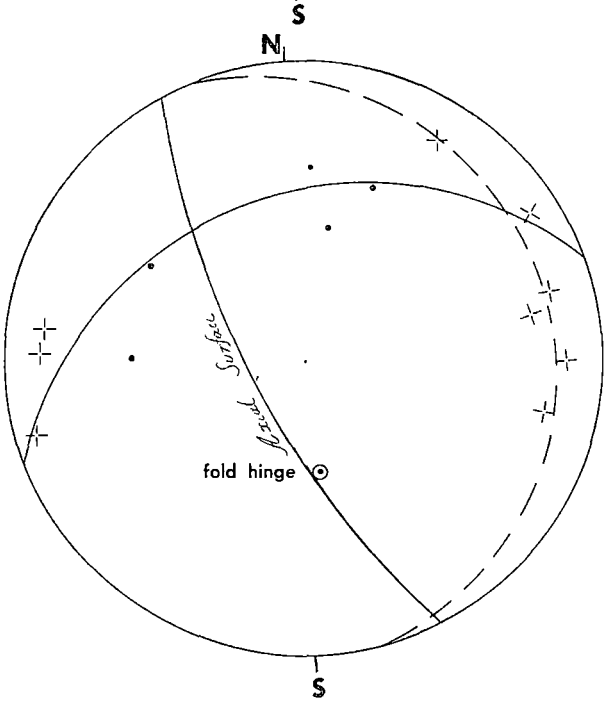

7(c)

FIG. 3:7

FIGURE 3:8

a. (i) Detailed field map of a D_{3c} fold.

(ii) Graph of orthogonal thickness against isogonic dip for the fold in (i).

b. (i) Fold profile produced using figure 3:8:c(iii).

(ii) Analysis of orthogonal thickness of the profile.

c. (i) A cylindrical semi-circular fold arc.

(ii) The effect of inhomogeneous flattening of the initial form.

(iii) As above, using different flattening figures.

d. (i) An initial cylindrical profile.

(ii) Inhomogeneous flattening which does not vary in a linear fashion.

(iii) Orthogonal thickness analysis of the profile shown in 3:8:d(ii).

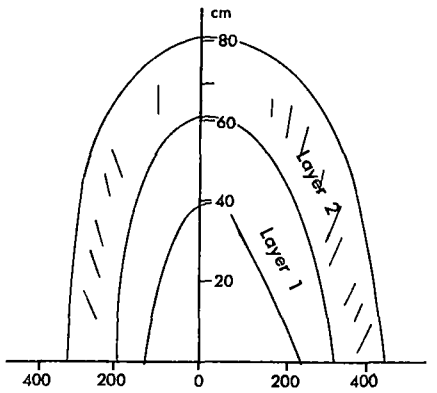

8(a) (i)

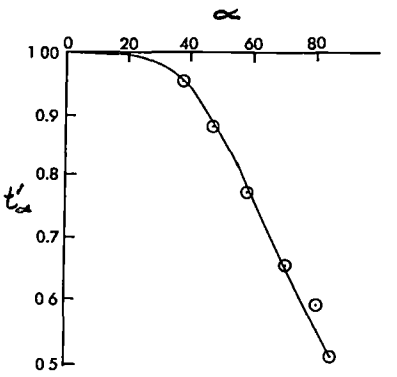

(ii)

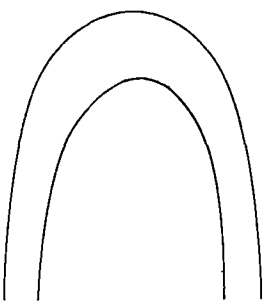

8(b) (i)

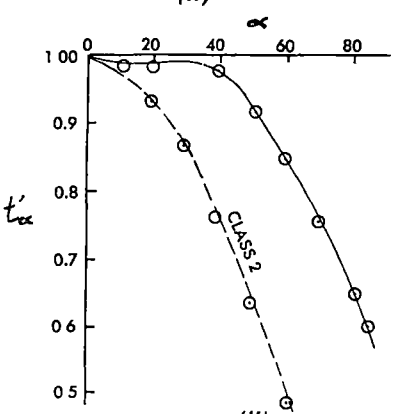

(ii)

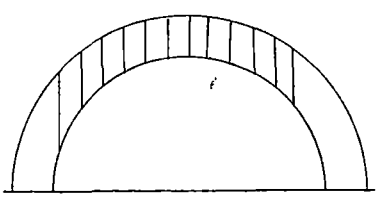

8(c) (i)

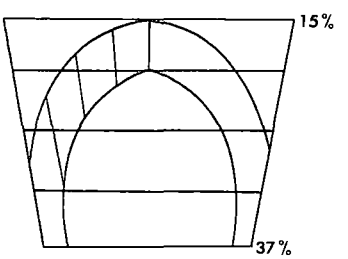

(ii)

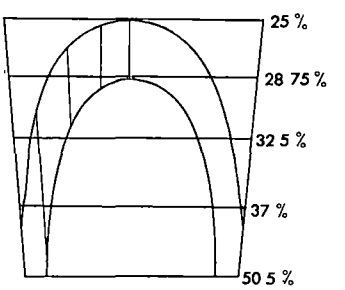

(iii)

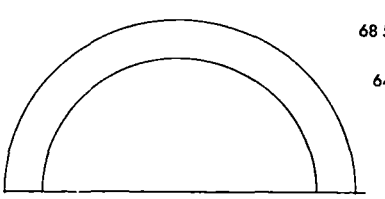

8(d) (i)

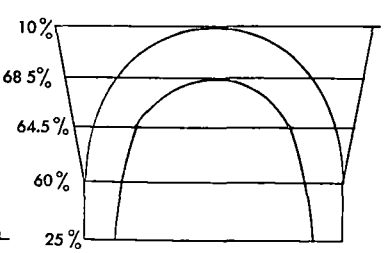

(ii)

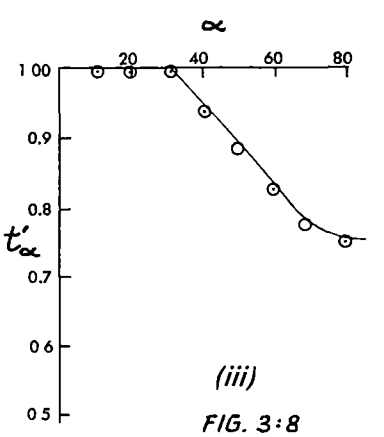

(iii)

FIG. 3:8

FIGURE 3:9

Analysis of orthogonal thickness variation of the fold shown in figure 3:10.

Each layer is analysed separately.

The "system" is an analysis using the thickness of the six beds as the "layer".

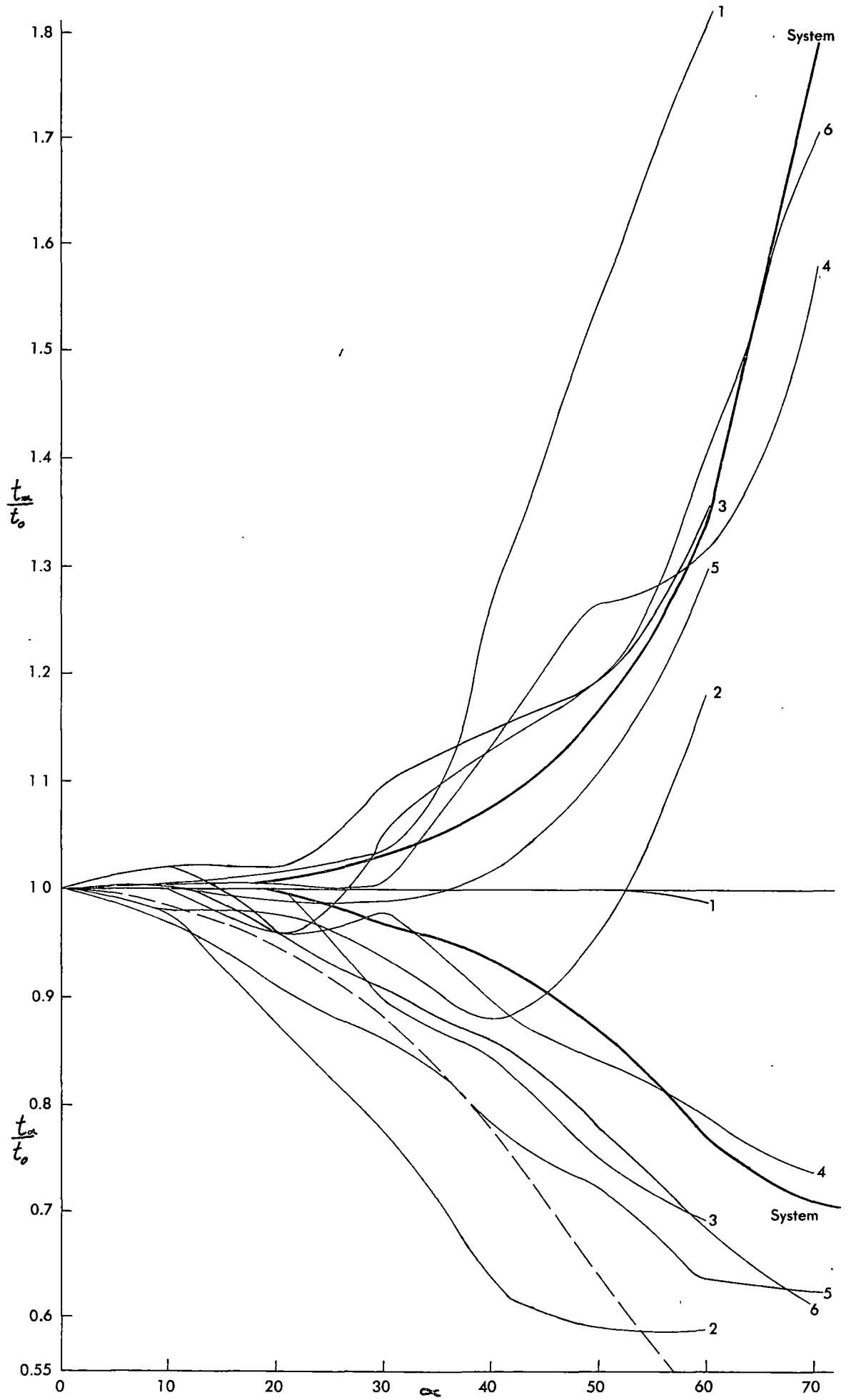
1.8
1.7
1.6
1.5
1.4
1.3
1.2
1.1
1.0
0.9
0.8
0.7
0.6
0.55
$\frac{t_m}{t_o}$
$\frac{t_a}{t_o}$
0
10
20
30
40
50
60
70
α
System
1
2
3
4
5
6

Fig. 3:9

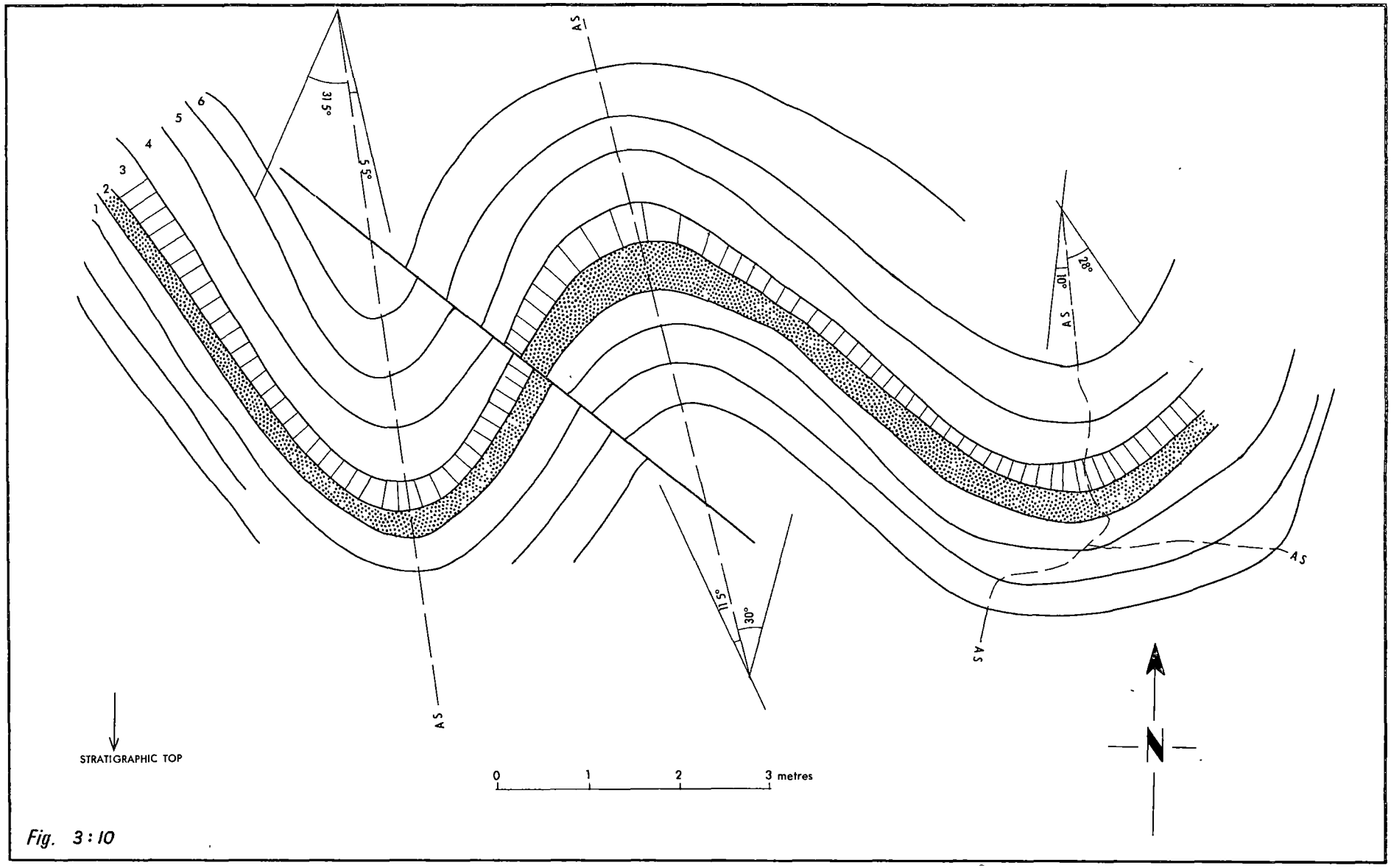
1
2
3
4
5
6
31 5°
53°
A S
28°
10°
A S
A S
A S
51°
30°
A S
STRATIGRAPHIC TOP
0
1
2
3 metres
N

Fig. 3 : 10

FIGURE 3:11

a. Graph of $\frac{dt'}{d\alpha}$ against α for layers 2 and 5 of the fold in figure 3:10.

b. Graph of $\frac{t'\alpha}{t_o}$ against α for the same layers.

c. Graph of $\frac{d^2t'}{d\alpha^2}$ against α for the same layers.

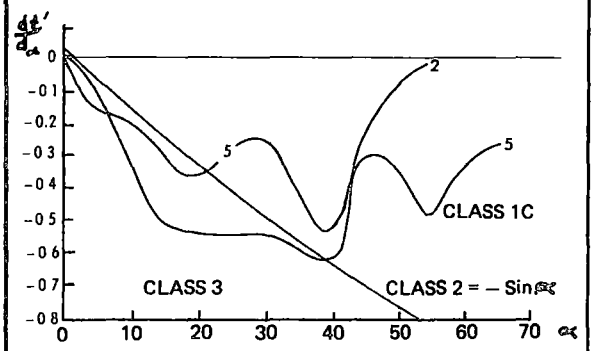

11 a

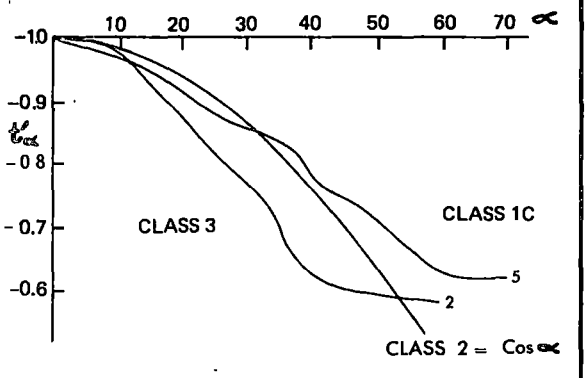

b

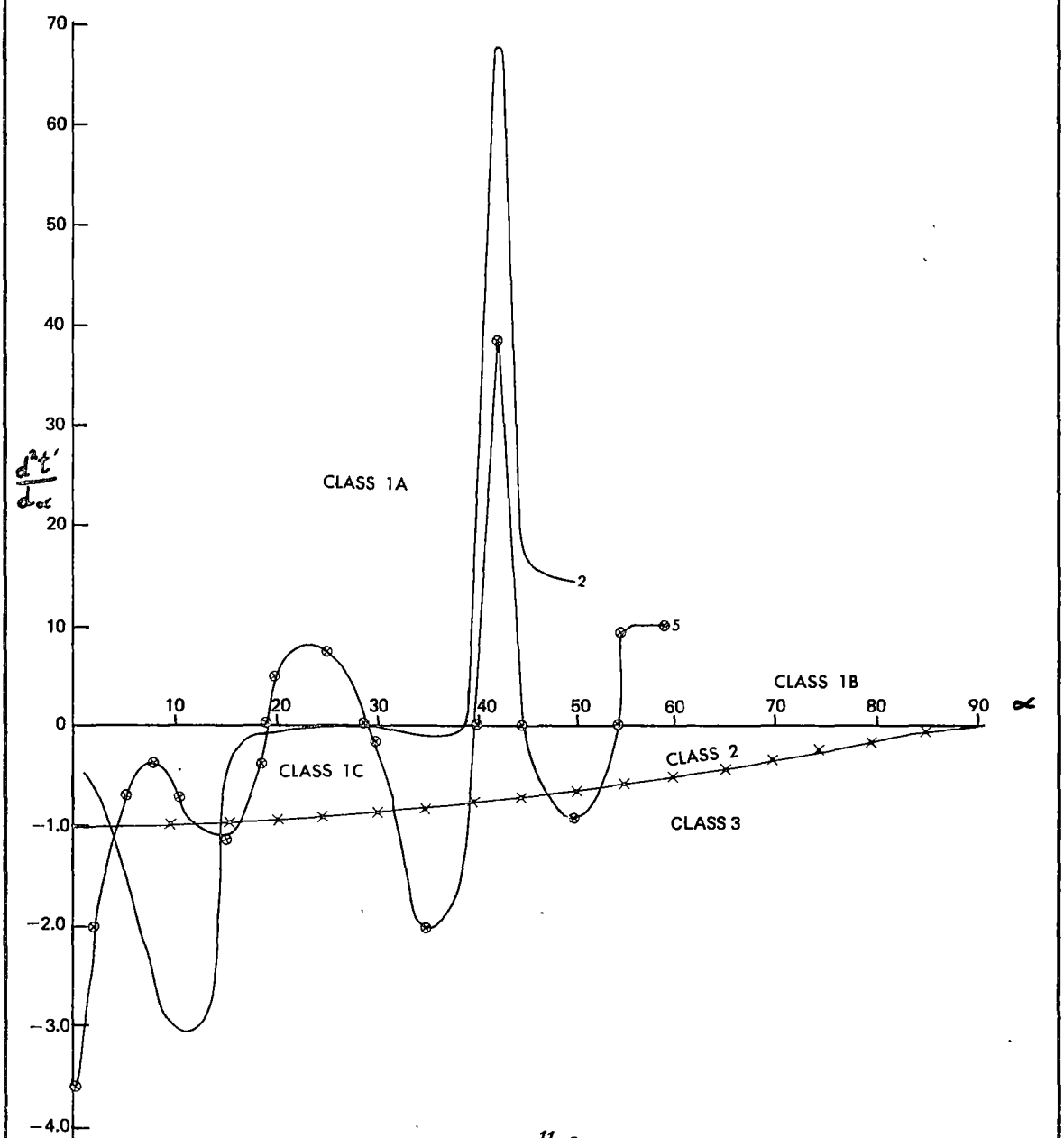

11 c

FIG. 3:11

FIGURE 3:12

Analysis of cleavage variations in the fold shown in figure 3:10.

The lower diagram shows bedding plane orientations.

Cleavage readings are from layer 3 (dotted).
Limb 1 in westernmost and limb 4 easternmost.

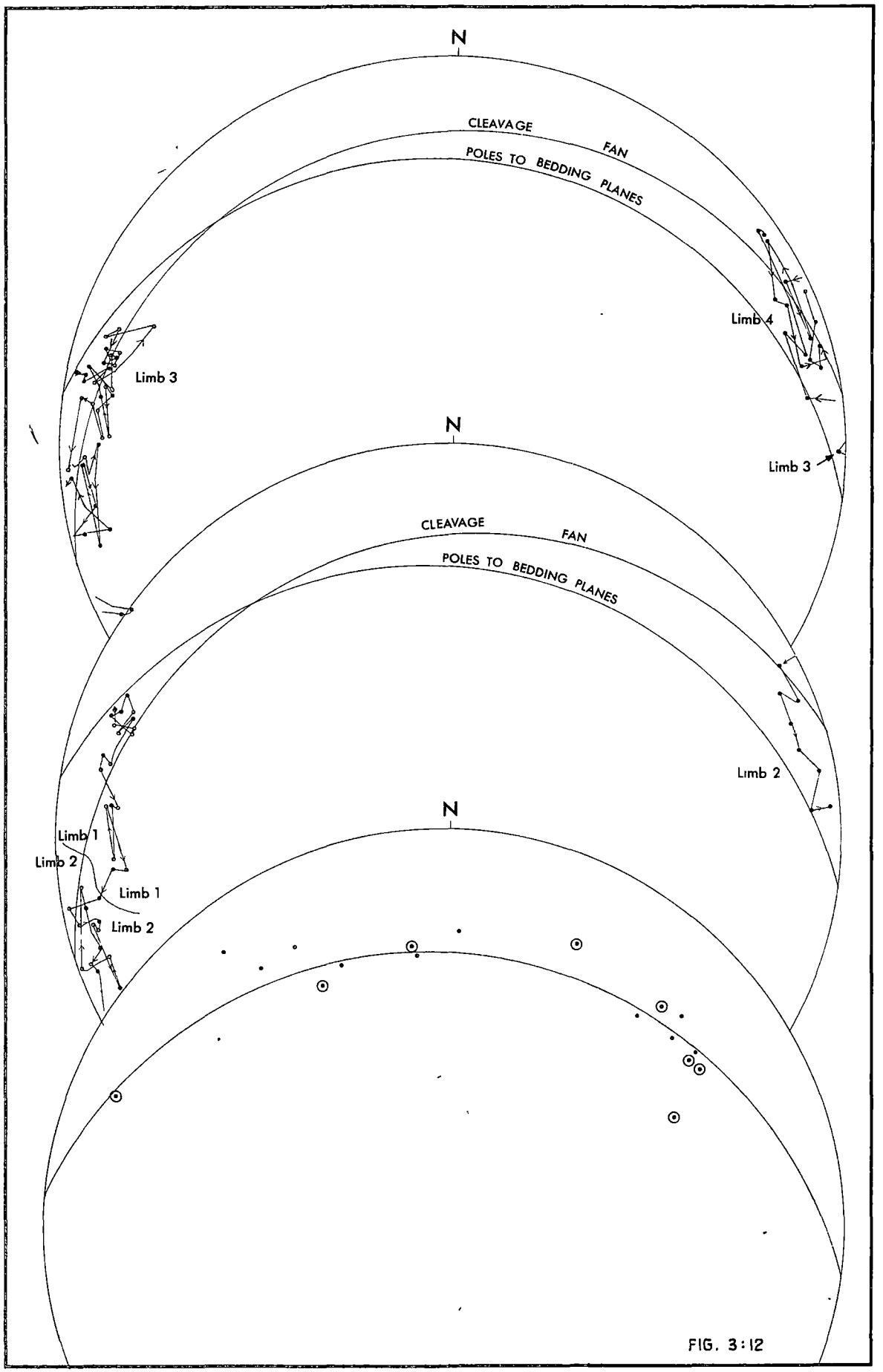
N
CLEAVAGE
FAN
POLES TO BEDDING PLANES
Limb 4
Limb 3
N
Limb 3
CLEAVAGE
FAN
POLES TO BEDDING PLANES
Limb 2
N
Limb 1
Limb 2
Limb 1
Limb 2

FIG. 3:12

FIGURE 3:13

FOLD STYLES DEVELOPED IN THE CLYTIE COVE GROUP

a. Folding and faulting during D_{3c}. Note the double hinge developed.

b. More open folds related to the D_{3c} event.

c. A sequence of F_{3c} folds with faults developed in the place of synclinal closures.

d. Variation in fold style along the axial surface direction.

e. Curved bedding traces resulting from the interference of D_{2c} and D_{3c} structures.

f. Earlier isoclinal and near isoclinal folds over-printed by D_3 structures.

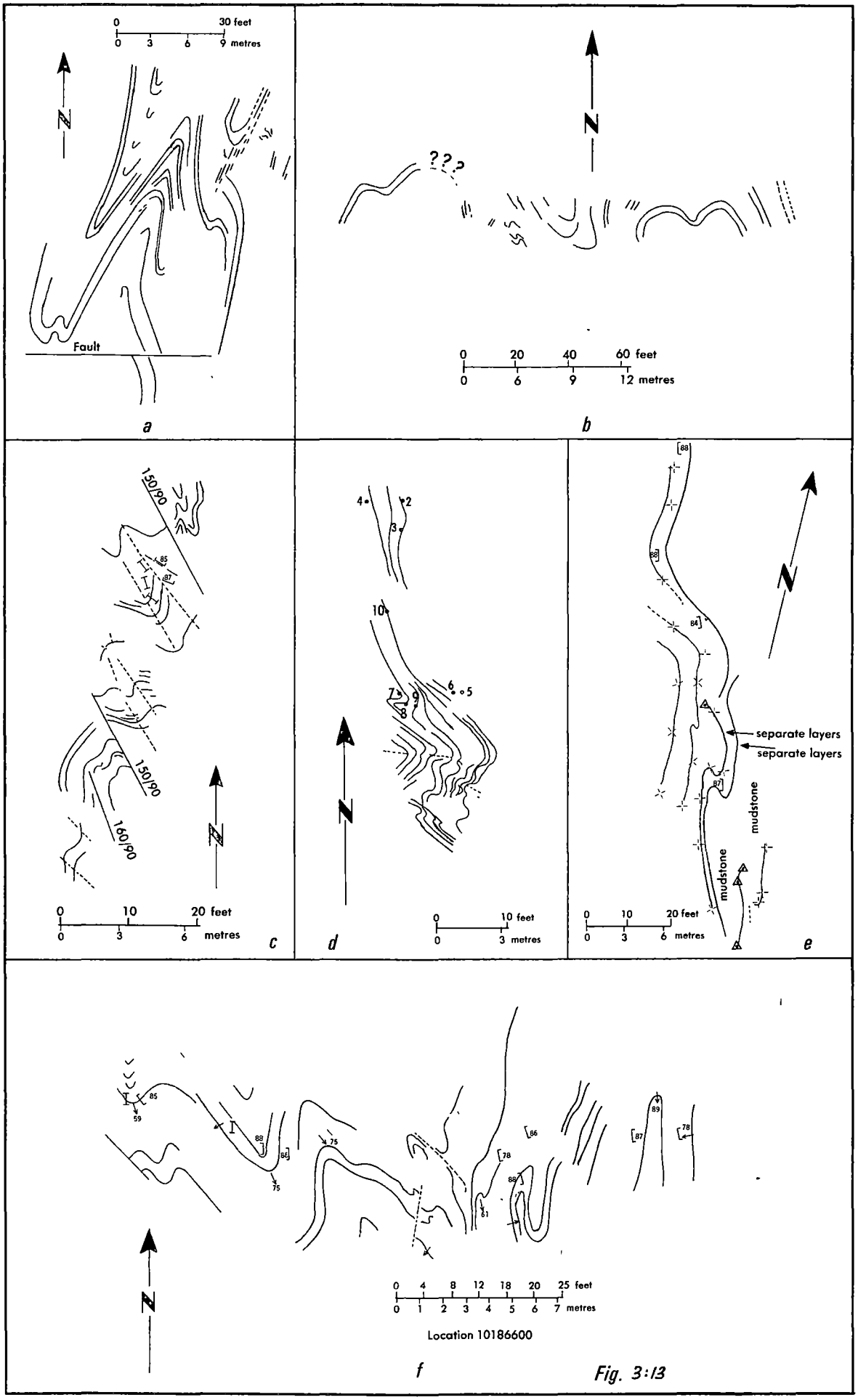
0 30 feet
0 3 6 9 metres
N
Fault
a
???
N
0 20 40 60 feet
0 6 9 12 metres
b
150/90
85
87
150/90
160/90
0 10 20 feet
0 3 6 metres
c
4
2
3
10
6
5
7
8
9
N
0 10 feet
0 3 metres
d
88
88
84
87
separate layers
separate layers
mudstone
mudstone
0 10 20 feet
0 3 6 metres
e
85
59
88
86
75
75
86
78
88
61
89
87
78
N
0 4 8 12 18 20 25 feet
0 1 2 3 4 5 6 7 metres
Location 10186600
f

Fig. 3:13

PLATE 3:10:a

Lithological banding parallel to S_{3c} cleavage scale in centimetres.

PLATE 3:10:b

Lithological banding parallel to cleavage refracted across bedding planes in a D_{3c} fold.

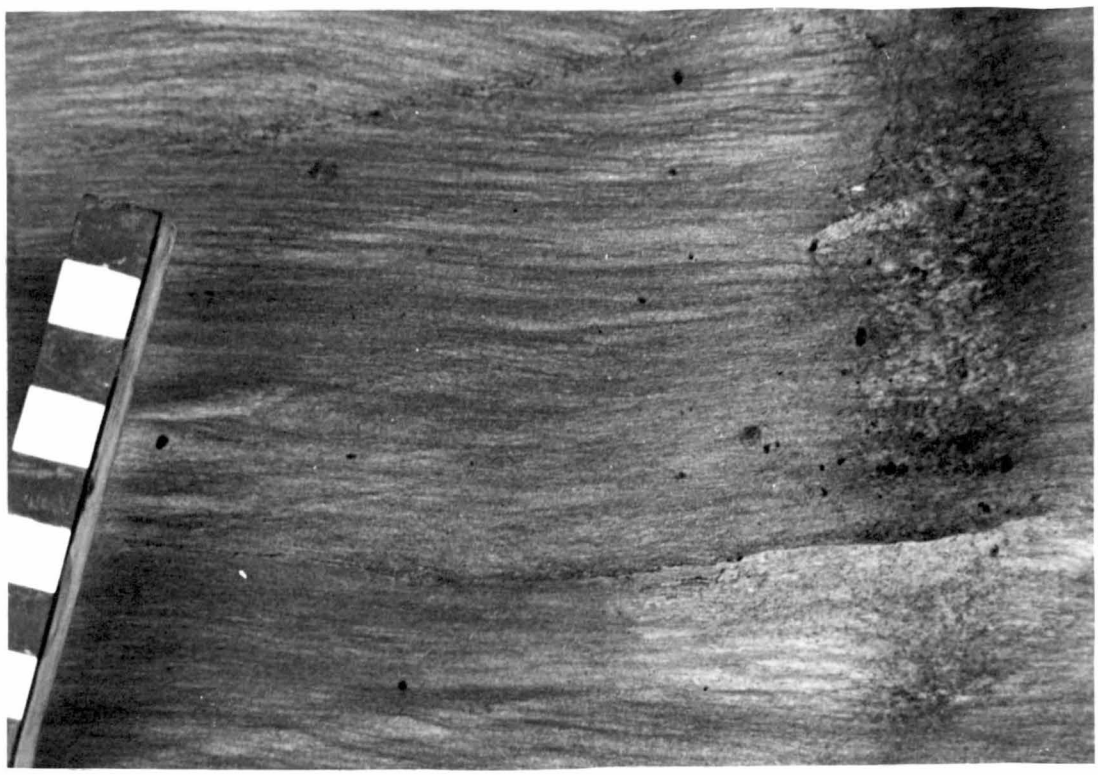

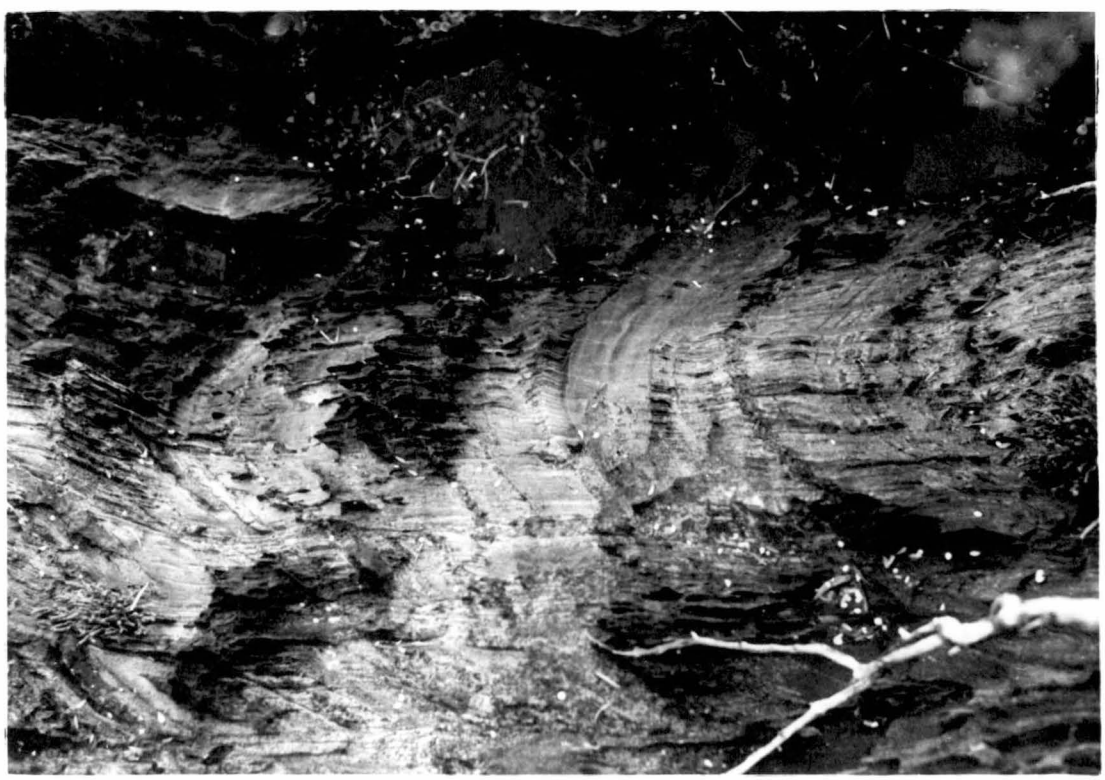

PLATE 3:11:a

Well developed lithological banding in a siltstone unit between sandstone beds. Cleavage in the sandstone bed is a grain alignment, but ghost banding penetrates into the sandstone in places.

PLATE 3:11:b

Lithological banding parallel to cleavage at a low angle to bedding, causing bedding transposition. In sandier layers the dark bands form thin wisps parallel to cleavage.


PENTAX

PLATE 3:12

Lithological banding parallel to the S_{3c} cleavage in the core of the Clytie Cove syncline. Ghost bedding is apparent.

PLATE 3:13

Form of the S_{3c} cleavage in hand specimen.

The formation of anticlinal folds without associated synclines is due to the removal of parts of the beds in the fold limbs by pressure solution. The concentration of mica and opaque minerals in the seams is by the same method.

Specimen 481.67.

PLATE 3:14

a. Widely spaced, wide micaceous seams with sharp boundaries formed in a thicker laminated sandstone bed. Mt Fulton region.

b. Wide, sharply defined seams with an anastomosing nature. Zones co-alesce towards the top of the bed, which is richer in mudstone.

PLATE 3:15

Widely spaced cleavage seams in the core of a fold. Very regular throughout the bed. Specimen 48168. Scale in centimetres.

PLATE 3:16

a. Load casts with cross-cutting cleavage seams. Loads have been aligned in the cleavage directions.

b. The seams are dominant on the peak of the flames, but also occur in the sandstone at an angle to the seams in the mudstone, and appear discontinuous. These seams in sandstone are less intensely developed. The load casts affected the position at which differentiation occurred.

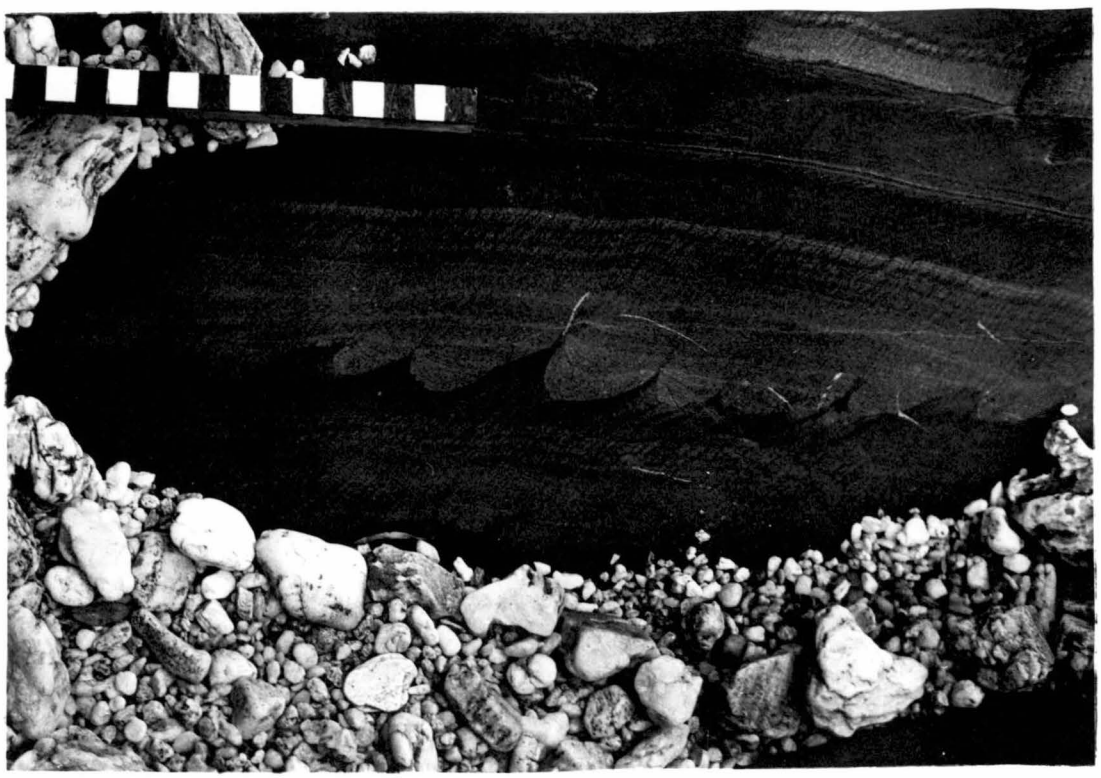

FIGURE 3:14

GEOMETRY OF CLEAVAGE FANS

a. Accurate field plot of an F_{3c} fold and associated cleavage.

b. Bedding (.) and (⊙) cleavage readings from the fold indicate a concordant cleavage fan.

c. Concordant cleavage and bedding folding from the folds shown in figure 3:13:c.

d. Folds from GR267997. Adjacent folds show a considerable variation in the direction of plunge. k = hinge of kink-bands.

e. Bedding readings from the fold shown in figure 3:8:a:

.	cleavage readings
⊗	inside of layer 1
+	outside of layer 1
◬	outside of layer 2

f. Combination of cleavage forming folds and D_{4c} folds.

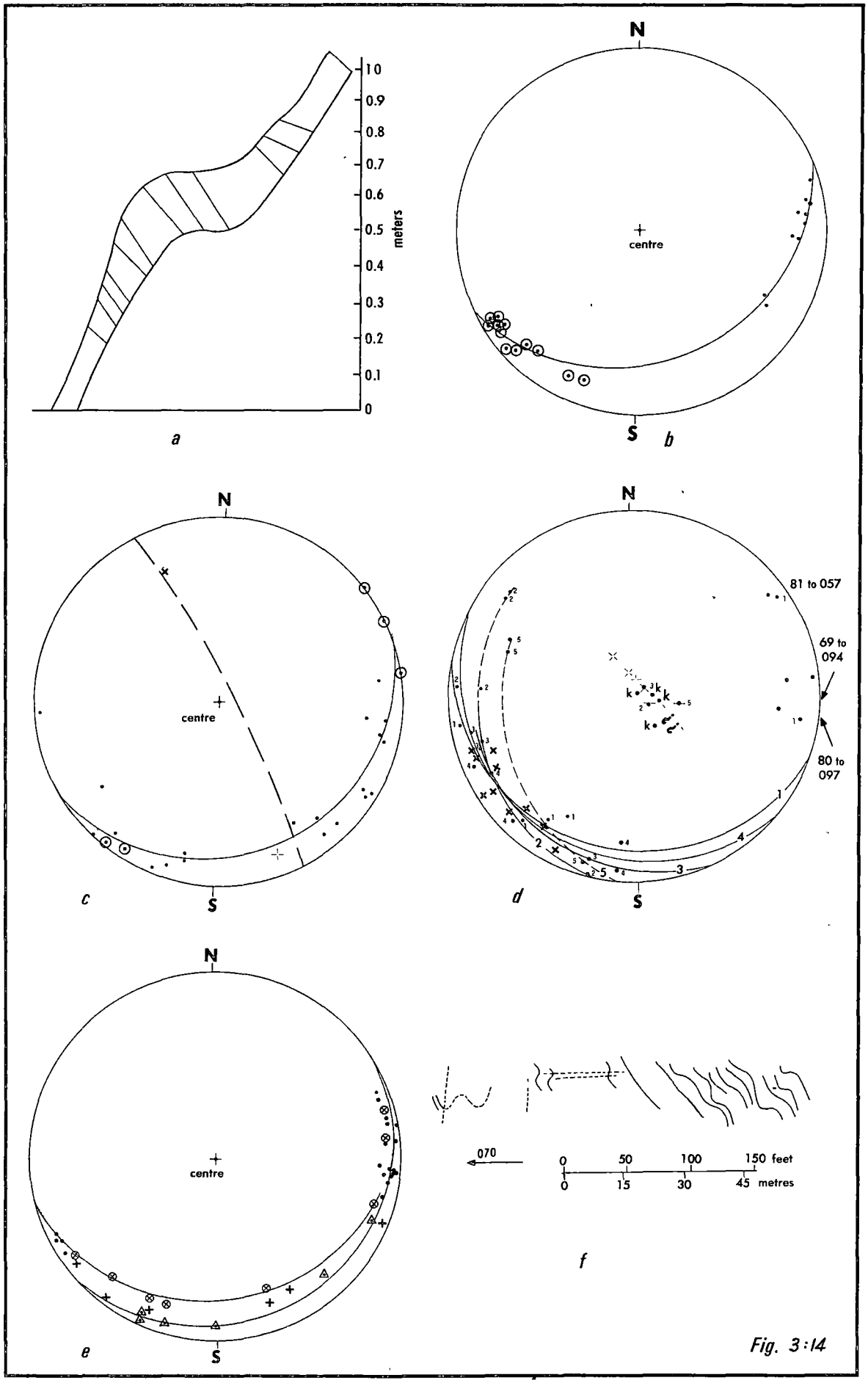
10
0.9
0.8
0.7
0.6
0.5
0.4
0.3
0.2
0.1
0
meters
a
N
centre
S
b
N
centre
S
c
N
81 to 057
69 to 094
80 to 097
k
1
2
3
4
5
S
d
N
centre
S
e
070
0
50
100
150 feet
0
15
30
45 metres
f

Fig. 3:14

FIGURE 3:15

a. Core of the Clytie Cove Syncline GR26520972.

b. Poles to bedding and cleavage from the core of the Clytie Cove Syncline.

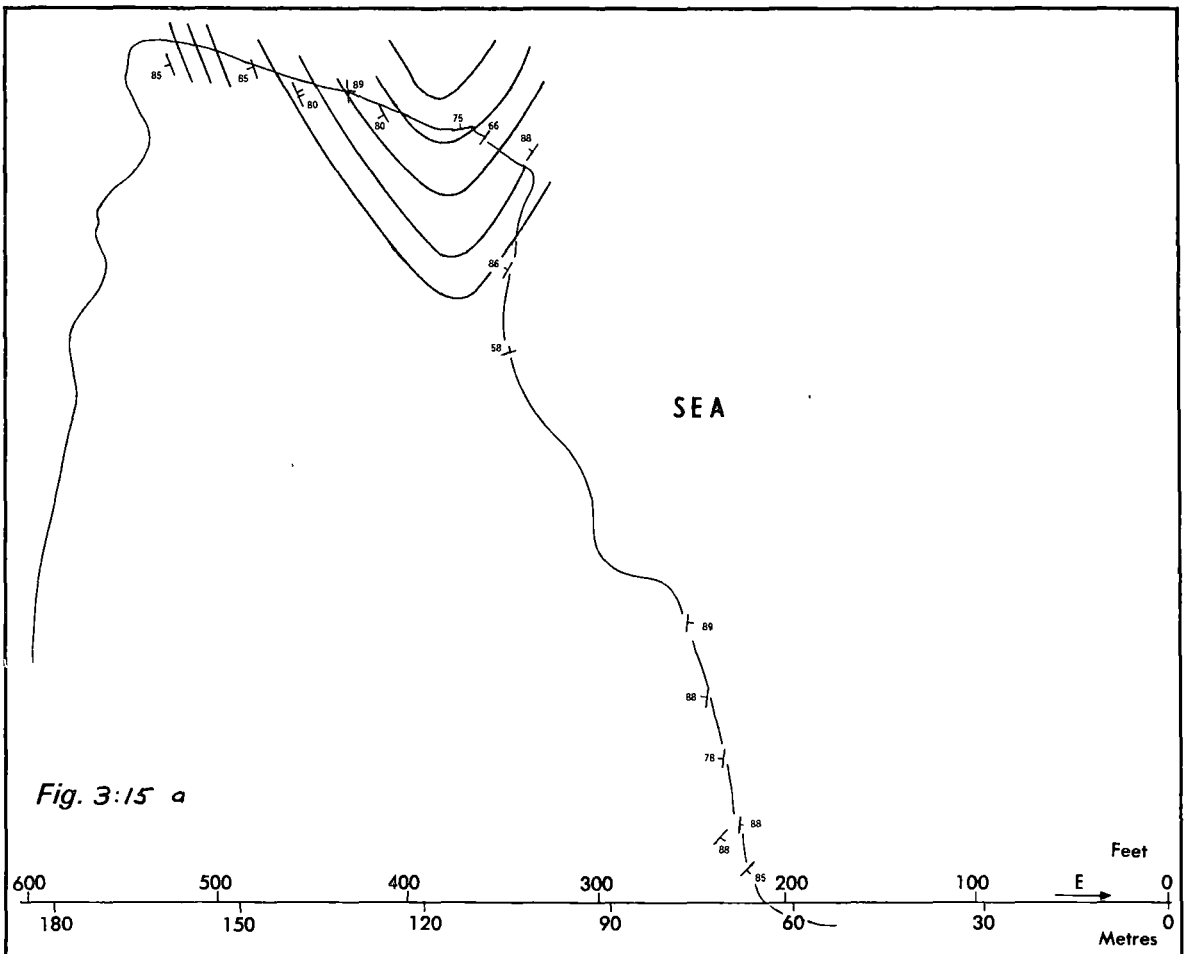

Fig. 3:15 a

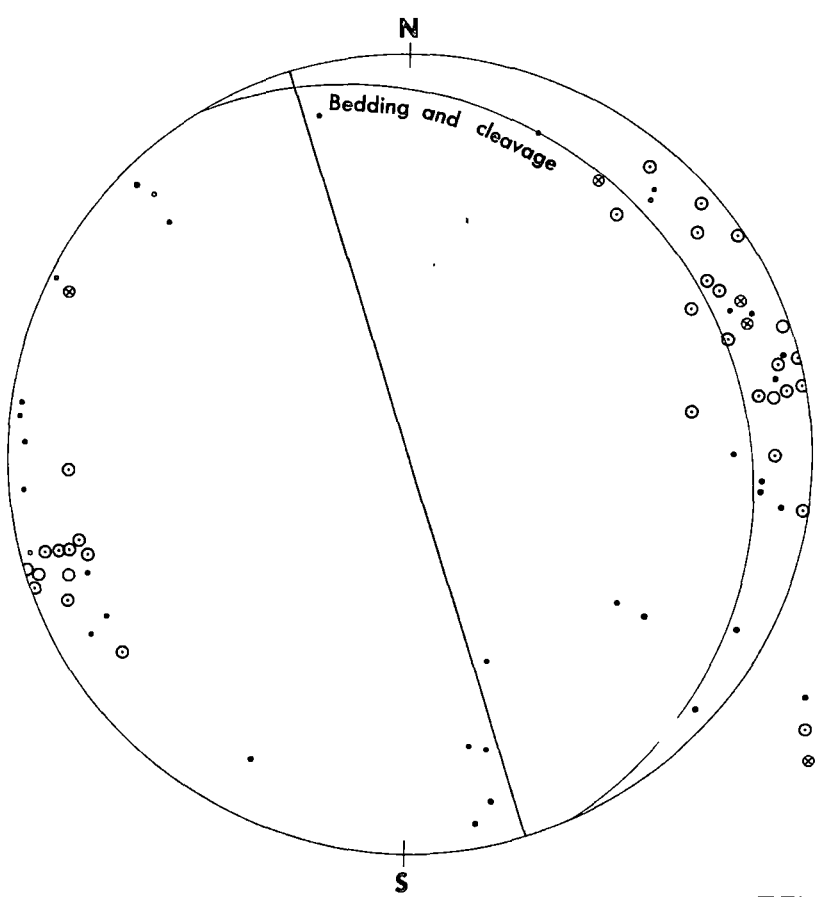

Fig. 3:15:b

PLATE 3:17

CLEAVAGE SEAMS

a. Cleavage seams disrupt bedding planes, and are more intensely developed in areas of high mudstone concentration. Specimen 48169, PPL, x 10.

b. Crenulation cleavage with associated seams superimposed on an earlier seam direction (vertical). Specimen 48167, PPL, x 10.

c. Detail of the crenulation cleavage in b. Mica flakes are dissolved strongly in limbs, and fold hinges are sharp. PPL, x 40.

d. Boundary between a cleavage zone and the surrounding rock. Specimen 48169. NX.

e. Cleavage seam, with quartz grain boundaries orientated at an angle to the seam cleavage. This direction represents an earlier cleavage. Specimen 48169.

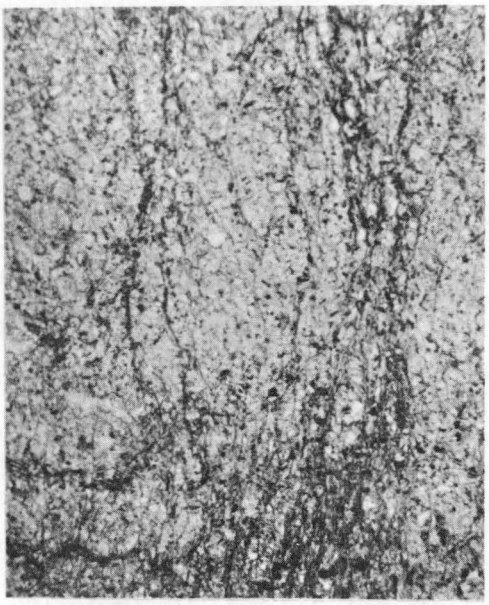

a

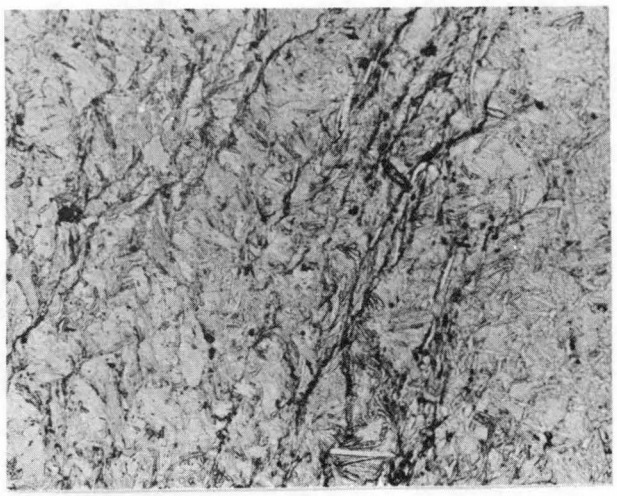

b

c

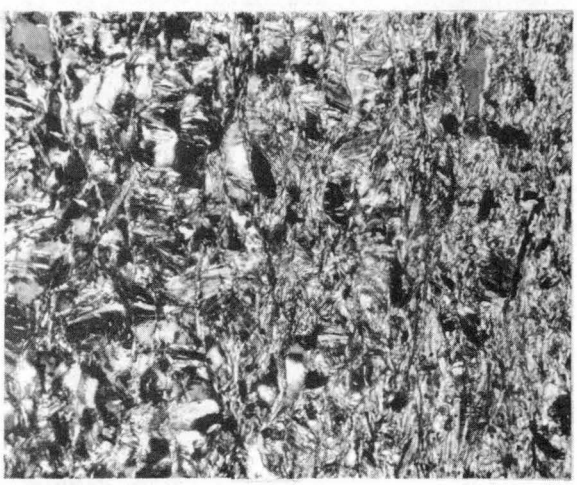

d

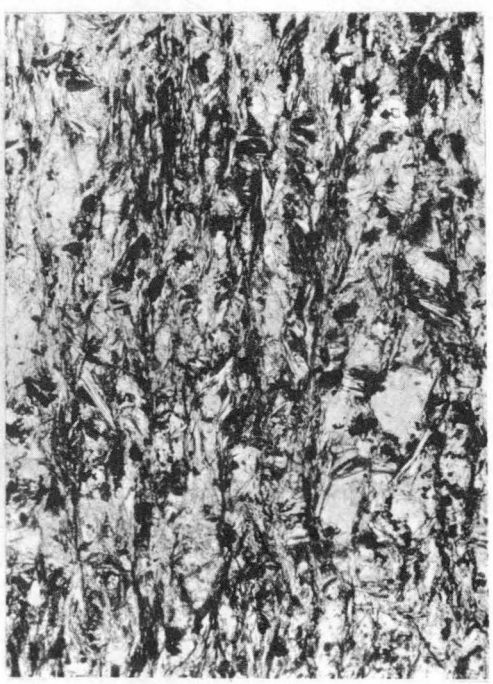

e

PLATE 3:17

PLATE 3:18

SEDIMENTARY MOBILISATION OF MUDSTONE

a. Flame structure, dominantly parallel to cleavage. Specimen 48170, PPL, x 10.

b. Detail of above. Straight flame boundary, and absence of quartz grains suggests forcible mud intrusion. PPL, x 40.

c. A mudstone intrusion parallel to a seam cleavage. Quartz grain boundaries suggest an earlier cleavage. In the mudstone, the seam cleavage is parallel to a crenulation cleavage. Specimen 48171, PPL, x 40.

d. Curved mudstone layers controlled by sandstone lens. Cleavage seams appear to truncate against the sedimentary layers. Specimen 48172, PPL, x 10.

e. Removal of a mudstone layer, by migration along weaknesses which are now preserved as micaceous seams. These are not structurally controlled. Specimen 48172. PPL, x 10.

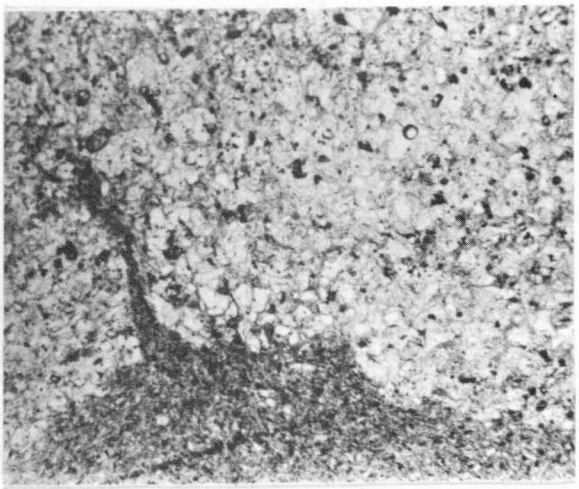

a

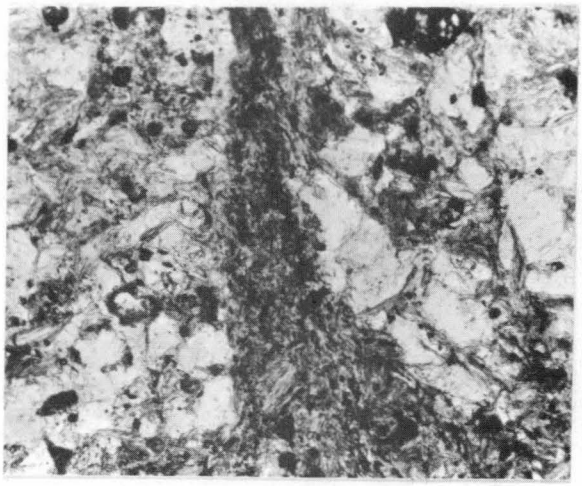

b

c

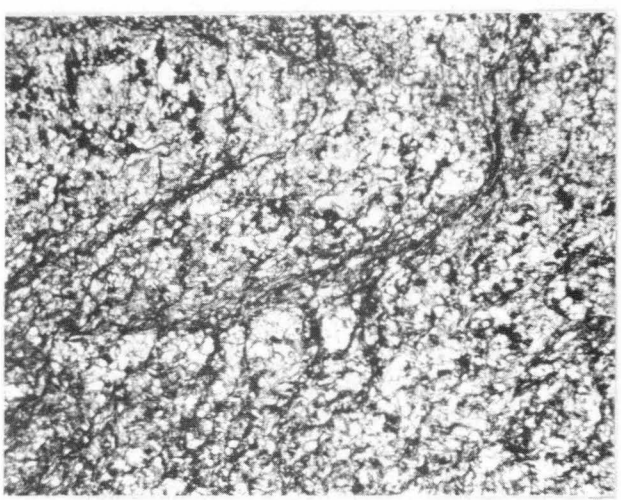

d

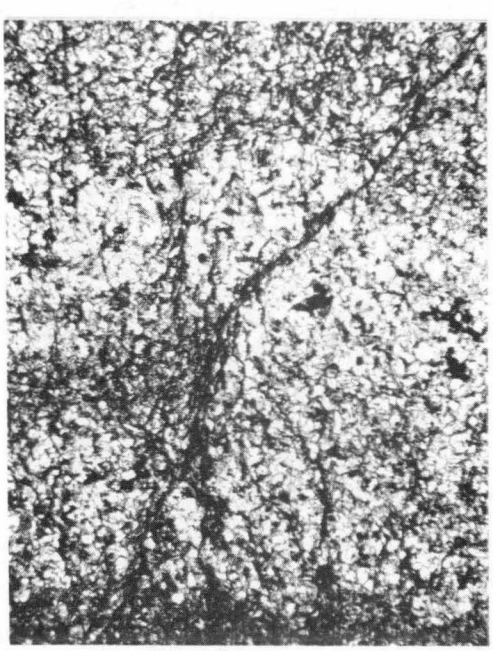

e

PLATE 3:18

PLATE 3:19

CLEAVAGE DEVELOPMENT IN OTHER ROCK TYPES

a. D_{3c} crenulation cleavage not affecting disharmonically folded sandstone layer.
Specimen 48162. PPL, x 10.

b. Crenulation cleavage in mudstone.
Specimen 48162, PPL, x 20.

c. Grain elongation and minor pressure shadows in poorly sorted sandstone.

d. Cleavage developed in phyllitic sandstone.
Specimen 48173. PPL, x 10.

e. Two cleavages formed in micaceous sandstone.
Specimen 48174. PPL, x 10.

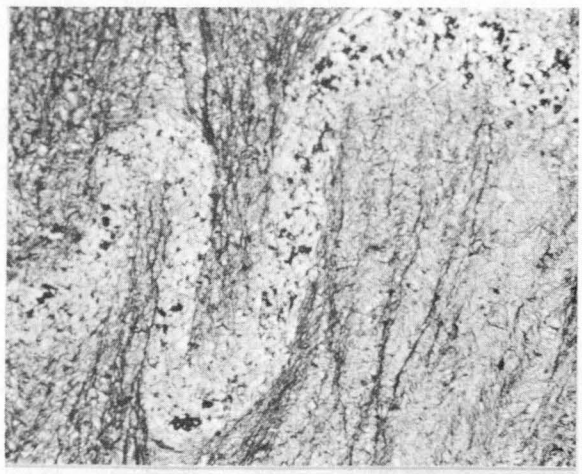

a

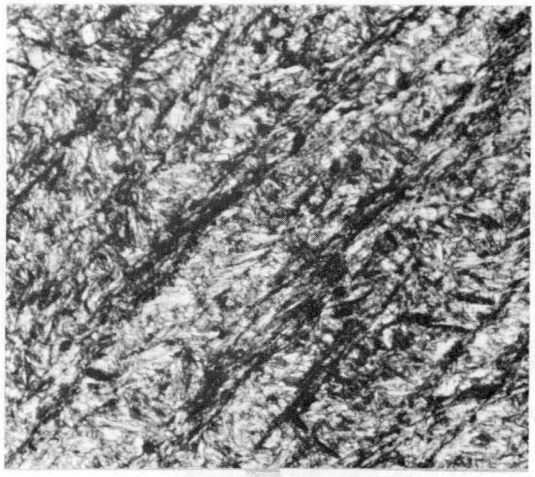

b

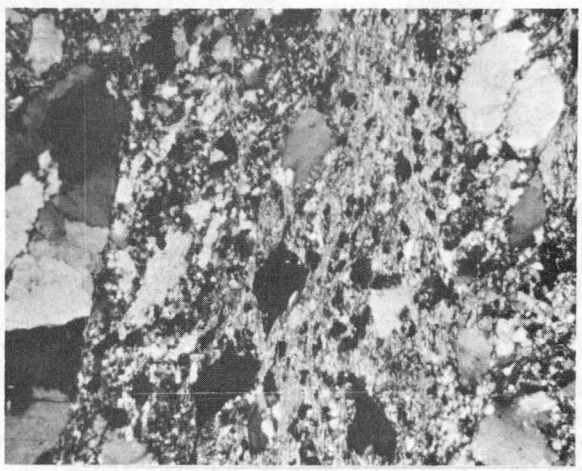

c

d

e

PLATE 3:19

PLATE 3:20

FORM OF WATER ESCAPE FOLDS, JOAN POINT SANDSTONE

a. Multiple fold formation, with two wavelengths of water escape channels present.

b. Elongation of folds in the S_{3c} cleavage direction. Cross-section.

c. Elongation of folds on the bedding plane, parallel to the bedding-cleavage intersection.

Scale in centimetres.

a

b

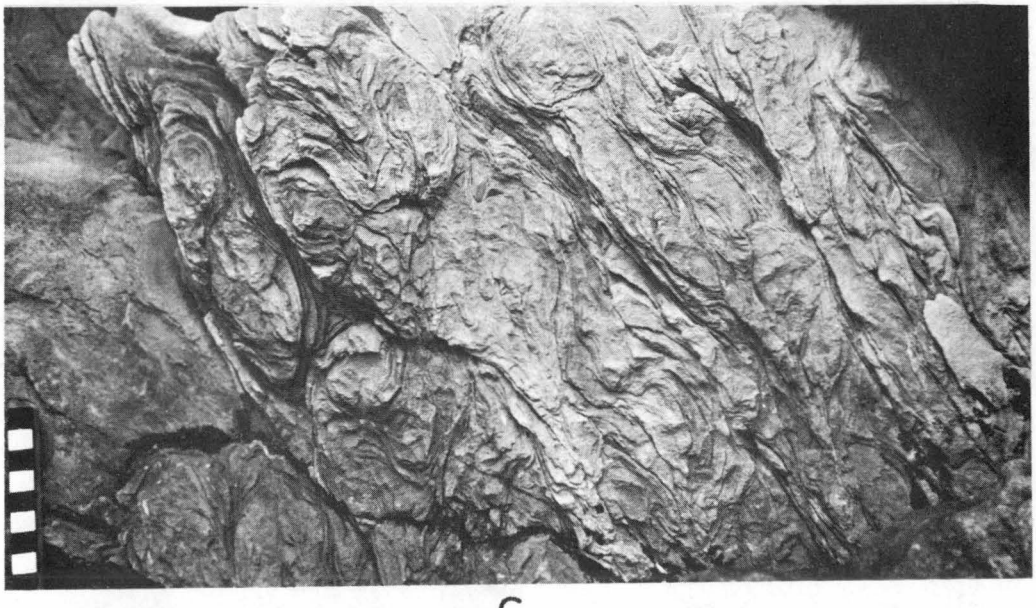

c

PLATE 3:20

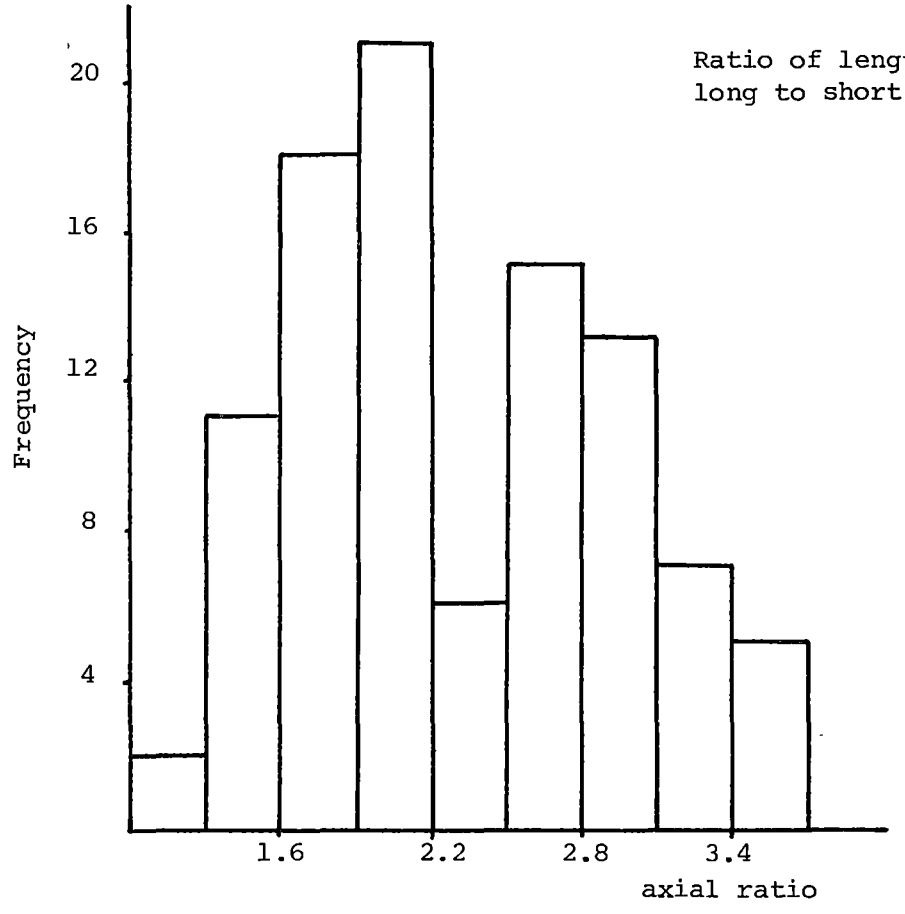

a.

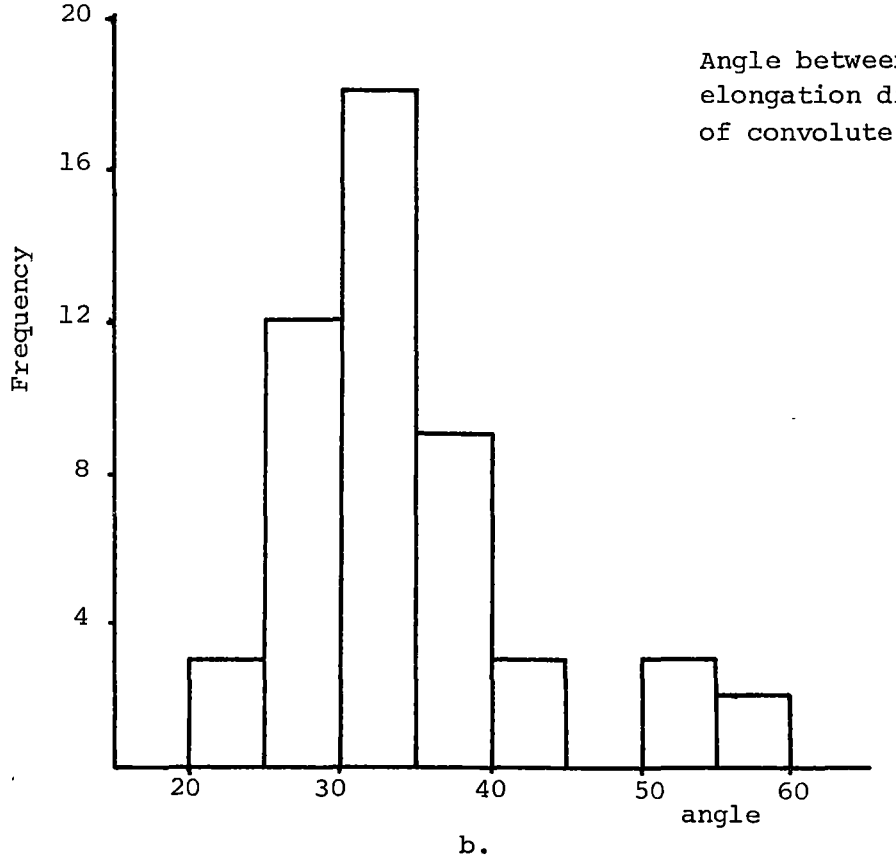

b.

GEOMETRY OF CONVOLUTE FOLDS

FIGURE 3:16

Figure 5:1

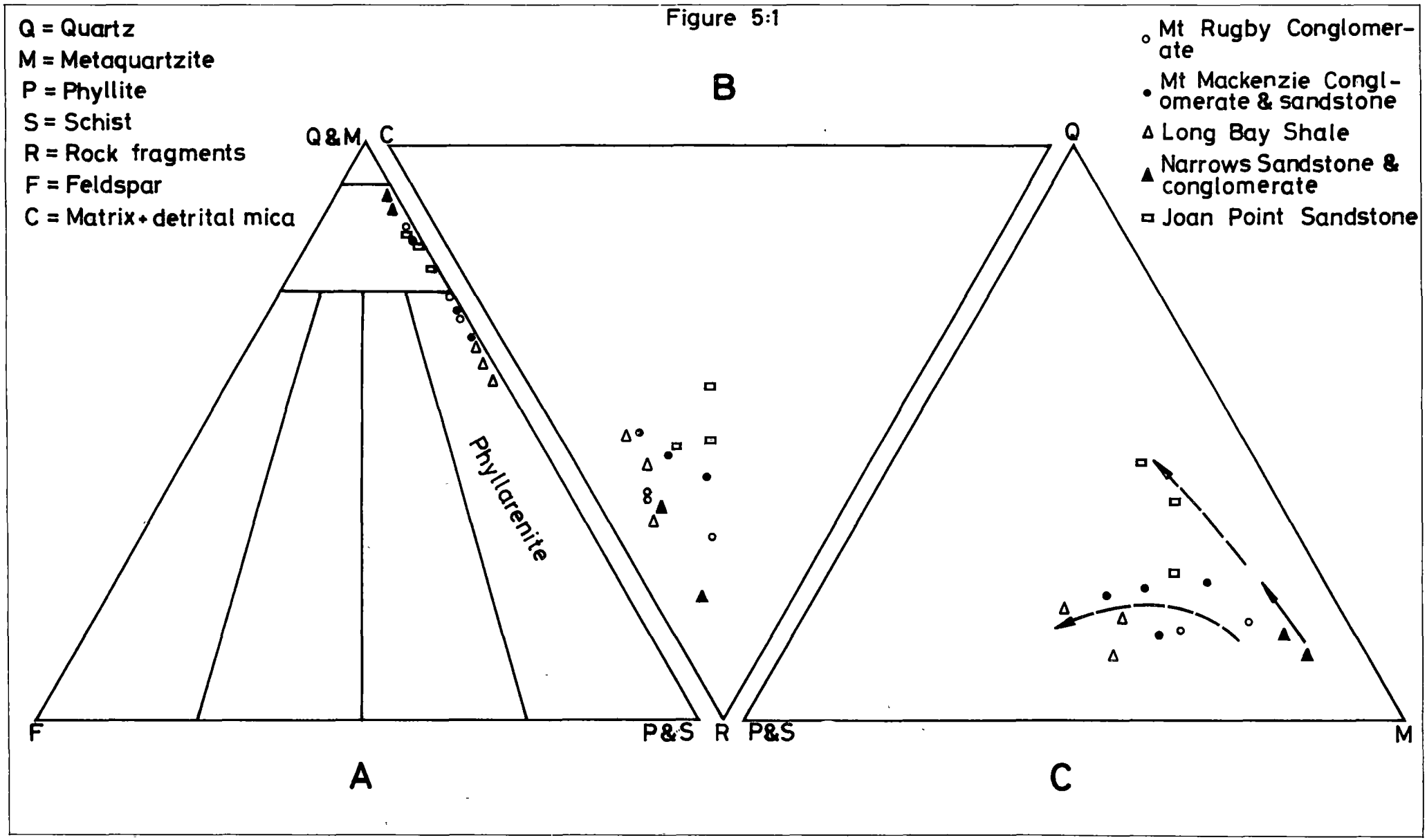
Q = Quartz
M = Metaquartzite
P = Phyllite
S = Schist
R = Rock fragments
F = Feldspar
C = Matrix + detrital mica
Mt Rugby Conglomerate
Mt Mackenzie Conglomerate & sandstone
Long Bay Shale
Narrows Sandstone & conglomerate
Joan Point Sandstone
B
Q&M
C
Q
Phyllarenite
F
P&S
R
P&S
M
A
C

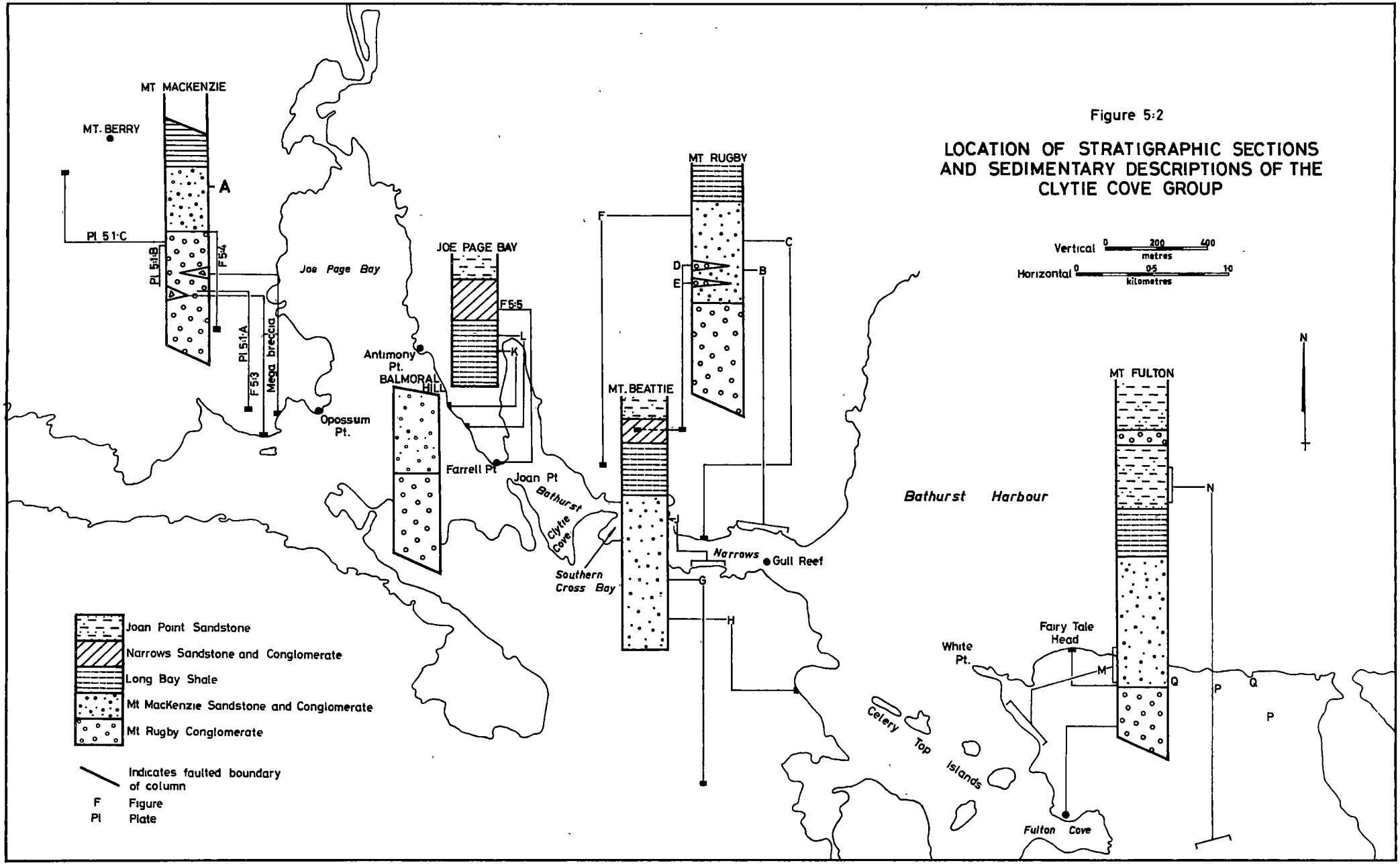

Figure 5:2

LOCATION OF STRATIGRAPHIC SECTIONS AND SEDIMENTARY DESCRIPTIONS OF THE CLYTIE COVE GROUP

PLATE 5:1

a. A typical boulder conglomerate of the Mt Rugby Conglomerate. Note crude graded bedding. Mt MacKenzie.

b. Non-spherical clasts showing a well developed grain alignment parallel to bedding. Some of the smaller grains have been rotated towards the cleavage direction (almost vertical). Mt MacKenzie Section.

c. Interdigitating sandstone and fine-grained conglomerate. Mt Berry.

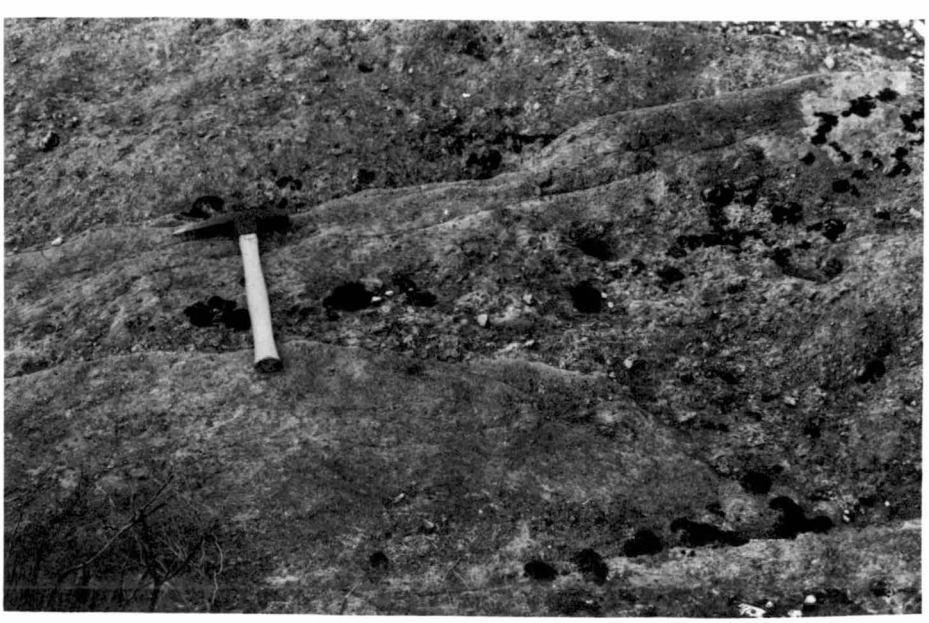

FIGURES 5:3 and 5:4

GRAINSIZE ANALYSES OF MT RUGBY CONGLOMERATE

a. From Mt MacKenzie (GR227014). Histogram of frequency against grainsize.

b. As above from GR225013.

c. Cumulative curves plotted from the histograms.

FIGURE 5:4

a. Mt Rugby Conglomerate (GR228010)

b. Alignment of discoidal clasts in the Mt Rugby Conglomerate (GR222020).

c. Grainsize against frequency from the Mt Rugby Conglomerate (GR220028).

d. Grainsize against frequency from the Mt MacKenzie formation, adjacent to the Mt Rugby Conglomerate (GR220028).

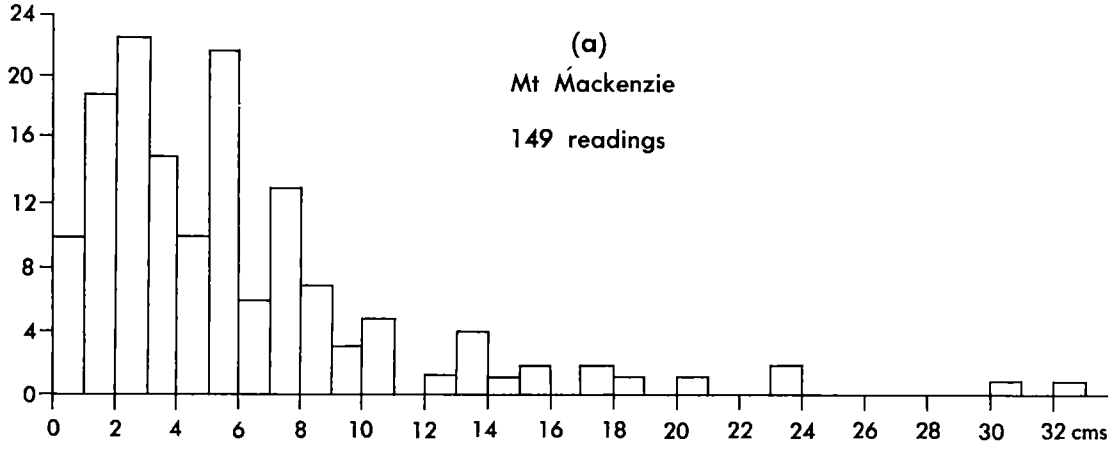

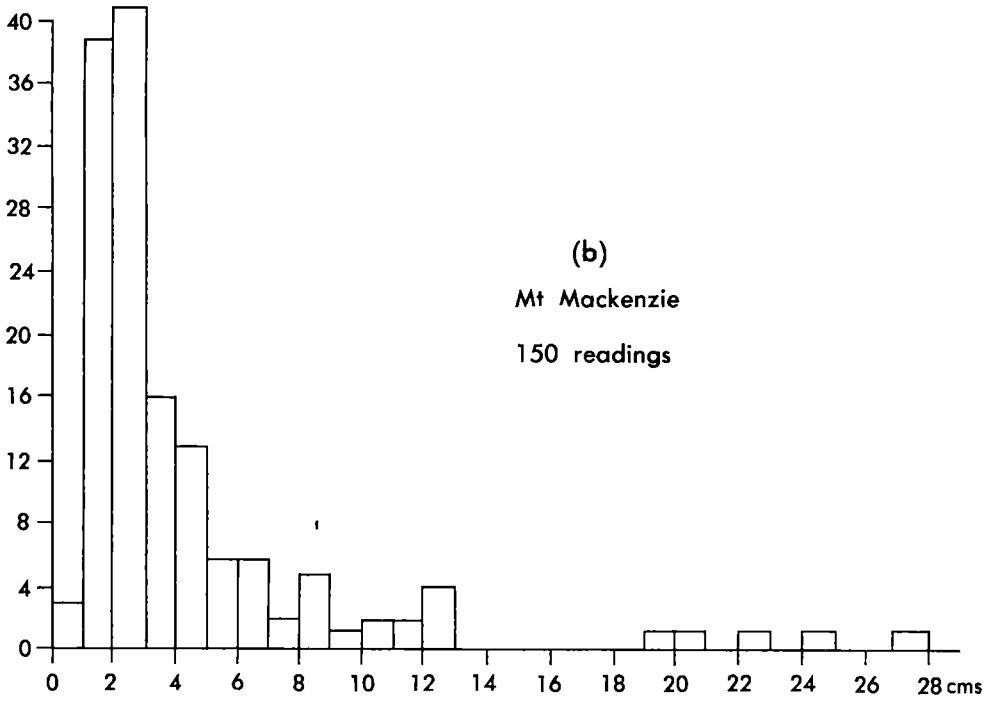

(c)
Cumulative curves;
Mt Mackenzie conglomerate

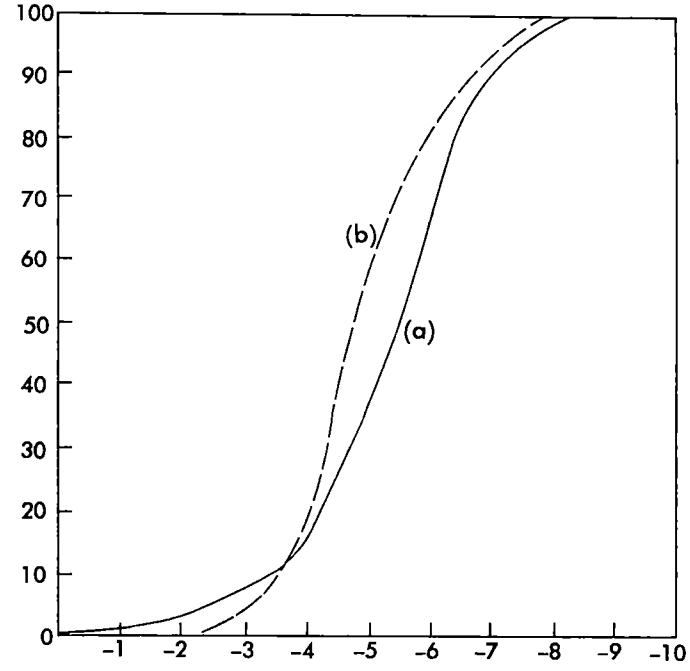

Figure 5:3

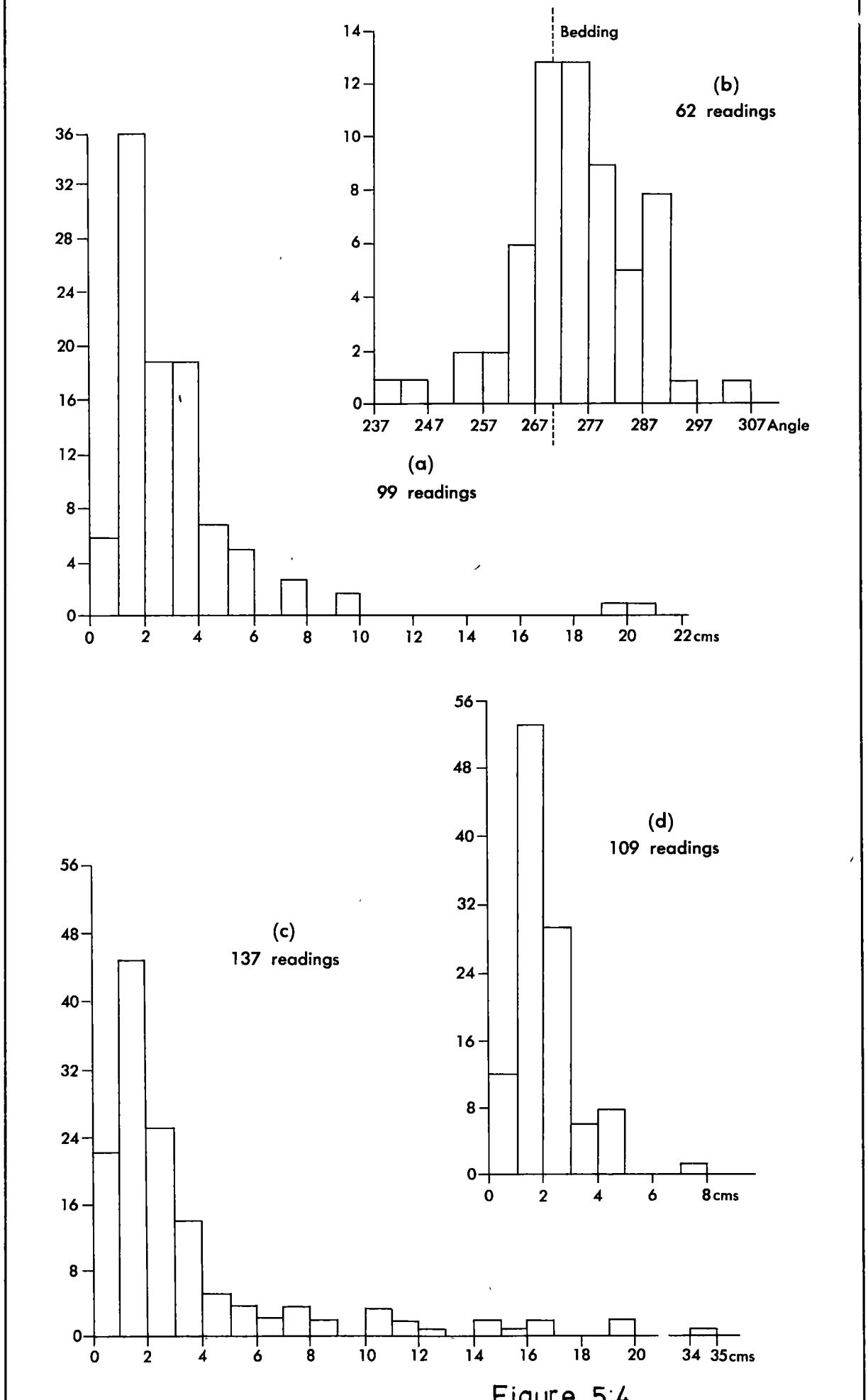
Bedding
(b)
62 readings
14
12
10
8
6
4
2
0
237 247 257 267 277 287 297 307 Angle
(a)
99 readings
36
32
28
24
20
16
12
8
4
0
0 2 4 6 8 10 12 14 16 18 20 22cms
(d)
109 readings
56
48
40
32
24
16
8
0
0 2 4 6 8cms
(c)
137 readings
56
48
40
32
24
16
8
0
0 2 4 6 8 10 12 14 16 18 20 34 35cms

Figure 5:4

PLATE 5:2

a. Matrix of Mt Rugby Conglomerate. Quartz, metaquartzite fragments are common, and phyllite fragments are aligned parallel to cleavage. Specimen 48196. PPL, x 10.

b. Matrix of Mt Rugby Conglomerate. Angular fragments are coated with opaque minerals. Specimen 48197. PPL, x 10.

c. As above, with crossed nicols, showing sutured grain boundaries and triple junctions.

d. Lithic greywacke from the Mt Rugby Conglomerate. The matrix is indistinguishable from deformed phyllite clasts. Specimen 48198. PPL, x 10.

e. Laminated siltstone from the Mt MacKenzie formation. Laminae are defined by phyllite fragments and mica flakes parallel to the bedding. Specimen 48199. PPL, x 40.

f. Polymict lithic greywacke from the Mt MacKenzie formation. Note angularity of the grains. Specimen 48203. PPL, x 10.

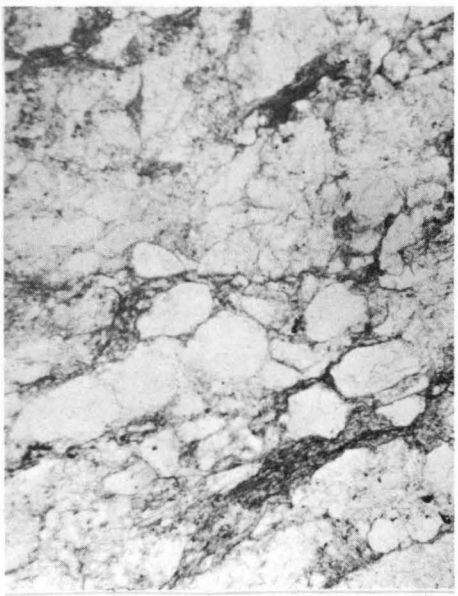

a

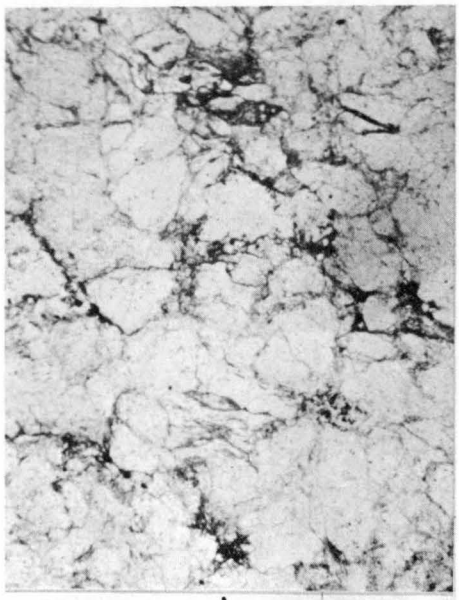

b

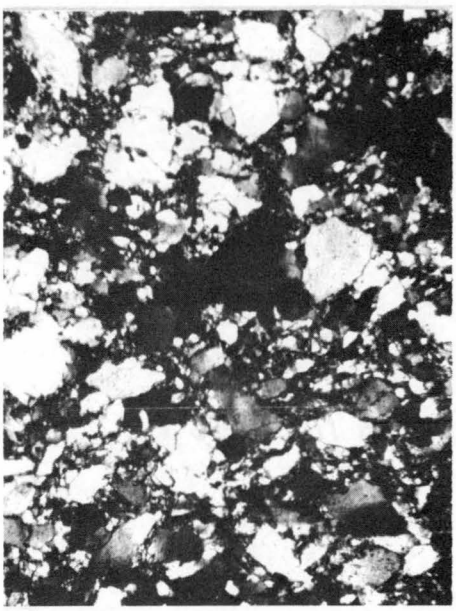

c

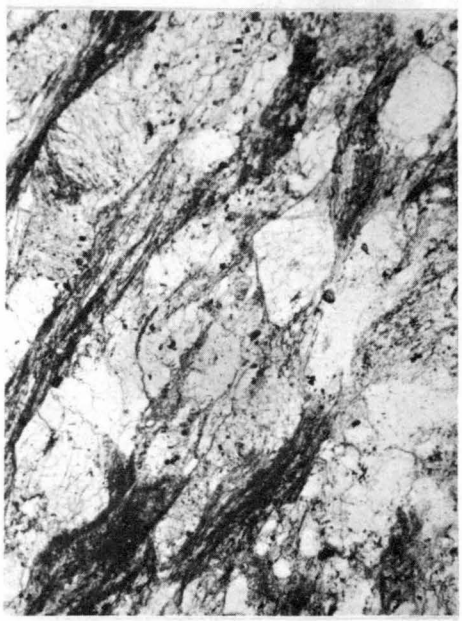

d

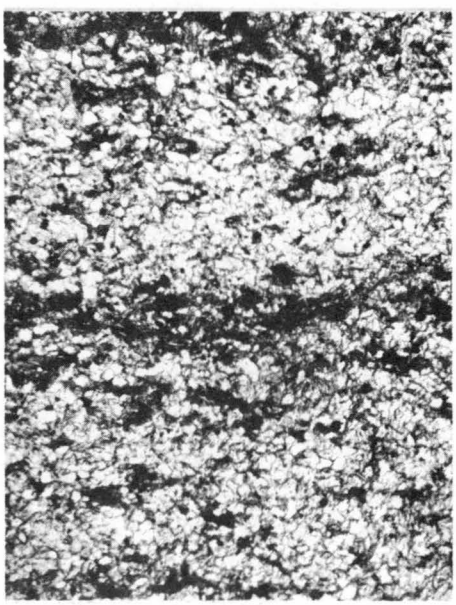

e

f

PLATE 5:2

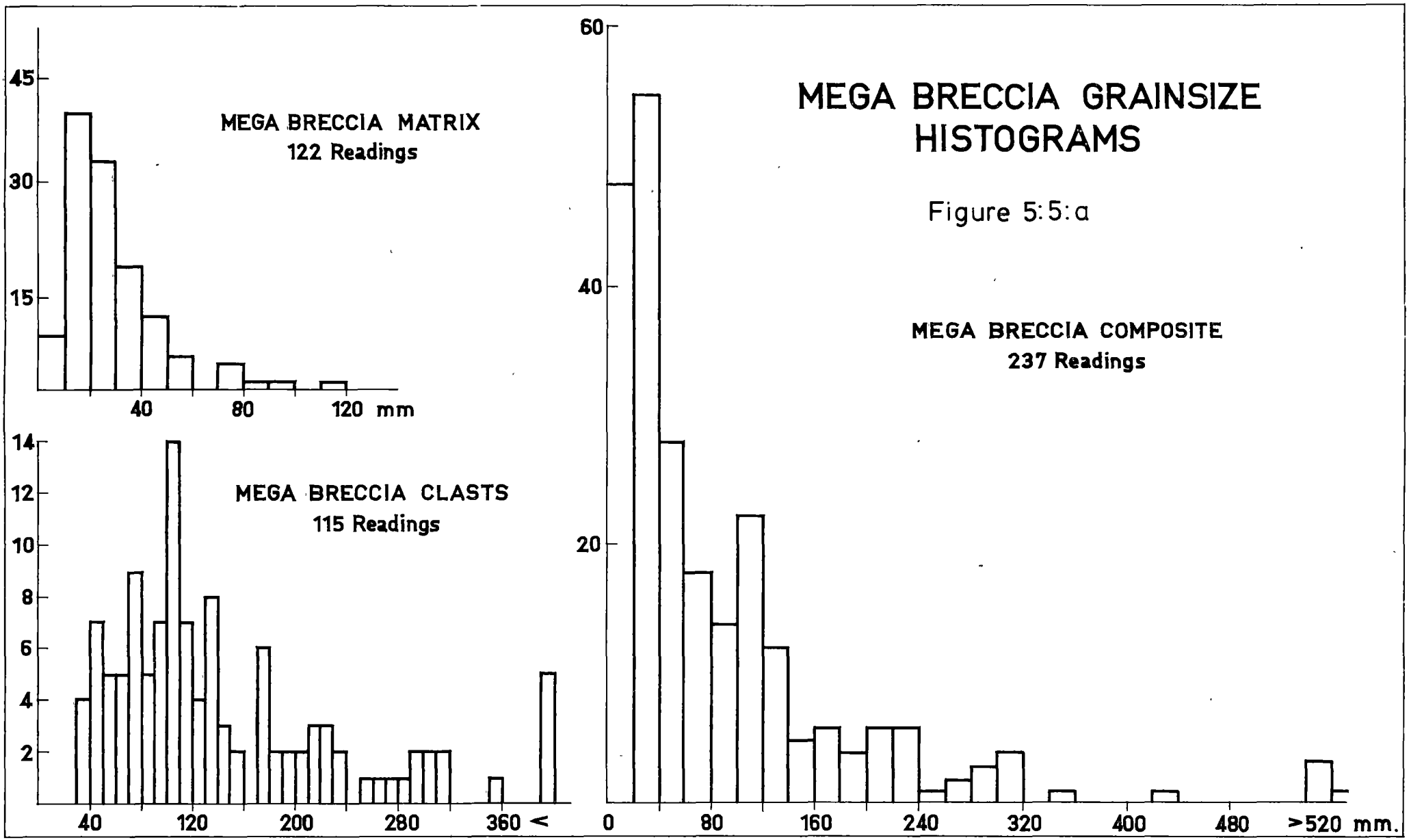
MEGA BRECCIA GRAINSIZE HISTOGRAMS
Figure 5:5:a
MEGA BRECCIA MATRIX
122 Readings
45
30
15
40
80
120 mm
MEGA BRECCIA CLASTS
115 Readings
14
12
10
8
6
4
2
40
120
200
280
360 <
MEGA BRECCIA COMPOSITE
237 Readings
60
40
20
0
80
160
240
320
400
480
>520 mm.

CUMULATIVE CURVES FOR MEGA BRECCIA
ARITHMETIC - PROBABILITY PLOT

Figure 5:5:b

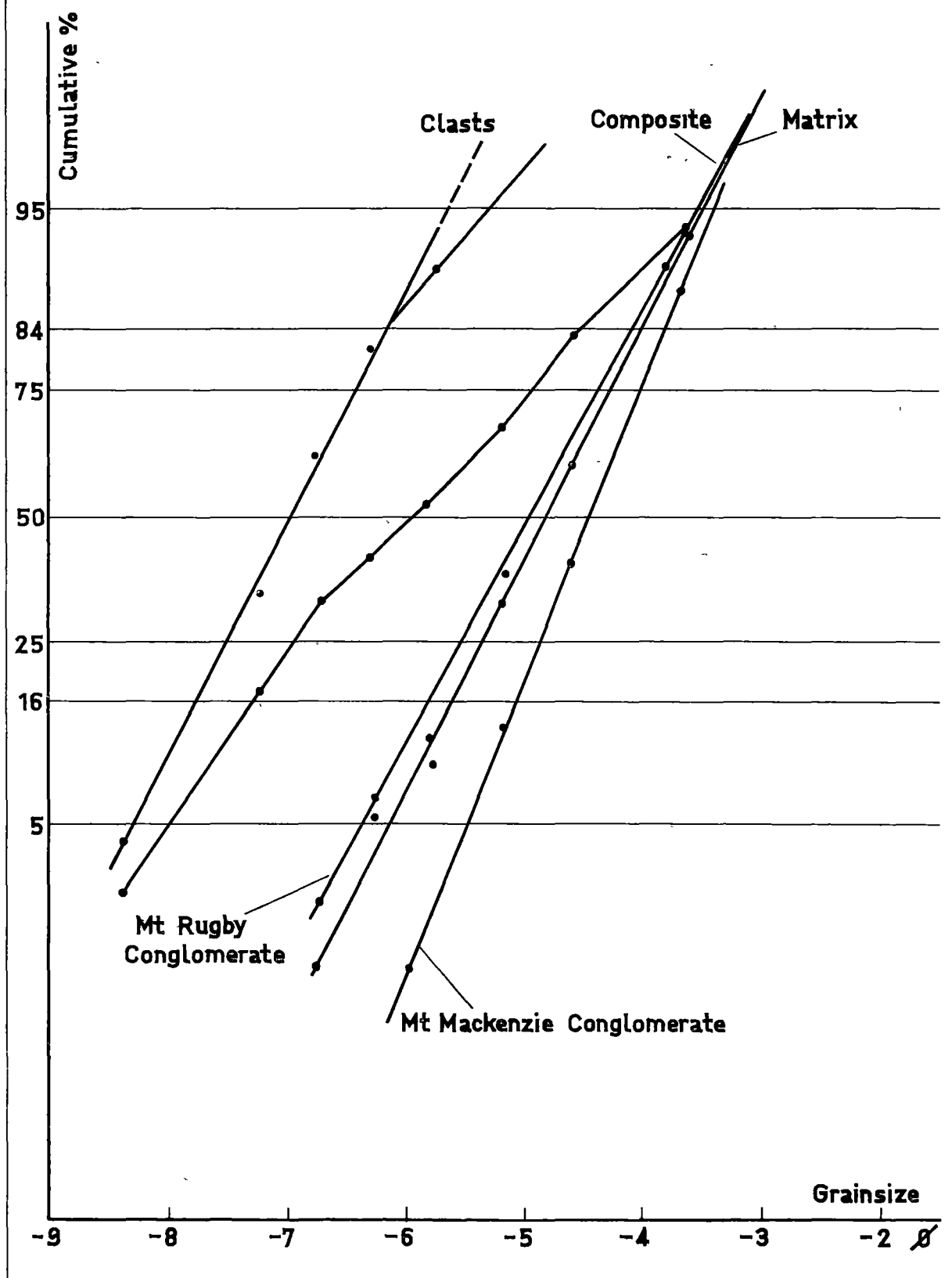

PLATE 5:3

a. Open framework conglomerate developed close to the contact between the Long Bay Shale and metamorphic rocks at Antimony Point. Photograph is looking downwards and clast alignment is parallel to the boundary fault, and a cataclastic cleavage. Scale divisions are centimetres.

b. Normally graded beds, 30 m stratigraphically above a. Faint lamination has developed above the graded interval. The beds are amalgamated.

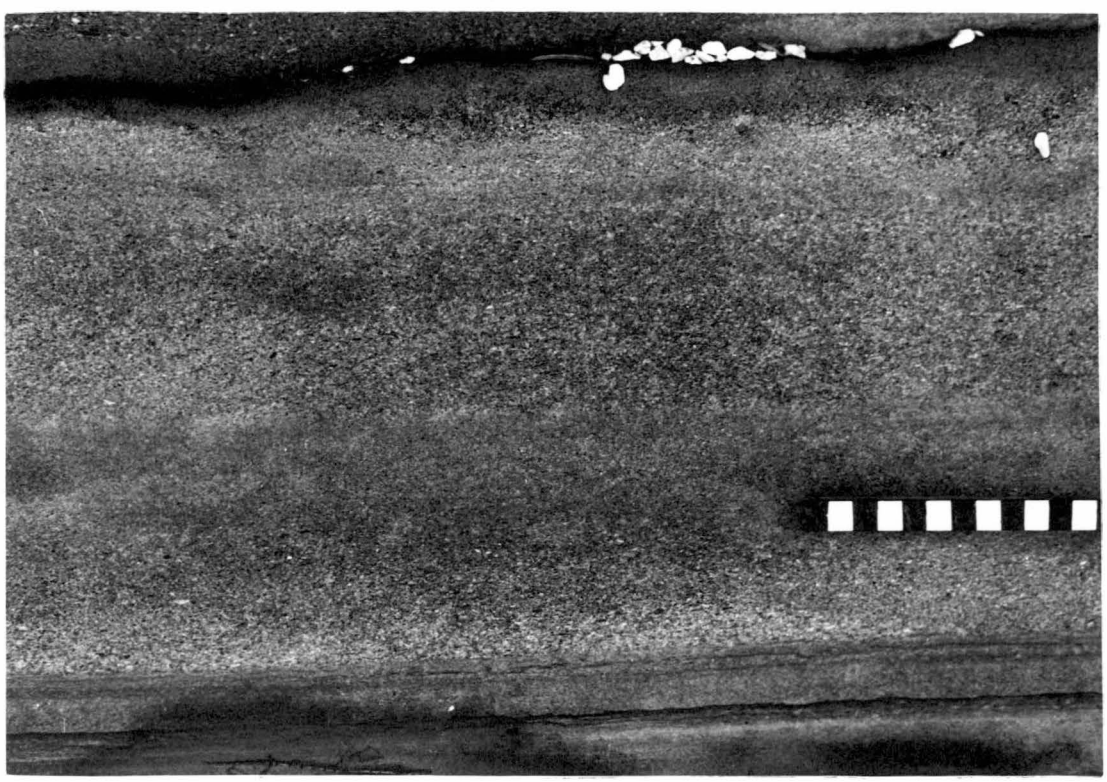

PLATE 5:4

a. Slump folds and contorted bedding confined between parallel bedded sequences. These are formed below a water interface as fold limbs are truncated by the overlying bed. Scale is in centimetres.

b. Coarser grained beds in the Long Bay Shale. Clasts have the appearance of lag deposits, the coarse-grained material collecting in bottom surface irregularities and being bypassed by the flow. The sand deposit is from a later part of the flow. Attests to the bottom hugging nature of the currents. Note the coarse clast alignment in the cleavage direction (parallel to scale), from an original bedding parallel fabric.

PLATE 5:5

a. Normal coarse-grained component of the Long Bay Shale. Clasts are of many types, have a low rounding and occur in poorly-sorted rocks. The structure is a load cast. Note the alignment of clasts parallel to the boundaries of the load.
Scale in centimetres.

b. Typical sequence of turbidite-deposited beds showing Bouma sequences and parts of Bouma sequences. Some very thin bedded layers are isolated ripple marks. These are also common in other, shallow water, environments.

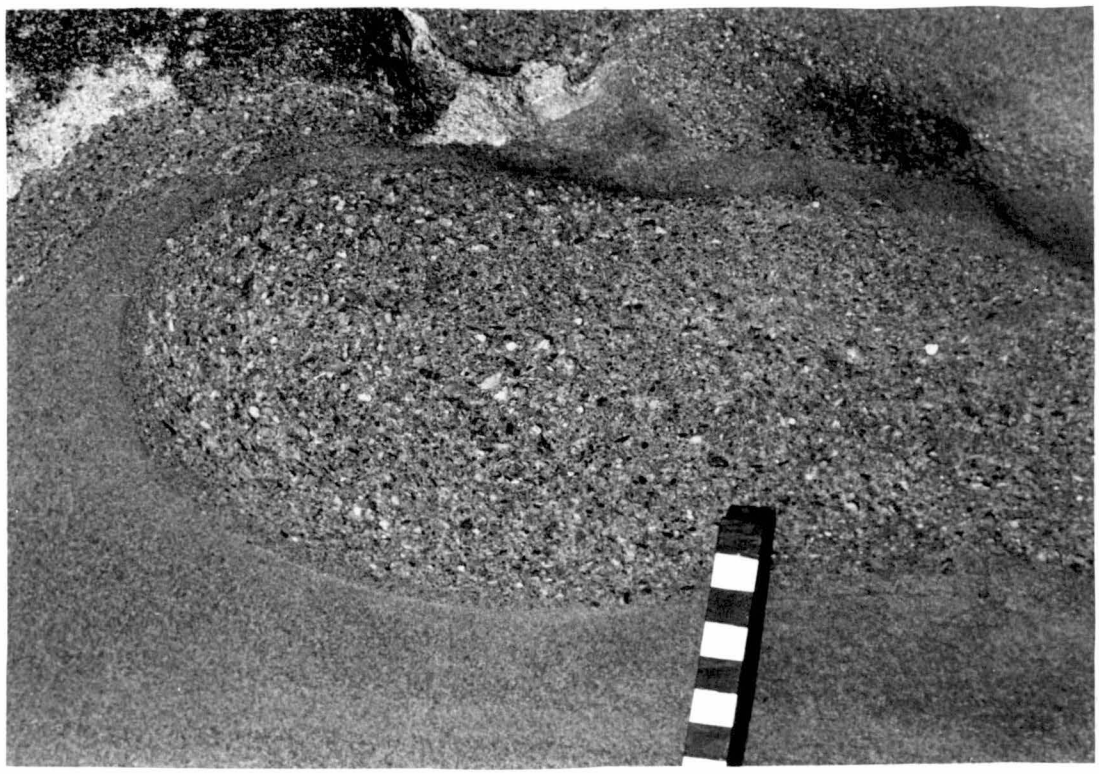

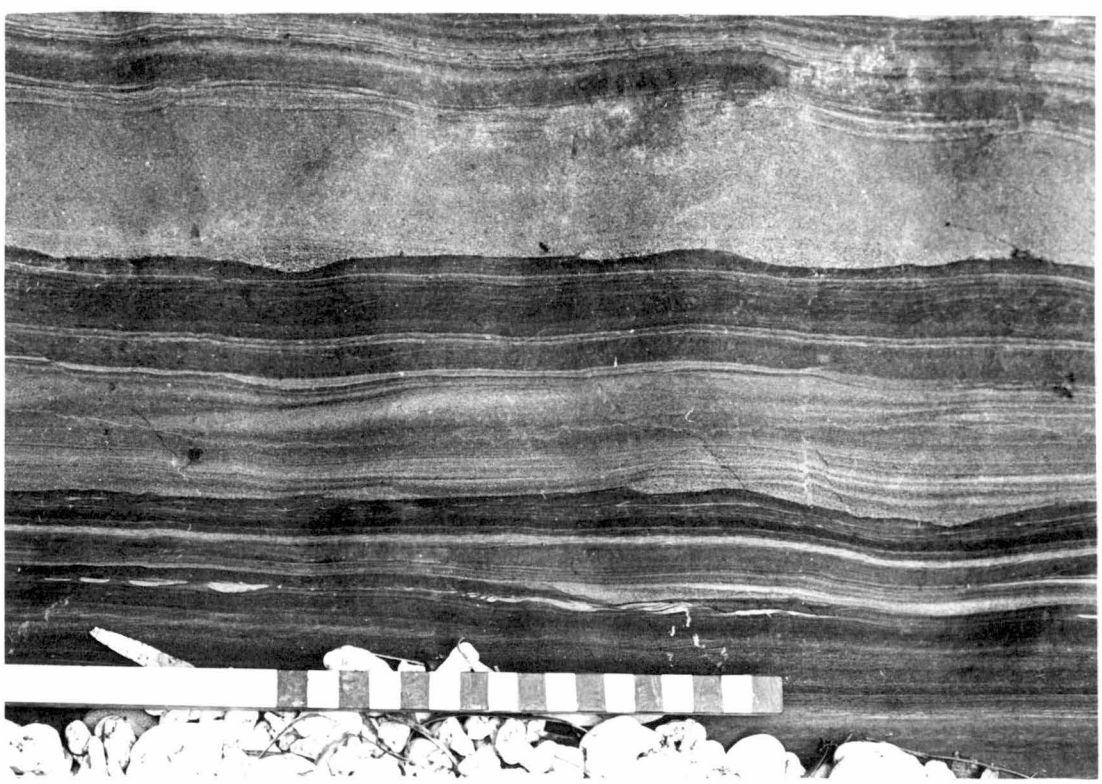

PLATE 5:6

a. A sequence of thin turbidite beds showing Bouma B and C divisions, with D divisions only poorly developed as occasional thin silty laminae. The mudstone may be a pelagic deposit.

b. A sequence of turbidites with well developed B and C divisions, with climbing ripples, but only very small amounts of interbedded mudstone. This is close to the Narrows Conglomerate and represents a lateral facies equivalent of much coarser and thicker flows of a prograding shallow channel system.

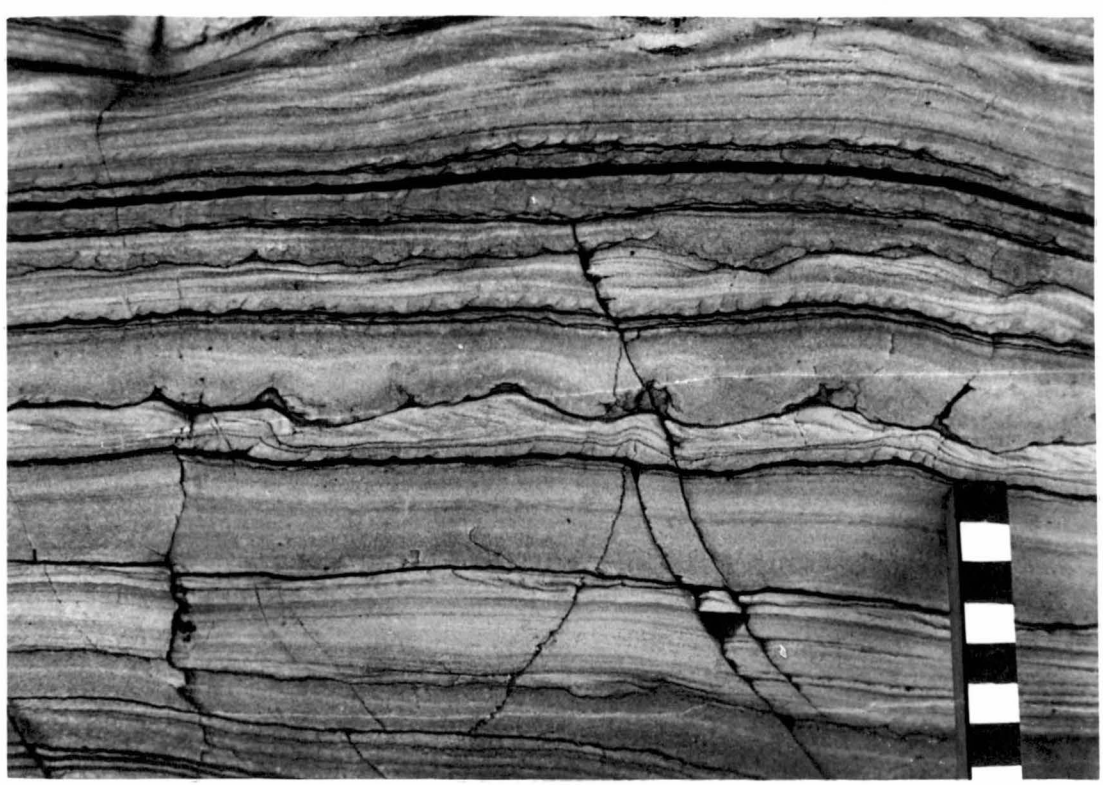

PLATE 5:7

a. Thin-bedded turbidites with the Bouma B and C divisions well developed. This shows a large number of flows in rapid succession, probably lateral equivalents of much thicker and possible coarser-grained flows.
Long Bay Shale, scale in centimetres.

b. Thin-bedded turbidites with a greater relative abundance of mudstone. The sandstone to mudstone ratio increase upwards. All beds imply that traction conditions were operating at deposition.
Long Bay Shale, just below the Narrows Formation.

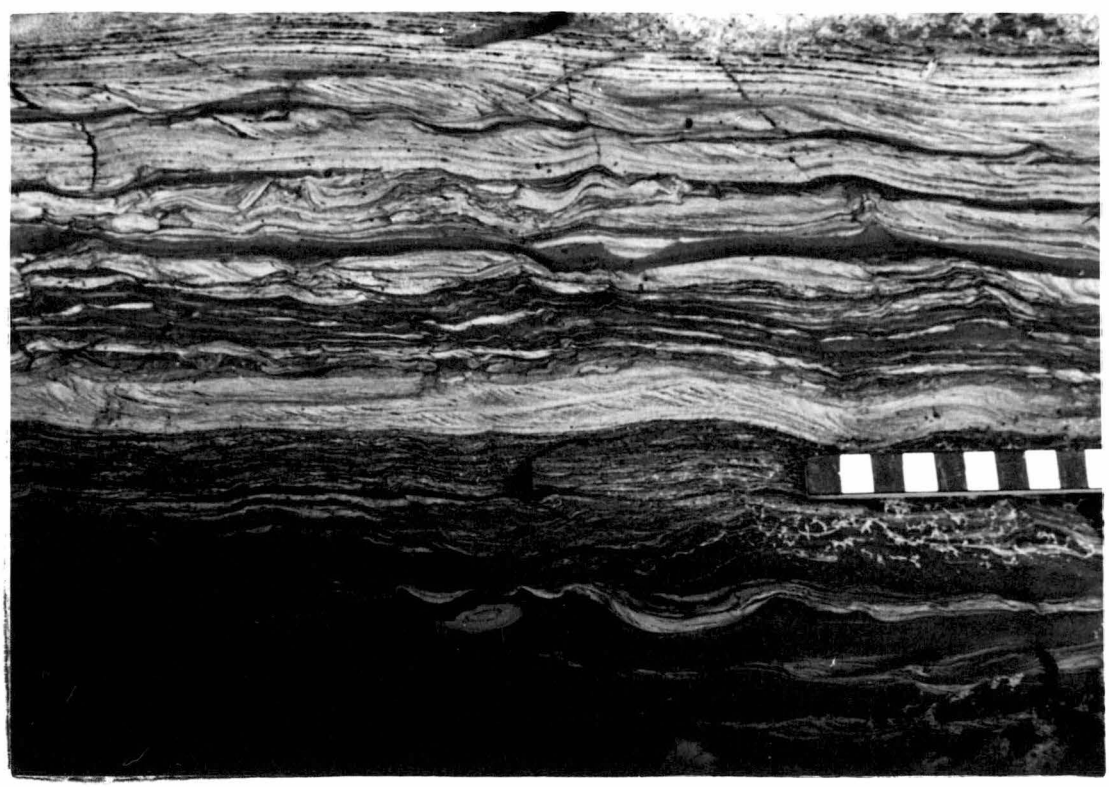

PLATE 5:8

a. Correlate of the Long Bay Shale. Shows poor sorting, high matrix component, low rounding and polymict nature of the lithic greywacke. Specimen 48173, PPL, x 10.

b. Narrows Sandstone and Conglomerate. Polymict lithic greywacke. Contains a lower matrix percentage than most greywacke from the formation. Specimen 48180, PPL, x 10.

c. Narrows Sandstone and Conglomerate. Cleaner sandstone showing the degree of grain boundary alteration. The original matrix component cannot be accurately determined. Specimen 48204, NX, x 10.

d. Joan Point Sandstone. The matrix component is about 10% and abundant detrital mica (phengite) is present. Opaque minerals are abundant. Specimen 48185, PPL, x 10.

e. Mt Rugby Correlate at Mt Fulton. Polymict sandstone with abundant opaque minerals and altered grain boundaries. Specimen 48206, PPL, x 40.

f. Mt Rugby Correlate at Mt Fulton. Fine-grained conglomerate with a continuous framework. All grainsizes are present down to the matrix. Specimen 48207, PPL, x 10.

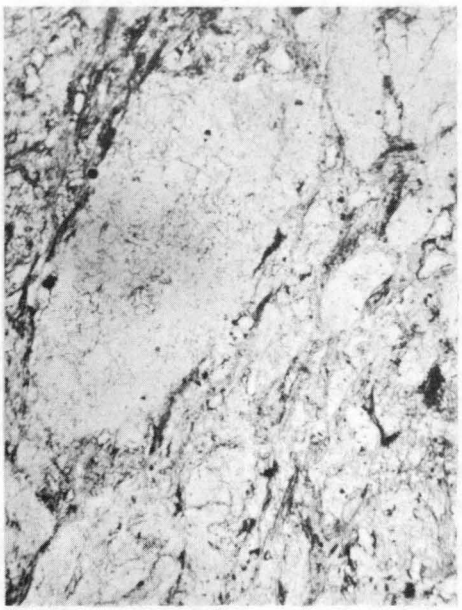

a

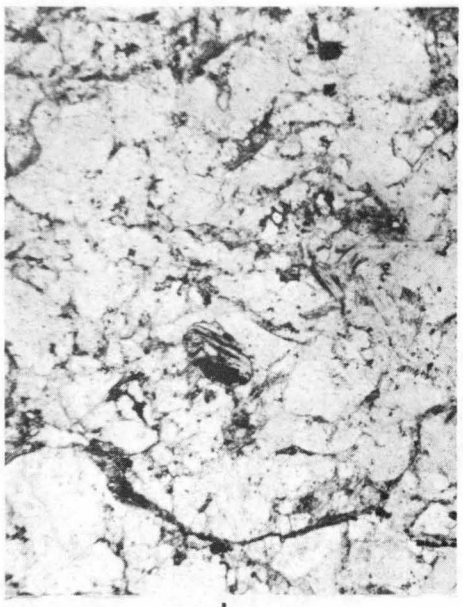

b

c

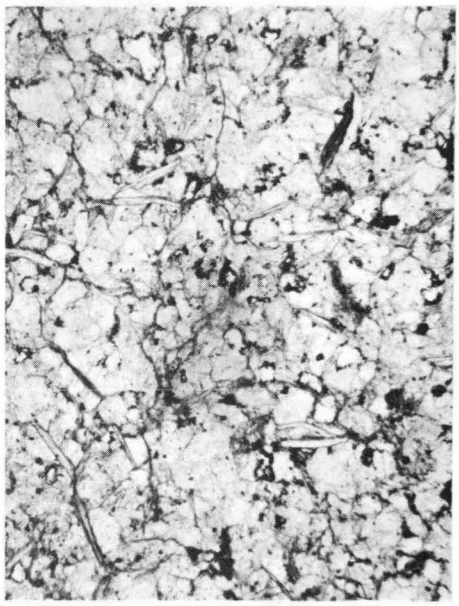

d

e

f

PLATE 5:8

PLATE 5:9

a. The basal bed of the Narrows Sandstone and Conglomerate. High angle imbrication is not parallel to cleavage. The bed is normally graded and contains a sedimentary clast with preserved bedding.
Scale is in centimetres.

b. Cross-bedding developed in a channel in the Narrows Formation. The direction of the channel is out of the page, at right angles to the dip direction of the cross-bedding laminae.

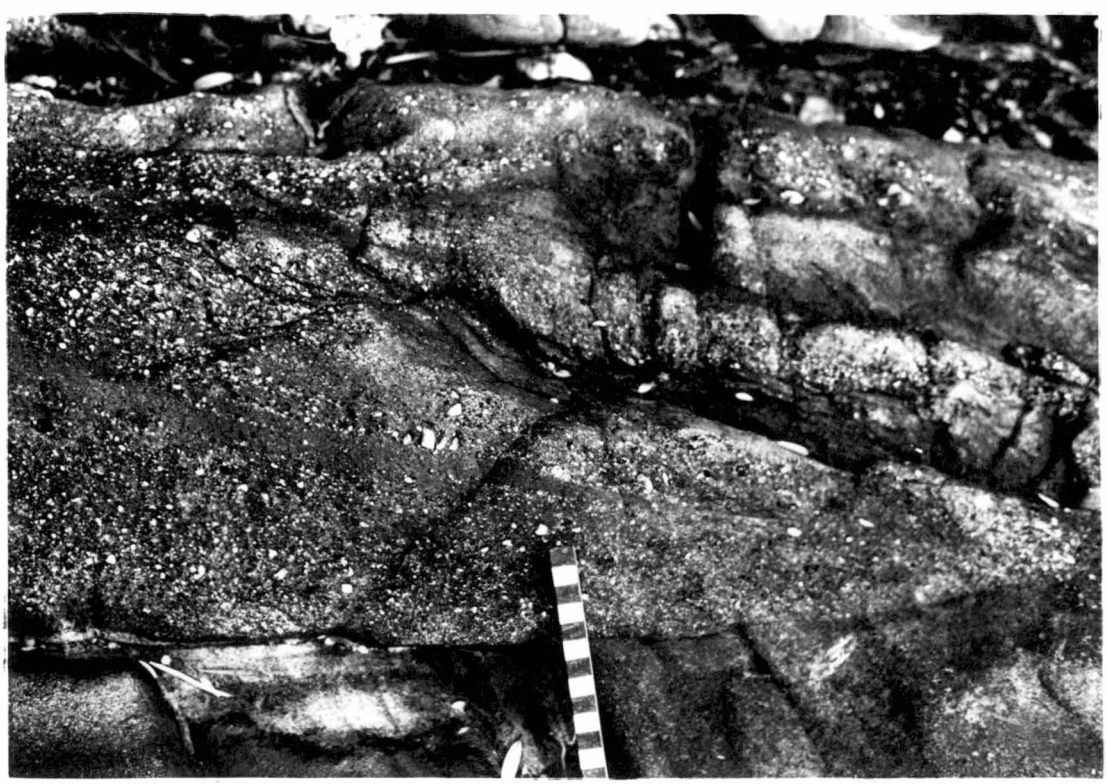

PLATE 5:10

a. Outsized clast in a graded sandstone bed from the Mt Rugby Correlate at Mt Fulton. Note well defined cleavage.
Lens cap is 50 mm in diameter.

b. Load structure at the base of a graded pebbly sandstone bed. The load has been accentuated tectonically and now has boundaries parallel to cleavage.


ASAHI
PENTAX


ASAHI
PENTAX

CHANNEL-FILL STRUCTURES, NARROWS FORMATION

Figure 5:6

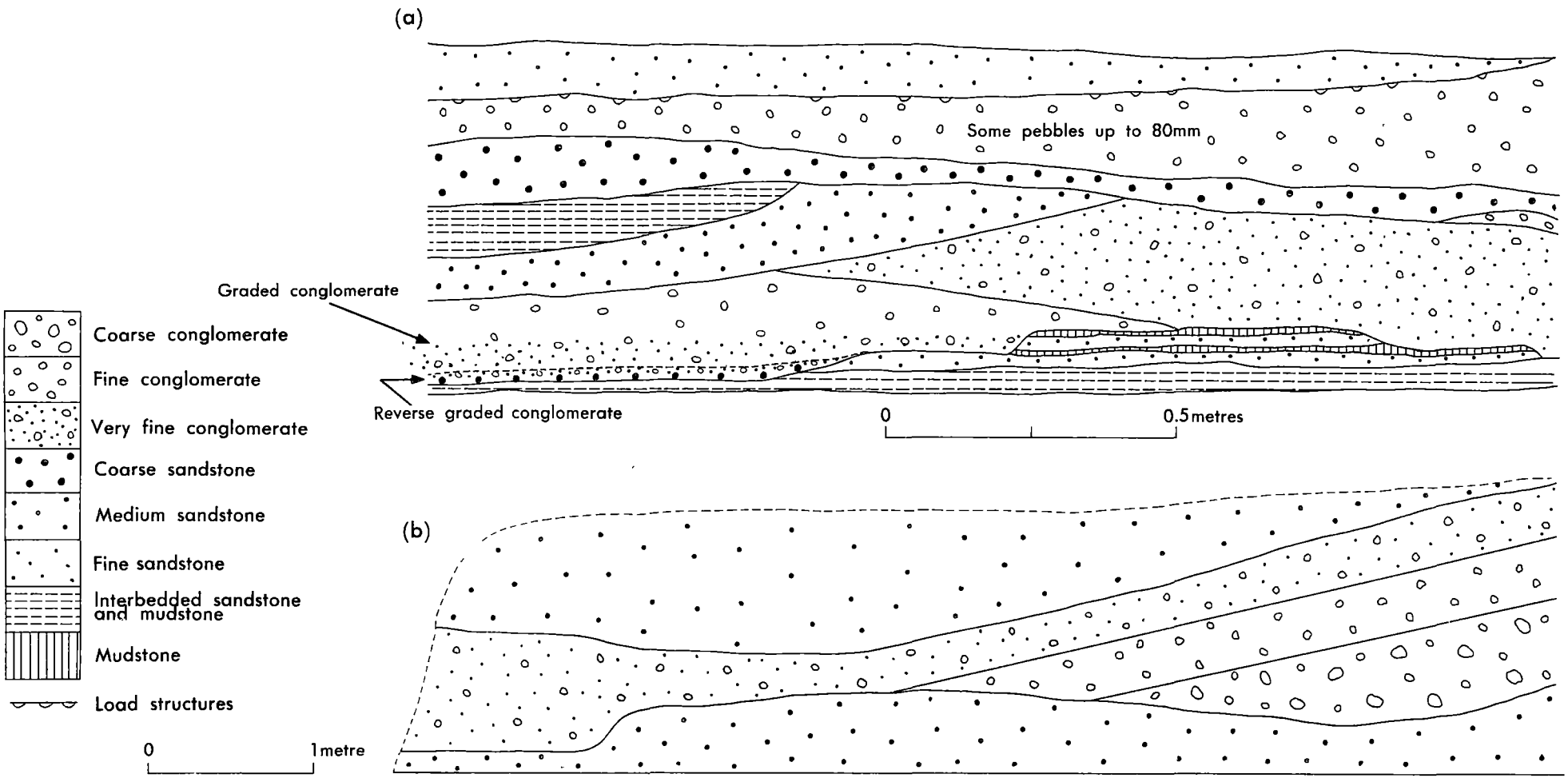

PLATE 5:11

a. A poorly sorted, thick-bedded conglomerate north-west of Fulton Cove. Numerous phyllite clasts occur. This is interbedded with thin sandstone beds.
Hammer is 0.6 m long.

b. An open framework conglomerate with sandy levels at the base and top of the bed. Note angularity of the grains.
Lens cap is 50 mm in diameter.


PENTAX

PLATE 5:12

a. Mt Rugby Correlate. Very poorly sorted lithic greywacke. Large clast has scalloped grain boundary, implying alteration. Specimen 48211. PPL, x 10.

b. Mt MacKenzie Sandstone and Conglomerate Correlate. Polymict lithic greywacke with angular clasts. Cleavage is well developed. Specimen 48158. PPL, x 10.

c. Sandstone-Conglomerate sequence, north of Mt Fulton. Poorly sorted lithic greywacke, continuous framework and high matrix component. Specimen 48181. PPL, x 10.

d. Sandstone-Conglomerate sequence. Discontinuous framework of lithic greywacke. Strongly deformed clasts. Specimen 48214. PPL, x 10.

e. Sandstone-Mudstone sequence. Silty mudstone with numerous opaque grains. Note the crenulation cleavage. Specimen 48216. PPL, x 10.

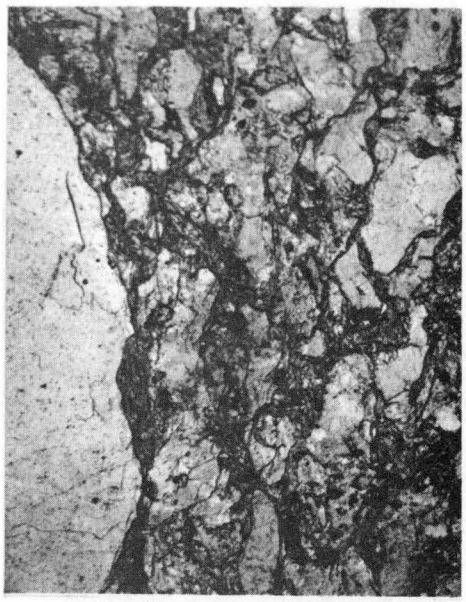

a

b

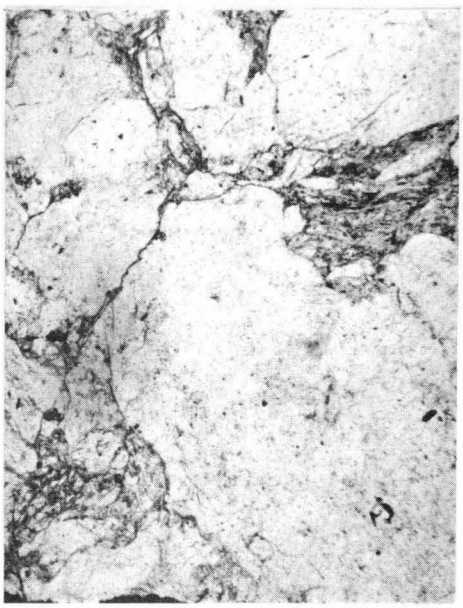

c

d

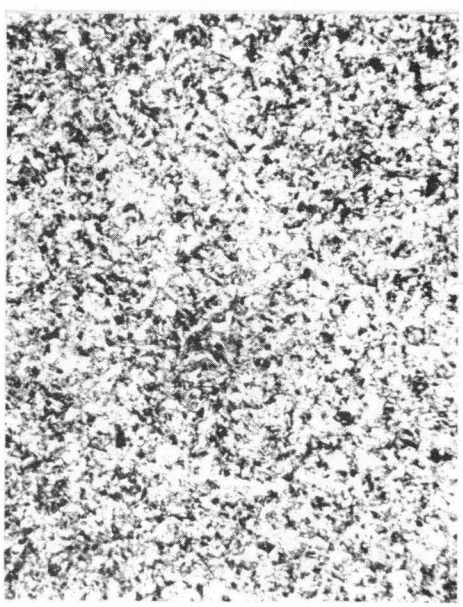

e

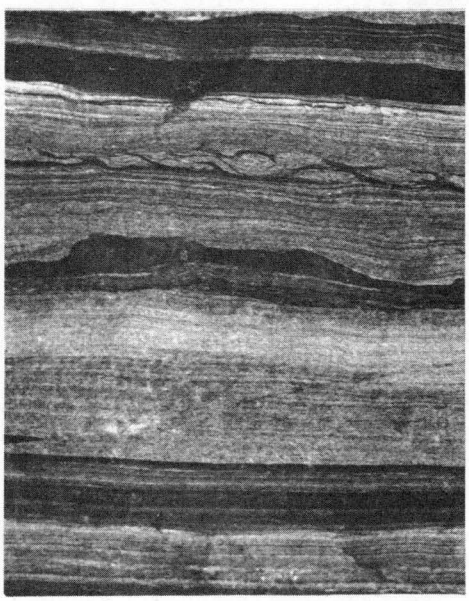

f

PLATE 5:12

PLATE 5:13

a. Fine-grained conglomerate bed overlying medium-grained sandstone with an erosional surface. Bedding-parallel grain alignment in the conglomerate is well developed.

b. Bulbous flute-casts at the base of a medium-grained sandstone bed. From the correlate of the Long Bay Shale at Mt Fulton.
Visible part of lens cap is 40 mm across.

ASAHI
PENTAX

PLATE 5:14

a. Lenticular sandstone beds indicating that scouring occurred and overlying units were deposited in channels.

b. Typical conglomerate bed in the Joan Point Sandstone Correlate. The Polymict nature of the bed and angularity of some clasts, along with the generally random nature of the bed suggest that the deposit was "dumped" or was a frozen debris flow.
The scalloped surface related to pebble concentrations implies that some clasts were trapped in eroded parts of the substrate.

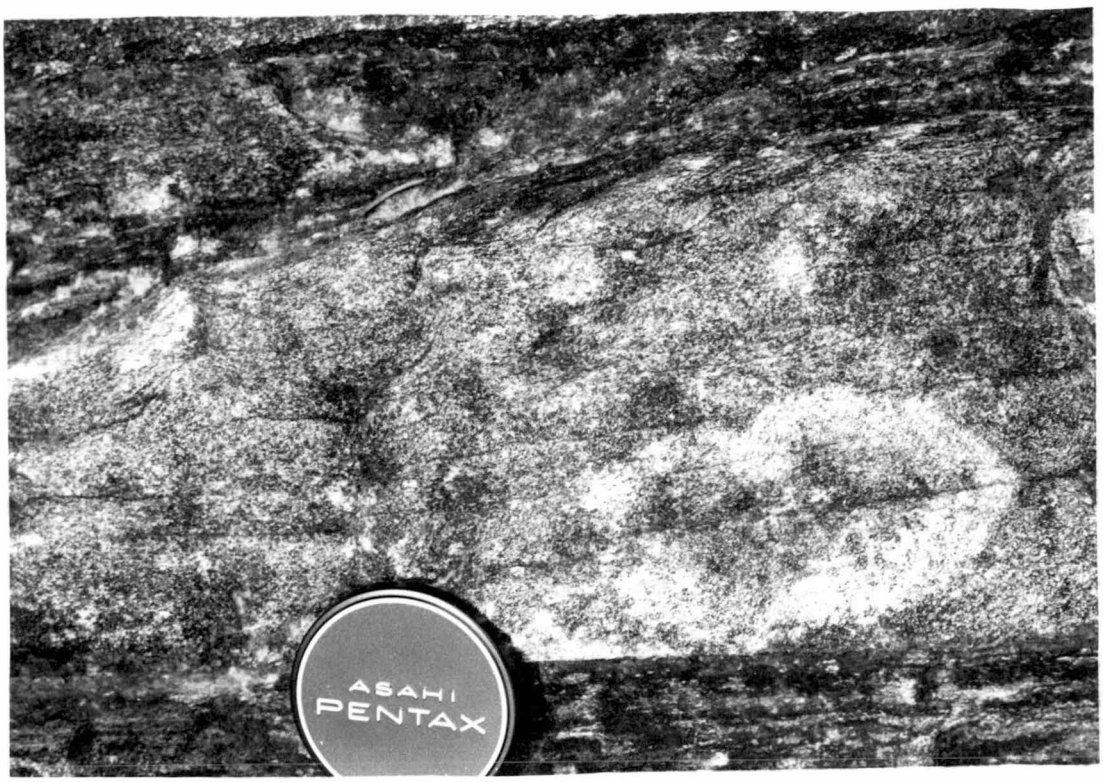
ASAHI
PENTAX

PLATE 5:15

a. Cross-bedded sandstone overlying a lenticular pebbly sandstone bed. The channel direction indicated for the conglomerate is perpendicular to the page, which suggests that the cross-bedding is of the channel-fill type.

b. Diffuse cross-bedding in medium- to coarse-grained sandstone bed.
Joan Point Sandstone Correlate at Mt Fulton.

FORM OF GRADED BEDDING

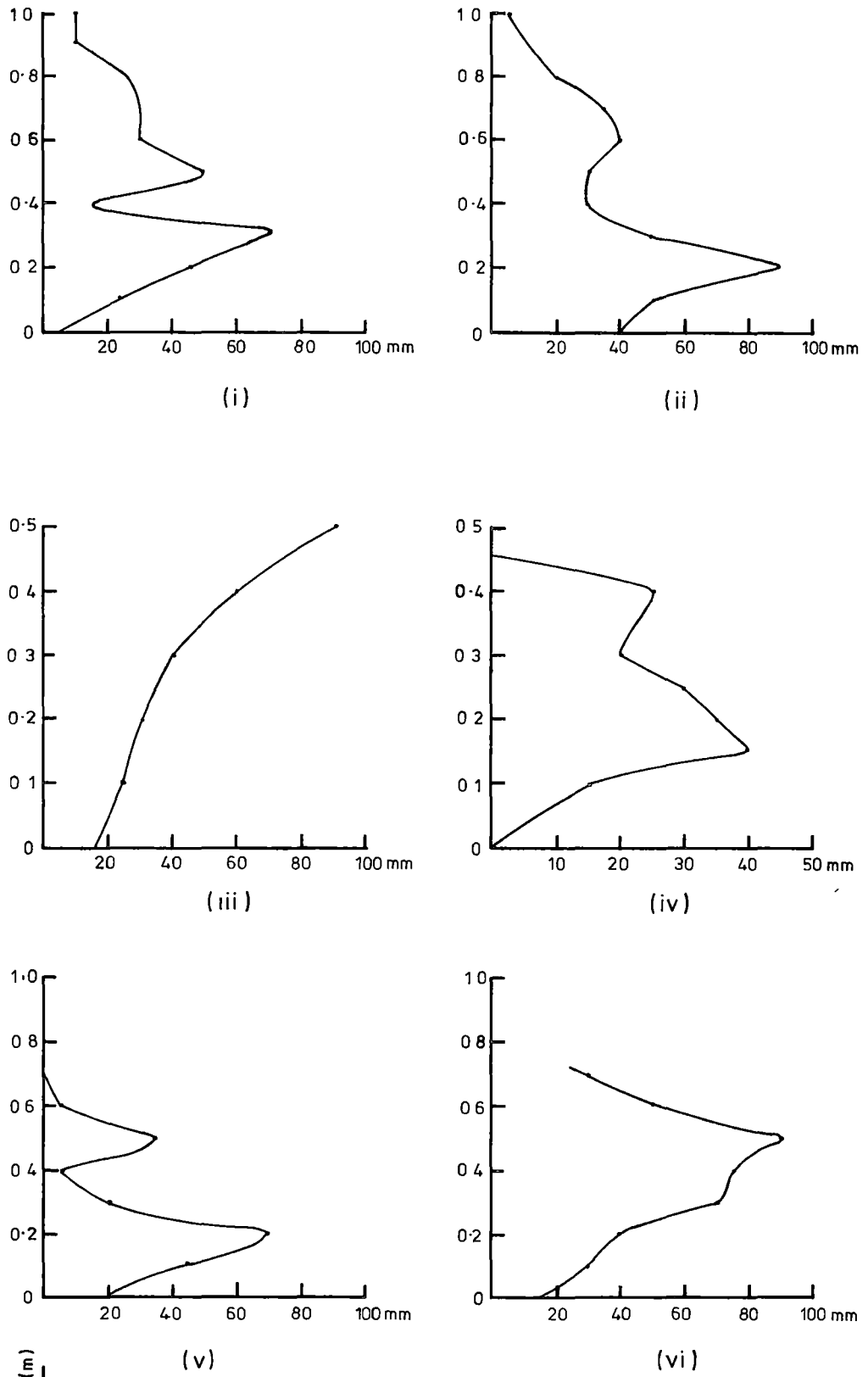

FIG. 5:7

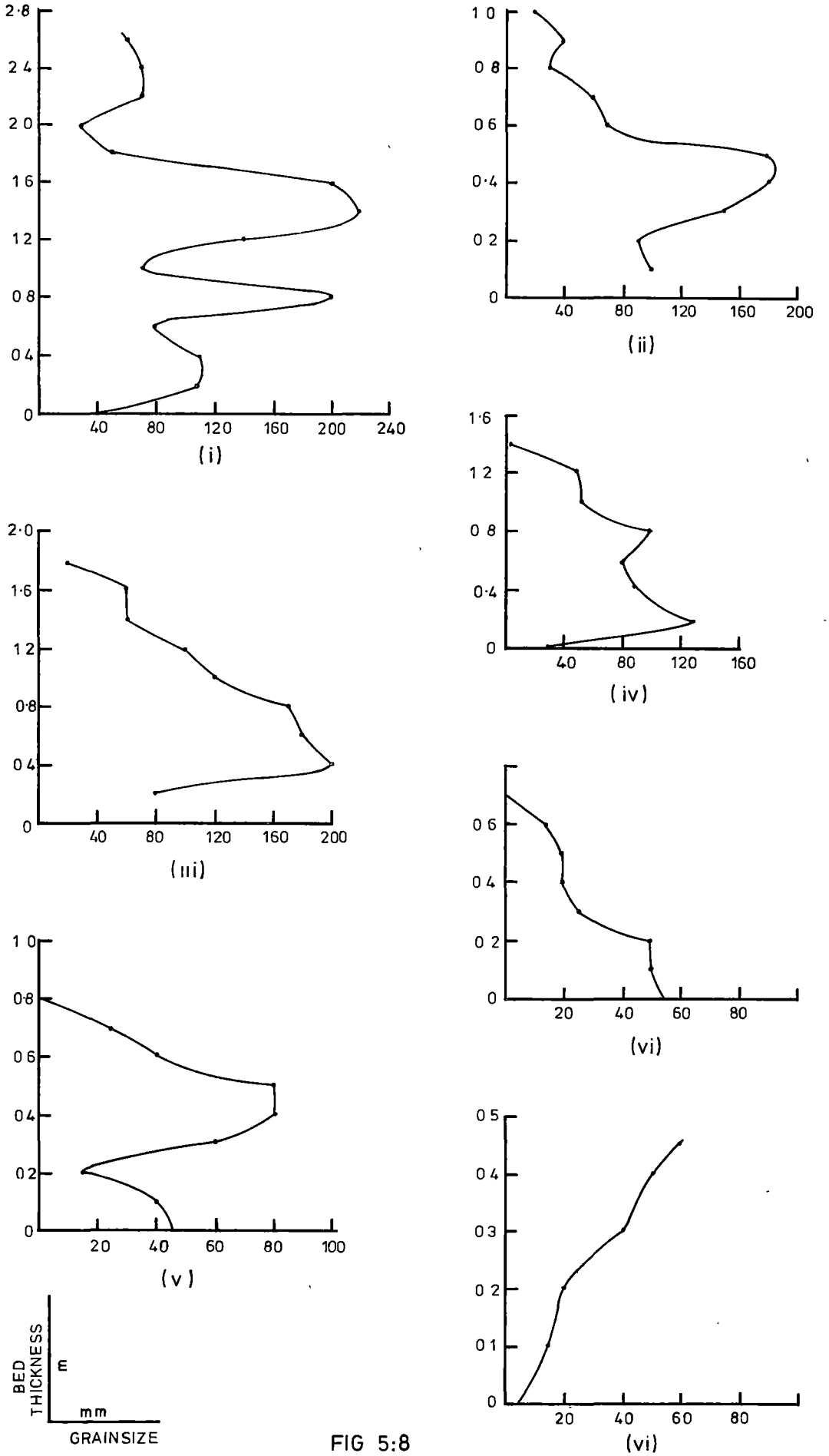
2·8
2 4
2 0
1 6
1 2
0 8
0 4
0
40 80 120 160 200 240
(i)
1 0
0 8
0 6
0·4
0 2
0
40 80 120 160 200
(ii)
2·0
1·6
1 2
0·8
0 4
0
40 80 120 160 200
(iii)
1·6
1 2
0 8
0·4
0
40 80 120 160
(iv)
1 0
0·8
0 6
0 4
0 2
0
20 40 60 80 100
(v)
0 6
0 4
0 2
0
20 40 60 80
(vi)
0 5
0 4
0 3
0 2
0 1
0
20 40 60 80
(vi)
BED THICKNESS
m
mm
GRAINSIZE

FIG 5:8

PLATE 5:16

a. A well-sorted fine-conglomerate bed showing inverse grading and normal grading. There is a well developed imbrication and the boundary with the underlying bed is planar. Note the diffuse boundary of the conglomerate and sandstone sections of the bed.

b. Inverse-to-normally graded bed of a more poorly sorted conglomerate with more angular clasts.

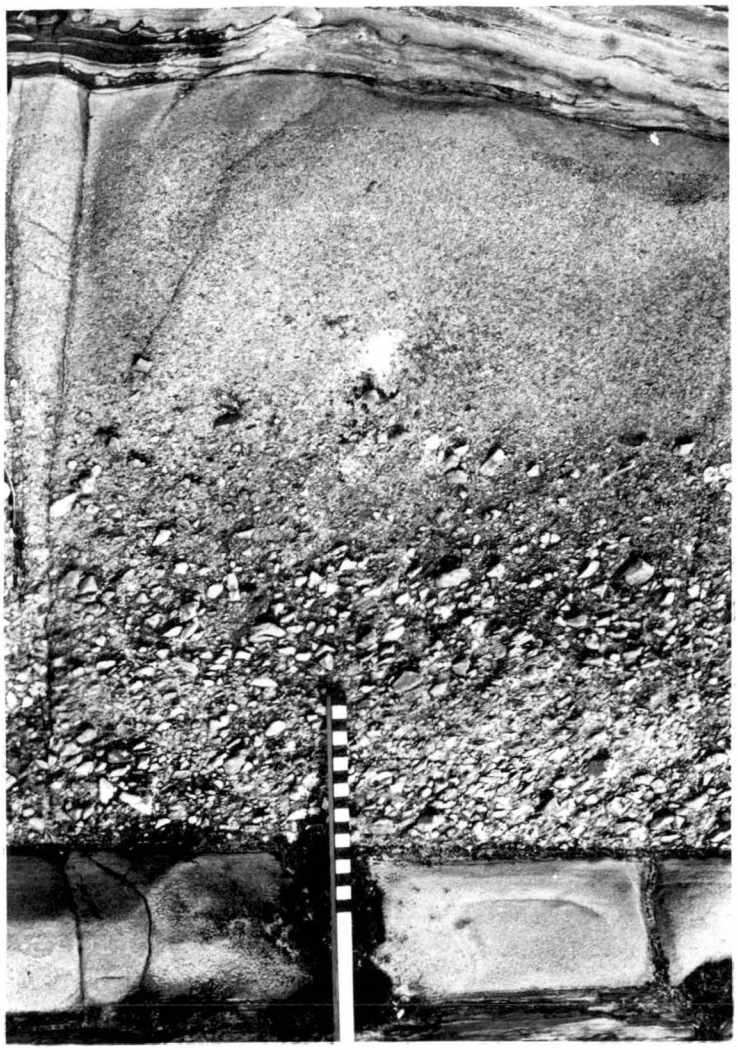

PLATE 5:17

a. Inverse-to-normally graded fine conglomerate bed. Little imbrication is present but numerous clasts are aligned parallel to bedding.

b. Large clasts with a low sphericity in open framework in a micaceous matrix. The deformation of laminae around the clast may be due to flow, or deposition of overlying material.


ASAHI
PENTAX

PLATE 5:18

a. A large clast projecting above the general level of the coarse-grained bed. Other clasts are also present at different levels.

b. Numerous large outsized isolated clasts in a pebbly sandstone bed. Lens cap is 50 mm. in diameter.

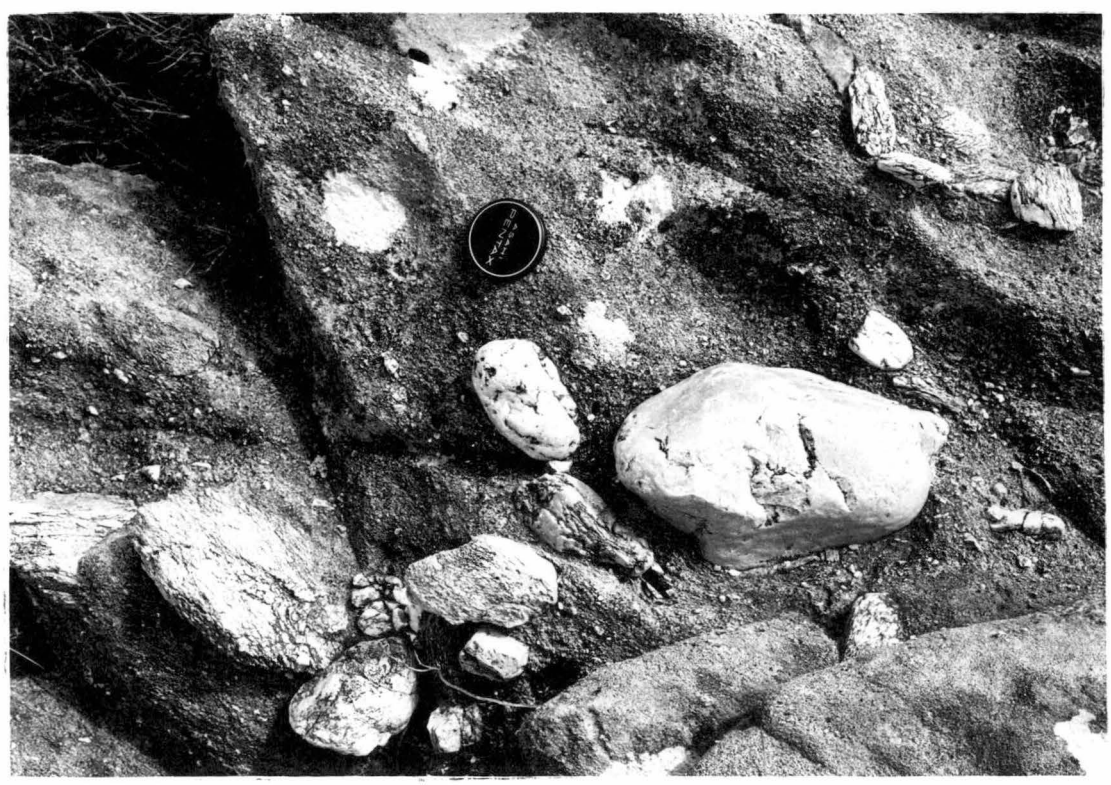

PLATE 5:19

a. A single isolated, outsized clast in unevenly bedded coarse-grained sandstone. Clast is 0.3 m. across.

b. Large clasts at the base of a crudely graded conglomerate. These have formed in scours and may be deposited from larger flows which eroded the substrate but deposited only occasional boulders. Hammer head is 0.16 m. long.

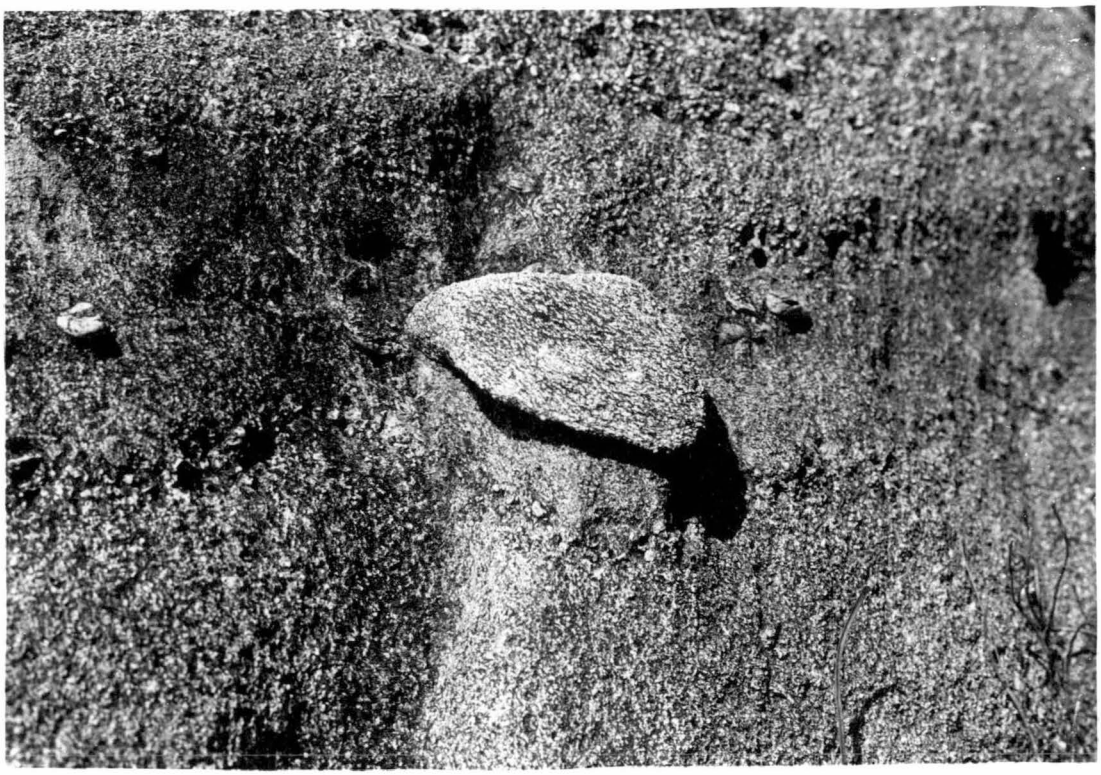

PLATE 5:2D

a. Two touching isolated clasts in a coarse-grained sandstone bed.

b. Clasts which formed at the bed surface. Two modes of origin of the protruding structure are possible.

(i) Prior to the pebble conglomerate deposition erosion occurred exposing a previously enclosed clast.

(ii) Coherent sandstone bed during transport picked up clasts and prevented them sinking.

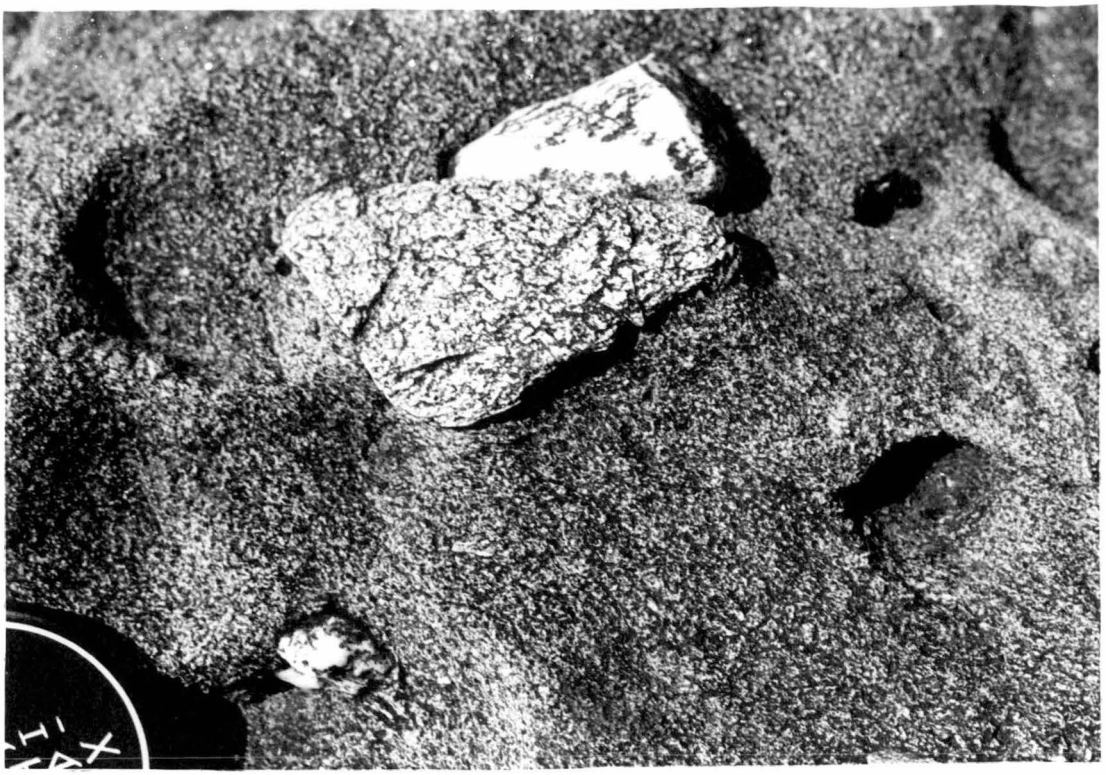

PLATE 5:21

a. Graded conglomerate deposited over an erosional contact with laminated sandstone. The bed has a continuous framework.
Facing is down the page.

b. Typical graded-stratified conglomerate.
An indication of a very thin reverse-graded horizon occurs near the base of the scale.

PLATE 5:22

Graded granule-conglomerate deposited in a deep scour in medium-grained sandstone. This is typical of the graded-bed group of conglomerate.


ASAHI
PENTAX

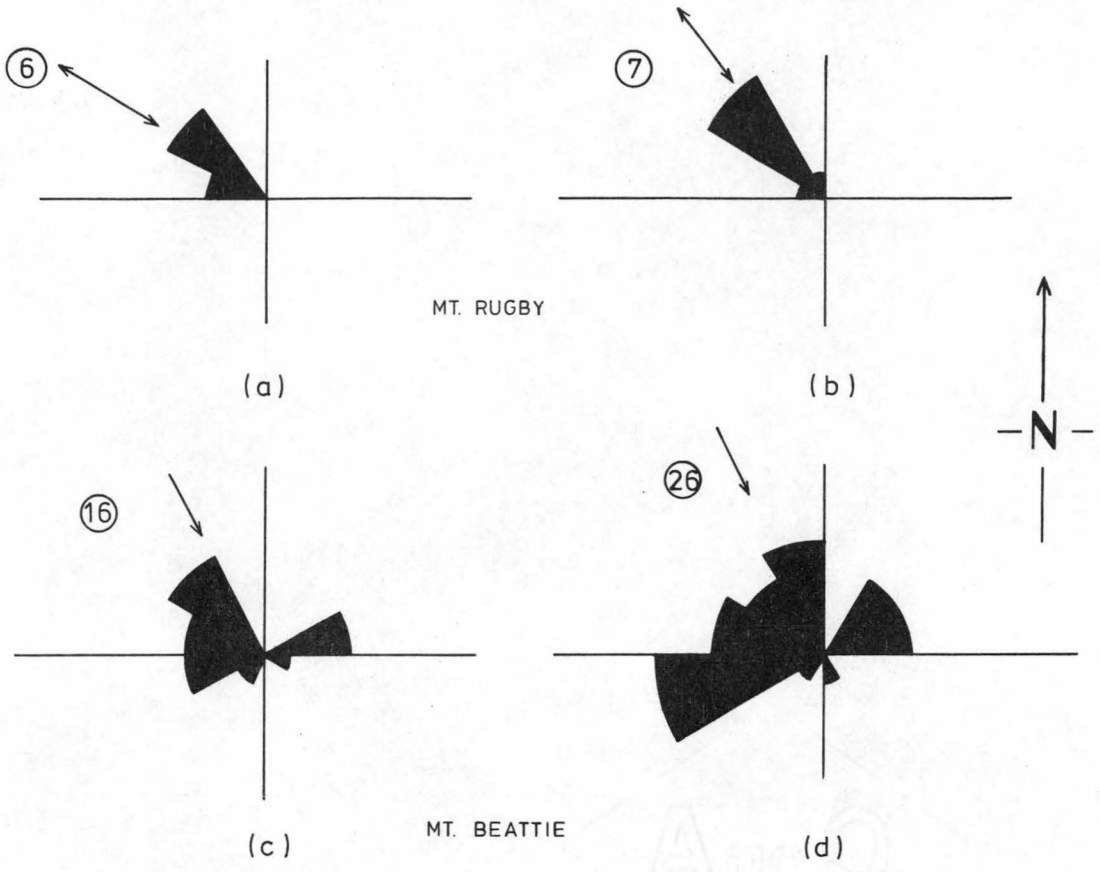
6
7
MT. RUGBY
(a)
(b)
N
16
26
MT. BEATTIE
(c)
(d)

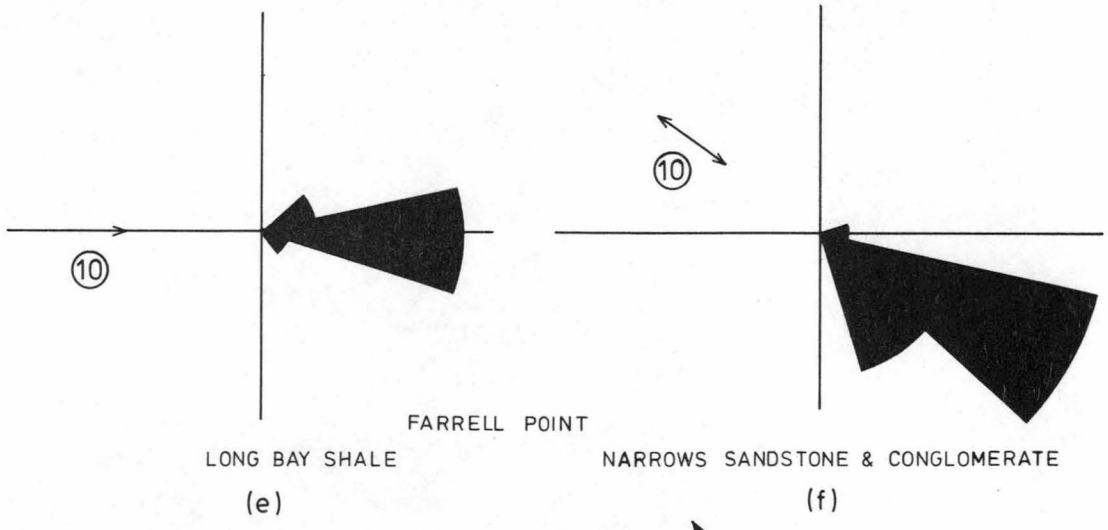
10
10
FARRELL POINT
LONG BAY SHALE
NARROWS SANDSTONE & CONGLOMERATE
(e)
(f)

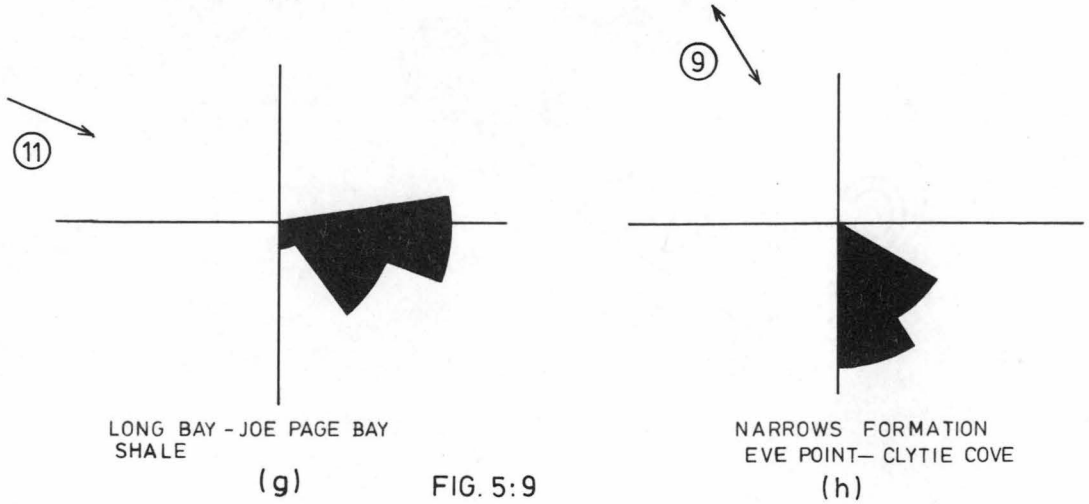
11
9
LONG BAY - JOE PAGE BAY SHALE
NARROWS FORMATION
EVE POINT— CLYTIE COVE
(g)
(h)

FIG. 5:9

LEGEND FOR STRATIGRAPHIC COLUMNS

1. Alignment:

Clasts aligned parallel to bedding

Clasts aligned parallel to cleavage

Clasts show imbrication

2. Lamination:

Fine lamination (0-2 mm)

Coarse lamination (>2 mm)

Coarse lamination with substantial grainsize variation (stratification)

Shaly partings

3. Lenticularity:

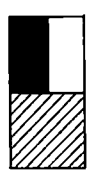

Contains lenticular pods of finer grained material.

Deposited on a low angle erosinal surface.

4. Bouma Divisions:

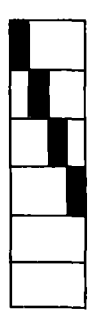

A	Division	present
B	"	"
C	"	"
D and/or E	"	"

5. Lithotype: Letters refer to facies groups defined by Walker and Mutti (1973).

6. Model: Letters refer to models defined by Walker (1975a; 1977). In addition:

L refers to structureless conglomerate

S refers to stratified conglomerate and pebbly sandstone.

(see over for details)

5. LITHOTYPE

FACIES A ... Coarse-grained sandstone and conglomerate.

A1 disorganised conglomerate

A2 organised conglomerate

(i.e. has internal sedimentary structures or a non-random grain fabric)

A3 disorganised pebbly sandstone

A4 organised pebbly sandstone

(i.e. has internal sedimentary structures or a non-random grain fabric)

FACIES B ... Medium to fine-grained or coarse-grained sandstone with no internal sedimentary structures.

FACIES C ... Medium to fine-grained sandstone, deposited from turbidity currents, the lower portion of the bed being graded.

FACIES D ... Fine-grained sandstone, deposited from turbidity currents, the lower portion of the bed being either plane-laminated or cross-bedded (ripple-drift type).

Modified from Walker and Mutti (1963).

6. MODEL

ING - Inverse-to-normally graded bed. Lower section is reverse graded, the upper section is normally graded.

MODEL (contd.)

GS - Graded-stratified beds. Sometimes crude cross-stratification occurs.

L - Structureless conglomerate bed, akin to the disorganised bed (Walker, 1975a).

S - Stratified conglomerate and pebbly sandstone. This does not occur in Walker's models.

G - Graded bed, containing no other structures (Walker, 1977).

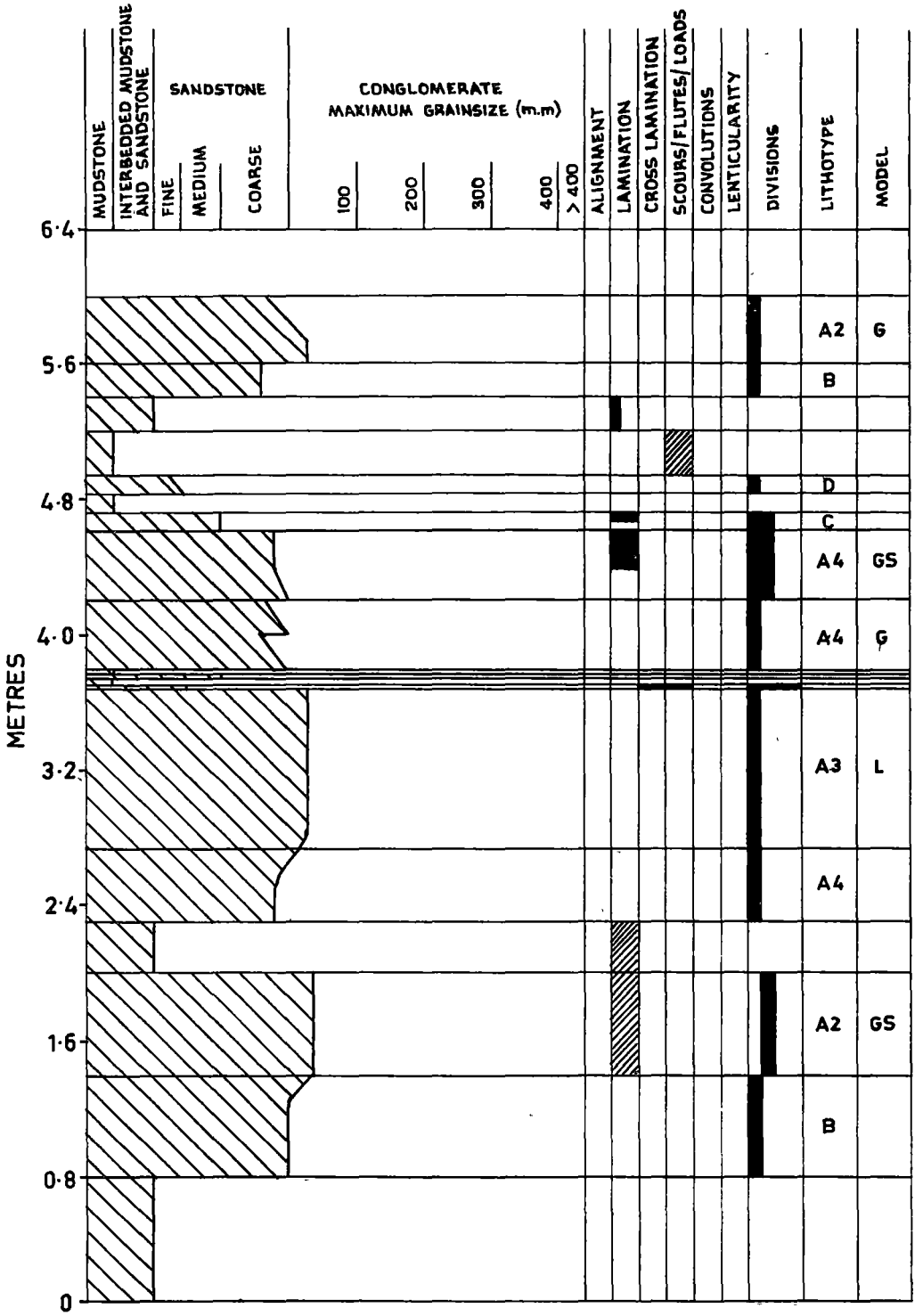

STRATIGRAPHIC SEQUENCE, MT. RUGBY FORMATION (TOP)
BALMORAL HILL

Figure 6:1:a

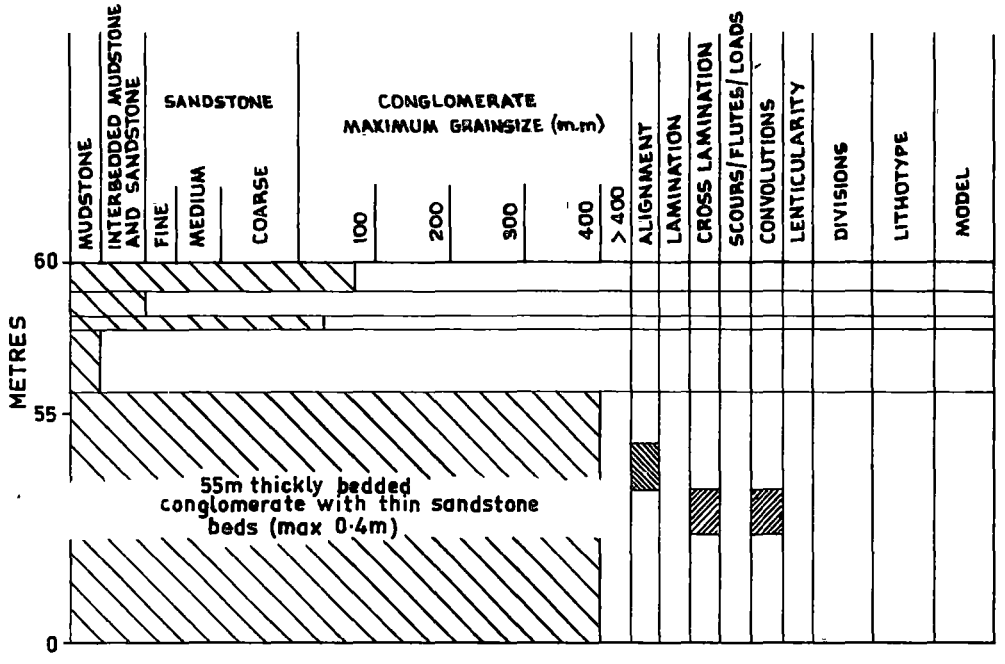

STRATIGRAPHIC SEQUENCE, MT. MACKENZIE FORMATION

Figure 6:1:b

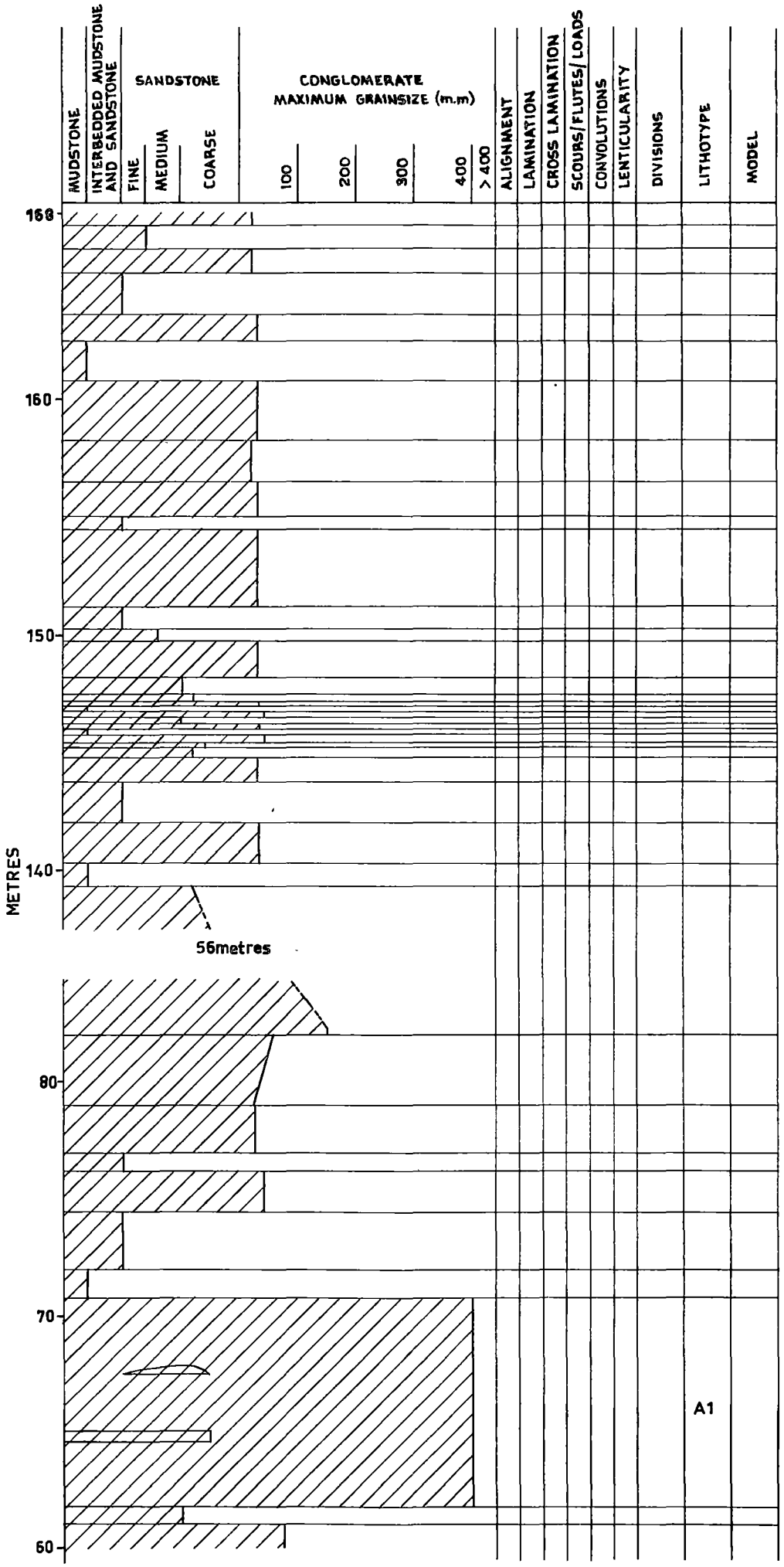
MUDSTONE
INTERBEDDED MUDSTONE AND SANDSTONE
SANDSTONE
FINE
MEDIUM
COARSE
CONGLOMERATE MAXIMUM GRAINSIZE (m.m)
100
200
300
400
> 400
ALIGNMENT
LAMINATION
CROSS LAMINATION
SCOURS/FLUTES/LOADS
CONVOLUTIONS
LENTICULARITY
DIVISIONS
LITHOTYPE
MODEL
METRES
160
150
140
80
70
60
56metres
A1

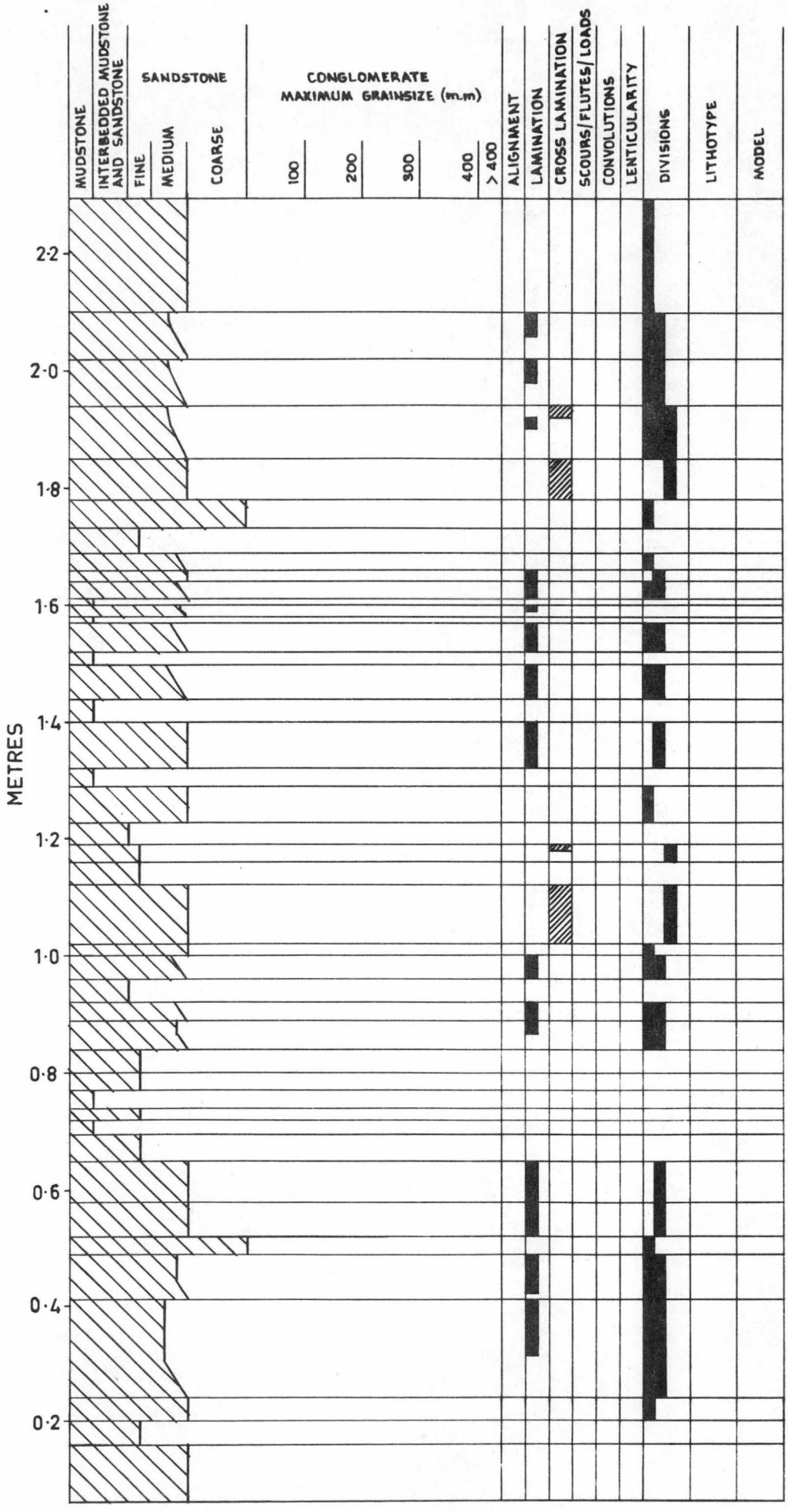

STRATIGRAPHIC SEQUENCE, LONG BAY SHALE

Figure 6:1:c

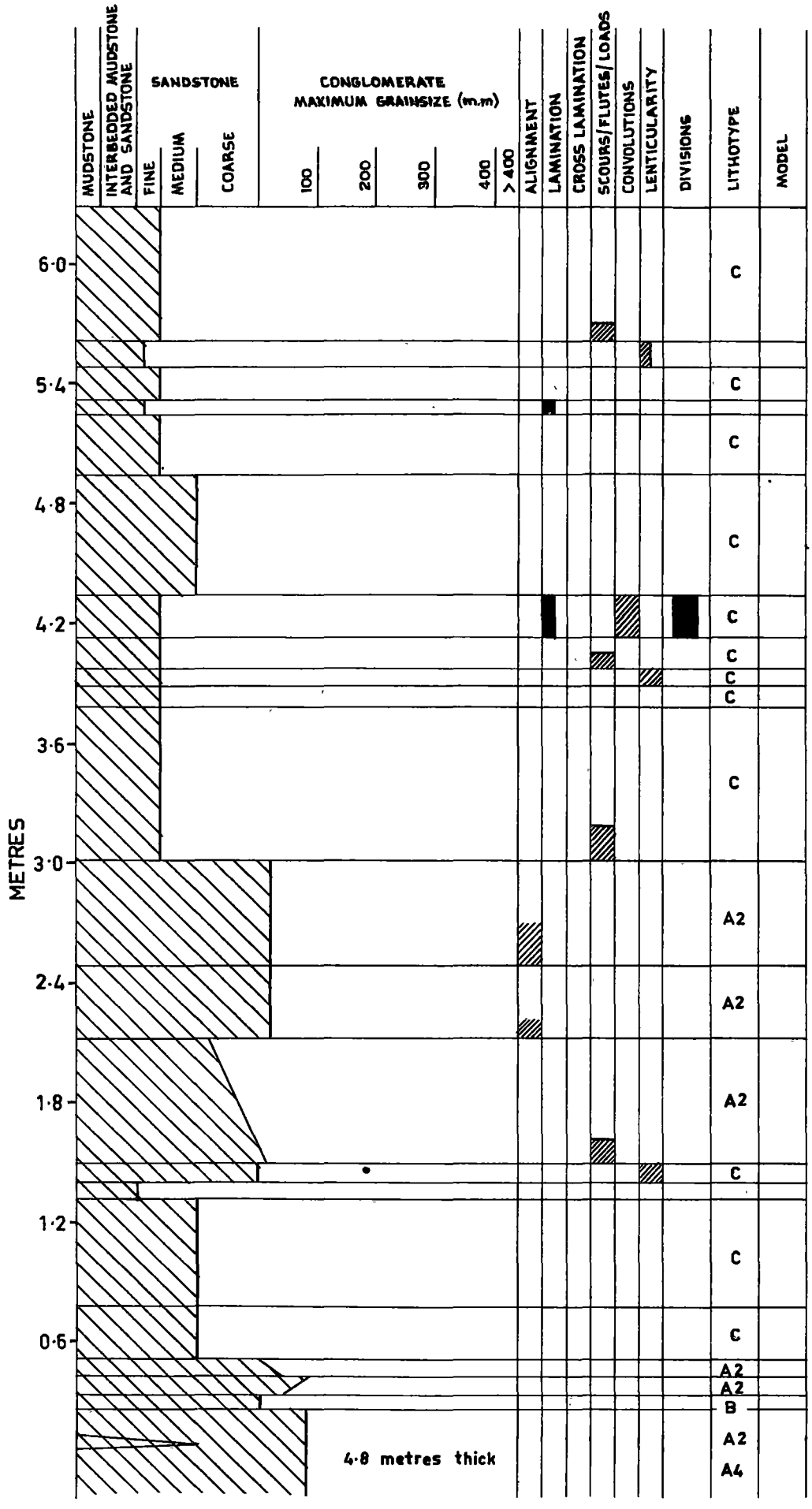

STRATIGRAPHIC SEQUENCE, BASE OF JOAN POINT SANDSTONE

Figure 6:1:d

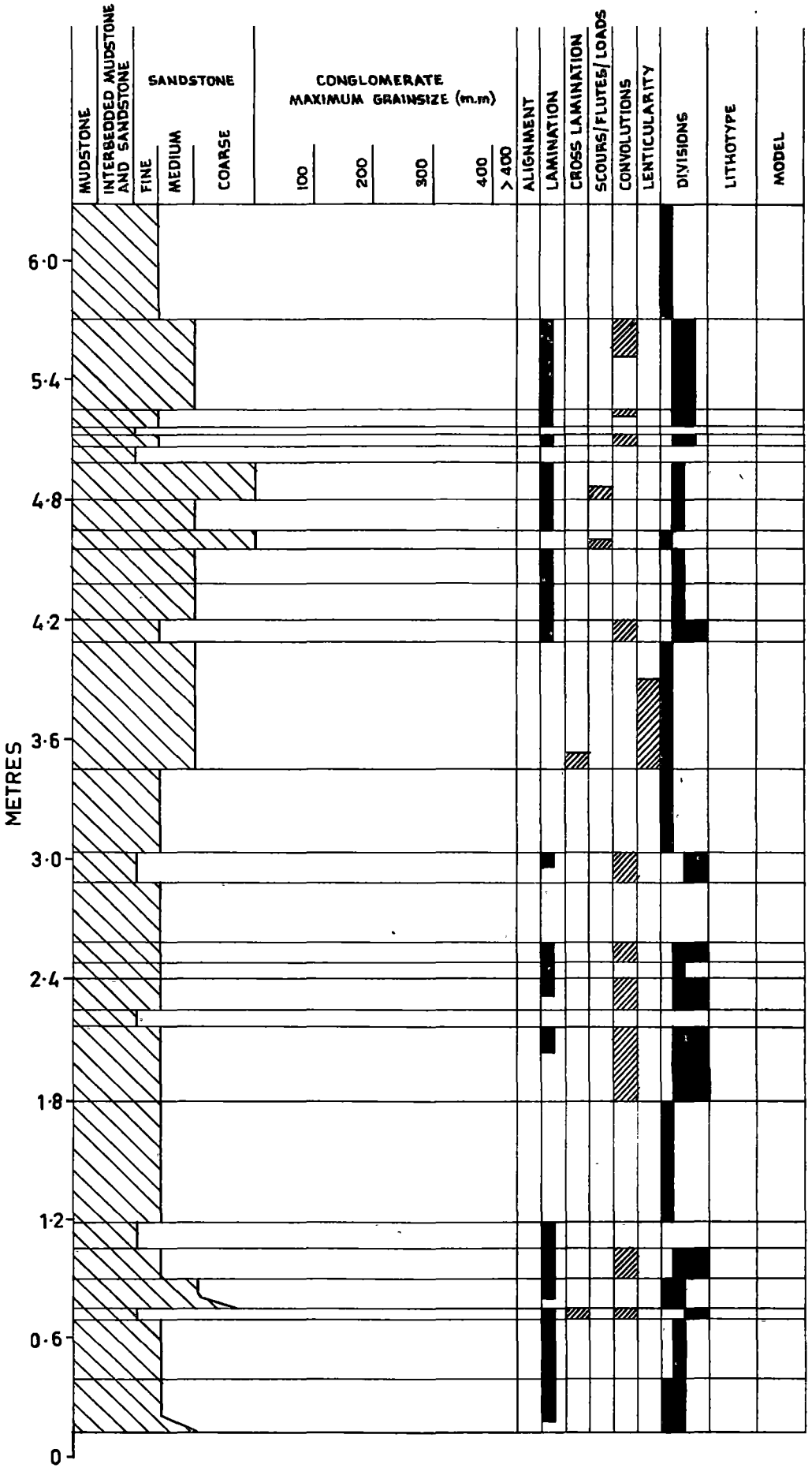

STRATIGRAPHIC SEQUENCE, JOAN POINT SANDSTONE

Figure 6:1:e

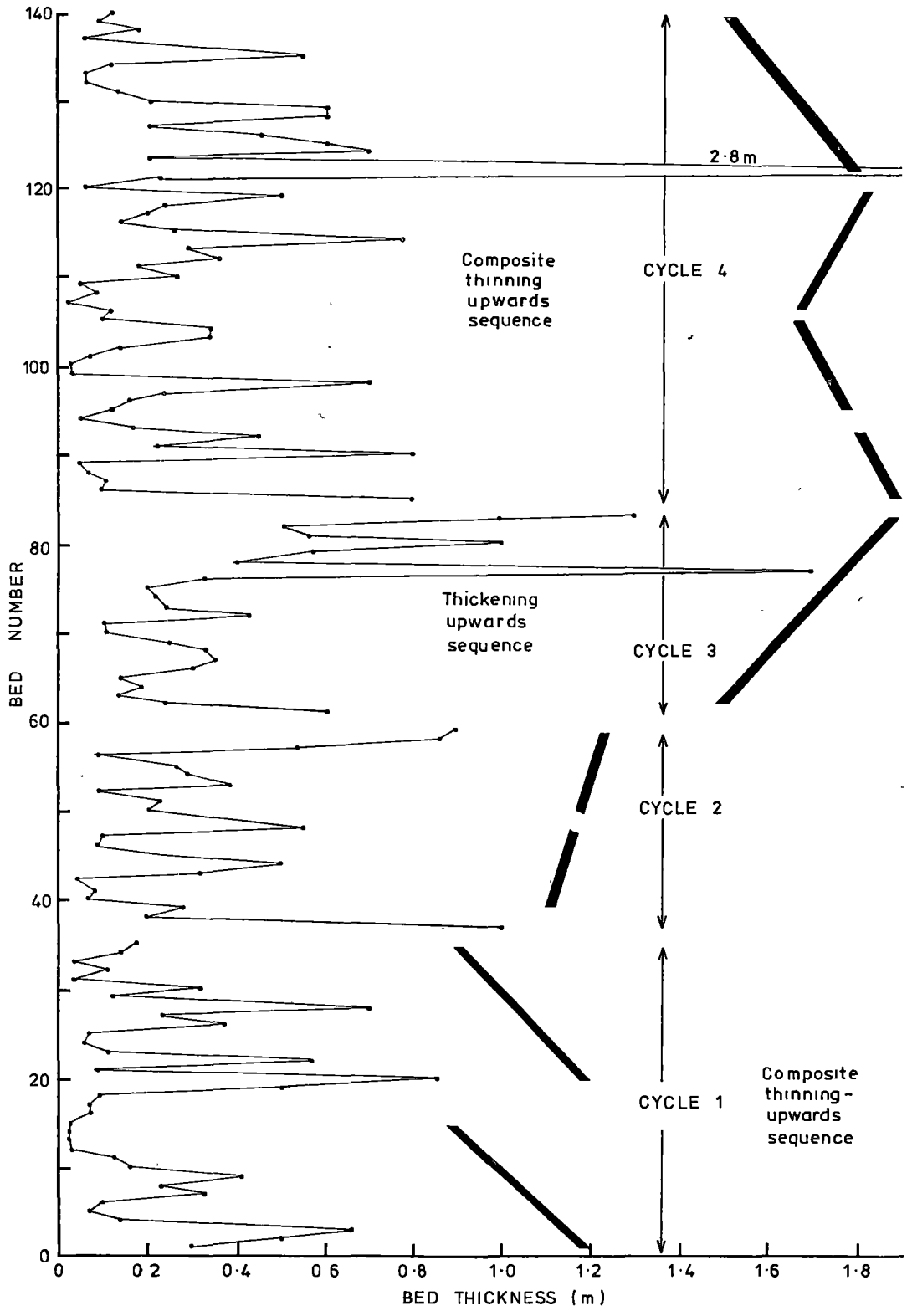

MT. RUGBY CONGLOMERATE
COARSE DIVISIONS

393·86 m logged
Total thickness = 445·864 m

FIGURE 6:2

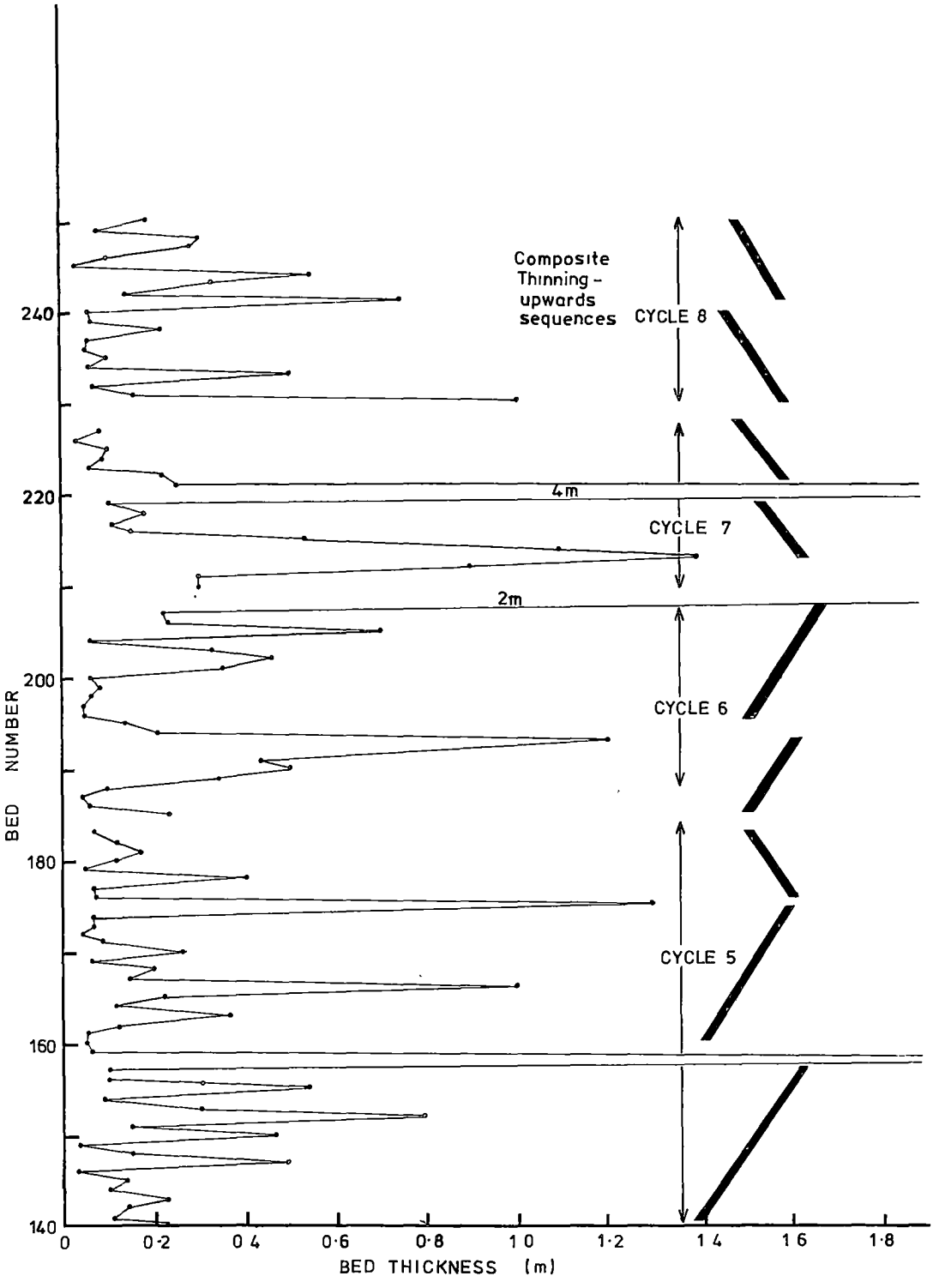
Composite
Thinning -
upwards
sequences
CYCLE 8
CYCLE 7
CYCLE 6
CYCLE 5
4m
2m
240
220
200
180
160
140
BED NUMBER
0
0·2
0 4
0·6
0·8
1 0
1·2
1 4
1 6
1·8
BED THICKNESS (m)

FIG. 6:2

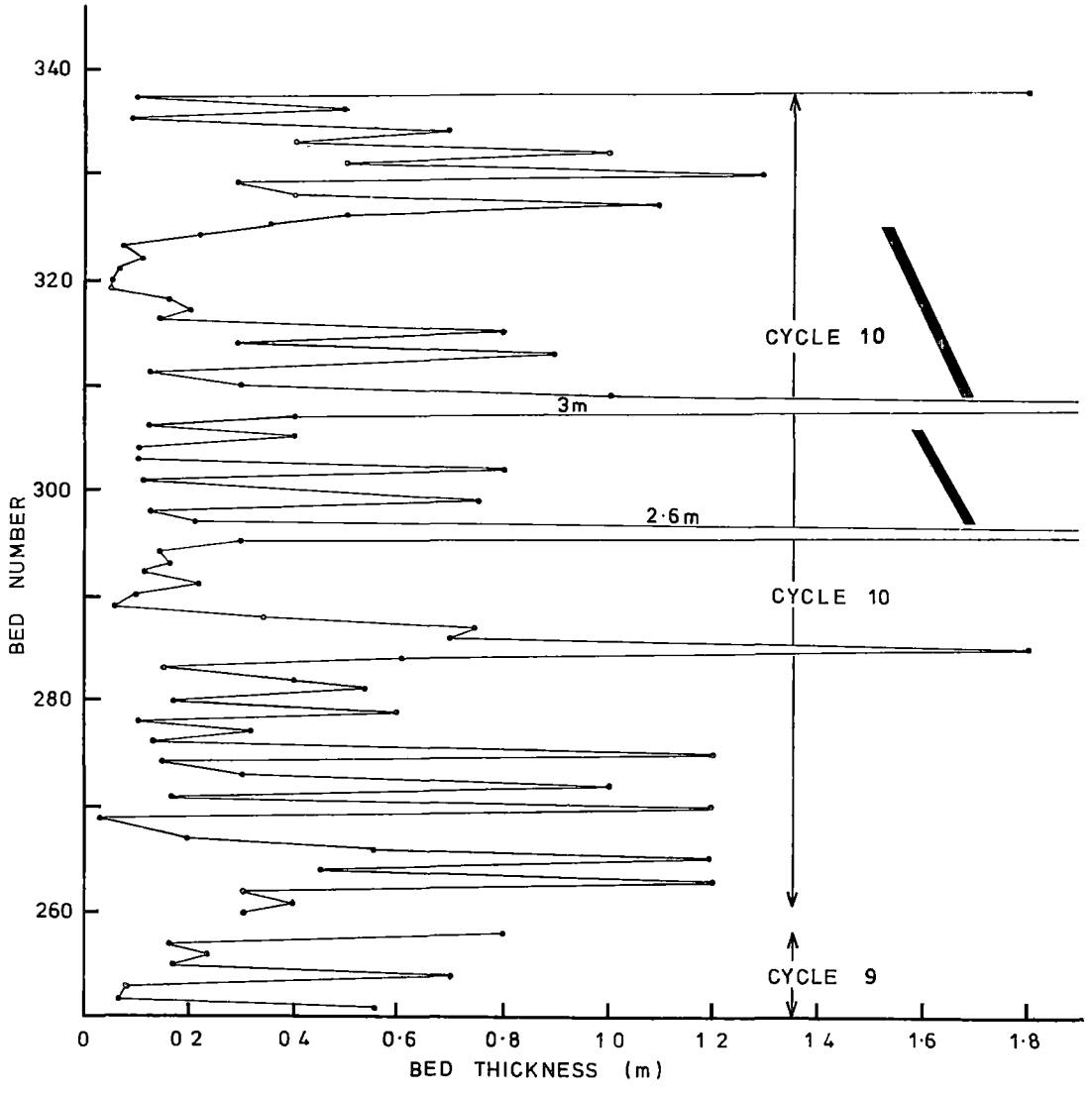
340
320
300
280
260
BED NUMBER
CYCLE 10
3m
2·6m
CYCLE 10
CYCLE 9
0
0 2
0 4
0·6
0·8
1 0
1 2
1 4
1·6
1·8
BED THICKNESS (m)

FIG. 6 : 2

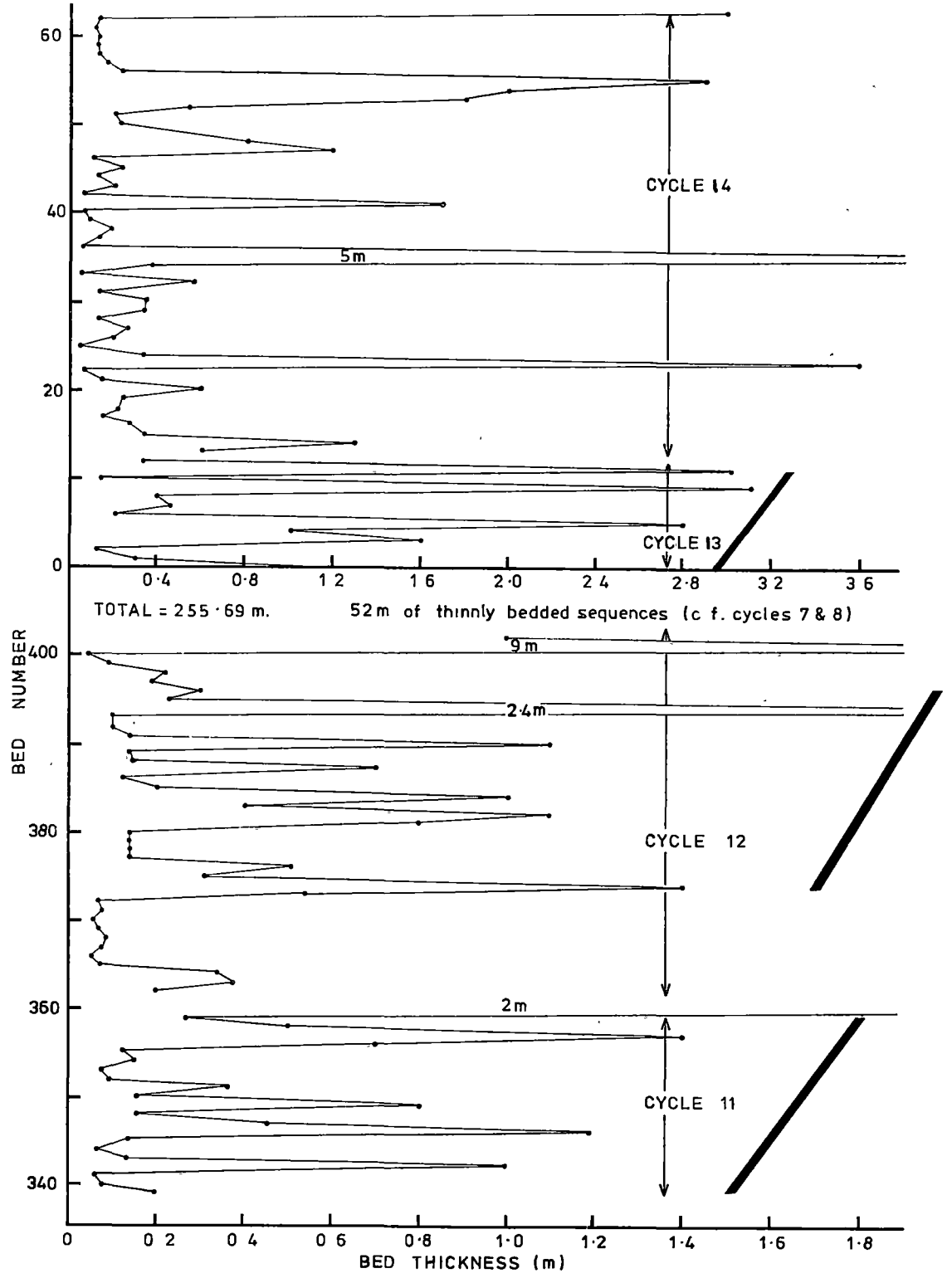
60
40
20
0
CYCLE 14
5m
CYCLE 13
0·4
0·8
1 2
1 6
2·0
2 4
2·8
3 2
3 6
TOTAL = 255 · 69 m.
52m of thinnly bedded sequences (c f. cycles 7 & 8)
BED NUMBER
400
380
360
340
9 m
2·4m
CYCLE 12
2m
CYCLE 11
0
0 2
0 4
0 6
0·8
1·0
1·2
1·4
1·6
1·8
BED THICKNESS (m)

FIG. 6:2

FIGURE 6 : 2

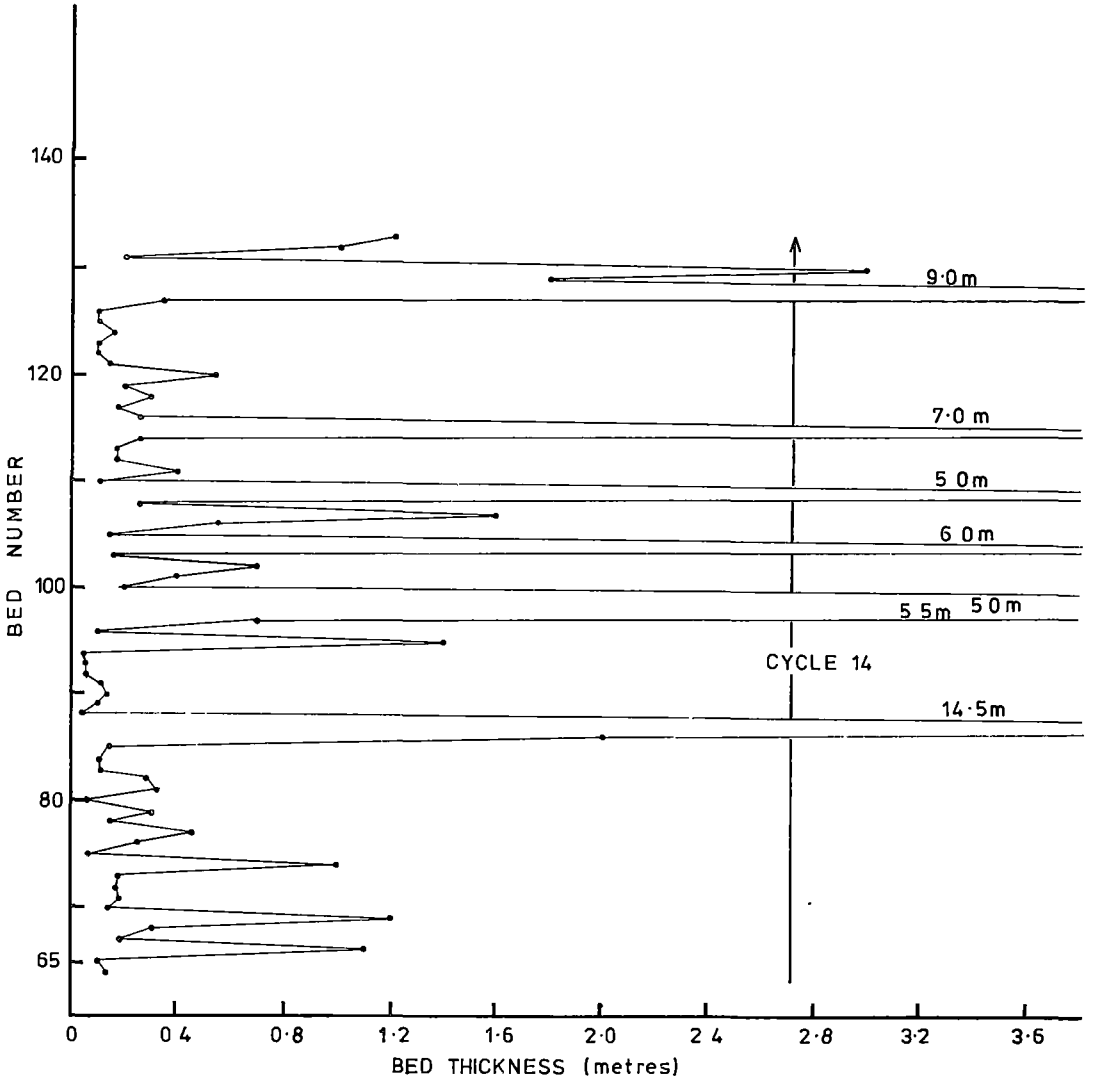
140
120
100
80
65
BED NUMBER
9·0m
7·0 m
5 0m
6 0m
5 5m
5 0m
CYCLE 14
14·5m
0
0 4
0·8
1·2
1·6
2·0
2 4
2·8
3·2
3·6
BED THICKNESS (metres)

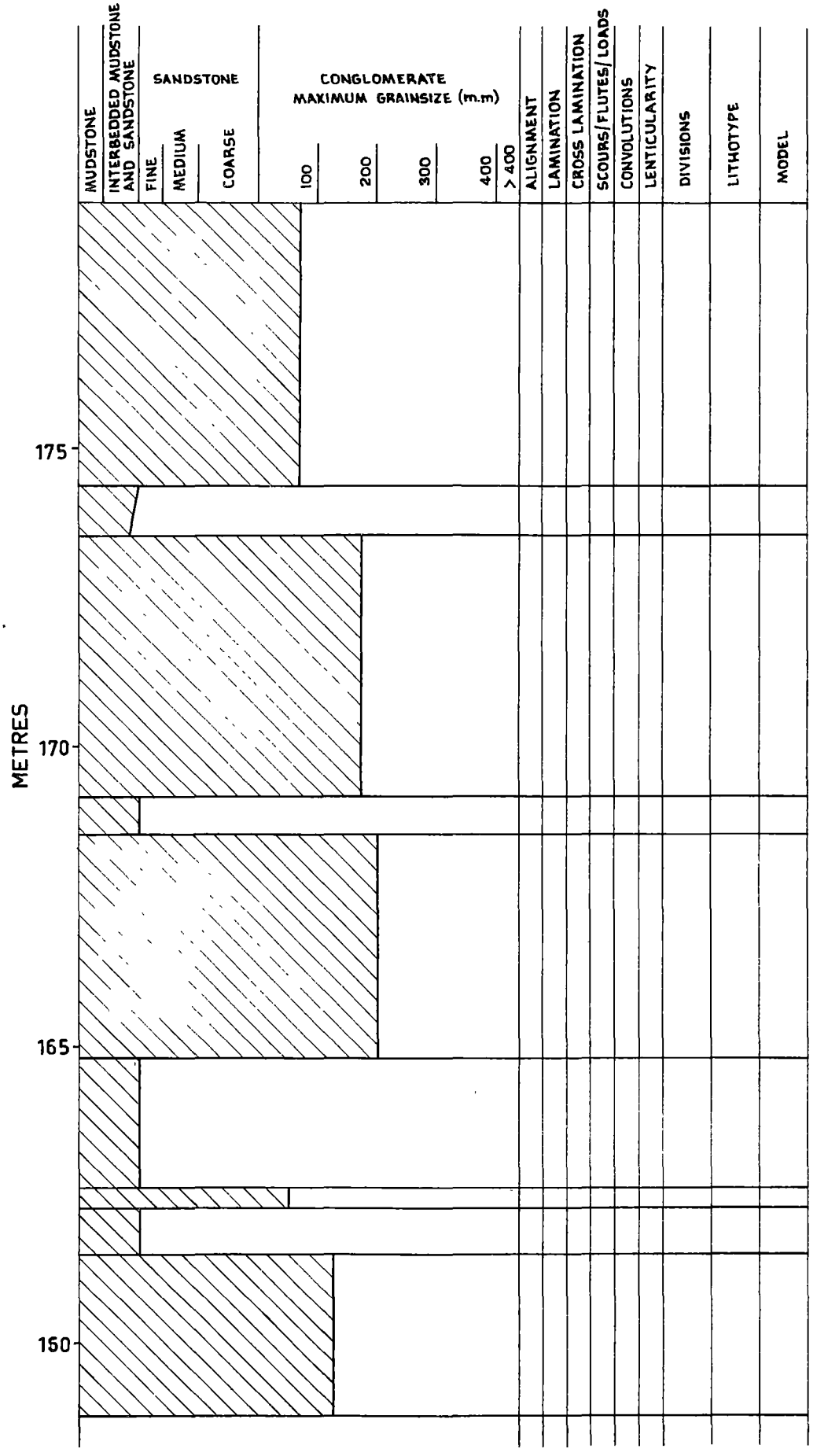
MUDSTONE
INTERBEDDED MUDSTONE AND SANDSTONE
SANDSTONE
FINE
MEDIUM
COARSE
CONGLOMERATE
MAXIMUM GRAINSIZE (m.m)
100
200
300
400
> 400
ALIGNMENT
LAMINATION
CROSS LAMINATION
SCOURS/FLUTES/LOADS
CONVOLUTIONS
LENTICULARITY
DIVISIONS
LITHOTYPE
MODEL
METRES
175
170
165
160

FIGURE 6:3

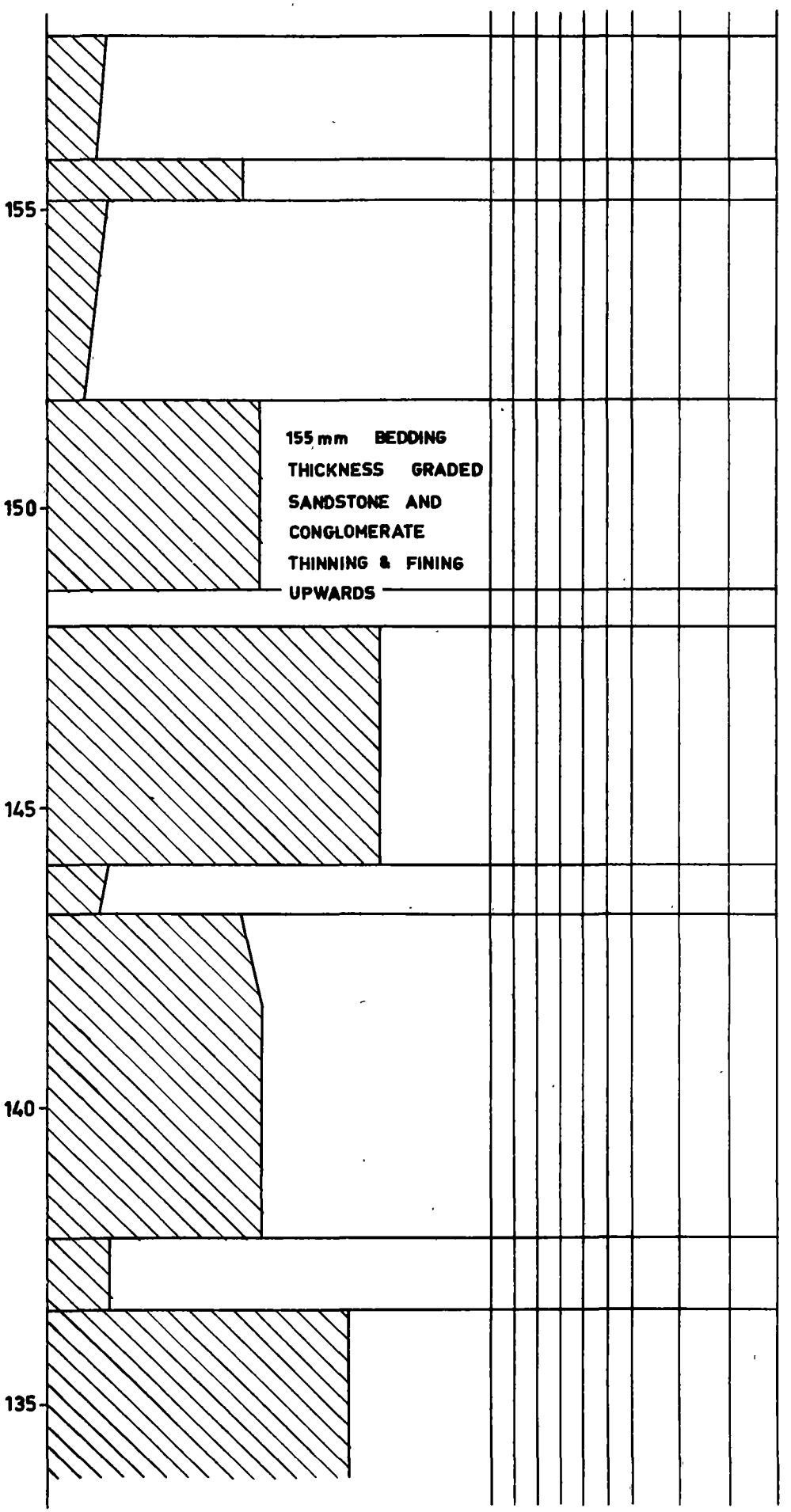
155
150
145
140
135
155 mm BEDDING THICKNESS GRADED SANDSTONE AND CONGLOMERATE THINNING & FINING UPWARDS

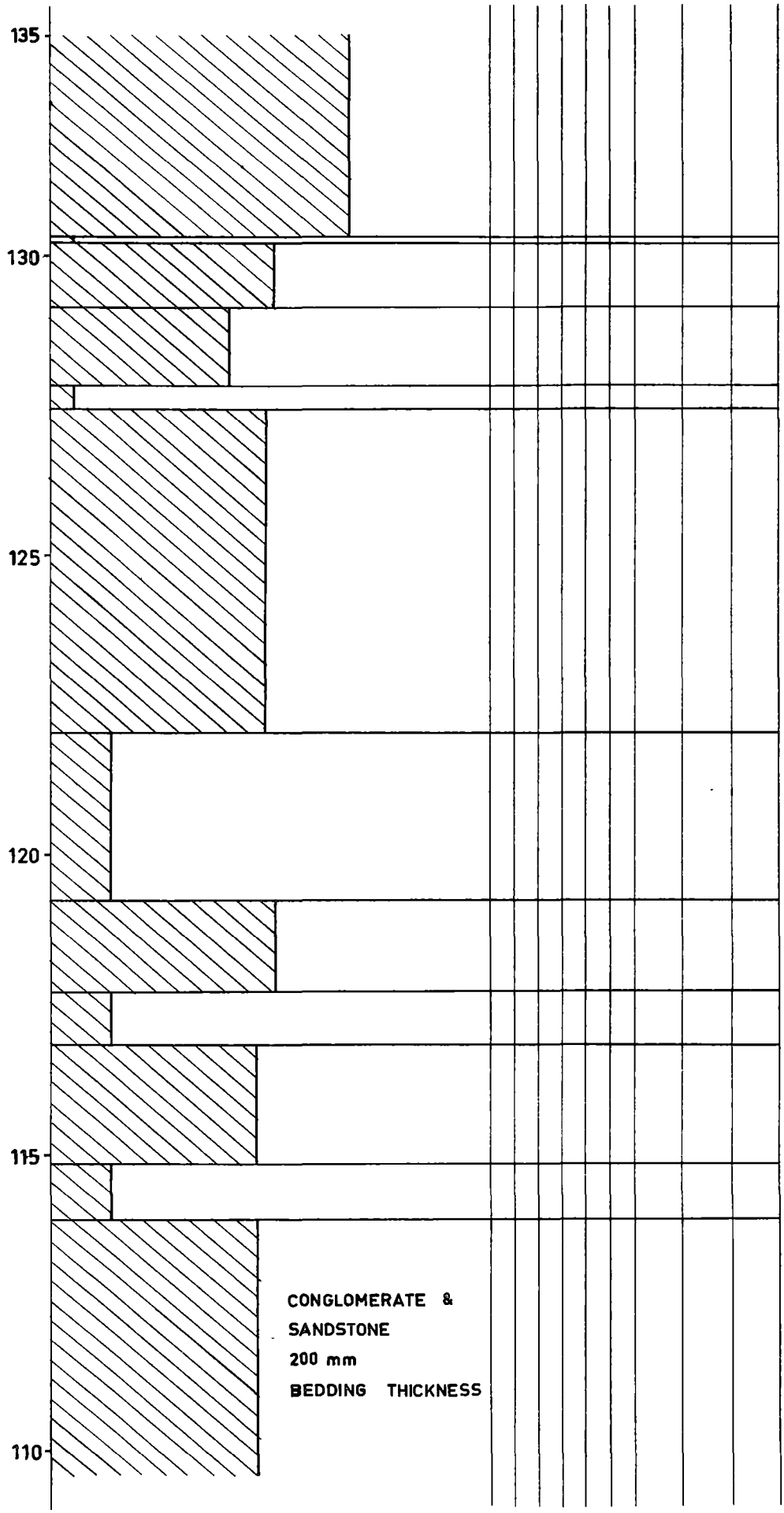
135
130
125
120
115
110
CONGLOMERATE &
SANDSTONE
200 mm
BEDDING THICKNESS

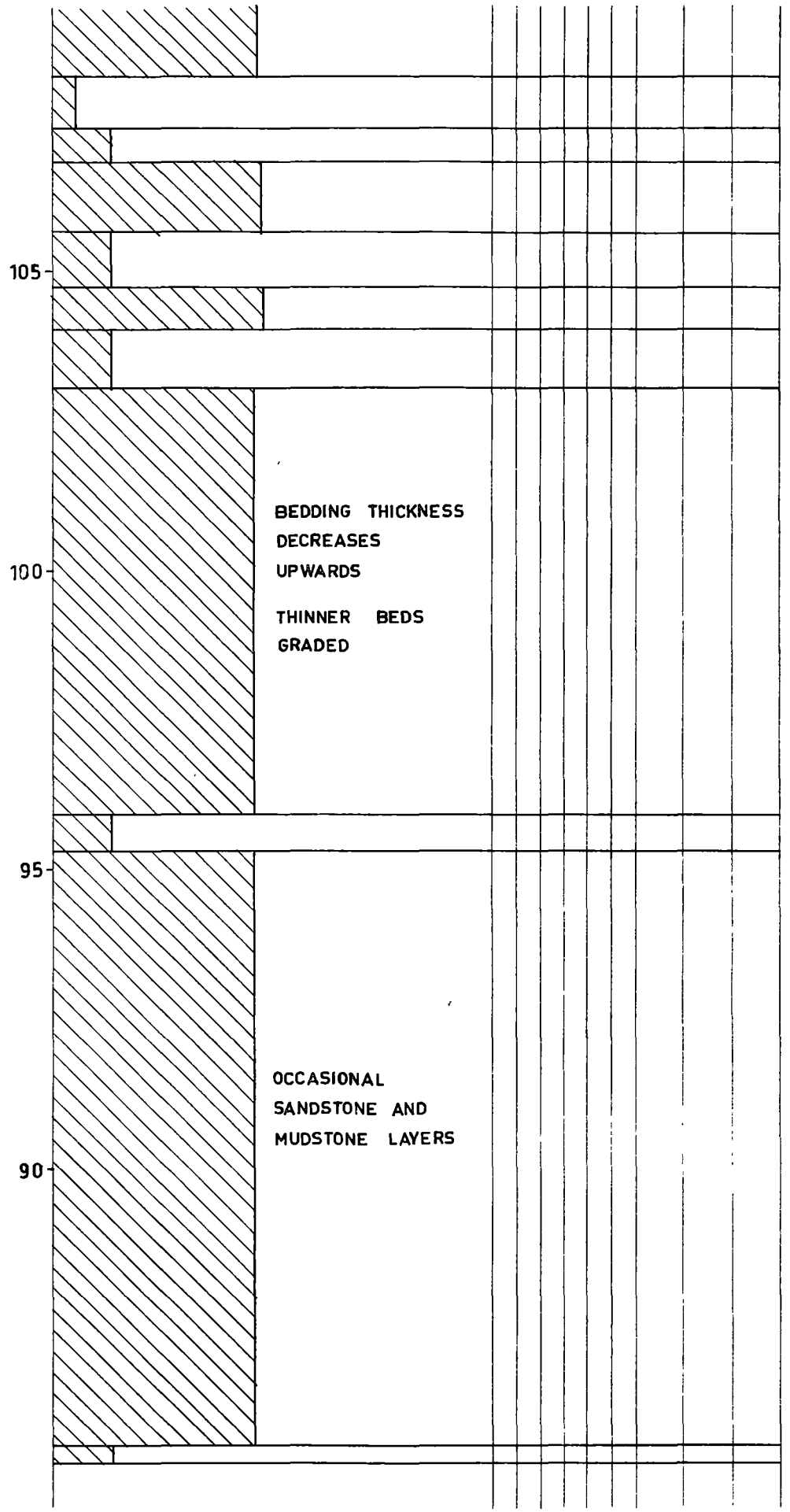
105
100
95
90
BEDDING THICKNESS
DECREASES
UPWARDS
THINNER BEDS
GRADED
OCCASIONAL
SANDSTONE AND
MUDSTONE LAYERS

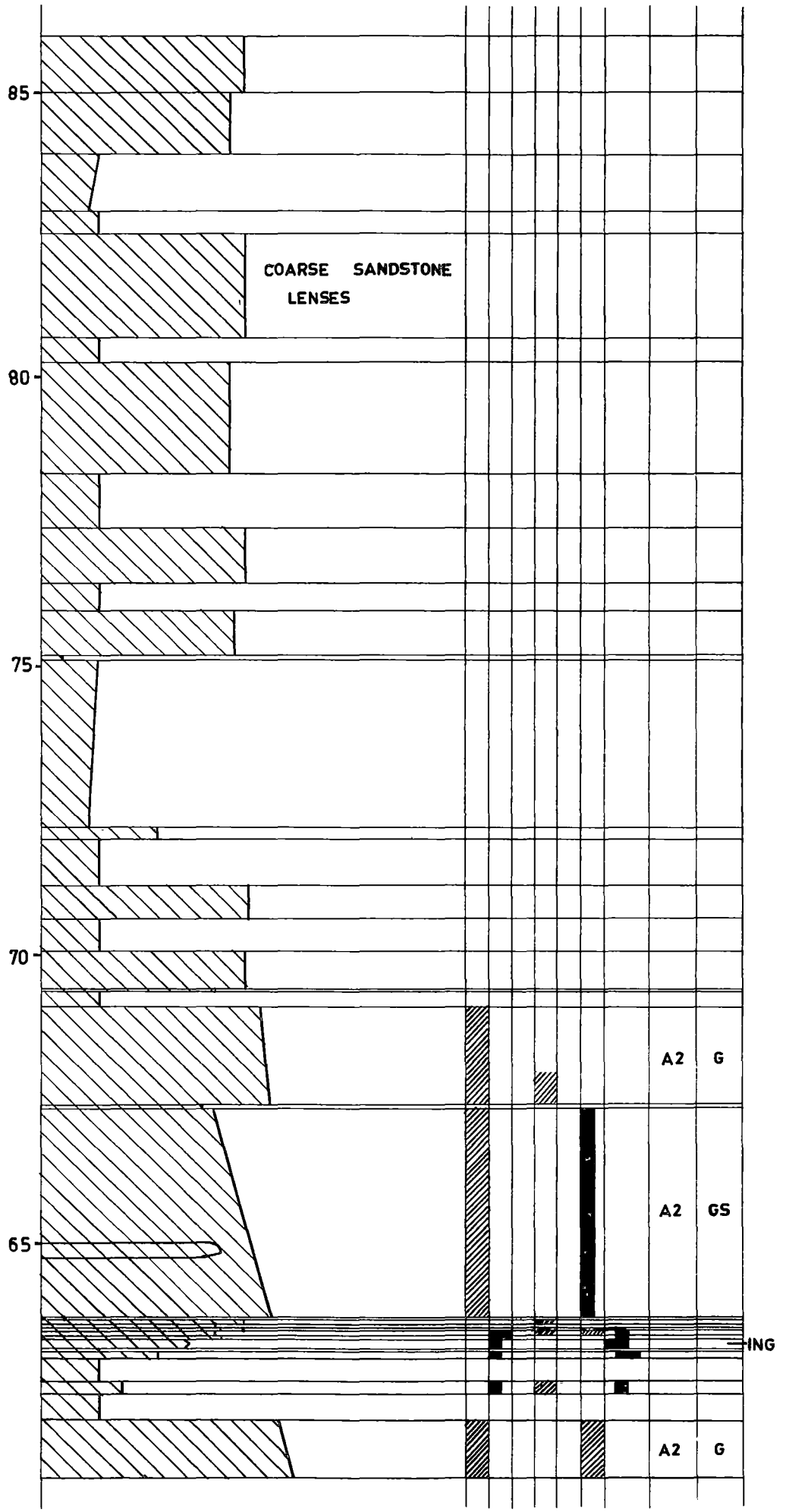
85
80
75
70
65
COARSE SANDSTONE
LENSES
A2
G
A2
GS
ING
A2
G

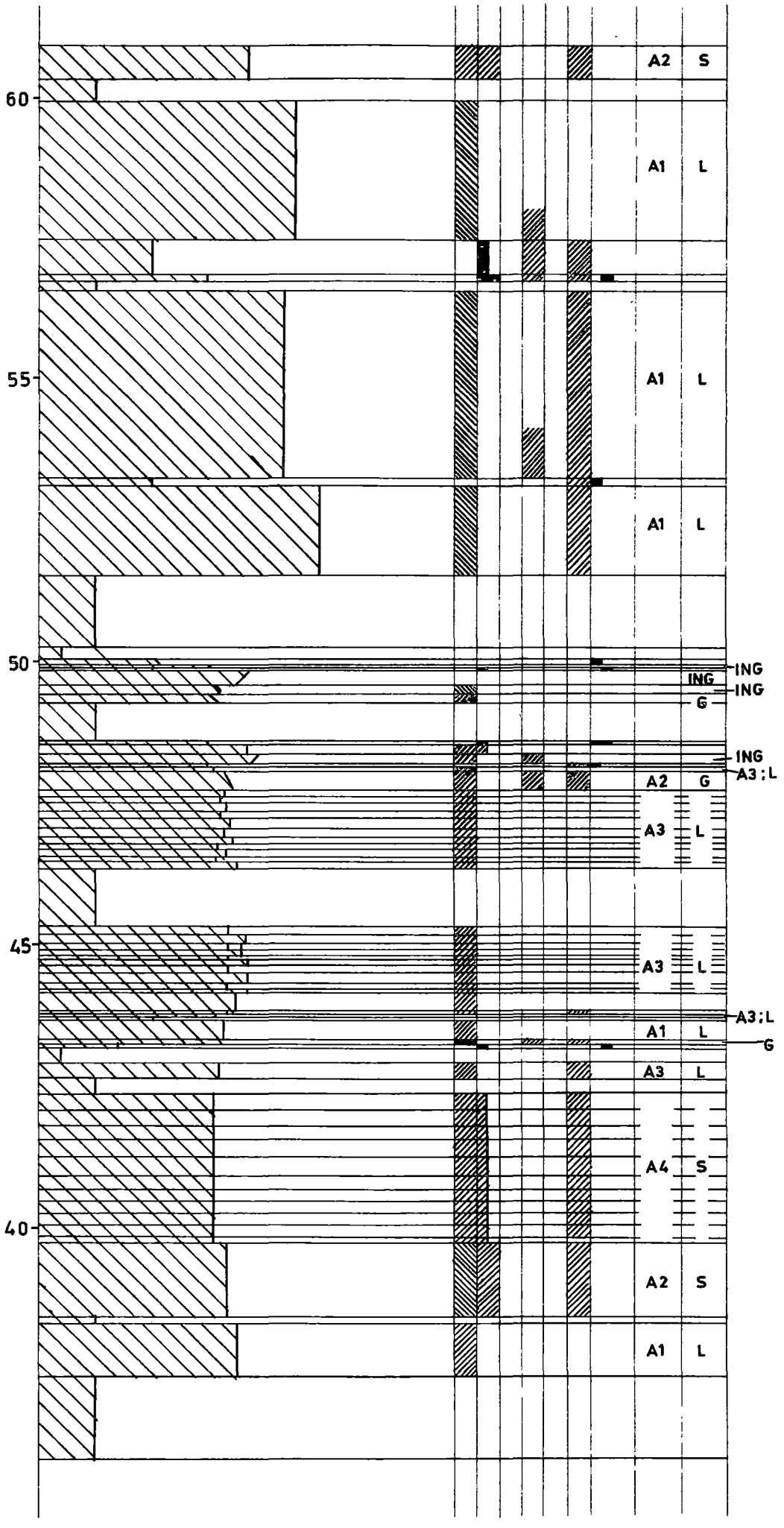
60
55
50
45
40
A2 S
A1 L
A1 L
A1 L
ING
ING
ING
G
ING
A3 ; L
A2 G
A3 L
A3 L
A3 ; L
A1 L
G
A3 L
A4 S
A2 S
A1 L

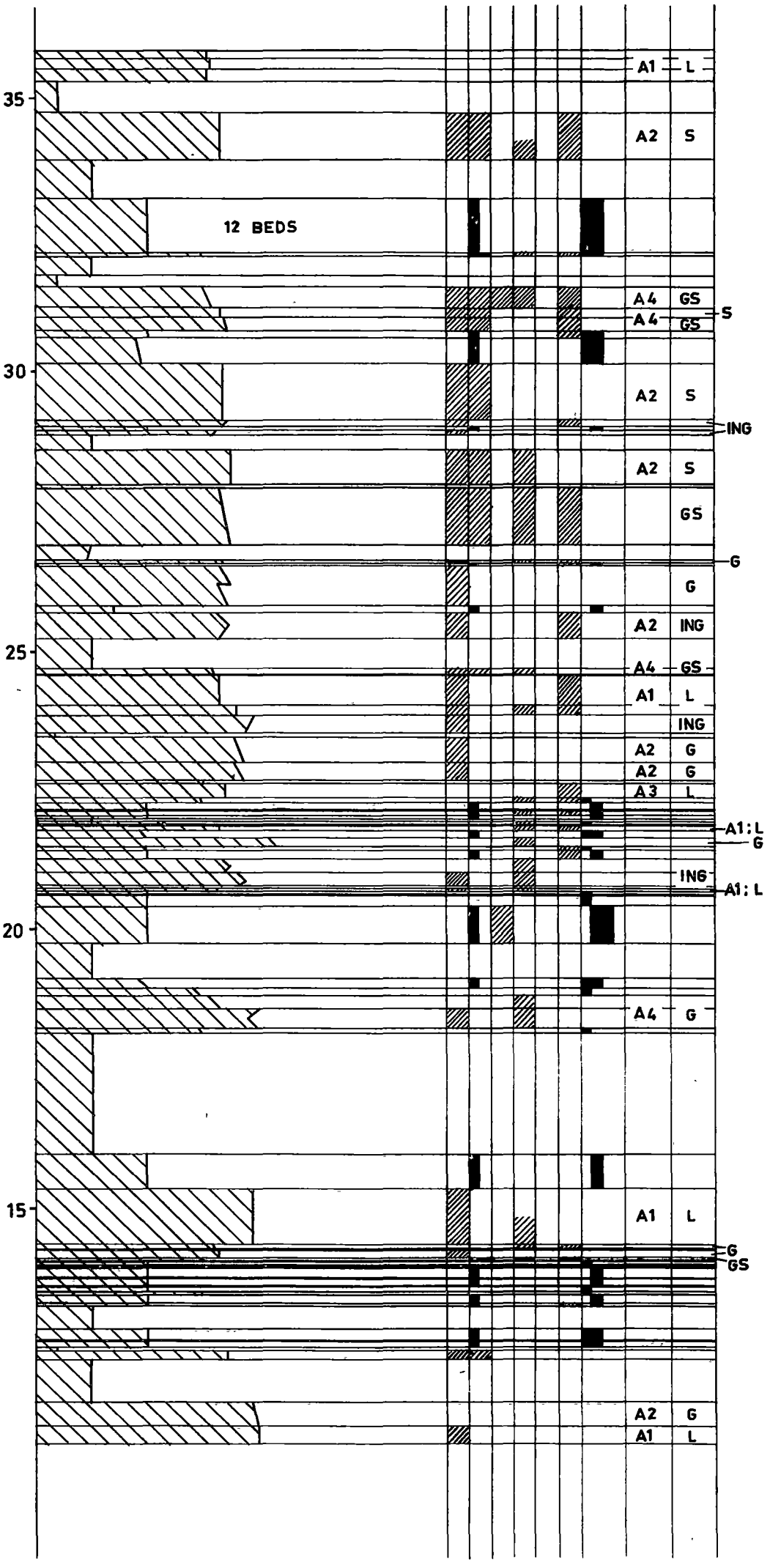
35
30
25
20
15
12 BEDS
A1 L
A2 S
A4 GS
A4 GS
A2 S
ING
A2 S
GS
G
G
A2 ING
A4 GS
A1 L
ING
A2 G
A2 G
A3 L
A1: L
G
ING
A1: L
A4 G
A1 L
G
GS
A2 G
A1 L

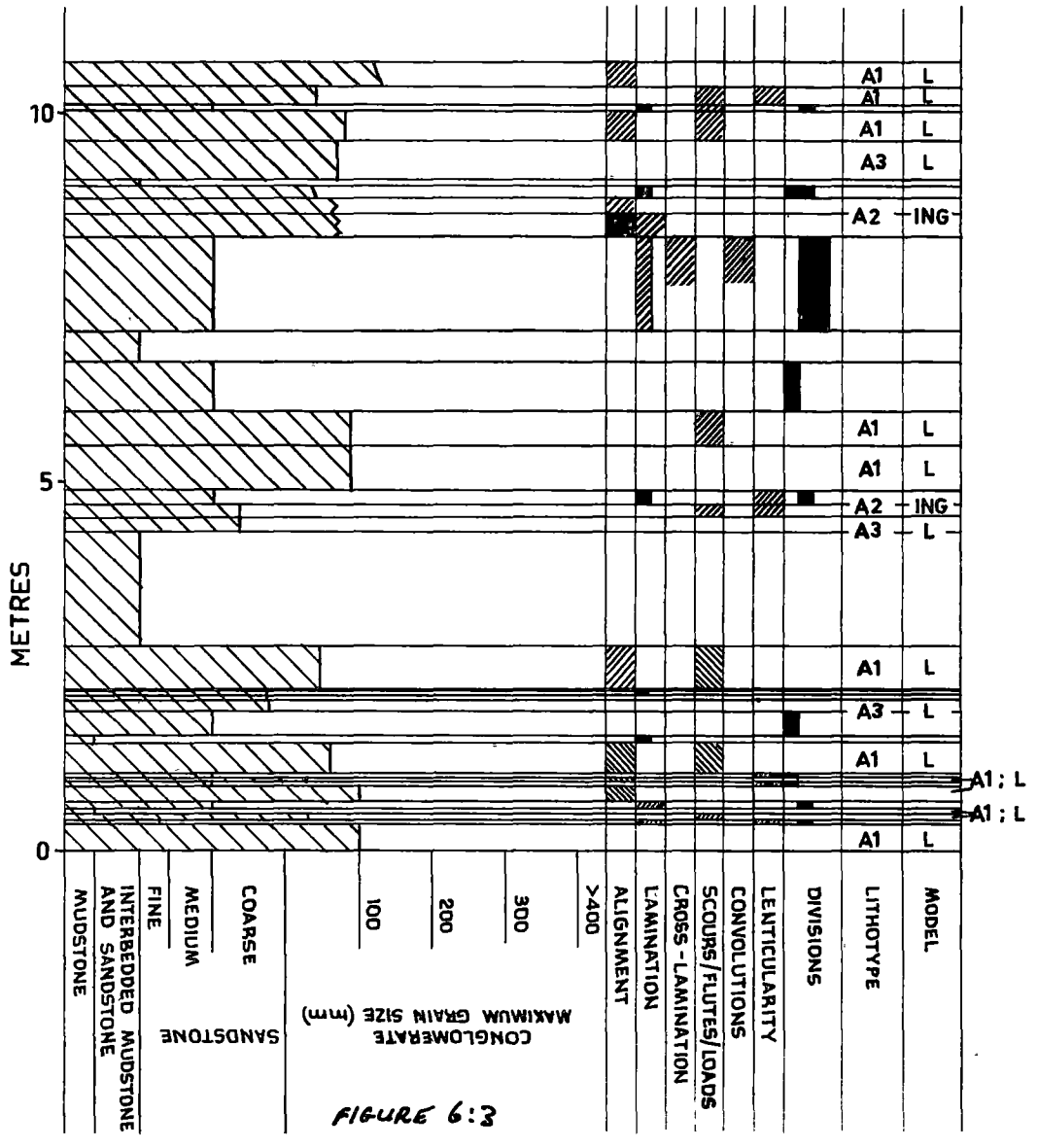
METRES
10
5
0
A1 L
A1 L
A1 L
A3 L
A2 ING
A1 L
A1 L
A2 ING
A3 L
A1 L
A3 L
A1 L
A1 ; L
A1 ; L
A1 L
MODEL
LITHOTYPE
DIVISIONS
LENTICULARITY
CONVOLUTIONS
SCOURS/FLUTES/LOADS
CROSS-LAMINATION
LAMINATION
ALIGNMENT
>400
300
200
100
MAXIMUM GRAIN SIZE (mm)
CONGLOMERATE
COARSE
MEDIUM
FINE
SANDSTONE
INTERBEDDED MUDSTONE AND SANDSTONE
MUDSTONE

FIGURE 6:3

WHITE POINT EAST

C.D. DIAGRAM LOWER 200 BEDS

Figure 6:4:a

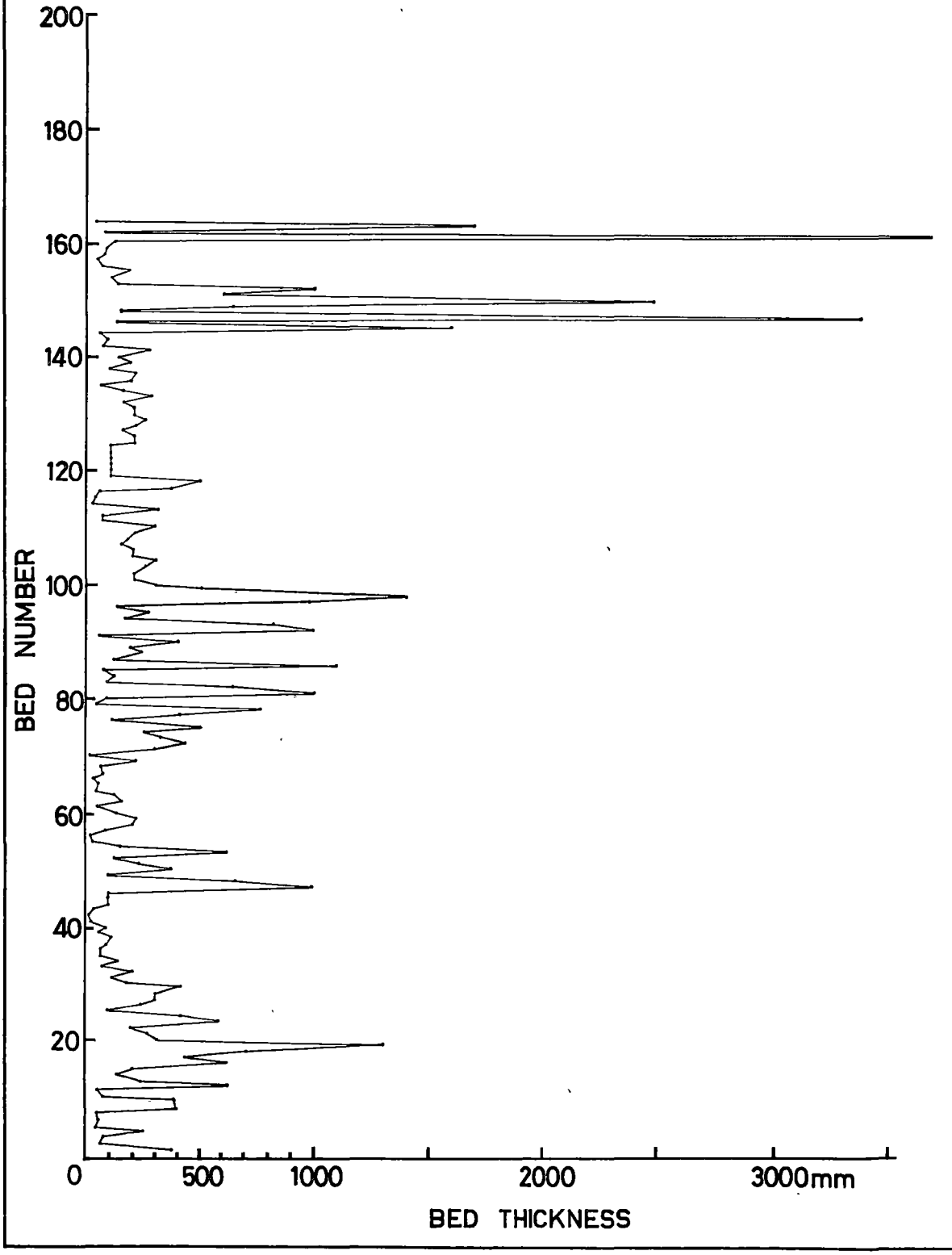

WHITE POINT EAST

SMOOTHED AVERAGE LOWER 200 BEDS

Figure 6:4:b

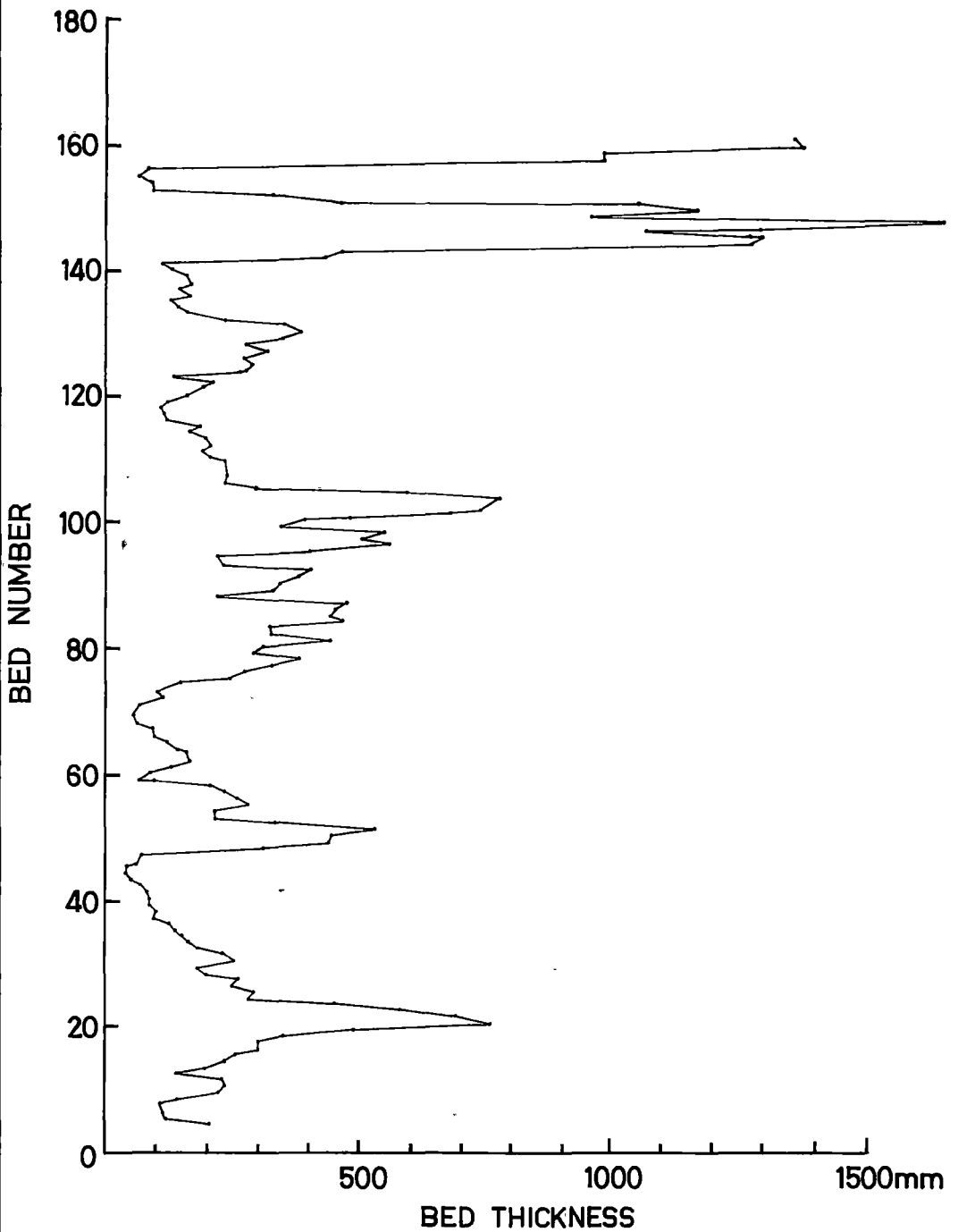

WHITE POINT

CONGLOMERATIC DIVISIONS

Figure 6:5

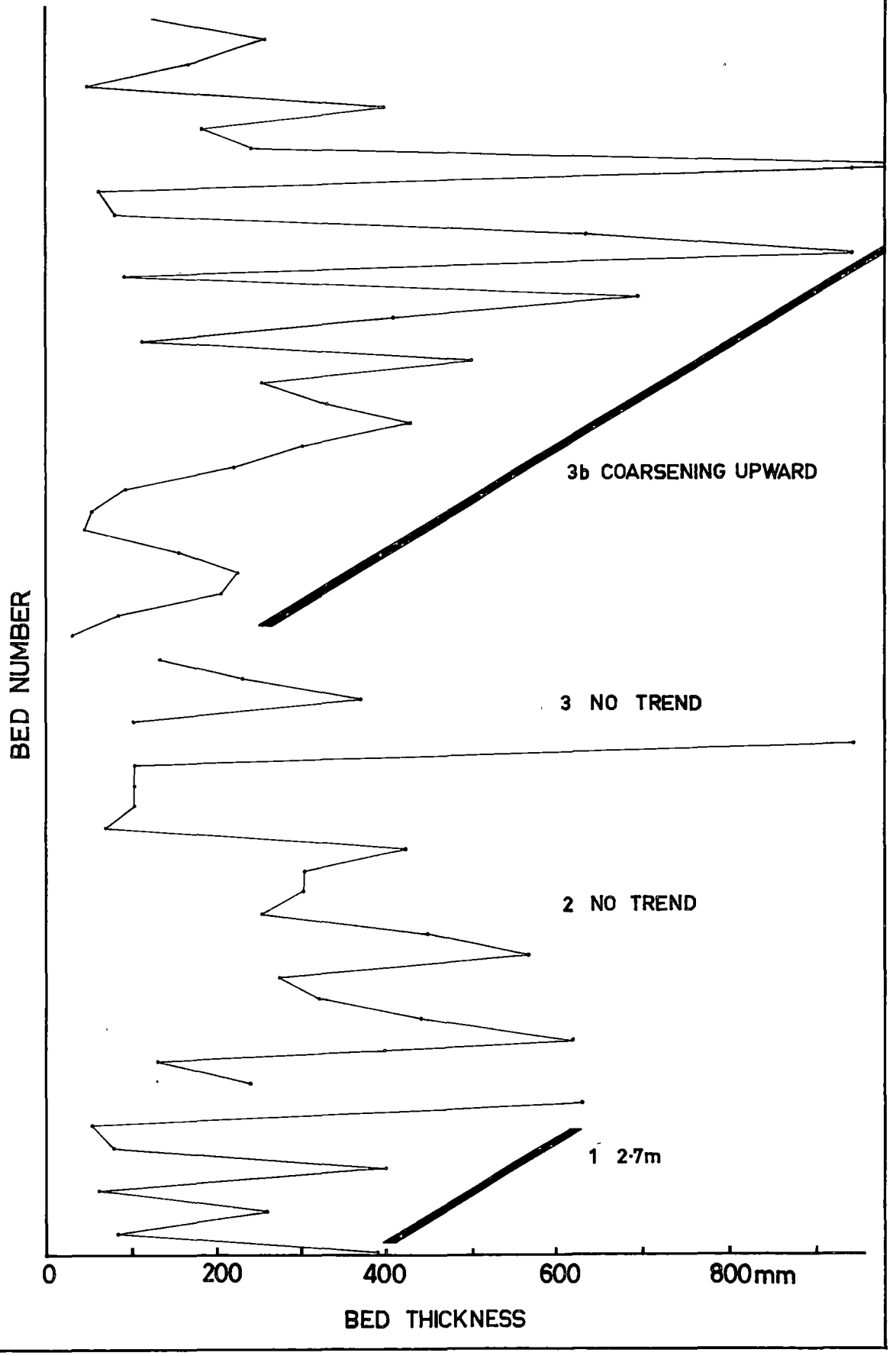

WHITE POINT

Figure 6:6

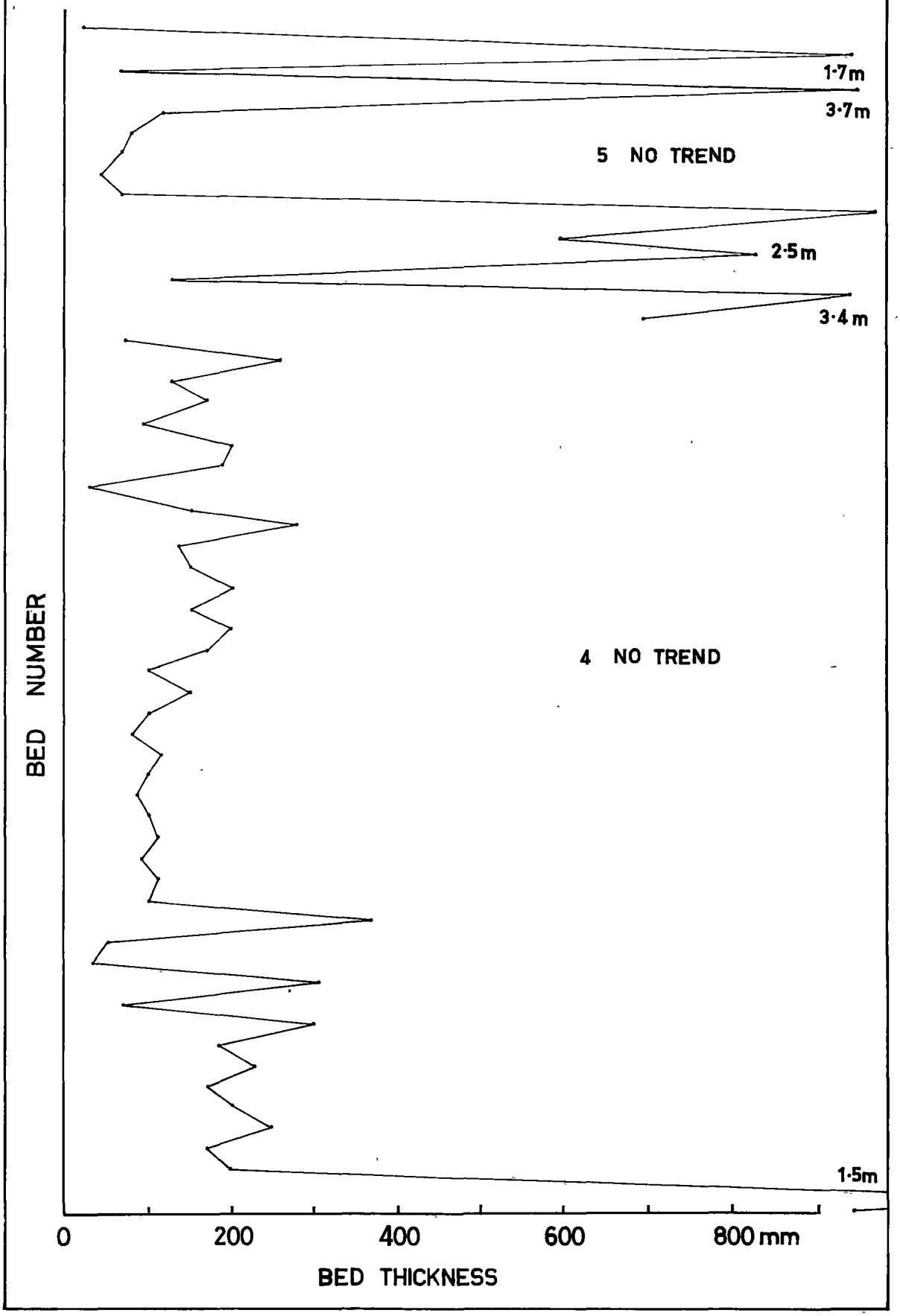

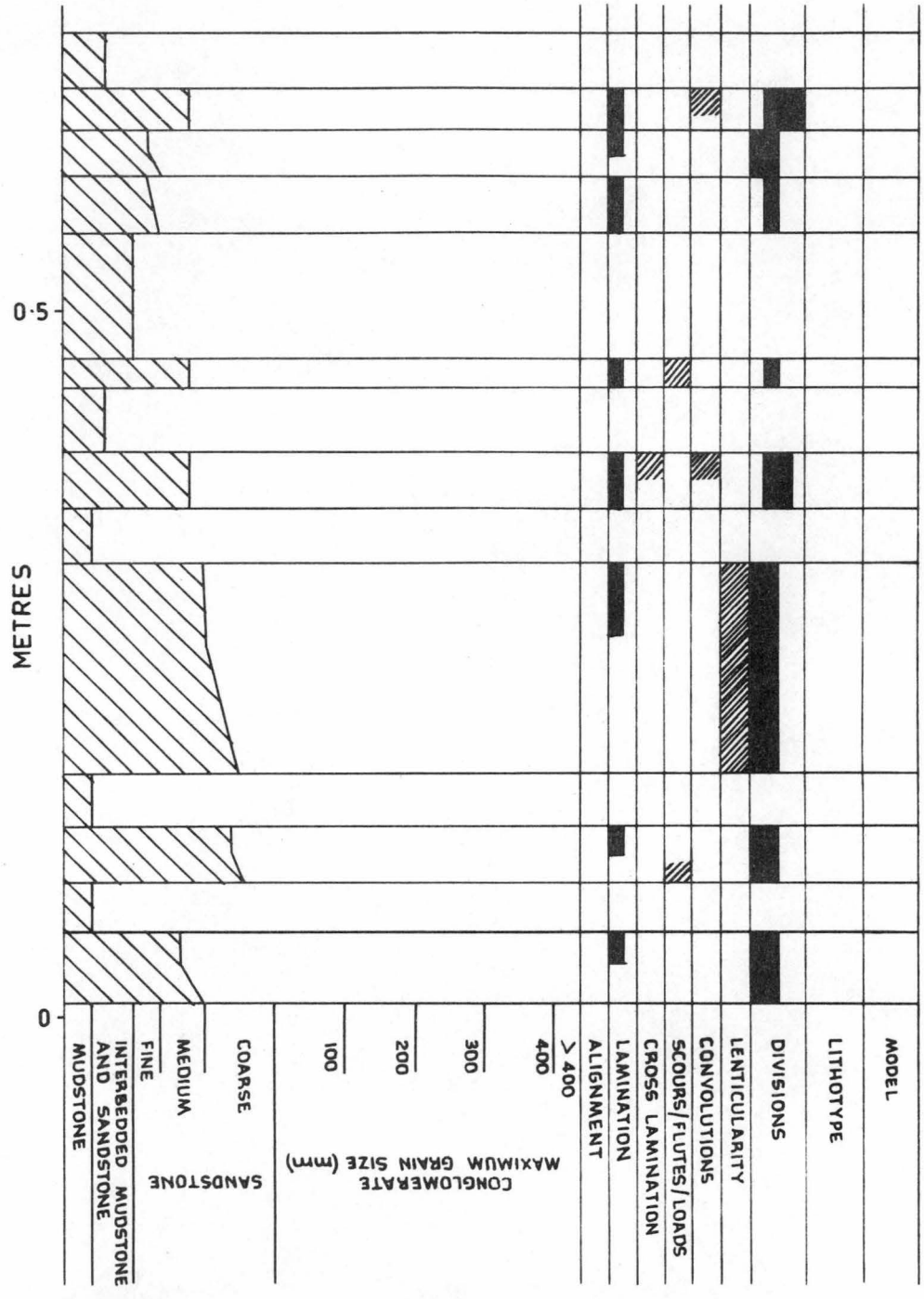

STRATIGRAPHIC SEQUENCE, LONG BAY SHALE

Figure 6:7:a

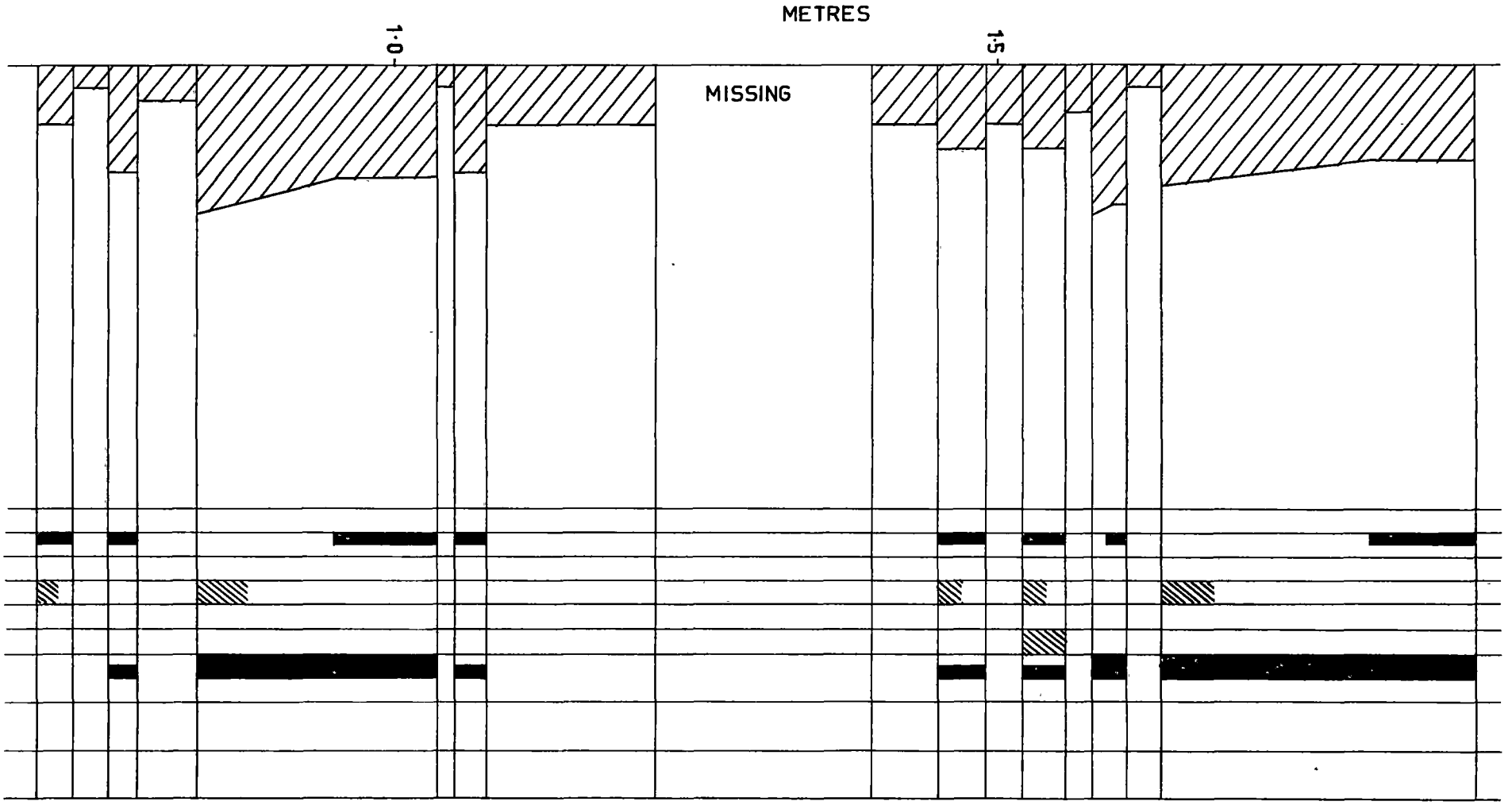
METRES
1·0
1·5
MISSING

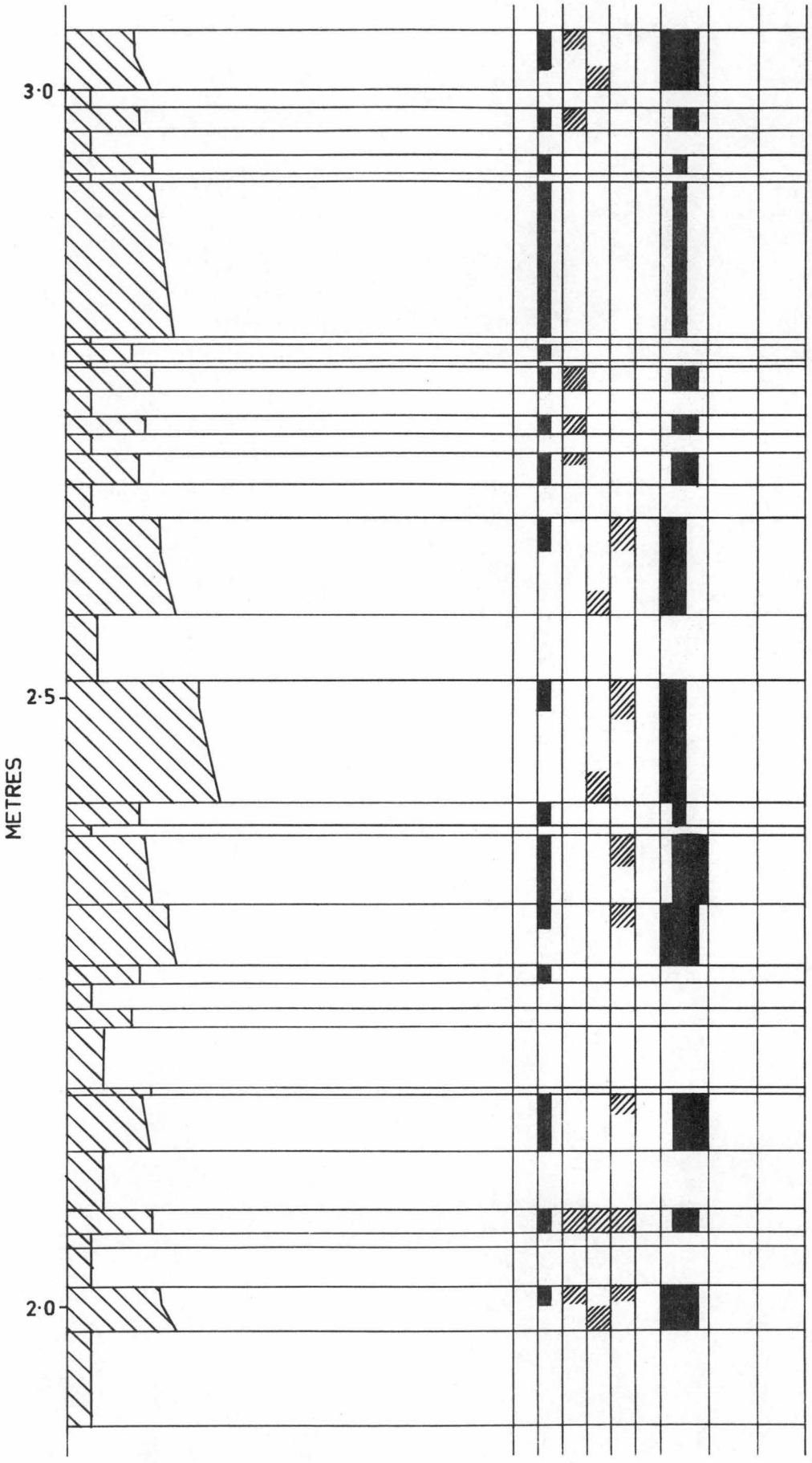
3·0
2·5
2·0
METRES

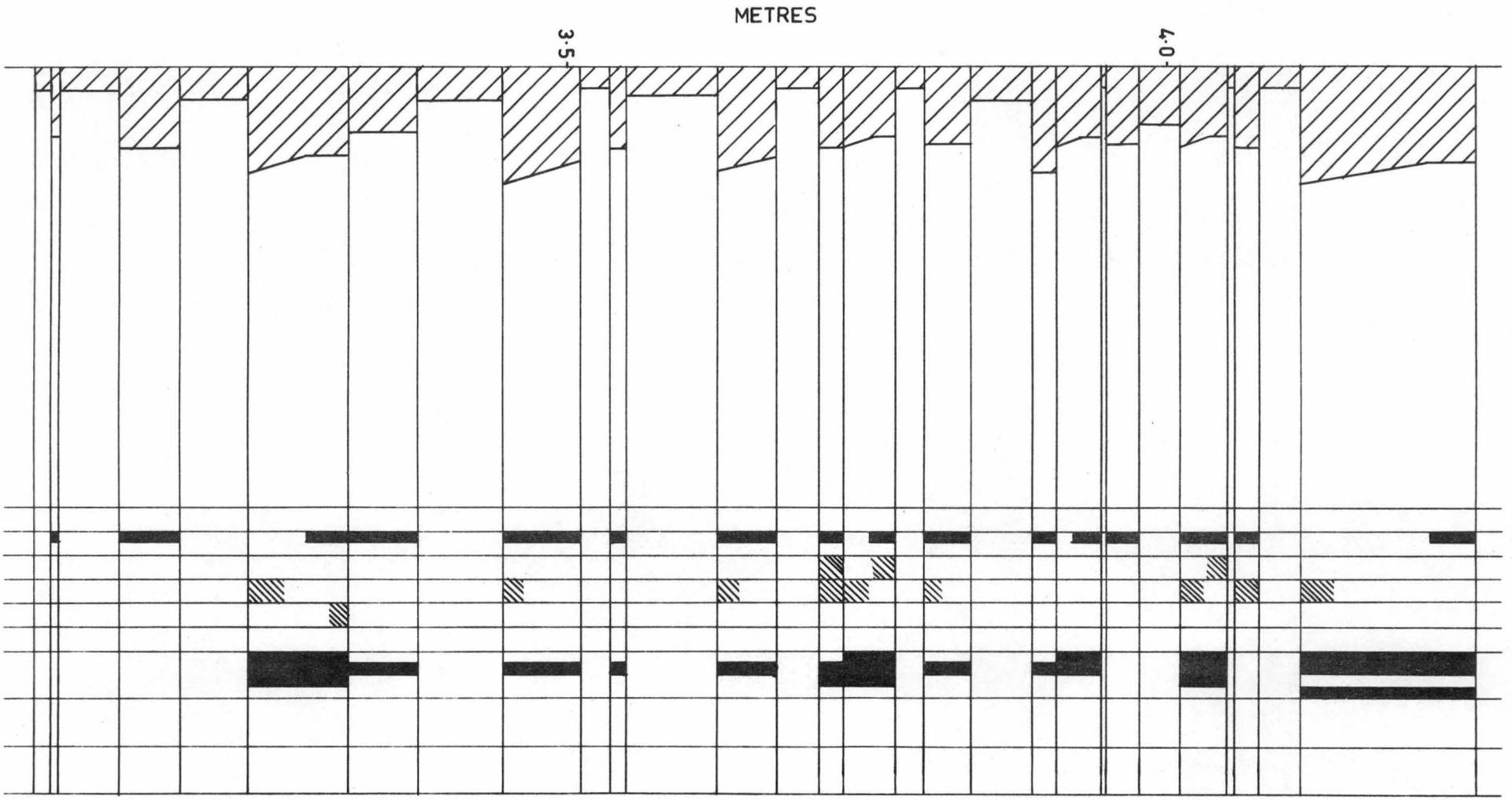
METRES
3·5
4·0

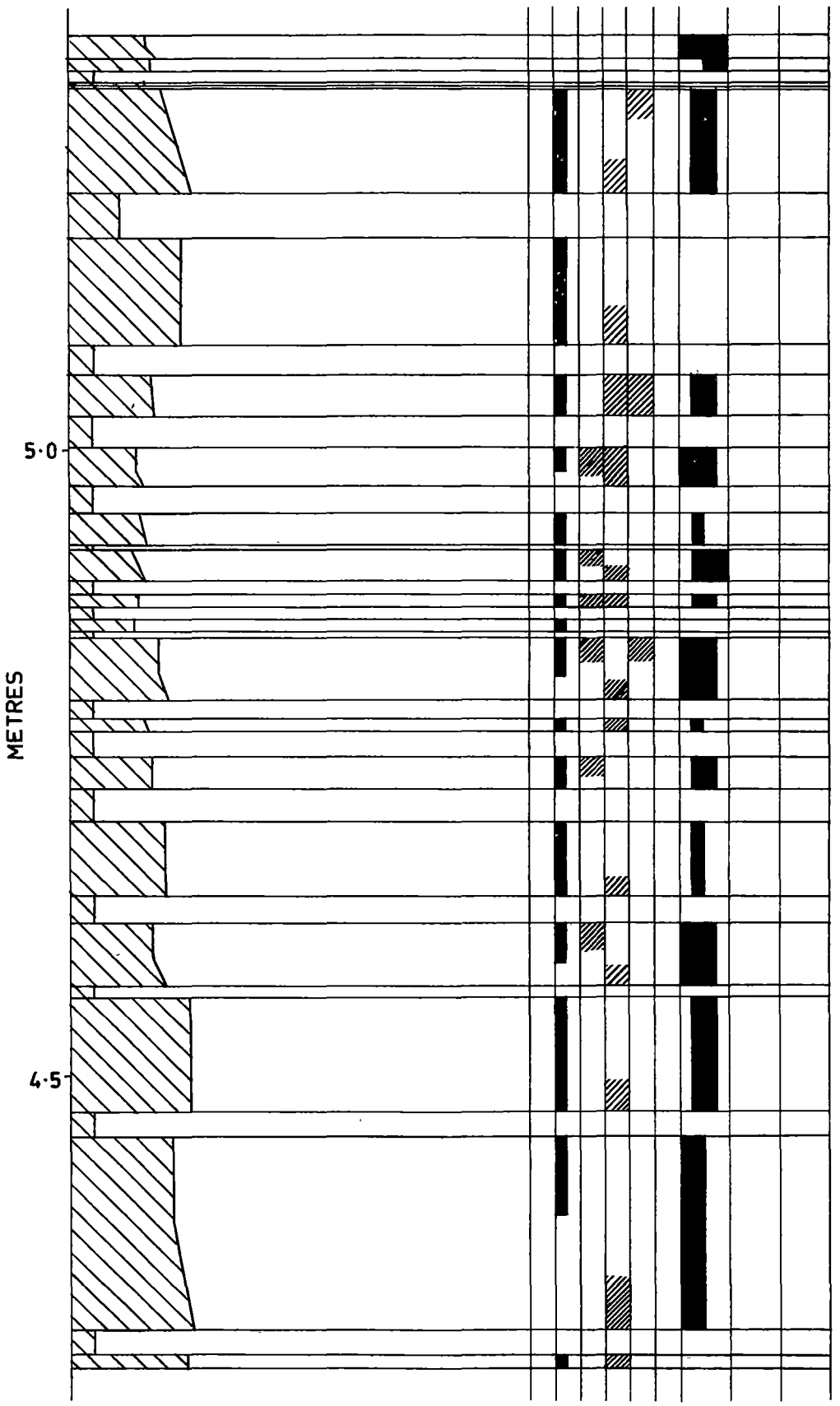
5·0
4·5
METRES

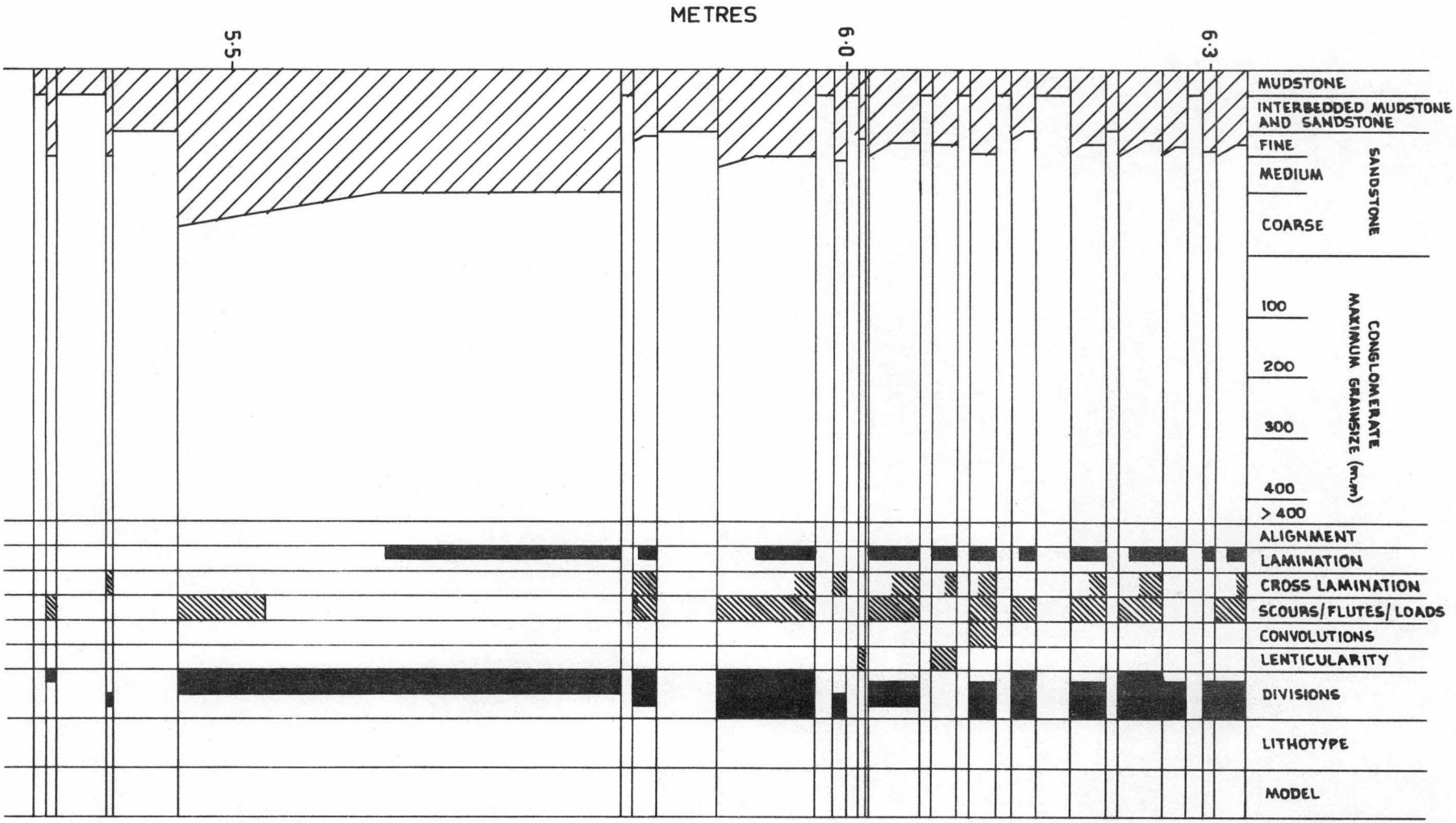
METRES
5·5
6·0
6·3
MUDSTONE
INTERBEDDED MUDSTONE AND SANDSTONE
SANDSTONE
FINE
MEDIUM
COARSE
CONGLOMERATE MAXIMUM GRAINSIZE (m.m)
100
200
300
400
> 400
ALIGNMENT
LAMINATION
CROSS LAMINATION
SCOURS/FLUTES/LOADS
CONVOLUTIONS
LENTICULARITY
DIVISIONS
LITHOTYPE
MODEL

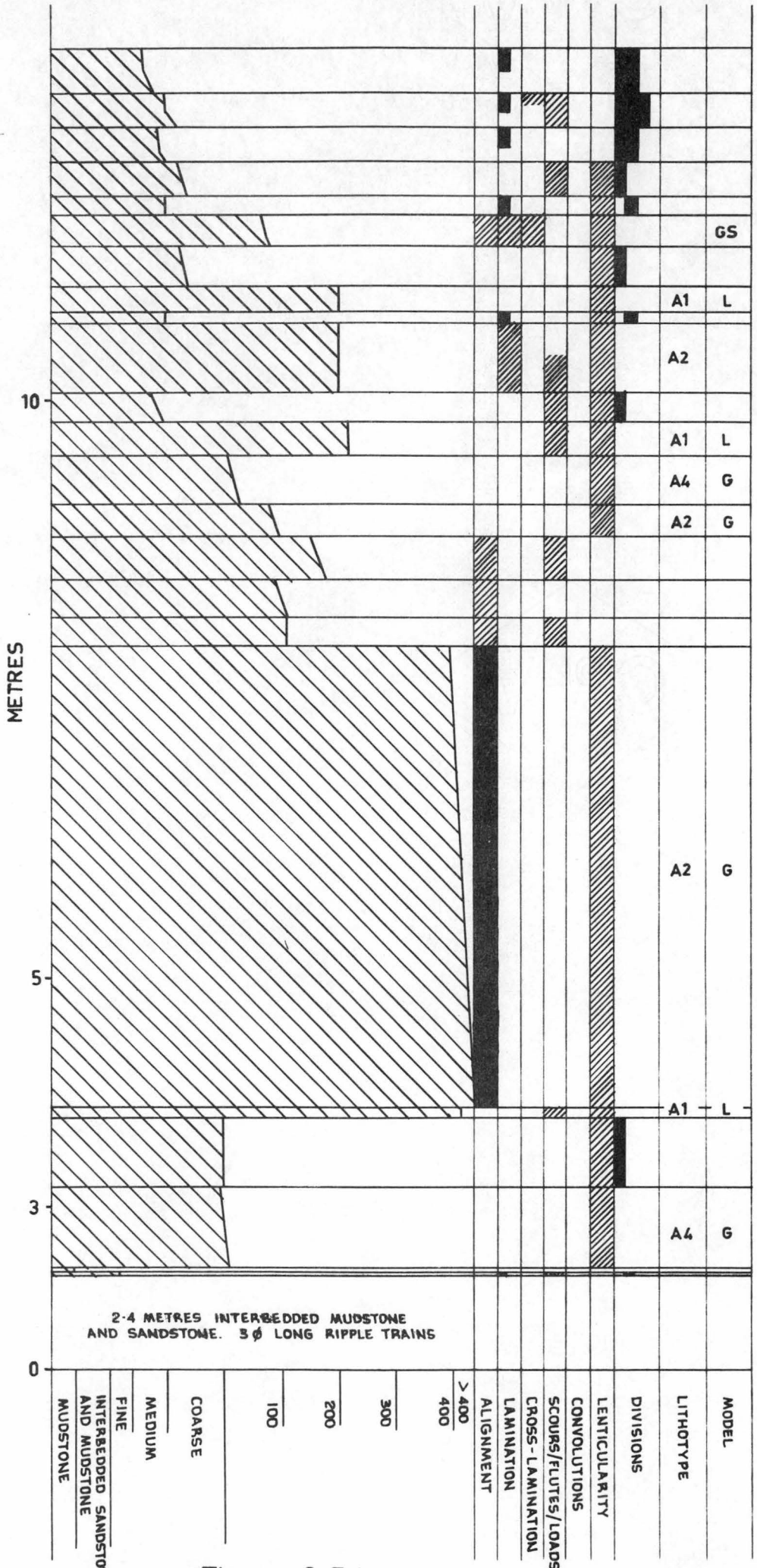
METRES
10
5
3
0
2·4 METRES INTERBEDDED MUDSTONE
AND SANDSTONE. 3ø LONG RIPPLE TRAINS
A1 L
A2
A1 L
A4 G
A2 G
A2 G
A1 L
A4 G
GS
MUDSTONE
INTERBEDDED SANDSTONE AND MUDSTONE
FINE
MEDIUM
COARSE
100
200
300
400
> 400
ALIGNMENT
LAMINATION
CROSS-LAMINATION
SCOURS/FLUTES/LOADS
CONVOLUTIONS
LENTICULARITY
DIVISIONS
LITHOTYPE
MODEL

Figure 6:7:b

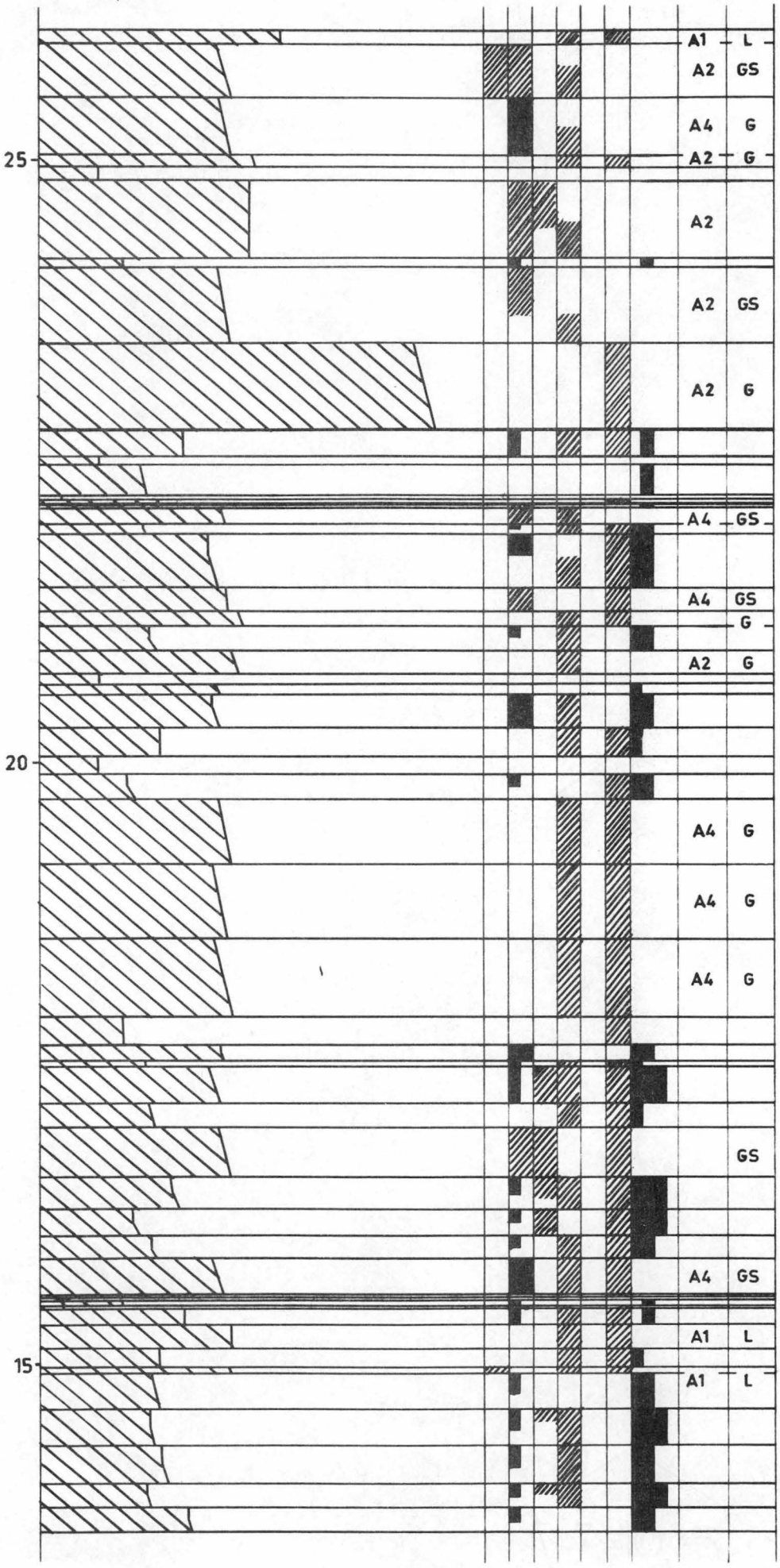
A1 L
A2 GS
A4 G
A2 G
25
A2
A2 GS
A2 G
A4 GS
A4 GS
G
A2 G
20
A4 G
A4 G
A4 G
GS
A4 GS
A1 L
A1 L
15

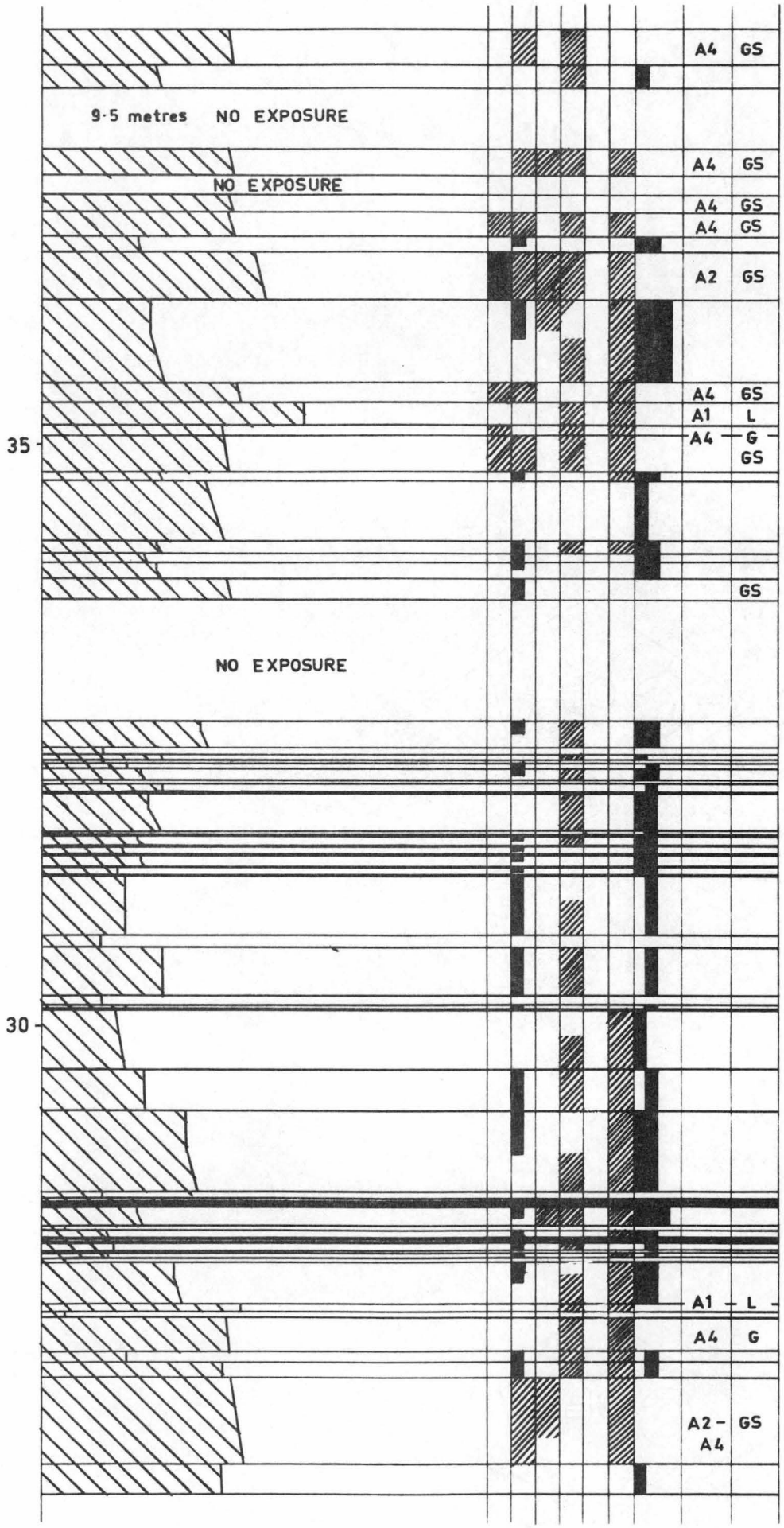
9·5 metres NO EXPOSURE
NO EXPOSURE
NO EXPOSURE
35
30
A4 GS
A4 GS
A4 GS
A4 GS
A2 GS
A4 GS
A1 L
A4 G
GS
GS
A1 L
A4 G
A2 GS
A4

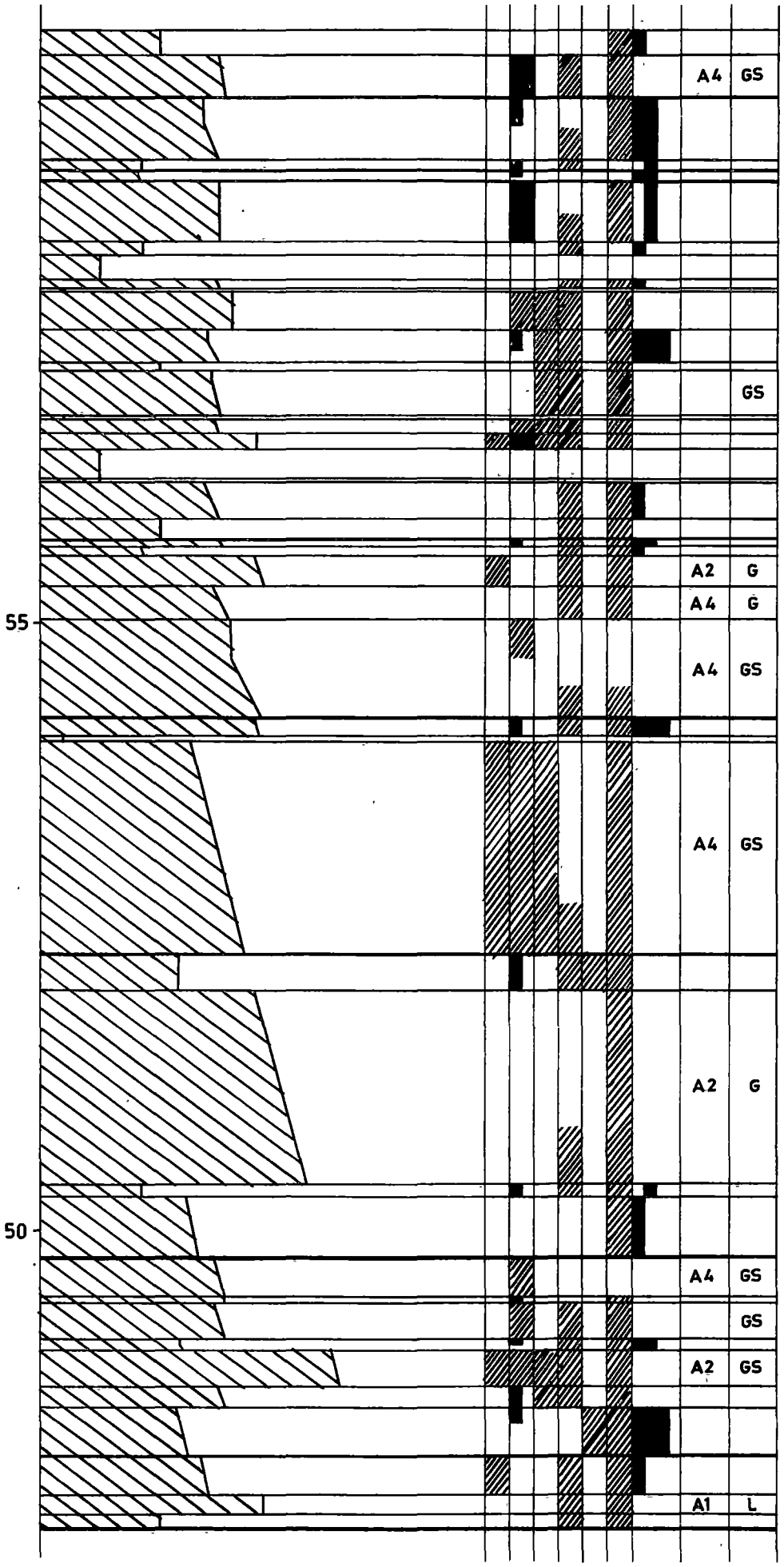
A4 GS
GS
A2 G
A4 G
55
A4 GS
A4 GS
A2 G
50
A4 GS
GS
A2 GS
A1 L

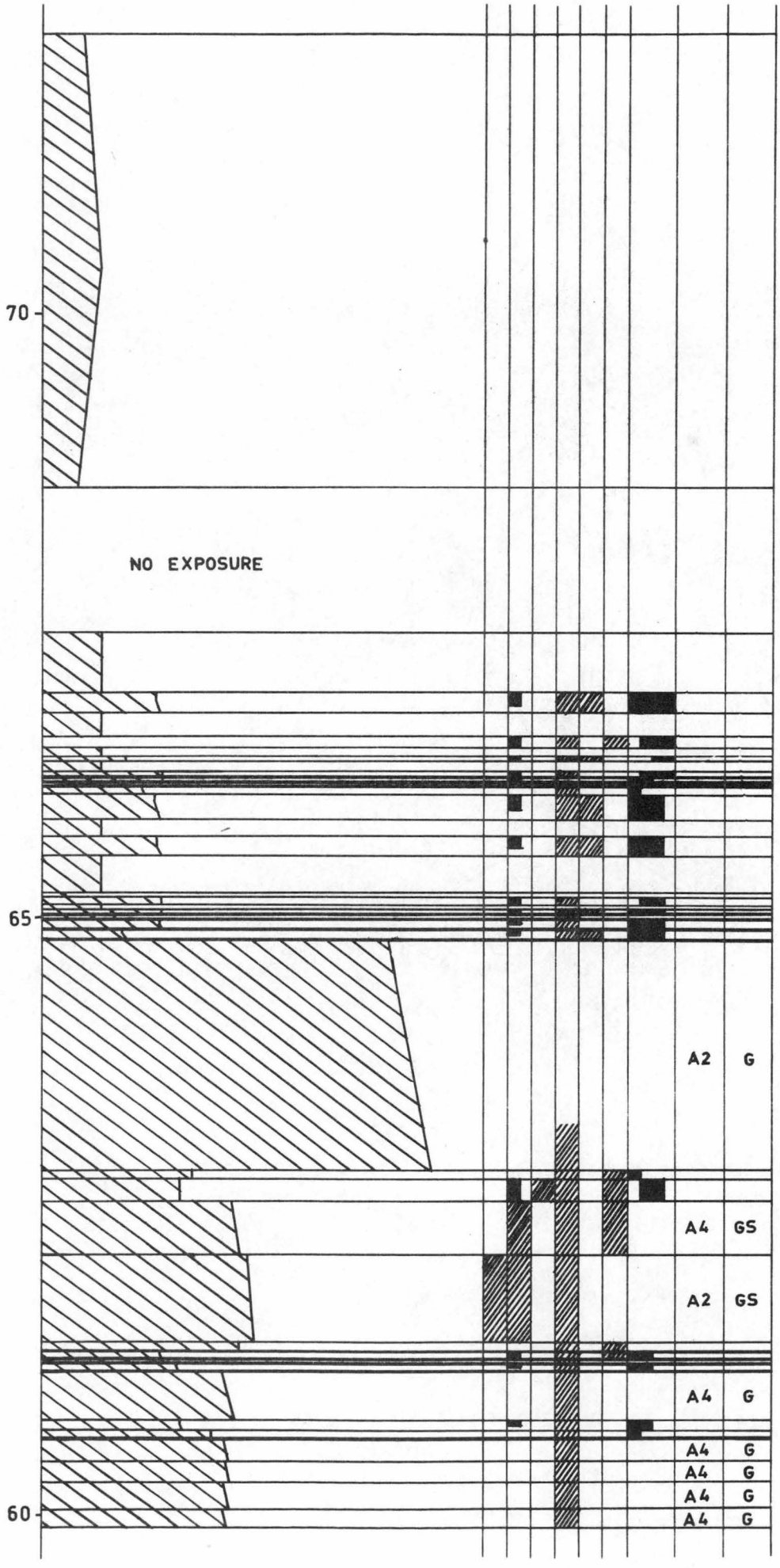
70
NO EXPOSURE
65
A2 G
A4 GS
A2 GS
A4 G
A4 G
A4 G
A4 G
A4 G
60

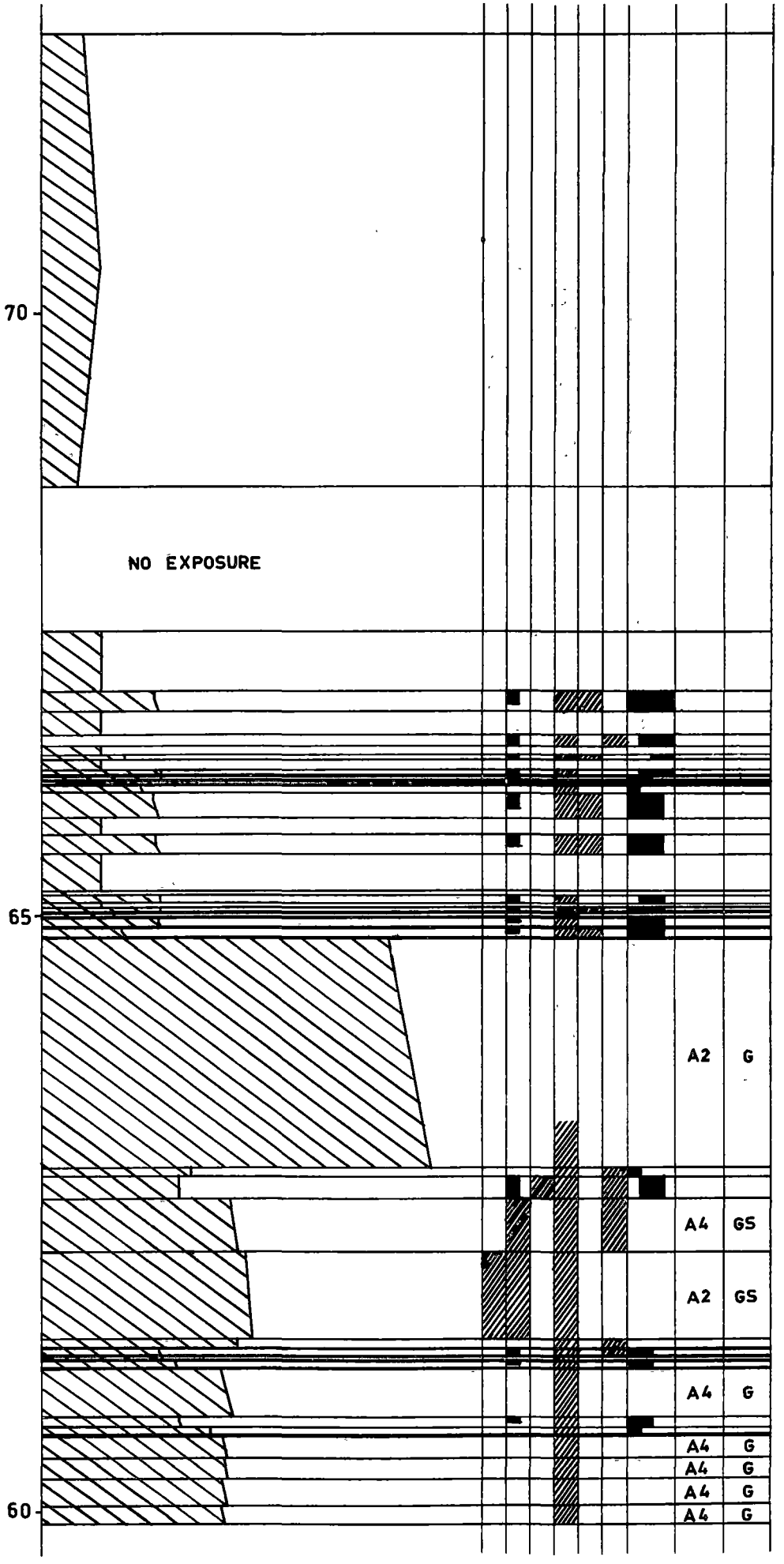
70
NO EXPOSURE
65
A2
G
A4
GS
A2
GS
A4
G
A4
G
A4
G
A4
G
A4
G
60

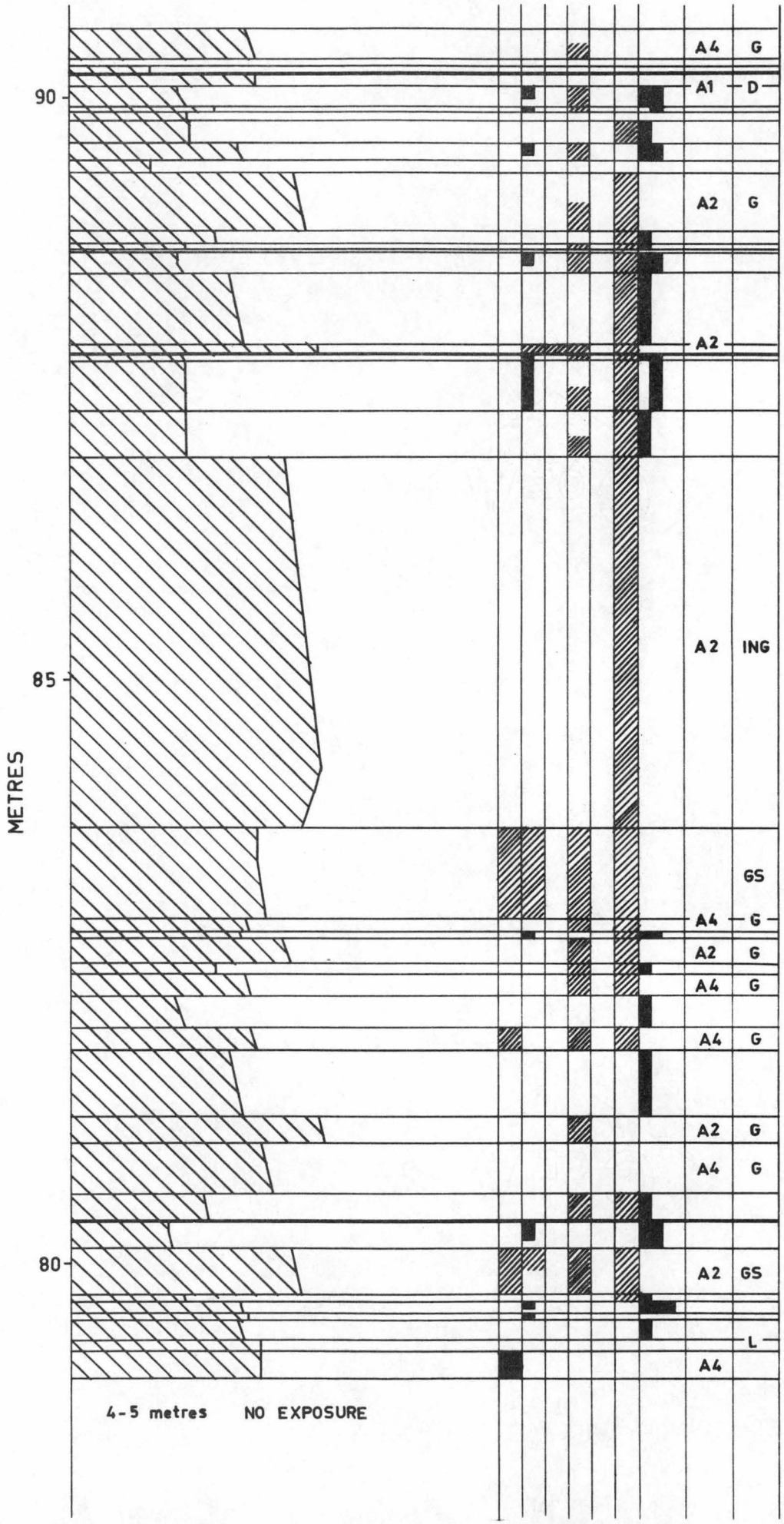
METRES
90
85
80
A4 G
A1 D
A2 G
A2
A2 ING
GS
A4 G
A2 G
A4 G
A4 G
A2 G
A4 G
A2 GS
L
A4
4-5 metres NO EXPOSURE

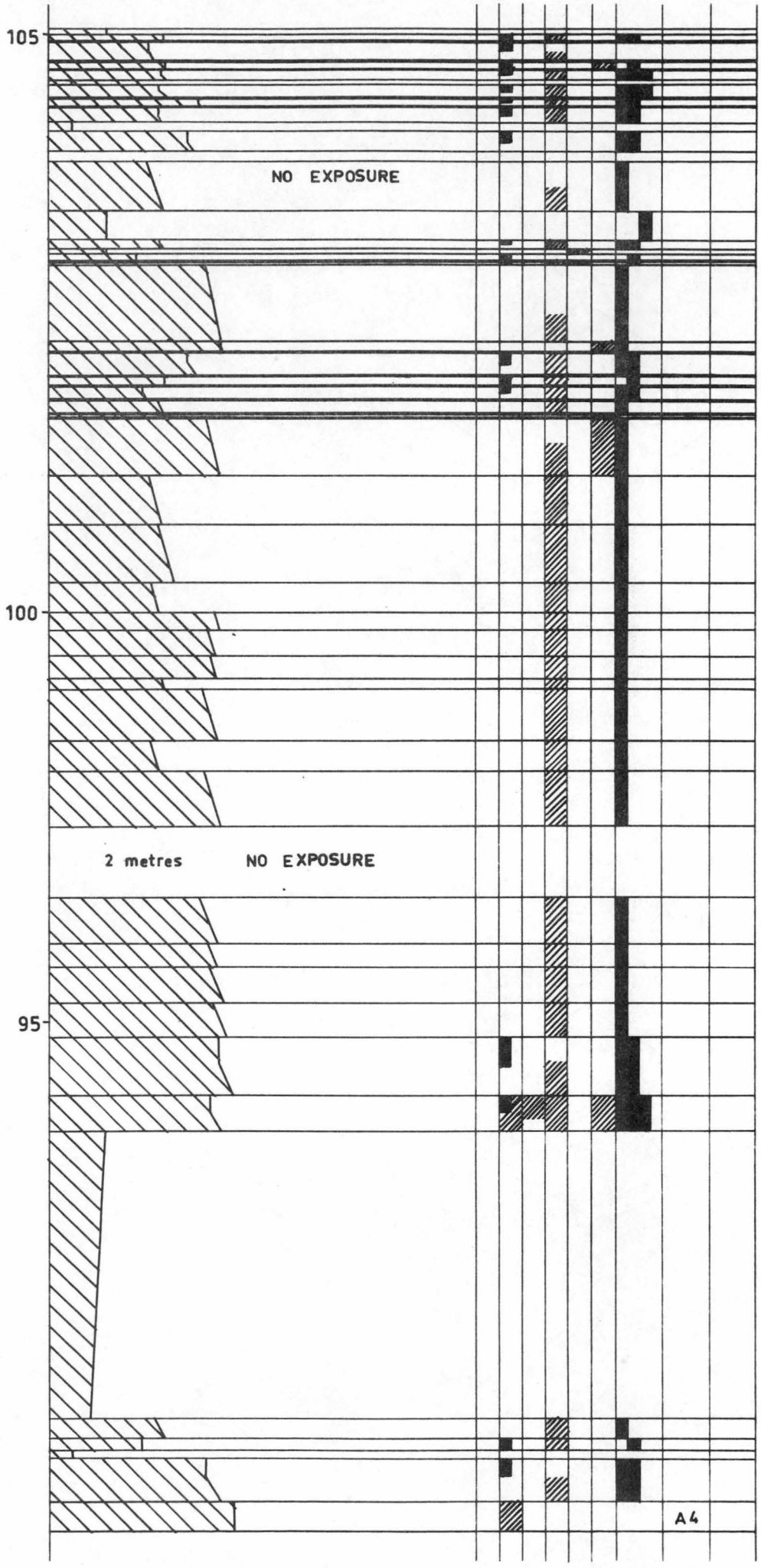
105
NO EXPOSURE
100
2 metres
NO EXPOSURE
95
A4

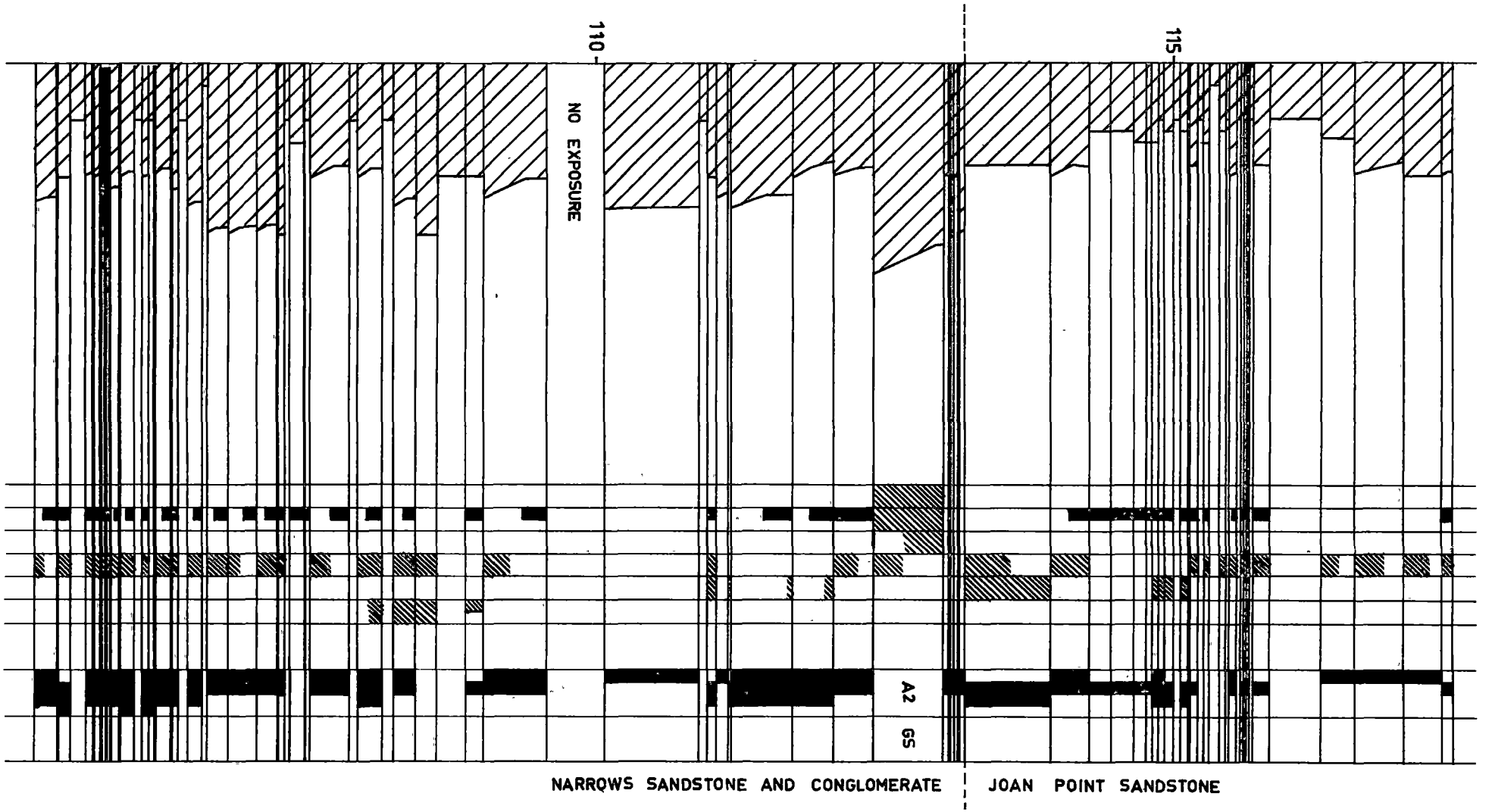
110
115
NO EXPOSURE
A2
GS
NARROWS SANDSTONE AND CONGLOMERATE
JOAN POINT SANDSTONE

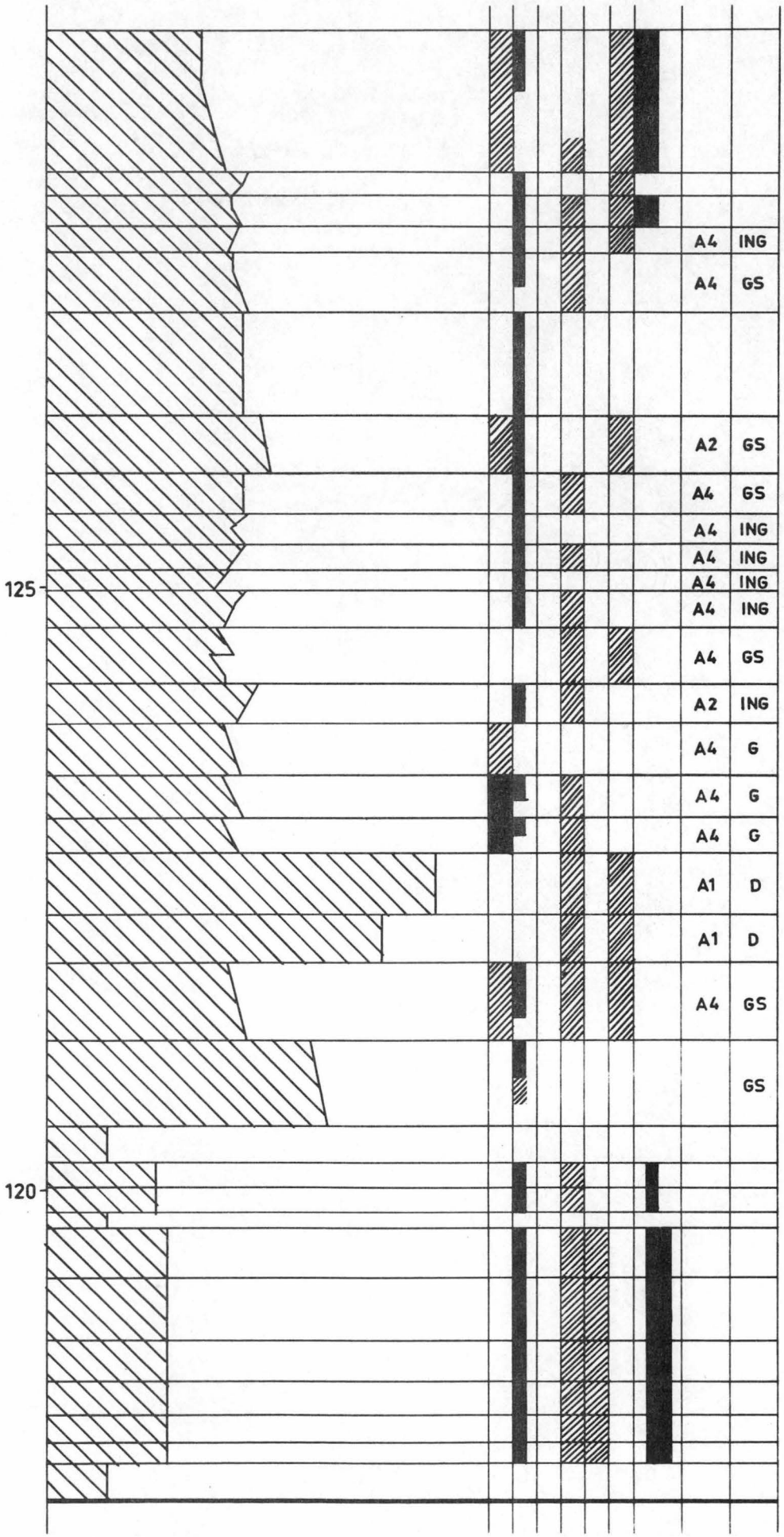
125
120
A4 ING
A4 GS
A2 GS
A4 GS
A4 ING
A4 ING
A4 ING
A4 ING
A4 GS
A2 ING
A4 G
A4 G
A4 G
A1 D
A1 D
A4 GS
GS

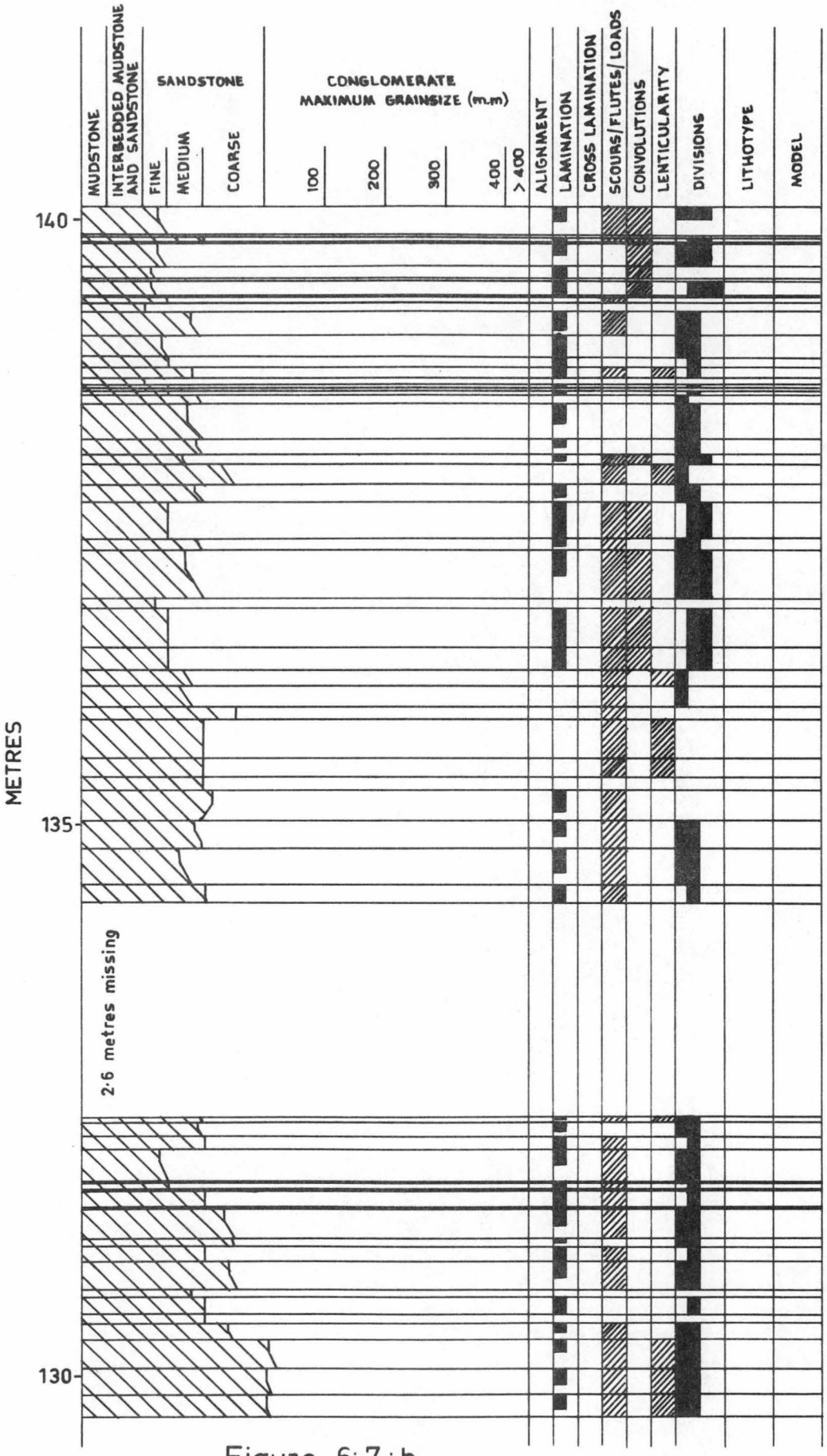
MUDSTONE
INTERBEDDED MUDSTONE AND SANDSTONE
SANDSTONE
FINE
MEDIUM
COARSE
CONGLOMERATE MAXIMUM GRAINSIZE (m.m)
100
200
300
400
> 400
ALIGNMENT
LAMINATION
CROSS LAMINATION
SCOURS/FLUTES/LOADS
CONVOLUTIONS
LENTICULARITY
DIVISIONS
LITHOTYPE
MODEL
METRES
140
135
130
2·6 metres missing

Figure 6:7:b

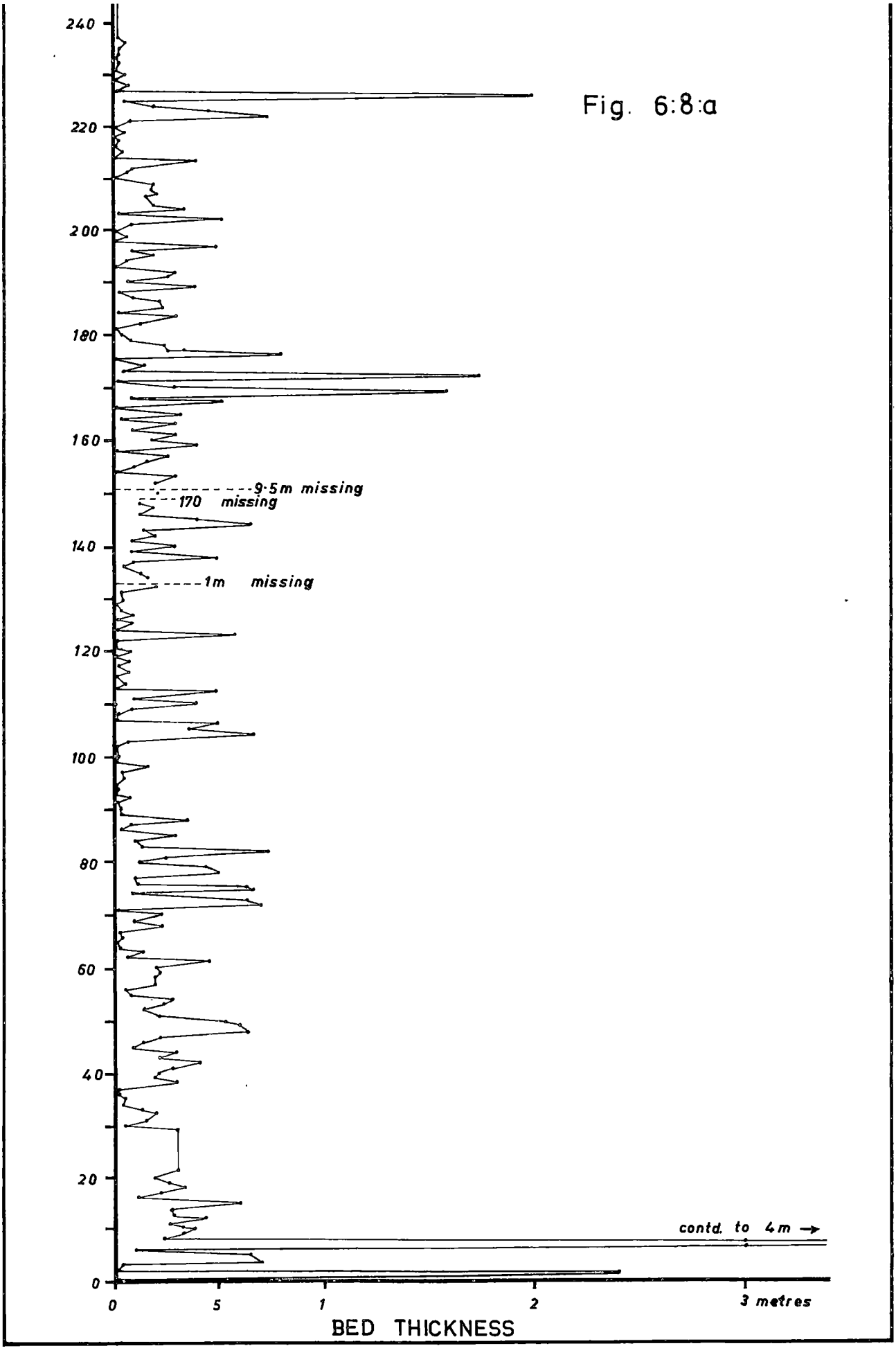
240
220
200
180
160
140
120
100
80
60
40
20
0
9·5m missing
170 missing
1m missing
contd. to 4m →
0
5
1
2
3 metres
BED THICKNESS

Fig. 6:8:a

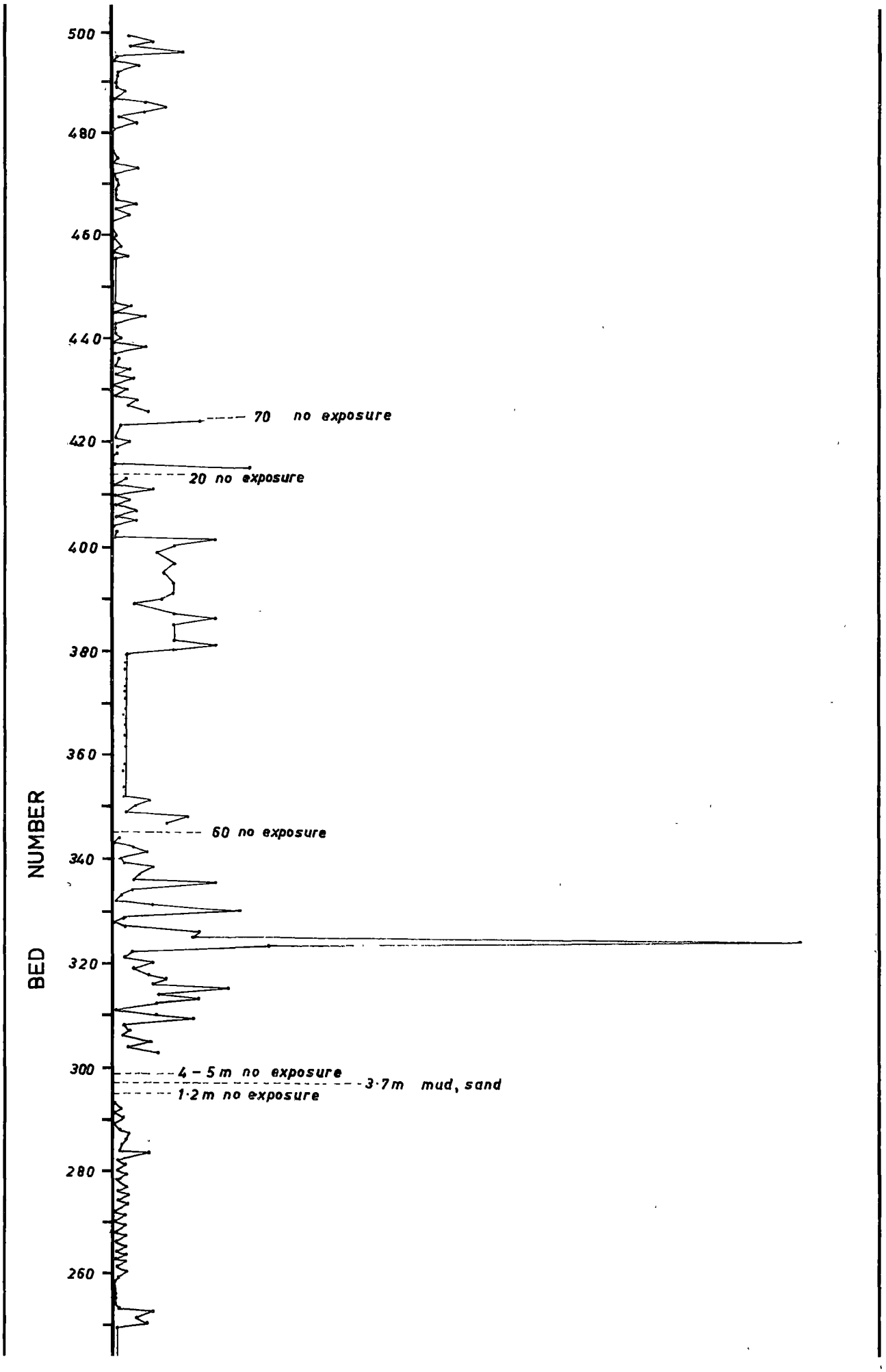
BED NUMBER
500
480
460
440
420
400
380
360
340
320
300
280
260
70 no exposure
20 no exposure
60 no exposure
4 – 5 m no exposure
3·7m mud, sand
1·2m no exposure

NARRROWS FORMATION—LAYER DIAGRAM

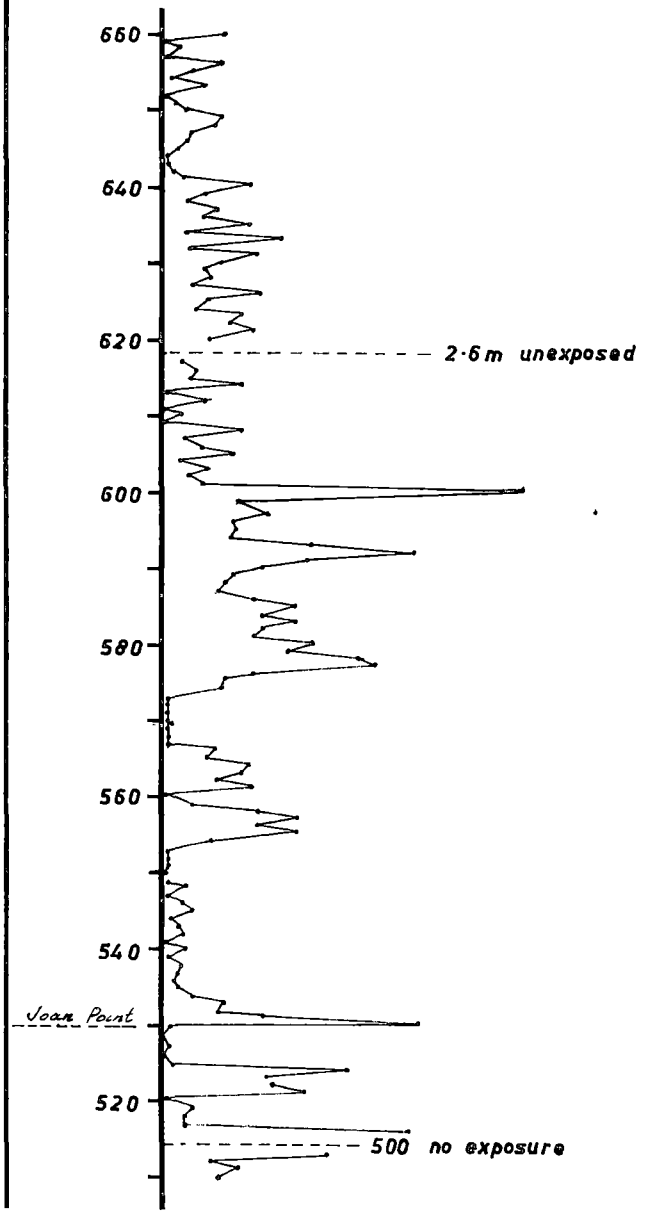

Figure 6:8:a

FARRELL POINT

CONGLOMERATE & SANDSTONE COARSE DIVISIONS

Figure 6:8:b

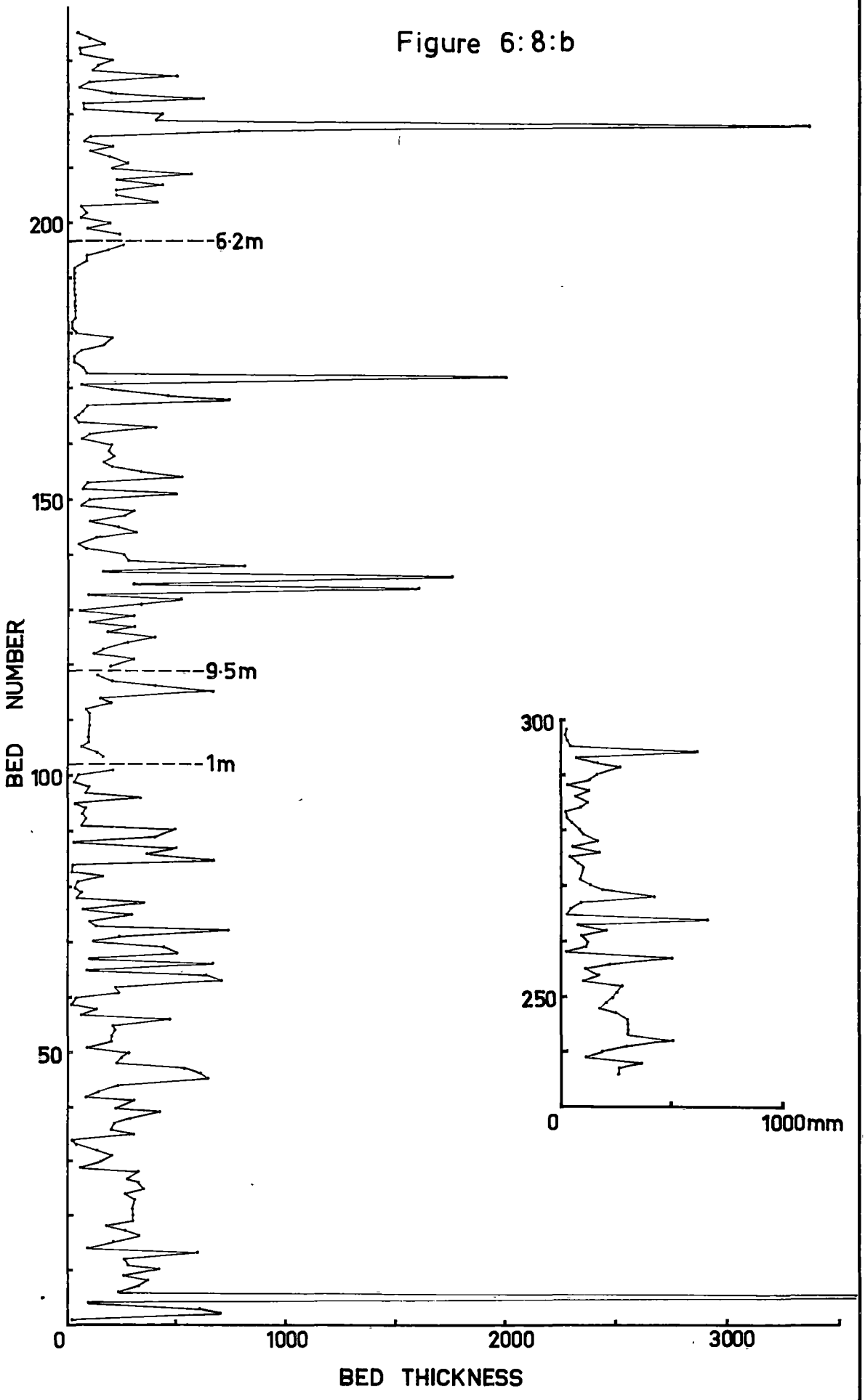

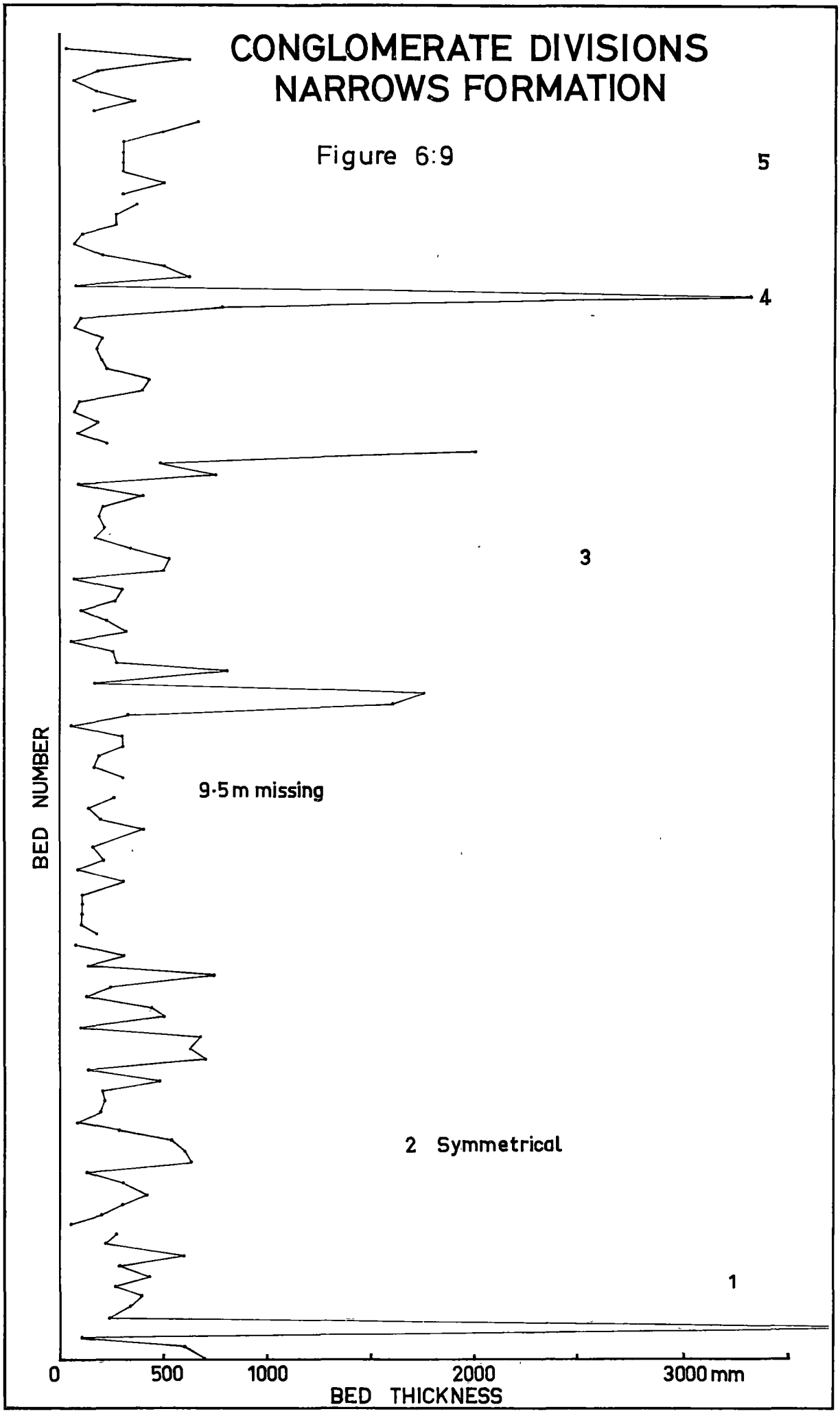
CONGLOMERATE DIVISIONS
NARROWS FORMATION
Figure 6:9
5
4
3
9·5 m missing
2 Symmetrical
1
BED NUMBER
0
500
1000
2000
3000 mm
BED THICKNESS

COARSE DIVISIONS
CLYTIE COVE GROUP GENERALISED

Figure 6:10

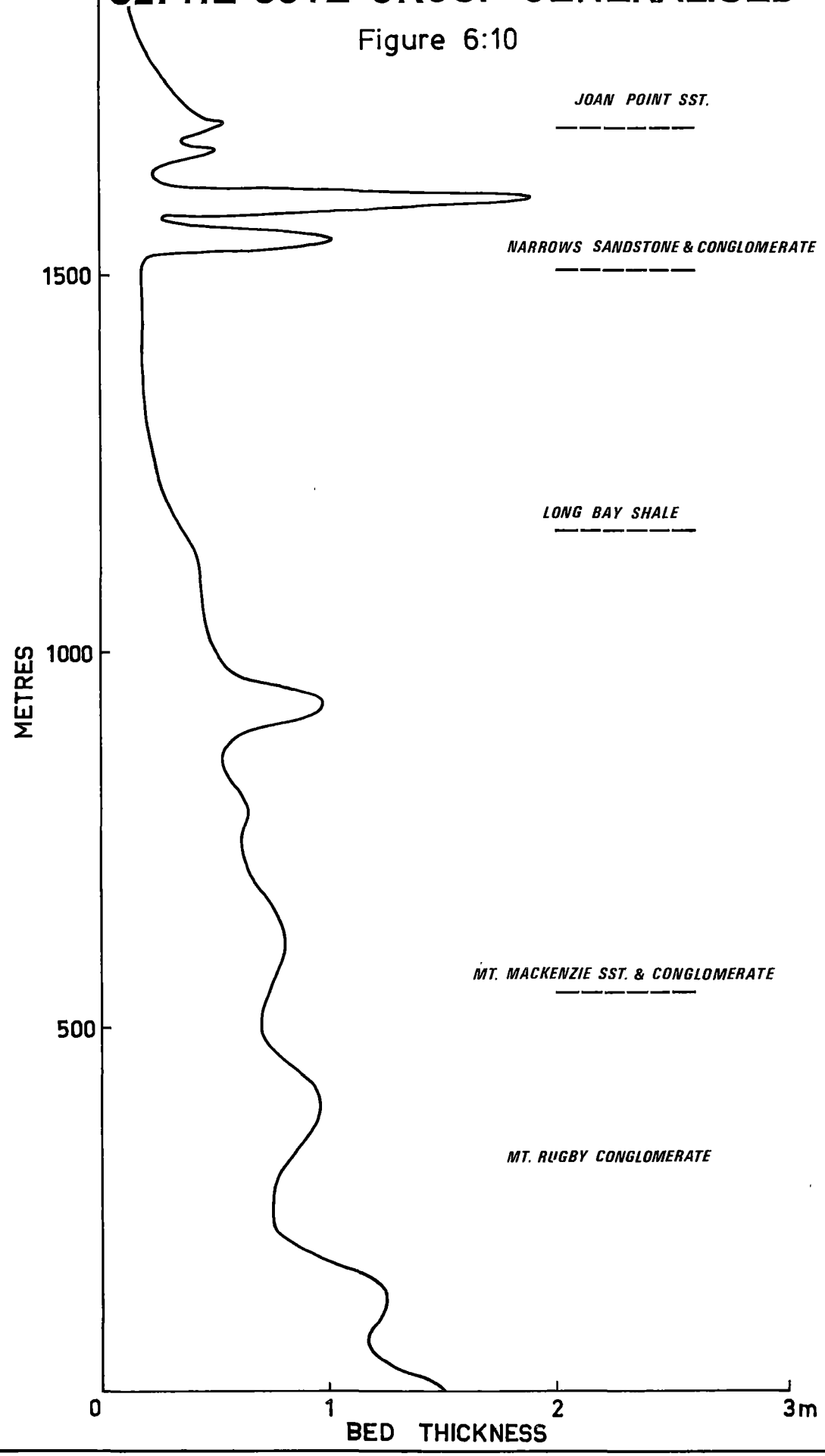

FIGURE 6 : 11

a. Relationship between Narrows Formation and the Long Bay Shale. Note non-erosional base of Narrows Formation sandstone lenses.

b. Mt. Mackenzie Formation is deposited in channels eroded in the Long Bay Shale. Indicates partial equivalence of both formations.

c. White Point area. Correlates of the equivalents of the Long Bay Shale and Mt. Mackenzie formations show both erosional and non-erosional relationships.

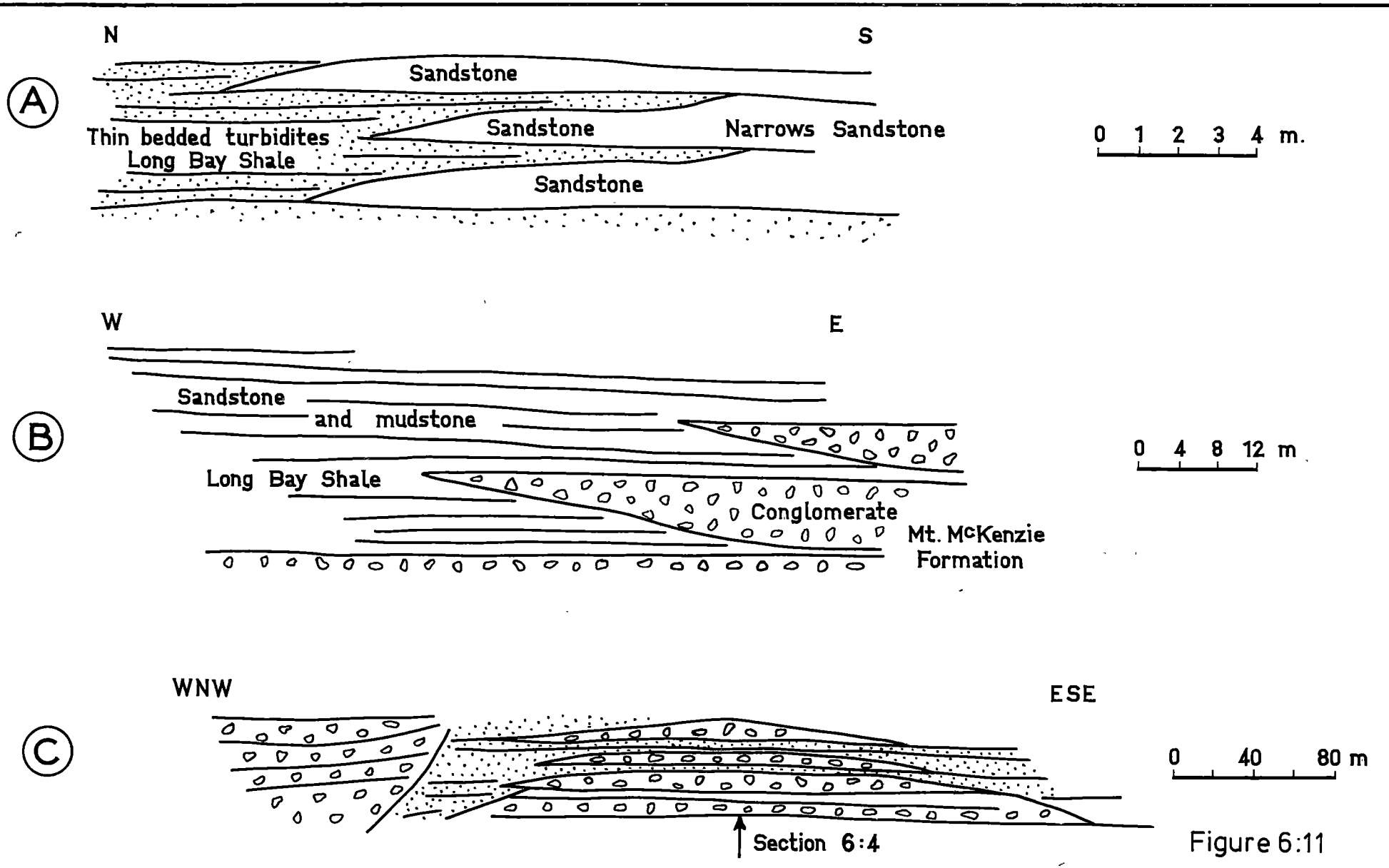
N
S
A
Sandstone
Thin bedded turbidites
Long Bay Shale
Sandstone
Narrows Sandstone
Sandstone
0 1 2 3 4 m.
W
E
B
Sandstone
and mudstone
Long Bay Shale
Conglomerate
Mt. McKenzie
Formation
0 4 8 12 m
WNW
ESE
C
Section 6:4
0 40 80 m

Figure 6:11

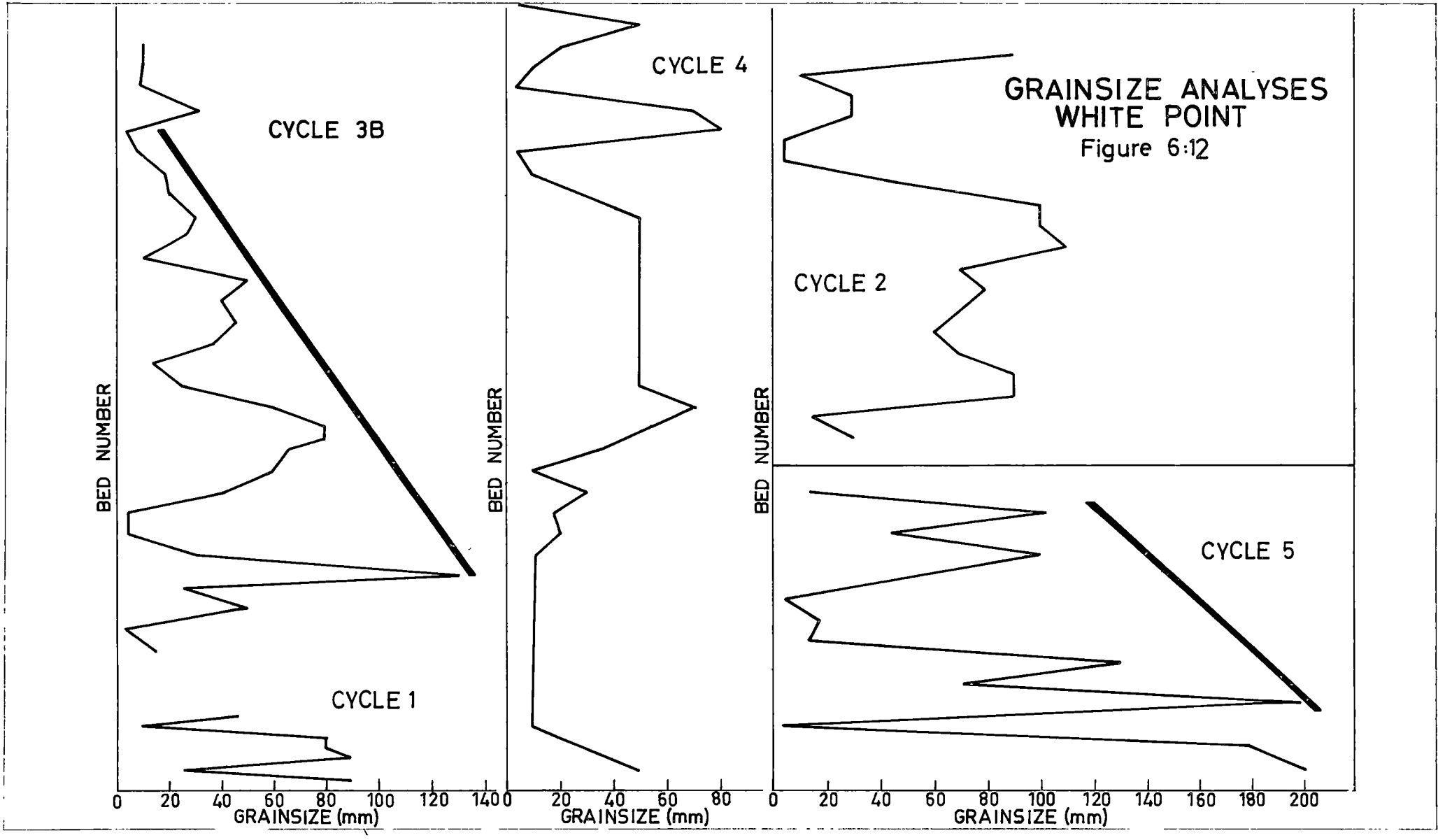
GRAINSIZE ANALYSES
WHITE POINT
Figure 6:12
CYCLE 3B
CYCLE 1
CYCLE 4
CYCLE 2
CYCLE 5
BED NUMBER
BED NUMBER
BED NUMBER
0 20 40 60 80 100 120 140
GRAINSIZE (mm)
0 20 40 60 80
GRAINSIZE (mm)
0 20 40 60 80 100 120 140 160 180 200
GRAINSIZE (mm)

RELATIONSHIP BETWEEN BED THICKNESS AND GRAINSIZE WHITE POINT SECTION

Figure 6·13

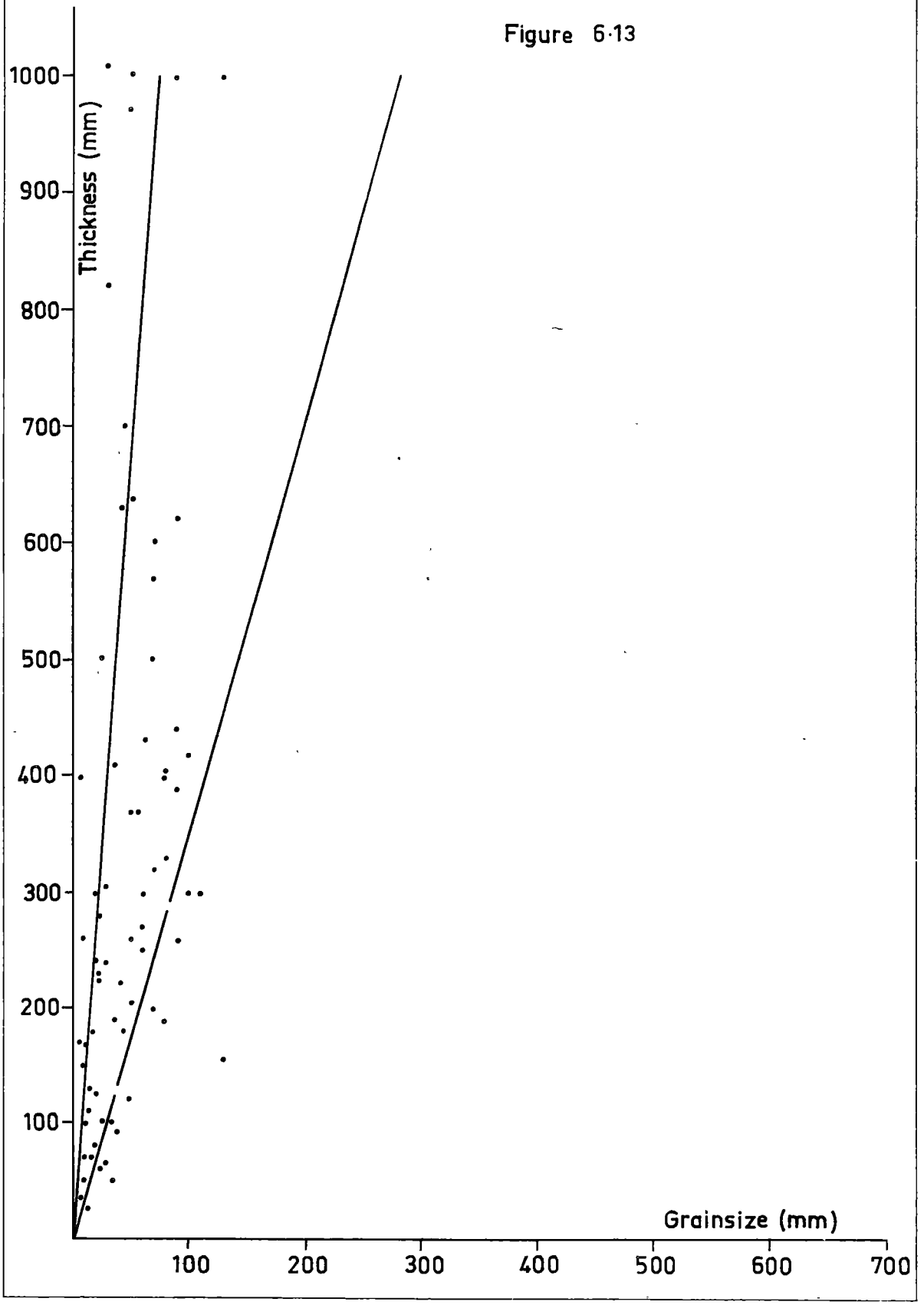

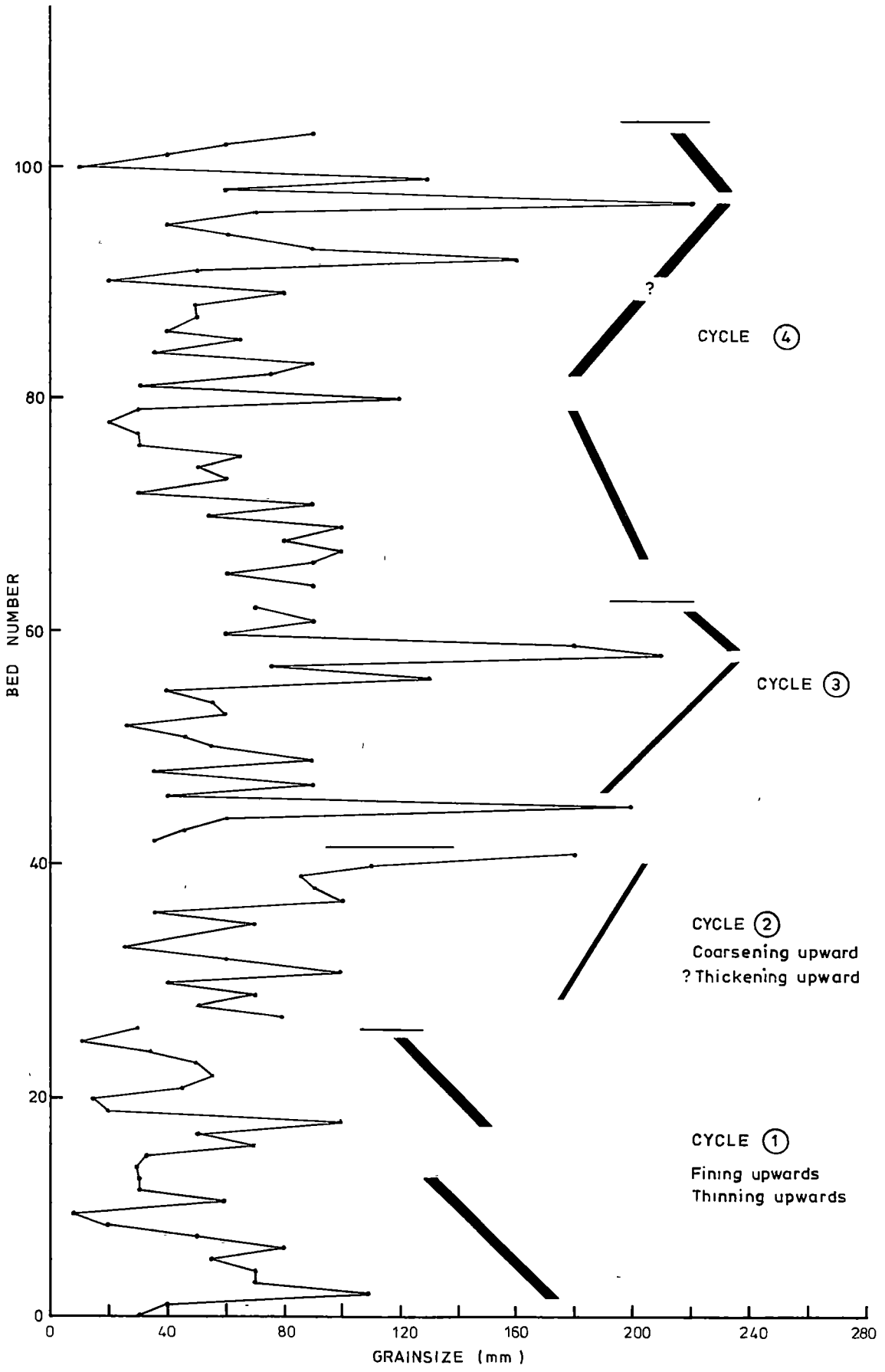
BED NUMBER
100
80
60
40
20
0
0
40
80
120
160
200
240
280
GRAINSIZE (mm)
?
CYCLE (4)
CYCLE (3)
CYCLE (2)
Coarsening upward
? Thickening upward
CYCLE (1)
Fining upwards
Thinning upwards

FIG 6:14

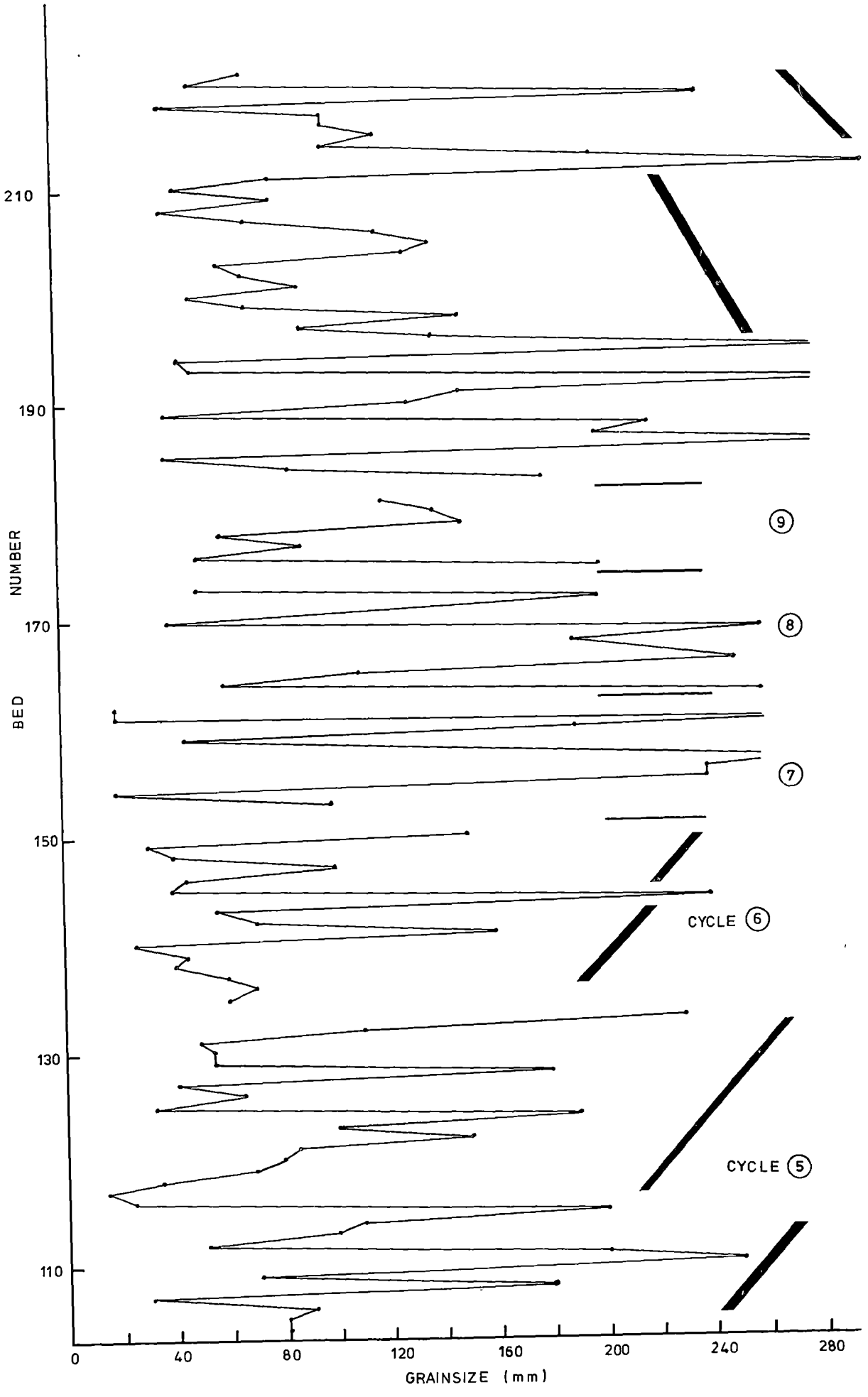
BED NUMBER
210
190
170
150
130
110
9
8
7
CYCLE 6
CYCLE 5
0
40
80
120
160
200
240
280
GRAINSIZE (mm)

FIG. 6:14

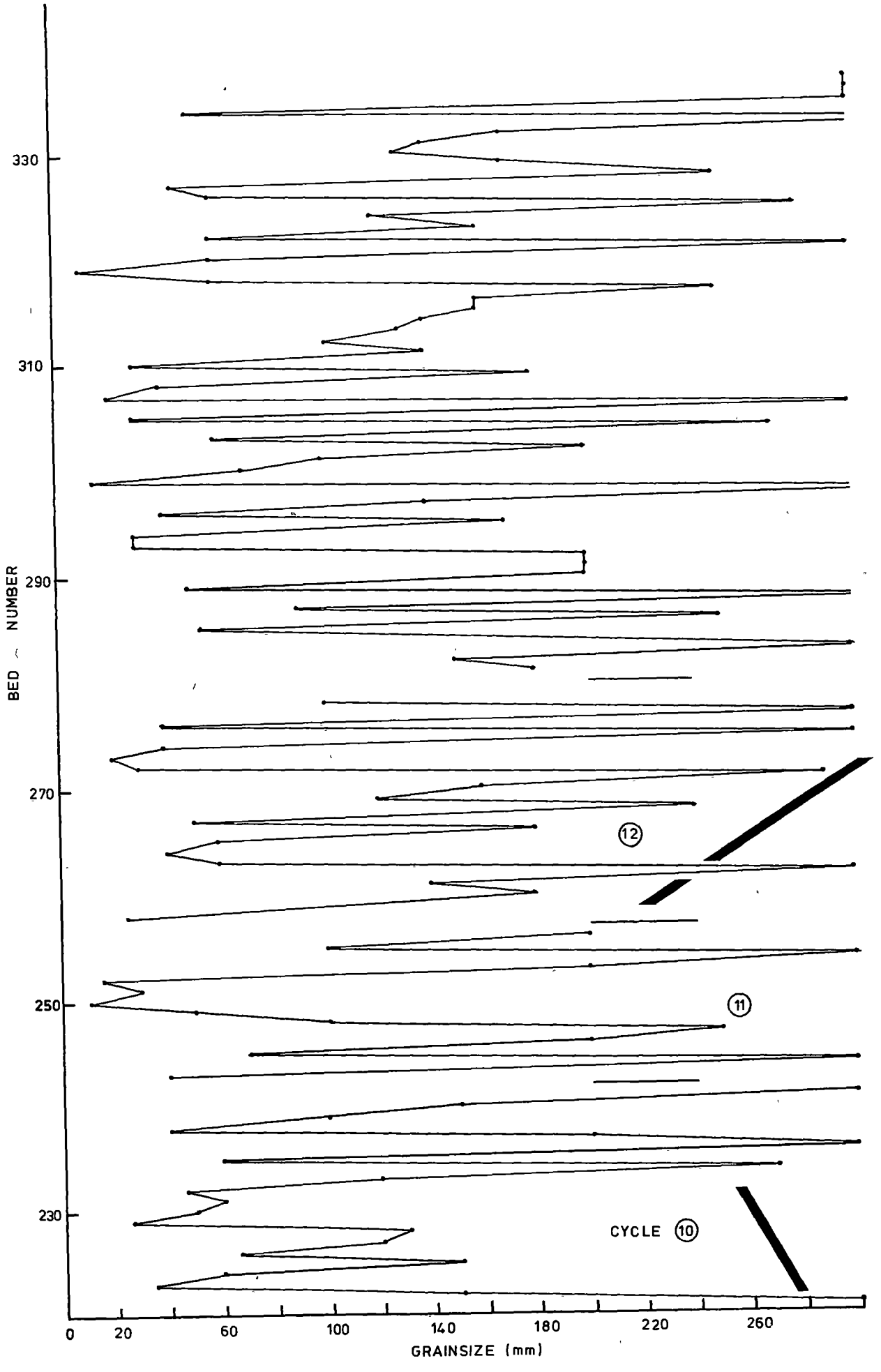
330
310
290
270
250
230
BED NUMBER
12
11
CYCLE 10
0
20
60
100
140
180
220
260
GRAINSIZE (mm)

FIG 6 : 14

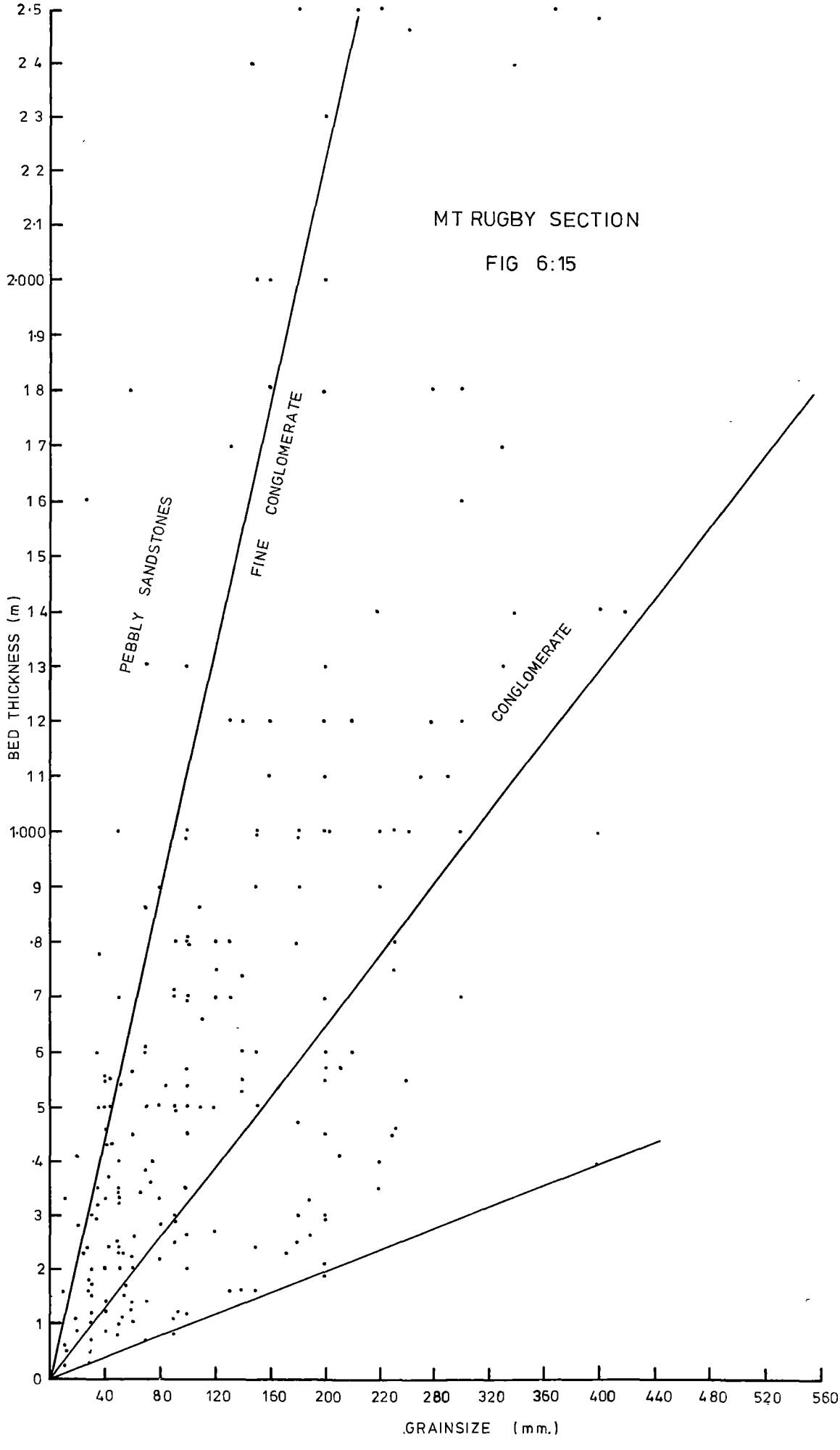
MT RUGBY SECTION
FIG 6:15
BED THICKNESS (m)
2·5
2 4
2 3
2 2
2·1
2·000
1·9
1 8
1 7
1 6
1 5
1 4
1 3
1 2
1 1
1·000
9
·8
7
6
5
·4
3
2
1
0
PEBBLY SANDSTONES
FINE CONGLOMERATE
CONGLOMERATE
40
80
120
160
200
220
280
320
360
400
440
480
520
560
GRAINSIZE (mm.)

GRAINSIZE VARIATION
NARROWS FORMATION

Figure 6:16

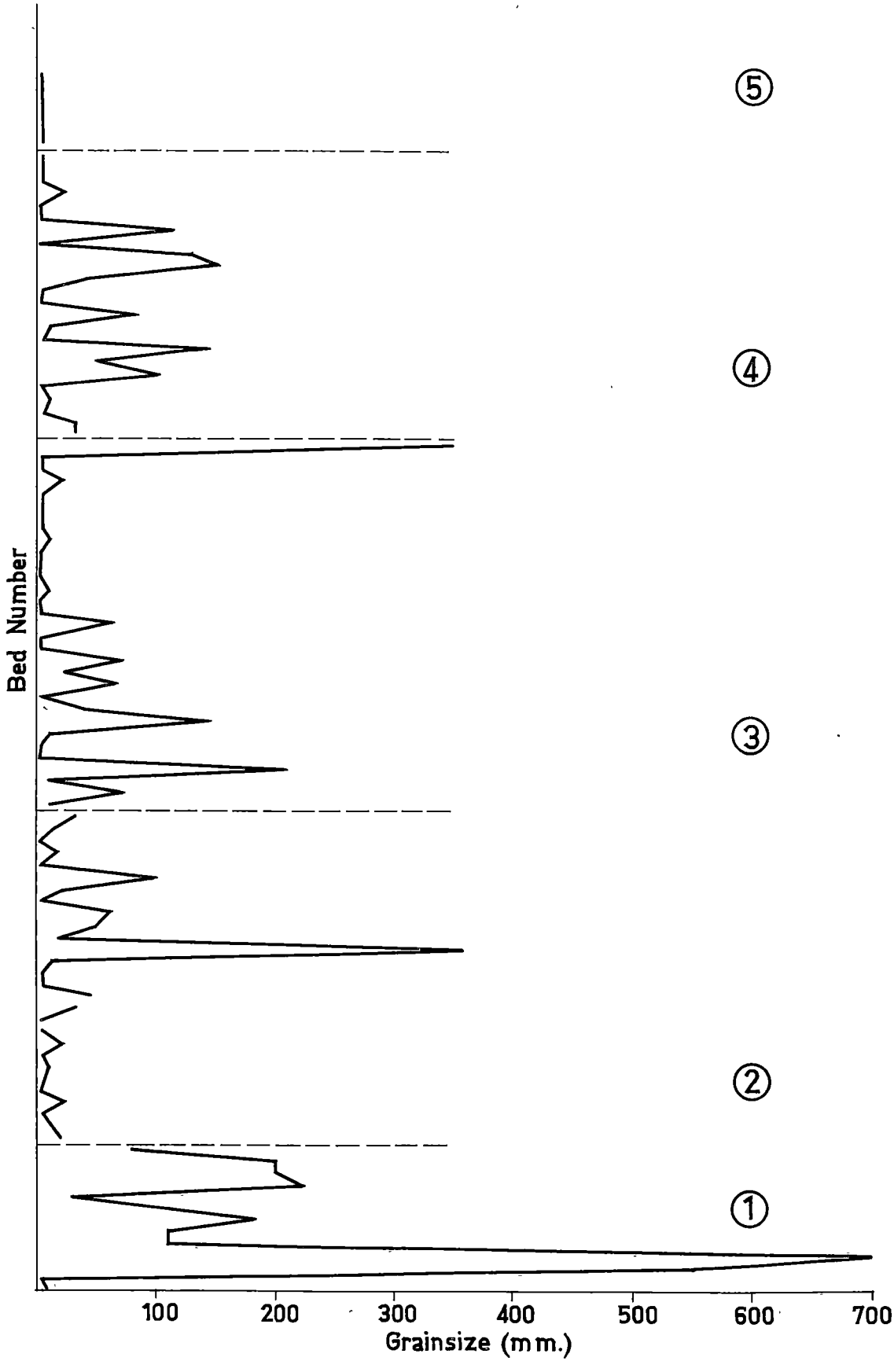

RELATIONSHIP BETWEEN BED THICKNESS AND GRAINSIZE NARROWS FORMATION

Figure 6:17

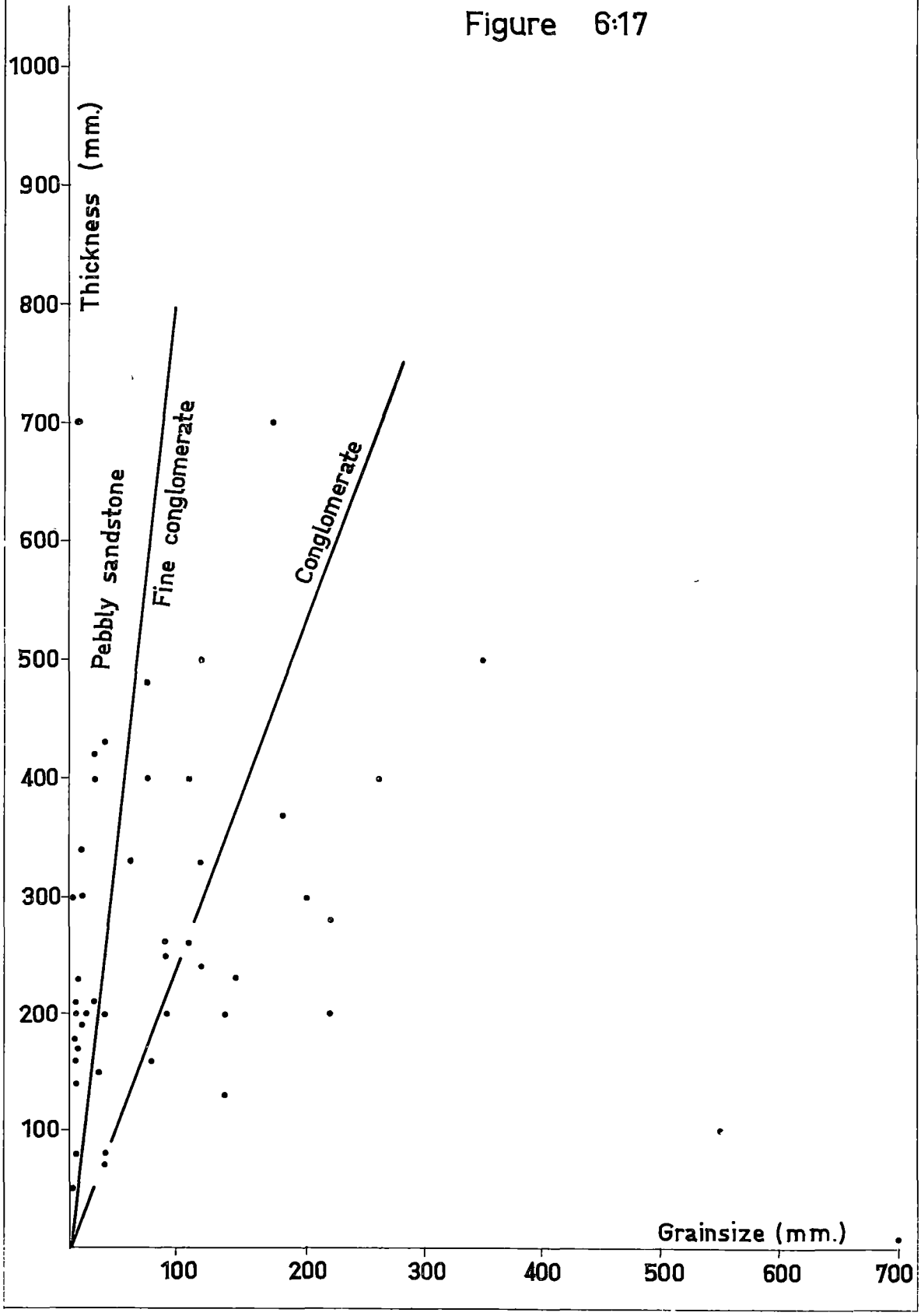

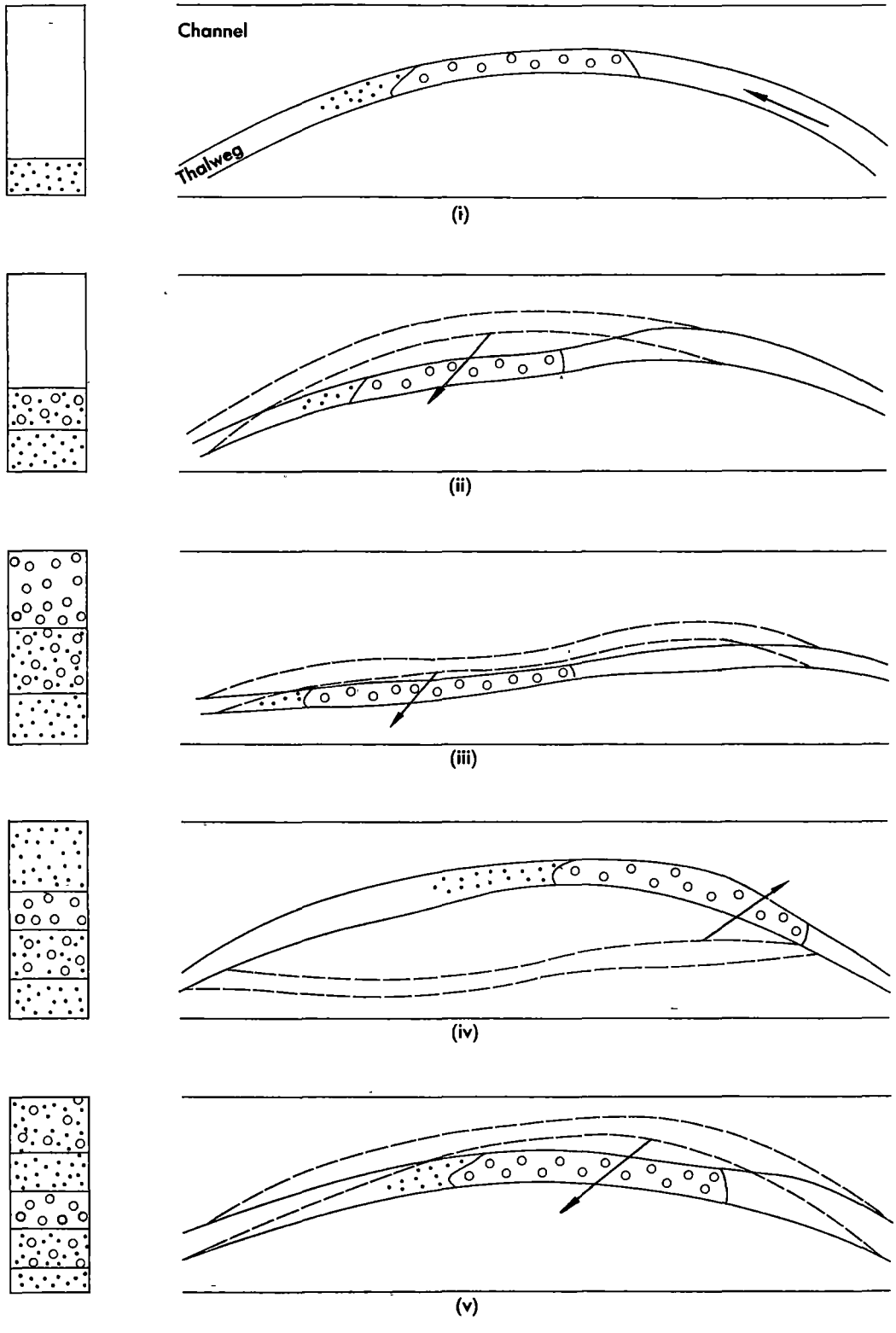

A PLAN VIEW OF A SHINGLING MODEL TO PRODUCE MULTIPLE THICKENING UPWARD SEQUENCES

Figure 6:187:a

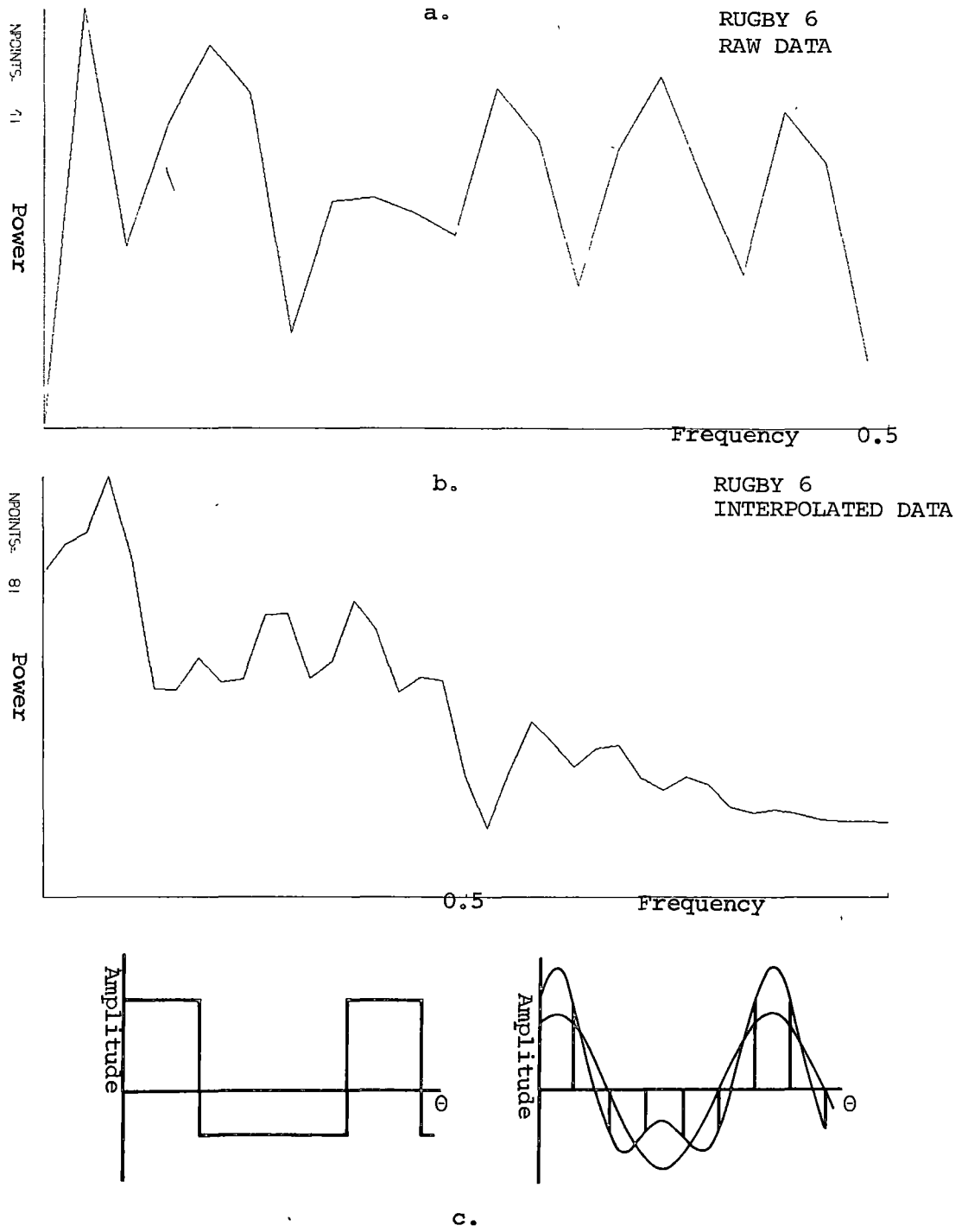
a.
RUGBY 6
RAW DATA
NPOINTS= 71
Power
Frequency
0.5
b.
RUGBY 6
INTERPOLATED DATA
NPOINTS= 81
Power
0.5
Frequency
Amplitude
Θ
Amplitude
Θ
c.

FIGURE 6:18

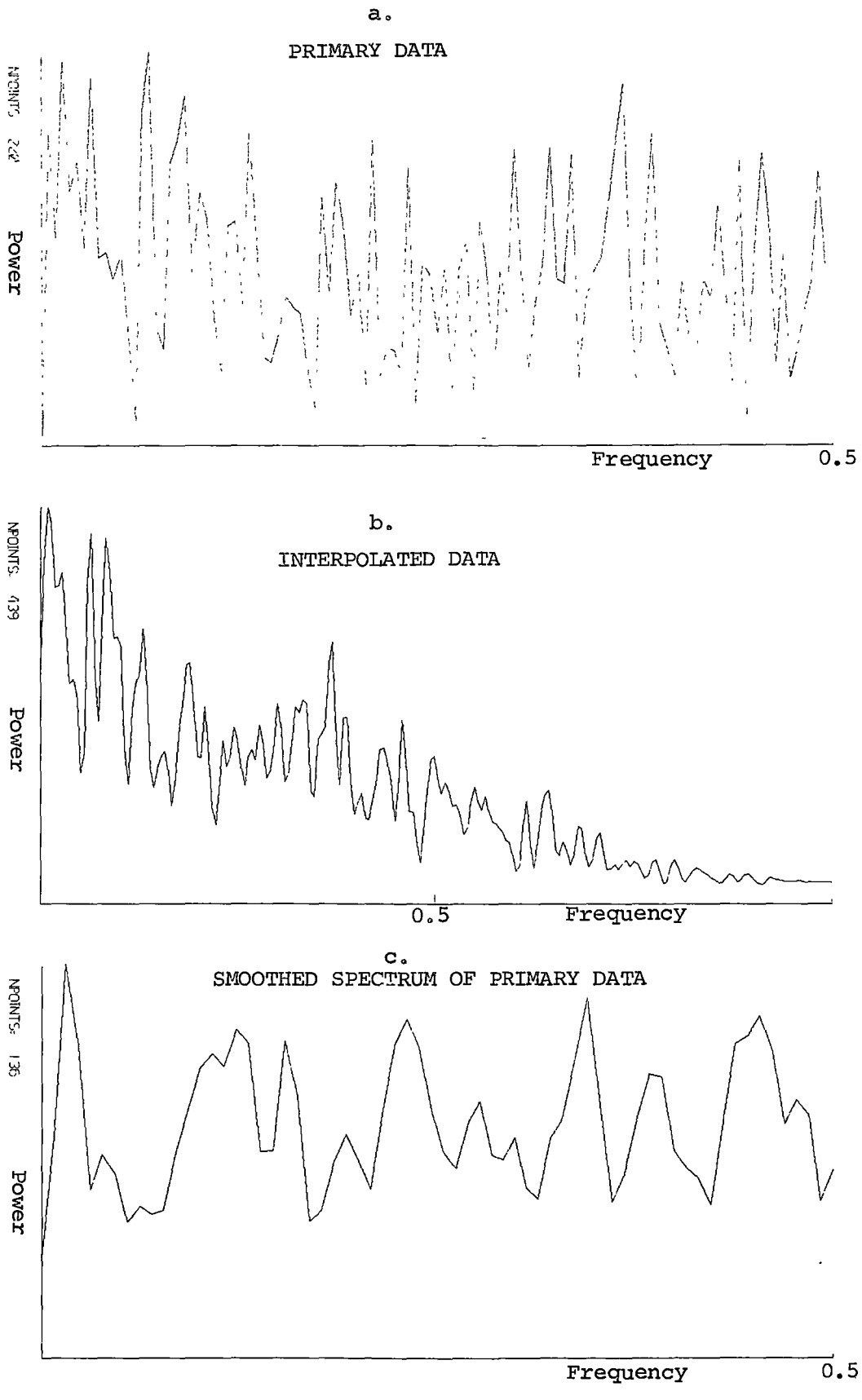

RUGBY 3, 4, 5 FOURIER SPECTRA

FIGURE 6:19

a.

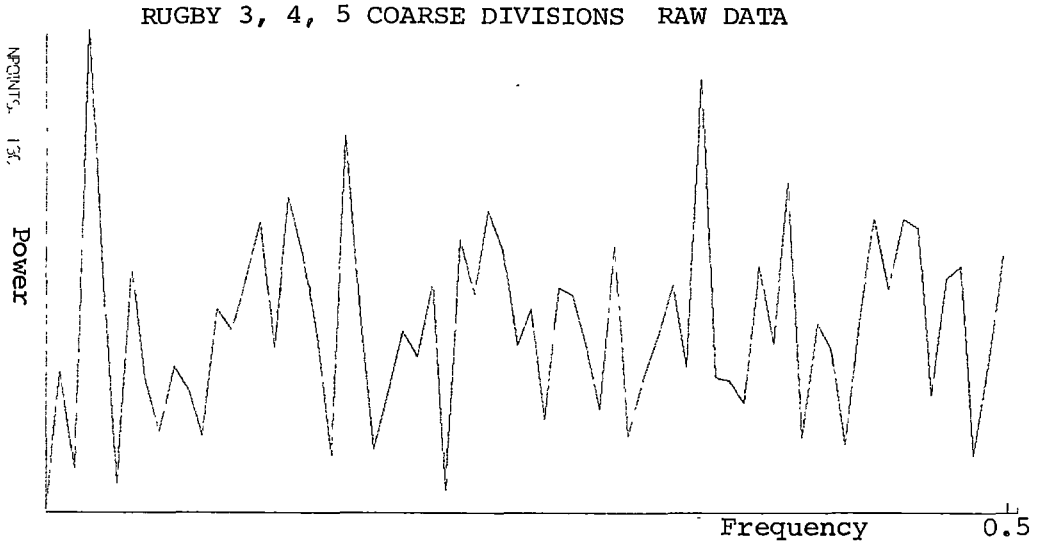

b.

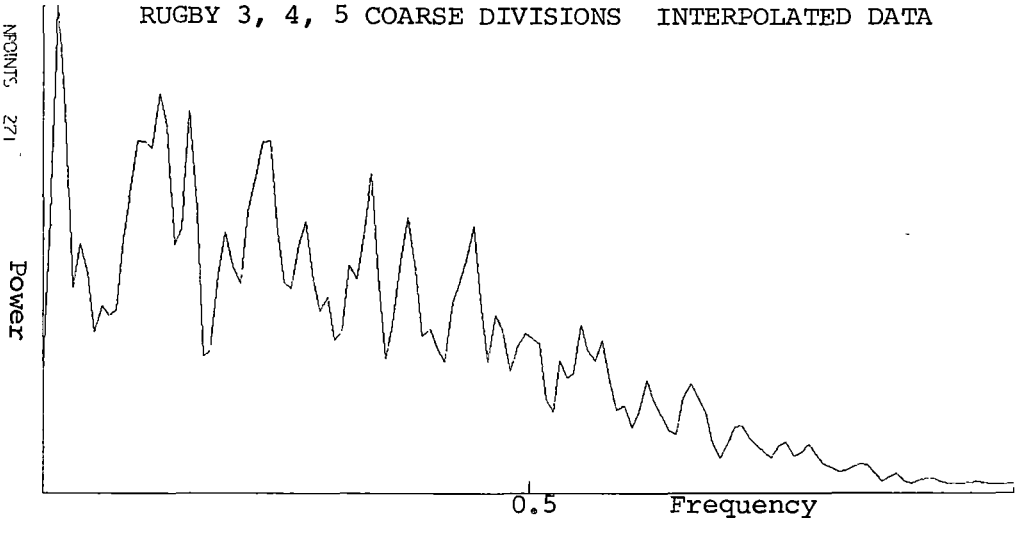

c.

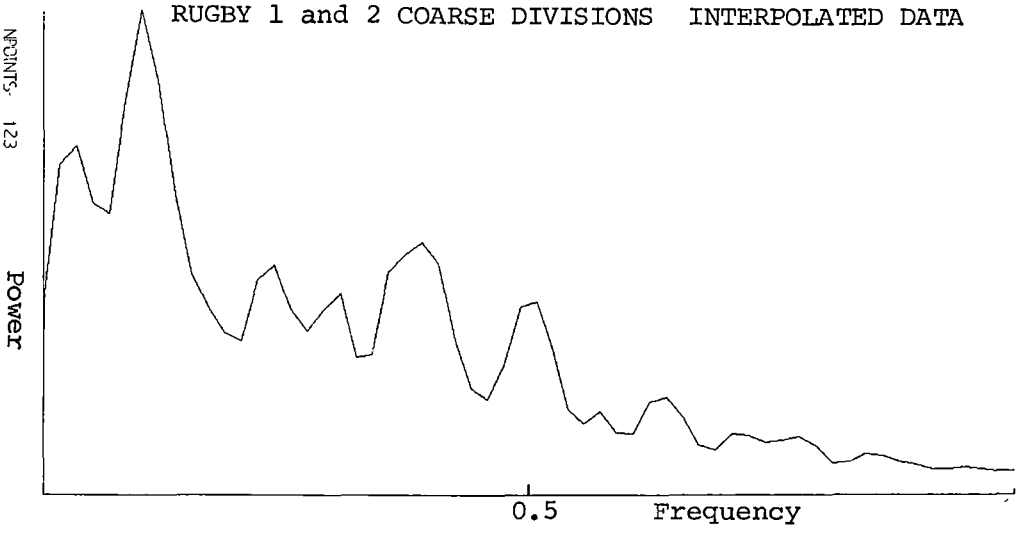

FOURIER SPECTRA

FIGURE 6:20

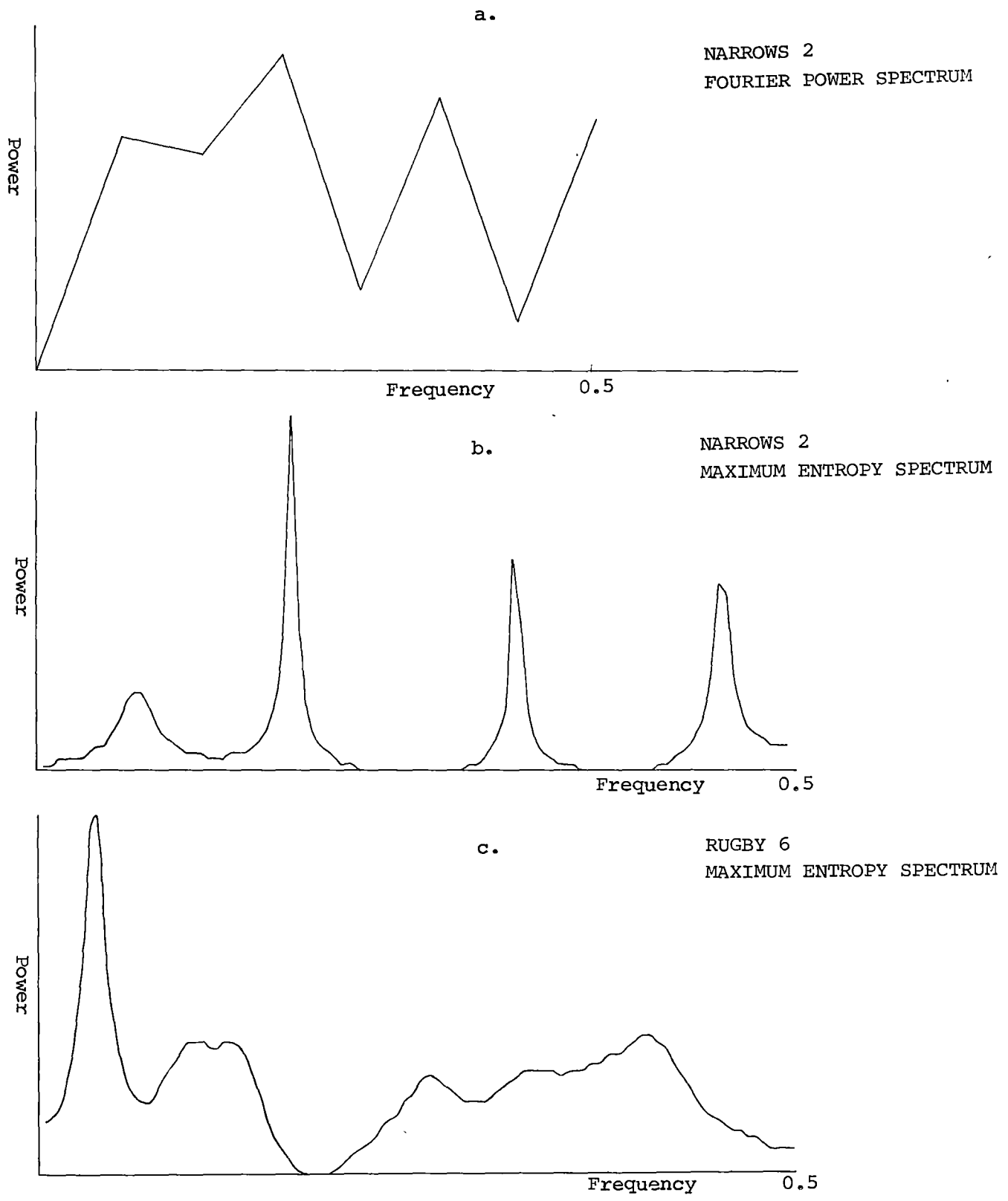
a.
NARROWS 2
FOURIER POWER SPECTRUM
Power
Frequency
0.5
b.
NARROWS 2
MAXIMUM ENTROPY SPECTRUM
Power
Frequency
0.5
c.
RUGBY 6
MAXIMUM ENTROPY SPECTRUM
Power
Frequency
0.5

FIGURE 6:21

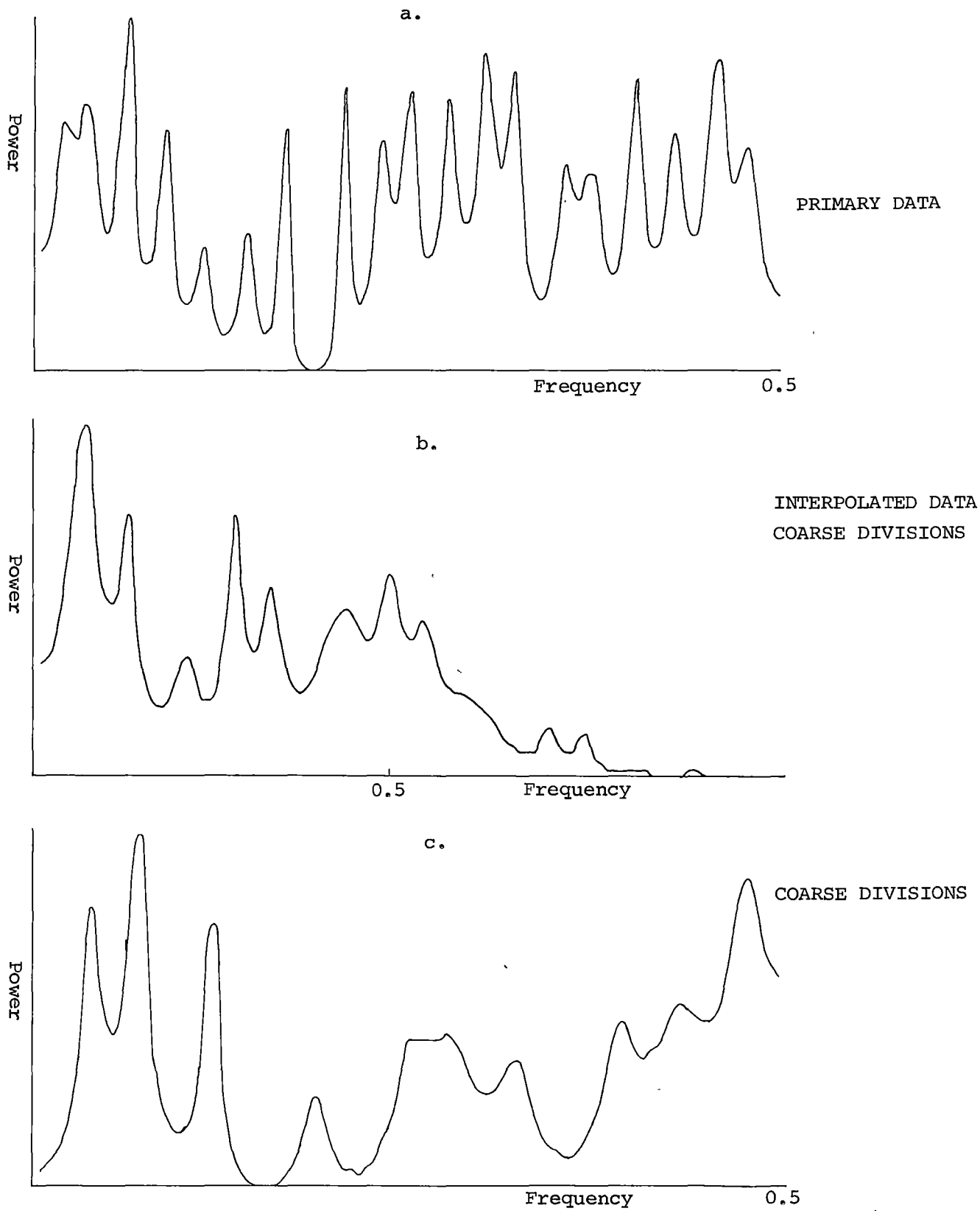

MAXIMUM ENTROPY SPECTRA NARROWS 2A

FIGURE 6:22

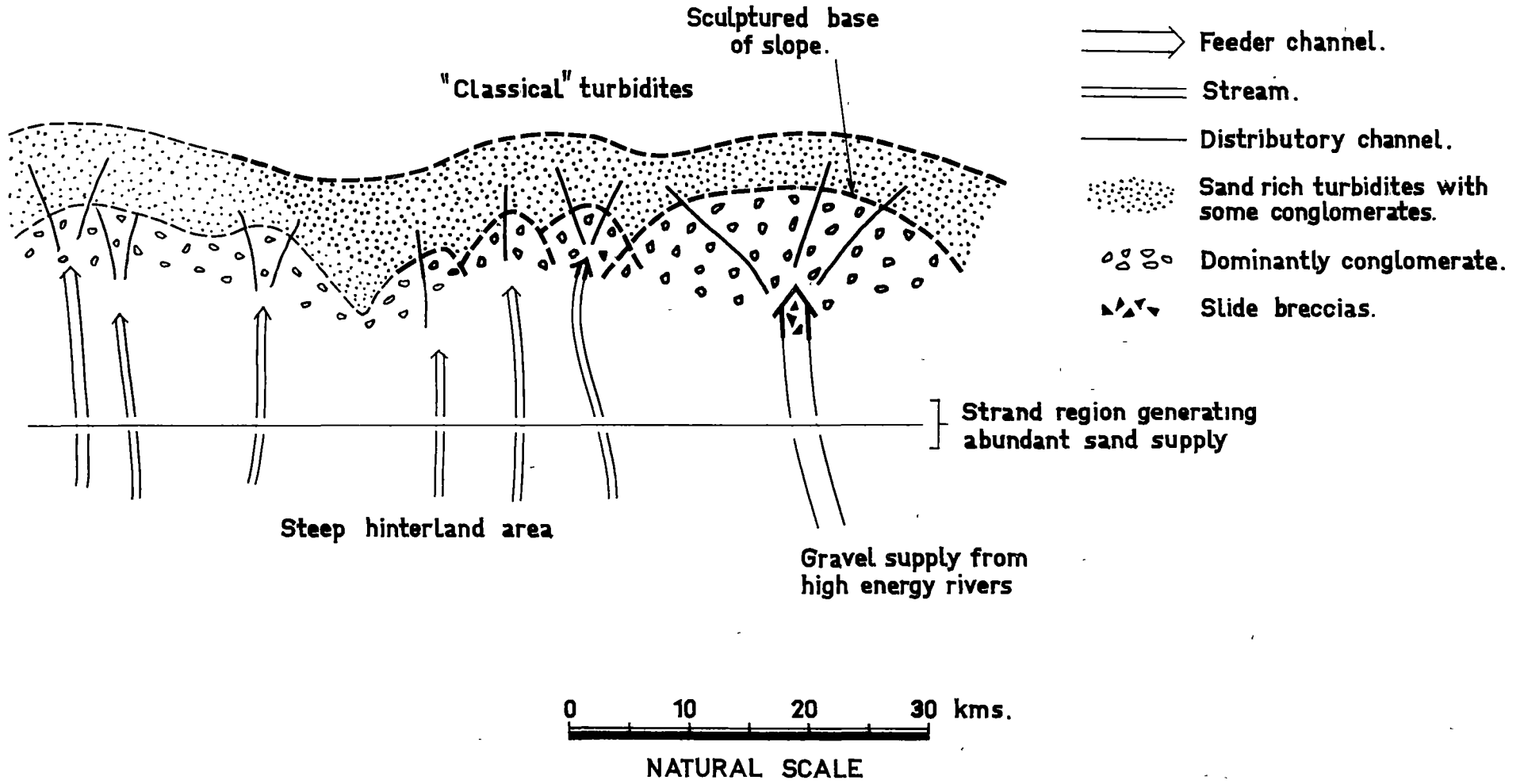
Sculptured base of slope.
"Classical" turbidites
Feeder channel.
Stream.
Distributory channel.
Sand rich turbidites with some conglomerates.
Dominantly conglomerate.
Slide breccias.
Strand region generating abundant sand supply
Steep hinterland area
Gravel supply from high energy rivers
0
10
20
30 kms.
NATURAL SCALE

Figure 7:1 :a

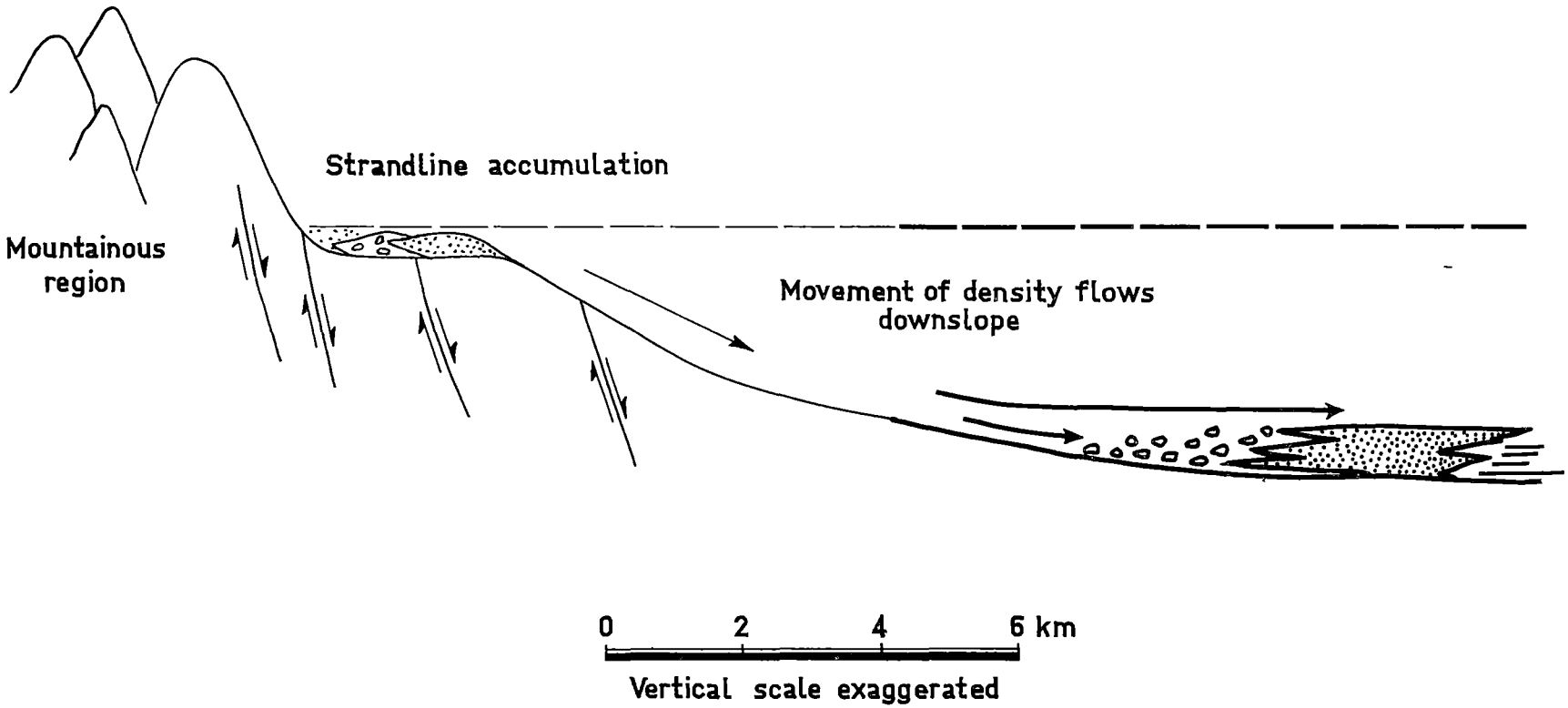
Strandline accumulation
Mountainous region
Movement of density flows downslope
0
2
4
6 km
Vertical scale exaggerated

Figure 7:1 :b